

# Hydrologic Conditions and Assessment of Water Resources in the Turkey Creek Watershed, Jefferson County, Colorado, 1998–2001

By Clifford R. Bossong, Jonathan Saul Caine, David I. Stannard,  
Jennifer L. Flynn, Michael R. Stevens, and Janet S. Heiny-Dash

---

U.S. GEOLOGICAL SURVEY

Water-Resources Investigations Report 03–4034

Prepared in cooperation with the  
JEFFERSON COUNTY PLANNING AND ZONING DEPARTMENT

Denver, Colorado  
2003

U.S. DEPARTMENT OF THE INTERIOR  
GALE A. NORTON, Secretary

U.S. GEOLOGICAL SURVEY  
Charles G. Groat, Director

The use of firm, trade, and brand names in this report is for identification purposes only and does not constitute endorsement by the U.S. Geological Survey.

---

For additional information write to:

District Chief  
U.S. Geological Survey  
Box 25046, Mail Stop 415  
Denver Federal Center  
Denver, CO 80225-0046

Copies of this report can be purchased  
from:

U.S. Geological Survey  
Information Services  
Box 25286  
Denver Federal Center  
Denver, CO 80225

# CONTENTS

Glossary of Special Terms .....	IX
Abstract .....	1
Introduction .....	2
Purpose and Scope .....	3
Location and Setting .....	3
Previous Investigations .....	3
Acknowledgments .....	3
Geologic Framework .....	5
Data Collection and Methods .....	9
Historical Data .....	9
Contemporary Data .....	13
Fracture Characteristics .....	13
Outcrop Selection .....	14
Methods of Fracture Measurement .....	14
Climatologic Data .....	14
Surface-Water Data .....	20
Ground-Water Data .....	20
Water-Quality Data .....	21
Runoff Modeling Methods .....	27
General Characteristics of the Precipitation-Runoff Modeling System .....	29
Watershed Characterization Using the Precipitation-Runoff Modeling System .....	30
Hydrologic Conditions .....	32
Evapotranspiration .....	32
Forest Site Results .....	32
Meadow Site and Comparison to Forest Site .....	40
Surface-Water Conditions .....	46
Watershed Conditions .....	46
Intrawatershed Conditions .....	48
Ground-Water Conditions .....	51
Time-Series Water Levels .....	51
Synoptic Water Levels .....	57
Analysis of State Engineer Well-Construction Data .....	58
Univariate Statistics .....	58
Variogram Analysis .....	61
Water-Quality Characteristics in the Turkey Creek Watershed .....	63
General Water-Quality Characteristics .....	63
Comparison to Historical Water-Quality Data .....	72
Tritium .....	73
Chloride to Bromide Ratios .....	74
Wastewater Compounds .....	75
Chloride Sources .....	76
Seasonality of Specific Conductance .....	77
Assessment of Water Resources .....	79
Estimates of Potential Fracture-Network Porosity .....	79
Runoff Modeling .....	83
Hydrologic Response Unit Delineation and Parameterization .....	83
Interflow and Base-Flow Reservoir Delineation and Parameterization .....	88
Distribution of Precipitation and Temperature Data .....	89
Model Calibration .....	90
Watershed Calibration Procedures .....	91
Intrawatershed Calibration Procedures .....	92
Final Calibration .....	92

Contemporary Simulations .....	92
Long-Term Simulations .....	102
Simulation Results and Their Implications to Water Supply .....	106
Summary .....	117
Selected References .....	120
Appendix .....	125
Brittle Structures of the Turkey Creek Watershed .....	127
Fracture Data Analysis, Model Construction, and Matching Models to Data .....	128
Fracture Set Designation .....	129
Fracture Length Simulation .....	130
Fracture Spacing .....	130
Fracture Intensity and Calibration of Fracture Network Models to Field Data .....	130
Spatial Analysis of Well-Construction Data and Ground-Water Levels .....	131
Evapotranspiration Measurement Methods .....	132
Quality Assurance and Quality Control .....	134
Milliequivalent Balances .....	134
Quality-Control Samples .....	135
Duplicate Samples .....	137

## FIGURES

1–8. Maps showing:	
1. Location of Turkey Creek watershed in Jefferson County, Colorado; identifier and locations for sites with specific-conductance measurement; and location of Bailey, Cheesman, and Elk Creek climatologic monitoring stations .....	4
2. Compilation of parts of the existing Evergreen, Indian Hills, Morrison, Conifer, and Meridian Hills U.S. Geological Survey Geologic Quadrangle Maps .....	6
3. Simplified geologic map, locations of outcrops where fracture characteristics were measured or observed, and fracture-orientation data for measurements at each location .....	7
4. Locations of surface-water streamflow measurement and sampling sites, stream gages, and irrigation ditches .....	11
5. Locations of permitted wells from the State Engineers Office .....	12
6. Spatial distribution of water-quality samples collected in previous studies in the Turkey Creek watershed .....	13
7. Location of climatologic monitoring sites .....	15
8. Schematic of the energy balance of a vegetated surface .....	16
9. Photograph of eddy-correlation evapotranspiration tower at forest site .....	19
10. Photograph of Bowen-ratio evapotranspiration tripod at meadow site .....	21
11. Map showing locations of water-level monitoring wells .....	23
12. Map showing location of ground-water sampling sites .....	27
13. Schematic diagram of selected physical processes characterized by Precipitation-Runoff Modeling System .....	31
14–22. Graphs showing:	
14. Daily evapotranspiration at forest site during (A) 1999, (B) 2000, and (C) 2001 .....	33
15. Daily precipitation and daily mean soil moisture at forest site during (A) 1999, (B) 2000, and (C) 2001 .....	34
16. Daily mean solar radiation at forest site during (A) 1999, (B) 2000, and (C) 2001 .....	35
17. Annual precipitation and infiltration at forest site during the study period .....	38
18. Daily precipitation and cumulative infiltration at forest site during (A) 1999, (B) 2000, and (C) 2001 .....	39
19. Daily evapotranspiration at meadow and forest sites during (A) 2000 and (B) 2001 .....	41
20. Daily precipitation at meadow site, and daily mean soil moisture at meadow and forest sites during (A) 2000 and (B) 2001 .....	42
21. Daily mean solar radiation at meadow site during (A) 2000 and (B) 2001 .....	43
22. Streamflow hydrographs for the three stream gages on Turkey Creek and annual precipitation at the Cheesman site .....	47

23.	Map showing locations of short-term record stream gages and sites of synoptic streamflow measurements.....	51
24.	Hydrographs from short-term records of streamflow ( <i>A</i> , log; <i>B</i> , arithmetic) .....	52
25–29.	Graphs showing:	
25.	Ground-water fluctuations in water-level monitoring wells.....	54
26.	Ground-water table in the Turkey Creek watershed, September 2001 .....	58
27.	Contours of depth to ground water for September 2001 .....	59
28.	Well yield and total depth for State Engineers Office permitted wells .....	63
29.	Variogram surface maps .....	64
30.	Stiff diagrams of selected water-quality constituents in the Turkey Creek watershed .....	69
31.	Trilinear diagram of quarterly ground-water and surface-water samples collected in the Turkey Creek watershed.....	70
32–35.	Maps showing:	
32.	Specific-conductance measurements in ground- and surface-water samples.....	71
33.	Concentrations of chloride in ground- and surface-water samples .....	72
34.	Concentrations of nitrate plus nitrite in ground- and surface-water sample.....	73
35.	Concentrations of boron in ground- and surface-water samples .....	74
36–38.	Graphs showing:	
36.	Plot of tritium concentrations in precipitation interpolated to Turkey Creek watershed location and decayed to year 2000 values, and boxplot of tritium concentrations in selected water wells in the Turkey Creek watershed.....	75
37.	Time-series plot of Turkey Creek watershed hydrologic variables and seasonal specific-conductance measurements collected at selected wells in fall 2000 and spring 2001 .....	78
38.	Correlation of specific conductance and streamflow and time-series plot showing seasonal variation of specific conductance and streamflow at Turkey Creek at mouth of canyon near Morrison .....	80
39.	Boxplot showing distribution of specific conductance at Turkey Creek at mouth of canyon (site A) and six comparison sites .....	82
40.	Graph showing plot of the log of total fracture model potential porosity for each locality.....	83
41.	Map showing Hydrologic Response Units delineated for use with the Precipitation-Runoff Modeling System in the Turkey Creek watershed .....	85
42.	Map showing interflow and base-flow reservoirs delineated for use with the Precipitation-Runoff Modeling System in the Turkey Creek watershed .....	89
43–45.	Graphs showing:	
43.	Watershed hydrographs of contemporary simulated and measured results.....	93
44.	Intrawatershed hydrographs of contemporary simulated and measured results.....	96
45.	Watershed hydrographs of long-term simulated results .....	107

## APPENDIX FIGURE

A1.	Flow chart showing how discrete fracture-network model parameters are modeled to lead to the construction of a single best-fit model.....	129
-----	---	-----

## TABLES

1.	Individual rock types assigned to rock groups in the Turkey Creek watershed.....	8
2.	List of sites with time-series records .....	10
3.	Univariate statistics for water-quality properties and constituents collected in previous studies.....	14
4.	Sensor type, data loggers, sensor heights, and measured variables at forest site .....	18
5.	Sensor type, heights, and measured variables at meadow site.....	20
6.	Site identifiers and selected characteristics for sites of surface-water-quality samples, short-term streamflow records, and synoptic streamflow measurements in the Turkey Creek watershed, Jefferson County, Colorado, 1998–2001 .....	22
7.	Well-construction details and miscellaneous data for ground-water level monitoring wells in the Turkey Creek watershed, Jefferson County, Colorado, 1998–2001.....	24

8. Site identifiers and selected characteristics for ground-water-quality sampling sites in the Turkey Creek watershed, Jefferson County, Colorado, 1998–2000.....	25
9. Water-quality properties and constituents included in analyses in water year 1999.....	28
10. Miscellaneous data collected in water year 2001, including analysis results for bromide, selected inorganic ions, wastewater compounds, and tritium .....	29
11. Climatic and water balance summary for calendar years 1999, 2000, 2001, and 3-year mean, at forest site .....	36
12. Climatic and water balance summary for calendar year 2001 at meadow and forest sites.....	44
13. Streamflow statistics for Turkey Creek.....	49
14. Measured precipitation and streamflow in and near the Turkey Creek watershed .....	50
15. Synoptic measurements of streamflow made at rock group sites and surface-water sampling sites .....	53
16. Univariate statistics and correlations for well-construction characteristics .....	60
17. Descriptive statistics for selected physical characteristics of permitted wells from the State Engineers Office, by rock group .....	61
18. Univariate statistics for reported well yields by rock type and group and through time .....	62
19. Univariate statistics for water-quality properties and constituents in selected ground-water samples collected September 1998 through November 1999.....	65
20. Univariate statistics for water-quality properties and constituents in selected surface-water samples collected September 1998 through November 1999.....	67
21. Specific-conductance data summary for Turkey Creek at mouth (site A) and eight comparison sites on the eastern slope of the Rocky Mountains in Colorado .....	81
22. Turkey Creek watershed hydrologic parameter estimates from previous work.....	82
23. Turkey Creek watershed fracture-model potential porosity results .....	84
24. Summary of Hydrologic Response Unit and base-flow reservoir characteristics, and hydrologic response unit accounting for contemporary simulation in the Turkey Creek watershed .....	86
25. Monthly means and selected summary statistics for measured precipitation .....	90
26. Watershed and intrawatershed calibration statistics.....	95
27. Monthly and annual summary statistics for contemporary simulations (January 1, 1999, through September 30, 2001) for the entire Turkey Creek watershed.....	97
28. Intrawatershed summary statistics for contemporary simulations (January 1, 1999, through September 30, 2001) for areas of (A) metamorphic, (B) intrusive, and (C) fault-zone rocks and (D) Pikes Peak Granite.....	98
29. Summary statistics of daily values for water-balance terms from contemporary simulations in (A) the entire Turkey Creek watershed and for areas of (B) metamorphic, (C) intrusive, and (D) fault-zone rocks and (E) Pikes Peak Granite .....	102
30. Annual summary statistics for long-term simulations (October 1, 1948, through September 30, 1999) in the entire Turkey Creek watershed.....	108
31. Intrawatershed summary statistics for long-term simulations (October 1, 1948, through September 30, 1999) for areas of (A) metamorphic, (B) intrusive, and (C) fault-zone rocks and (D) Pikes Peak Granite in the Turkey Creek watershed .....	109
32. Summary statistics of daily values for water-balance terms from long-term simulations for (A) the entire Turkey Creek watershed and for areas of (B) metamorphic, (C) intrusive, and (D) fault-zone rocks and (E) Pikes Peak Granite .....	113

## APPENDIX TABLES

A1. Frequency distribution for milliequivalent balances .....	135
A2. List of detections in quality-control samples .....	136
A3. Statistics for relative percent differences in duplicate samples.....	137
A4. Selected site characteristics for water levels measured in fall 2001 .....	138

## CONVERSION FACTORS, VERTICAL DATUM, AND ABBREVIATIONS

	Multiply	By	To obtain
<b>Length</b>			
	inch	2.54	centimeter (cm)
	inch	25.4	millimeter (mm)
	foot (ft)	0.3048	meter (m)
	mile (mi)	1.609	kilometer (km)
<b>Area</b>			
	acre	4,047	square meter (m <sup>2</sup> )
	acre	0.004047	square kilometer (km <sup>2</sup> )
	square mile (mi <sup>2</sup> )	2.590	square kilometer (km <sup>2</sup> )
	square mile (mi <sup>2</sup> )	640	acre
<b>Volume</b>			
	liter (L)	0.2642	gallon
	acre-foot (acre-ft)	1,233	cubic meter (m <sup>3</sup> )
	acre-foot (acre-ft)	0.001233	cubic hectometer (hm <sup>3</sup> )
<b>Flow</b>			
	cubic foot per second (ft <sup>3</sup> /s)	0.02832	cubic meter per second (m <sup>3</sup> /s)
	cubic foot per second per square mile [(ft <sup>3</sup> /s)/mi <sup>2</sup> ]	0.01093	cubic meter per second per square kilometer [(m <sup>3</sup> /s)/km <sup>2</sup> ]
	gallon per minute (gal/min)	0.06309	liter per second (L/s)
<b>Power</b>			
	watt	1	joules per second

Temperature in degrees Celsius (°C) may be converted to degrees Fahrenheit (°F) as follows:

$$^{\circ}\text{F} = 1.8 (^{\circ}\text{C}) + 32$$

Temperature in degrees Fahrenheit (°F) may be converted to degrees Celsius (°C) as follows:

$$^{\circ}\text{C} = (^{\circ}\text{F} - 32) / 1.8$$

Vertical coordinate information is referenced to the National Geodetic Vertical Datum of 1929. Horizontal is referenced to the North American Datum of 1927.

**Elevation**, as used in this report, refers to distance above or below NGVD29. NGVD29 can be converted to the North American Vertical Datum of 1988 by using the the National Geodetic Survey Conversion Utility available at URL <http://www.ngs.noaa.gov/TOOLS/Vertcon/vertcon.html>

**Specific conductance** is given in microsiemens per centimeter at 25 degrees Celsius (μS/cm at 25°C).

**Concentrations of chemical constituents** in water are given either in milligrams per liter (mg/L) or micrograms per liter (μg/L).

### Additional Abbreviations

mL	milliliter
m <sup>2</sup> /m <sup>3</sup>	square meter per cubic meter
g m <sup>-2</sup> s <sup>-1</sup>	gram per square meter per second
Wm <sup>-2</sup>	watt per square meter
kPa	kilopascal
J	joule
min	minute

## GLOSSARY OF SELECTED TERMS

The following terms are defined as they are used in this report.

*Aperture.*—The width of individual fracture openings in rock. Aperture is measured across the fracture, perpendicular to the fracture length.

*Base flow.*—Streamflow that emanates from ground water contained in a conceptual base-flow reservoir that exists in the subsurface. It is base flow that typically sustains streamflow during rainless periods.

*Brittle structures.*—Fractures, joints, and faults in rocks that are the result of brittle rather than ductile deformation.

*Contemporary.*—This term is used in this report to indicate data that were collected as part of this study, or to indicate methods that were applied to data that were collected for this study.

*Evapotranspiration.*—The process of moisture moving from the surface and near-surface areas of the Earth to the atmosphere; it is the sum of evaporation from wet surfaces (leaves, wet soils and rock, surface-water bodies, for example), sublimation from snow or ice, and transpiration, which is water evaporated from plant stomates.

*Fracture set.*—A group of fractures that have a set of properties such as orientation or length, or both, that are similar.

*Fracture network.*—A group of fracture sets that comprise all of the fractures in a volume of rock.

*Fracture porosity.*—Porosity resulting from open fractures, faults, or cracks.

*Ground water.*—As used in this report, water in the subsurface under water-table conditions. Some unknown amount of ground water is not associated with local streamflow. As used in this report, ground water represents the contents of interflow and base-flow reservoirs and additional unaccounted for ground water that is not associated with local streamflow.

*GSNK.*—Ground water that percolates to a conceptual area of the watershed that is not available to support local streamflow.

*Hydrologic response unit (HRU).*—A land surface with similar slope and aspect properties defined for modeling surface and near-surface hydrologic processes.

*Interflow.*—Streamflow that emanates from ground water in direct response to precipitation or snowmelt, or both, that is contained in a conceptual interflow reservoir in the subsurface. Interflow may consist of streamflow contributions from subsurface areas that are saturated or perched, or some combination of both.

*Interflow and base-flow reservoirs.*—Conceptual subsurface portions of the watershed used for accounting purposes in runoff modeling.

*Overland flow.*—That part of precipitation that passes over the surface of the land and into the nearest surface-water body without first passing beneath the surface. Generally in direct response to precipitation.

*Potential porosity.*—An estimate of porosity made on the basis of mathematical characterizations of outcrop fracture measurements extrapolated to rock groups.

*Recharge.*—As used in this report, water added to the subsurface below the soil zone; it is the residual of precipitation, evapotranspiration, and overland flow. Recharge supports interflow, base flow, and underflow.

*Rock group.*—An assemblage of mappable rock types aggregated into a group on the basis of similarities.

*Transmissivity.*—Rate of movement of a volume of fluid through a medium. Units of measurement are  $L^2/T$ , where L is length and T is time.

*Underflow.*—Ground water that leaves the watershed by means other than streamflow or evapotranspiration.



# Hydrologic Conditions and Assessment of Water Resources in the Turkey Creek Watershed, Jefferson County, Colorado, 1998–2001

By Clifford R. Bossong, Jonathan Saul Caine, David I. Stannard, Jennifer L. Flynn, Michael R. Stevens, and Janet S. Heiny-Dash

## Abstract

The 47.2-square-mile Turkey Creek watershed, in Jefferson County southwest of Denver, Colorado, is relatively steep with about 4,000 feet of relief and is in an area of fractured crystalline rocks of Precambrian age. Water needs for about 4,900 households in the watershed are served by domestic wells and individual sewage-disposal systems. Hydrologic conditions are described on the basis of contemporary hydrologic and geologic data collected in the watershed from early spring 1998 through September 2001. The water resources are assessed using discrete fracture-network modeling to estimate porosity and a physically based, distributed-parameter watershed runoff model to develop estimates of water-balance terms.

A variety of climatologic and hydrologic data were collected. Direct measurements of evapotranspiration indicate that a large amount (3 calendar-year mean of 82.9 percent) of precipitation is returned to the atmosphere. Surface-water records from January 1, 1999, through September 30, 2001, indicate that about 9 percent of precipitation leaves the watershed as streamflow in a seasonal pattern, with highest streamflows generally occurring in spring related to snowmelt and precipitation. Although conditions vary considerably within the watershed, overall watershed streamflow, based on several records collected during the 1940's, 1950's, 1980's, and 1990's near the downstream part of watershed, can be as high as about 200 cubic feet per

second on a daily basis during spring. Streamflow typically recedes to about 1 cubic foot per second or less during rainless periods and is rarely zero. Ground-water level data indicate a seasonal pattern similar to that of surface water in which water levels are highest, rising tens of feet in some locations, in the spring and then receding during rainless periods at relatively constant rates until recharged. Synoptic measurements of water levels in 131 mostly domestic wells in fall of 2001 indicate a water-table surface that conforms to topography. Analyses of reported well-construction records indicate a median reported well yield of 4 gallons per minute and a spatial distribution for reported well yield that has relatively uniform conditions of small-scale variability. Results from quarterly samples collected in water year 1999 at about 112 wells and 22 streams indicate relatively concentrated calcium-bicarbonate to calcium-chloride type water that has a higher concentration of chloride than would be expected on the basis of chloride content in precipitation and evapotranspiration rates. Comparison of the 1999 data to similar data collected in the 1970's indicates that concentrations for many constituents appear to have increased. Reconnaissance sampling in the fall of 2000 indicates that most ground water in the watershed was recharged recently, although some ground water was recharged more than 50 years ago. Additional reconnaissance sampling in the spring and fall of 2001 identified some compounds indicative of human wastewater in ground water and surface water.

Outcrop fracture measurements were used to estimate potential porosities in three rock groups (metamorphic, intrusive, and fault zone) that have distinct fracture characteristics. The characterization, assuming a uniform aperture size of 100 microns, indicates very low potential fracture porosities, on the order of hundredths of a percent for metamorphic and intrusive rocks and up to about 2 percent for fault-zone rocks. A fourth rock group, Pikes Peak Granite, was defined on the basis of weathering characteristics. Short-term continuous and synoptic measurements of streamflow were used to describe base-flow characteristics in areas of the watershed underlain by each of the four rock groups and are the basis for characterization of base flow in a physically based, distributed-parameter watershed model.

The watershed model, the Precipitation-Runoff Modeling System (PRMS), was used to characterize hydrologic conditions on the basis of precipitation and air temperature in 112 hydrologic response units for which physical characteristics were derived from mostly digital data. The watershed model also was used to characterize hydrologic conditions in subsurface portions of the watershed that are associated with streamflow. The model was conditioned, using a relatively small set of parameters, to match measurements of watershed and intrawatershed streamflow and point measurements of evapotranspiration, air temperature, and soil moisture. Results from the watershed model provide simulated estimates for water-balance terms in a contemporary simulation (January 1, 1999, through September 30, 2001) using precipitation and adjusted temperature data from within the watershed, and in a long-term simulation (October 1, 1948, through September 30, 1999) using precipitation and temperature data from near the watershed. The results of both simulations indicate that, on a watershed scale, base-flow reservoirs consistently contain about enough water to cover the watershed with 0.1 to 0.2 inch of water. The long-term simulations indicate that during a year with about 14 inches of precipitation, the watershed base-flow reservoir may have about a -0.06 inch

change in contents during periods with relatively small amounts of recharge. The results from watershed simulations also indicate that contents of base-flow reservoirs vary within the watershed; base-flow reservoirs contain little or no recoverable water for significant portions of many years in about 90 percent of the watershed. In areas where base-flow reservoirs contain no water, the only source of water for wells is water that has percolated to relatively deep parts of the system that are not associated with local streamflow; water withdrawn under these conditions will need to be replaced before base flow can resume. Estimates of the amount of water withdrawn by wells in 2001 in the Turkey Creek watershed are equal to a watershed depth of about 0.43 to 0.65 inch (about 0.0012 to 0.0018 inch per day).

## INTRODUCTION

Water quality, water quantity, and population growth in the foothill portions of Jefferson County are of concern to the Jefferson County Board of County Commissioners and the Planning and Zoning Department. The Planning and Zoning Department desires to meet the needs of current residents for adequate supplies of good quality water and to prepare for the projected growth and demands on the water resource from future development. The Turkey Creek watershed is representative of the foothills portions of Jefferson County. Contemporary (2001) population in the Turkey Creek watershed is estimated at 11,064 residents with projected population growth, using a 2-percent per year rate, at 13,186 residents in 2010, and 15,313 residents in 2020 (Jefferson County Planning and Zoning Department, written commun., 2001).

Water supply in the foothills portions of Jefferson County is typically derived from domestic wells developed in the fractured crystalline rocks. There are many anecdotal reports of wells “going dry” or requiring modifications to maintain production, and the prospect of continued development raises some questions regarding water supply. In addition, domestic water is treated in individual sewage-disposal systems (ISDS) and returned to the local system as ISDS effluent from leach fields, and this has raised some concerns regarding the quality of water.

An understanding of hydrologic processes, especially those related to ground water, is a fundamental step in assessing contemporary (2001) quality and quantity of ground water. Together, the U.S. Geological Survey (USGS) and Jefferson County undertook a cooperative study of hydrologic conditions and assessment of water resources in Turkey Creek watershed beginning in 1998.

## **Purpose and Scope**

The purpose of this report is to describe contemporary (2001) hydrologic conditions and to provide a hydrologic assessment of water resources in the Turkey Creek watershed. Hydrologic conditions are described on the basis of evapotranspiration, surface water, ground water, and water quality. In addition, a description of rock-fracture characteristics based on outcrop-scale measurements is included. The watershed assessment includes estimates of fracture porosity and a characterization of water-balance terms using a watershed precipitation-runoff model.

The scope of the study includes historical climatologic data collected by study-area residents, contemporary data collected during the study from 1998 to 2001, and historical data from agencies such as the Colorado Climate Center, State Engineers Office (SEO), and the USGS. Various methods, including geologic mapping and precipitation-runoff modeling, were used to assess water resources in the study area.

## **Location and Setting**

The study area is the 47.2-mi<sup>2</sup> Turkey Creek watershed (fig. 1), in Jefferson County southwest of Denver, Colo., in the foothills of the Front Range Section of the Southern Rocky Mountains physiographic province (Fenneman, 1931). Included in the study area are many developed areas such as Conifer, Aspen Park, and Indian Hills. It is estimated that there are about 4,900 households in the study area, or, on average, about one household for every 6 acres (Jefferson County Planning and Zoning Department, written commun., 2001). About 62 percent of households in the watershed are single-family detached homes.

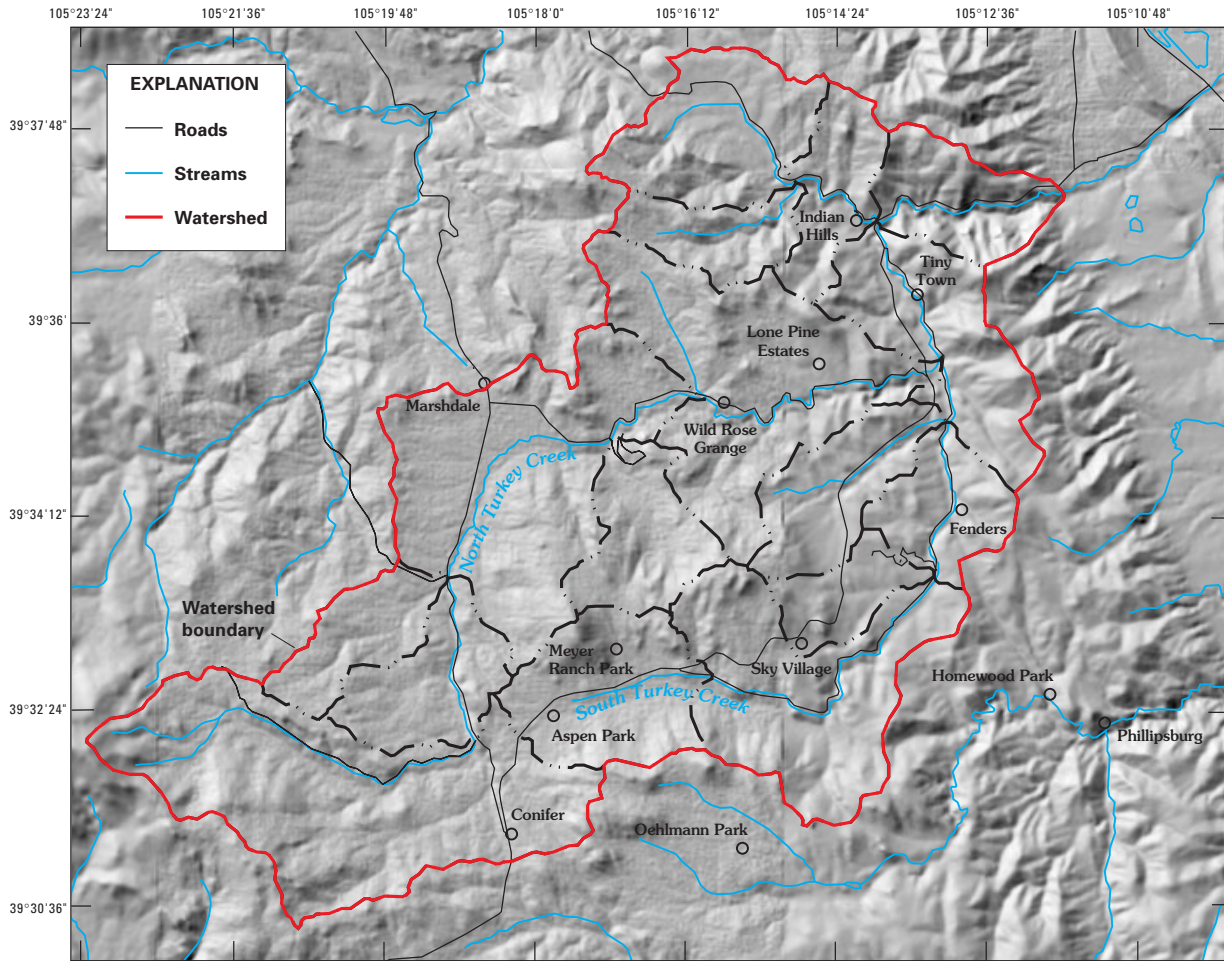
The watershed topography is mostly steep and often rocky with elevations ranging from about 10,500 ft in the southwestern part of the watershed to about 6,000 ft at the mouth of Turkey Creek canyon where the stream exits the foothills. Numerous bedrock outcrops in the study area border relatively gentle, open parks, such as Aspen Park, and stream valleys, such as North and South Turkey Creeks. Bedrock consists of fractured igneous and metamorphic crystalline rocks of Precambrian age that are extensively deformed. A more detailed geologic description is presented in the “Geologic Framework” section.

## **Previous Investigations**

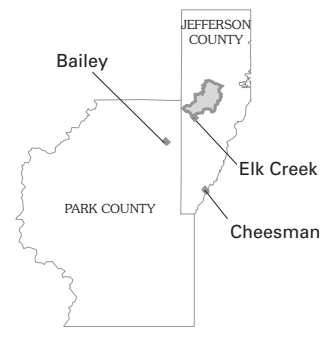
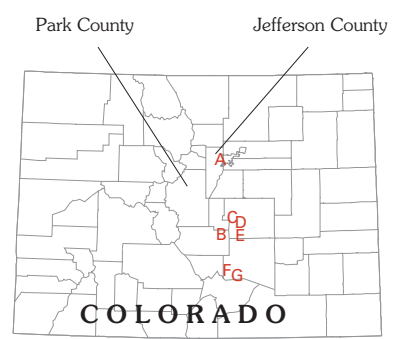
Several previous studies have been done on the chemical quality and physical quantity of the water resource in the Turkey Creek watershed. Snow (1968, 1972) and Waltz (1972) discussed the importance of fractured-bedrock aquifer characteristics in influencing the ground-water flow regime. Hofstra and Hall (1975a, 1975b) collected, compiled, and analyzed water-quality data for Phase I of an investigation to determine the effects of development on the water availability, water quality, and controlling factors in several mountain communities. Phase II of that investigation (Hall and Johnson, 1979) indicated that, although water quality was degrading, it was still acceptable for drinking. Seasonal fluctuations in water levels were observed (Hall and Johnson, 1979), and over a 3-year period there was an overall decline in water levels that may reflect short-term climatological factors or increased withdrawal from ground water. Recent work by Bruce and McMahon (1997) and Stevens and others (1997) provides water-quality data from the Turkey Creek watershed and other Front Range mountainous settings that can be compared to the results of this study.

## **Acknowledgments**

The authors thank various local, State, and Federal agencies for their cooperation in providing information and data that were used in preparing this report, specifically the Colorado Department of Public Health and Environment; Colorado Division of Water Resources; Jefferson County Board of Commissioners; Jefferson County Planning and Zoning Department;



Base modified from U.S. Geological Survey digital data for 1:24,000 maps



**EXPLANATION**  
 C Site with specific-conductance measurement

**Figure 1.** Location of Turkey Creek watershed in Jefferson County, Colorado; identifier and locations for sites with specific-conductance measurement; and location of Bailey, Cheesman, and Elk Creek climatologic monitoring stations.

members of the Mountain Ground-Water Resource Study Steering Committee; and the U.S. Environmental Protection Agency, Region VIII. Thanks also to Stephanie R.A. Tomusiak, Department of Geological Sciences, University of Colorado, Boulder, for her contributions to the fracture-data collection, analyses, and modeling efforts. Field assistance for outcrop measurements of fracture characteristics was provided by Ari Menitove, Jessica Beck, Sonya Cadle, Ben Glass, David Gardner, and Jared Lewis. Special appreciation also is expressed to Dick Burrows and Dorothy Hatch, dedicated volunteers that made monthly water-level measurements throughout the watershed during the study, as well as individuals who collected precipitation data, and homeowners who allowed various activities on their property such as water-level measurements, precipitation measurements, access to outcrops for fracture measurements, access to stream-sampling sites, and ground-water sample collection.

## GEOLOGIC FRAMEWORK

A compilation of existing USGS geologic quadrangle maps for the Turkey Creek watershed shows a complex arrangement of Precambrian-age crystalline metamorphic and intrusive rock types (fig. 2 and table 1; Char, 2000, modified from Sheridan and others, 1972; Bryant and others, 1973; Scott, 1972; Bryant, 1974). Figure 3 is a simplified version of the geology shown in figure 2 and the rock types in table 1, produced by combining individual rock types into rock groups. Rock groups were identified on the basis of lithologic similarity, structural history, and geologic setting. For each rock group it is assumed that (1) ground-water flow and storage predominantly occurs in fracture networks, and that (2) because each rock group is composed of similar rock types that have a similar geological history and response to brittle deformation, they will exhibit similar hydrogeological properties (for example, porosity). Three important rock groups that contain subgroups were used to aid in establishing a geologic and hydrologic framework model. The rock groups are (1) metamorphosed and foliated gneisses and schists, referred to as the “metamorphic rock group;” (2) large-scale intrusive quartz monzonites found in plutons and consisting mostly of the Silver Plume Quartz Monzonite, referred to as the “intrusive rock group;” and (3) major fault zones that cut all rock types, referred to as the “fault-zone rock group” (fig. 3). Further division of the metamorphic and intrusive rock

groups results in three subgroups: (1a) amphibolites, calc-silicates, and quartzites, (2a) the Pikes Peak Granite, and (2b) granitic pegmatite dikes that cross-cut the metamorphic and intrusive rock groups (table 1). The metamorphic, intrusive, and fault-zone rock groups plus subgroup 2a (the Pikes Peak Granite) are collectively referred to as the “four rock groups” in this report; group 1a is included in the metamorphic rocks and group 2b is included in the intrusive rocks.

The major rock types include approximately 1.7-billion-year-old gneisses and schists (metamorphic rocks). These rocks are typically well layered due to original compositional variations and metamorphic processes (Bryant, 1974; Bryant and others, 1975). They are part of the Turkey Creek Formation and are similar to the rocks in the Idaho Springs Formation (Lickus and LeRoy, 1968). The metamorphic rocks are intruded or cut by the approximately 1.4-billion-year-old Silver Plume Quartz Monzonite, which is a rock type similar to granite (intrusive rocks) (Bryant, 1974). These intrusive rocks are heterogeneously distributed in the watershed. The intrusive bodies range in size from small, dike-like features 50–100 ft long to large and irregular pluton-like bodies with large apophyses miles long. Pegmatitic dikes also cut the intrusive rocks. The pegmatites are highly irregular in shape and size and are less than a few feet to several miles long.

The major geologic structures in the watershed include folds and fault zones. The layering in the metamorphic rocks is generally steeply to moderately tilted and generally strikes northwest to southeast. This tilting is associated with the proximity of the observed outcrops to the limbs of several regional scale folds (Bryant and others, 1973). Many local-to outcrop-scale folds and highly contorted layering zones are present throughout the watershed.

A variety of brittle fault structures or fault zones are present in the watershed (fig. 3), and the Appendix contains a detailed discussion of these features. Brittle fault zones are in the form of unusually wide fracture networks (tens of feet to greater than miles wide) where most of the zone is composed of open fractures with little offset on them and a few discrete fractures where most of the offset has occurred. Other brittle fault zones are relatively narrow (a few feet wide) fault breccia zones that have anastomosing and discrete fractures where motion has taken place and where fracture networks have been mineralized with quartz, calcite, and other associated minerals.

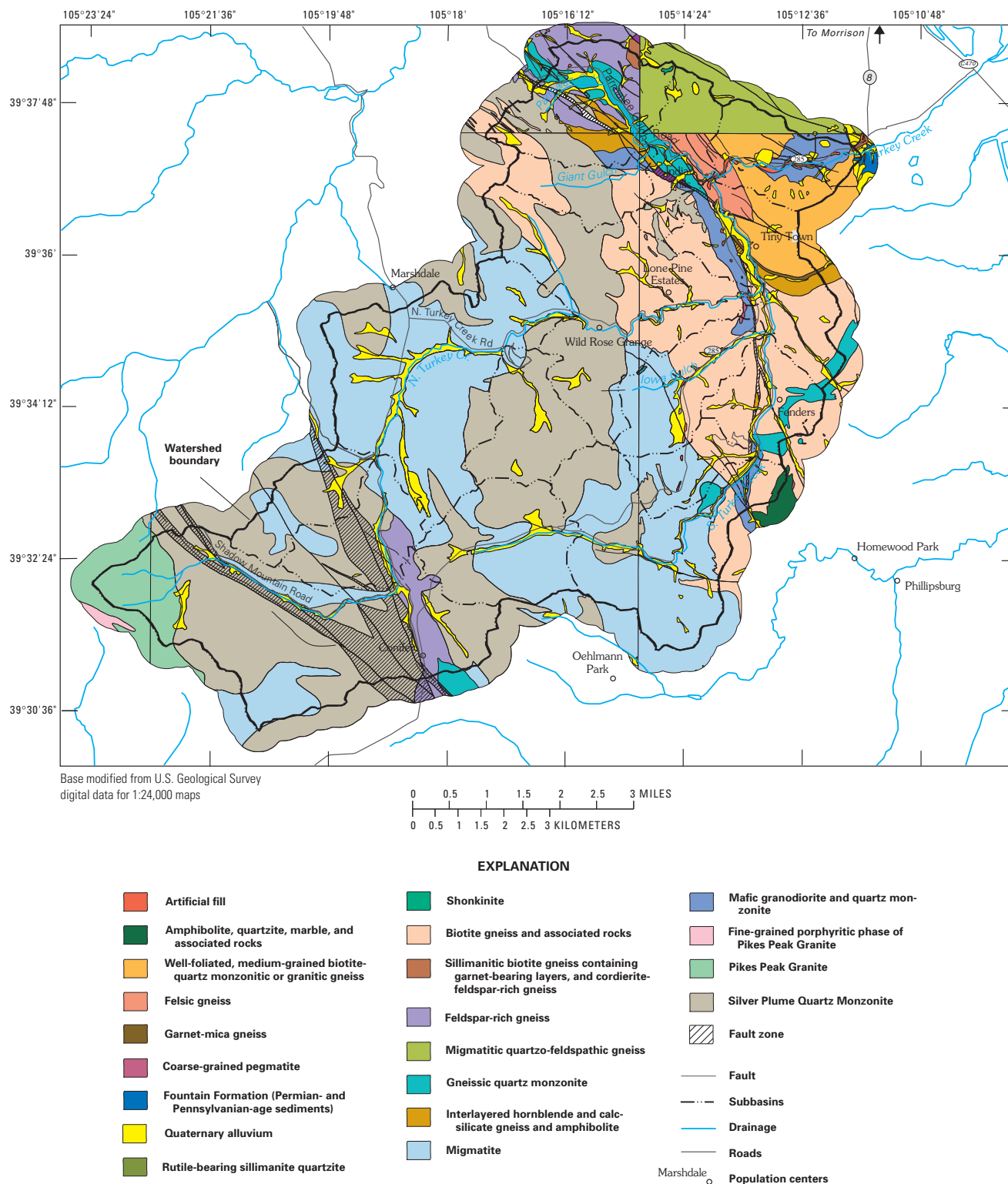


**Figure 2.** Compilation of parts of the existing Evergreen, Indian Hills, Morrison, Conifer, and Meridian Hills U.S. Geological Survey Geologic Quadrangle Maps.

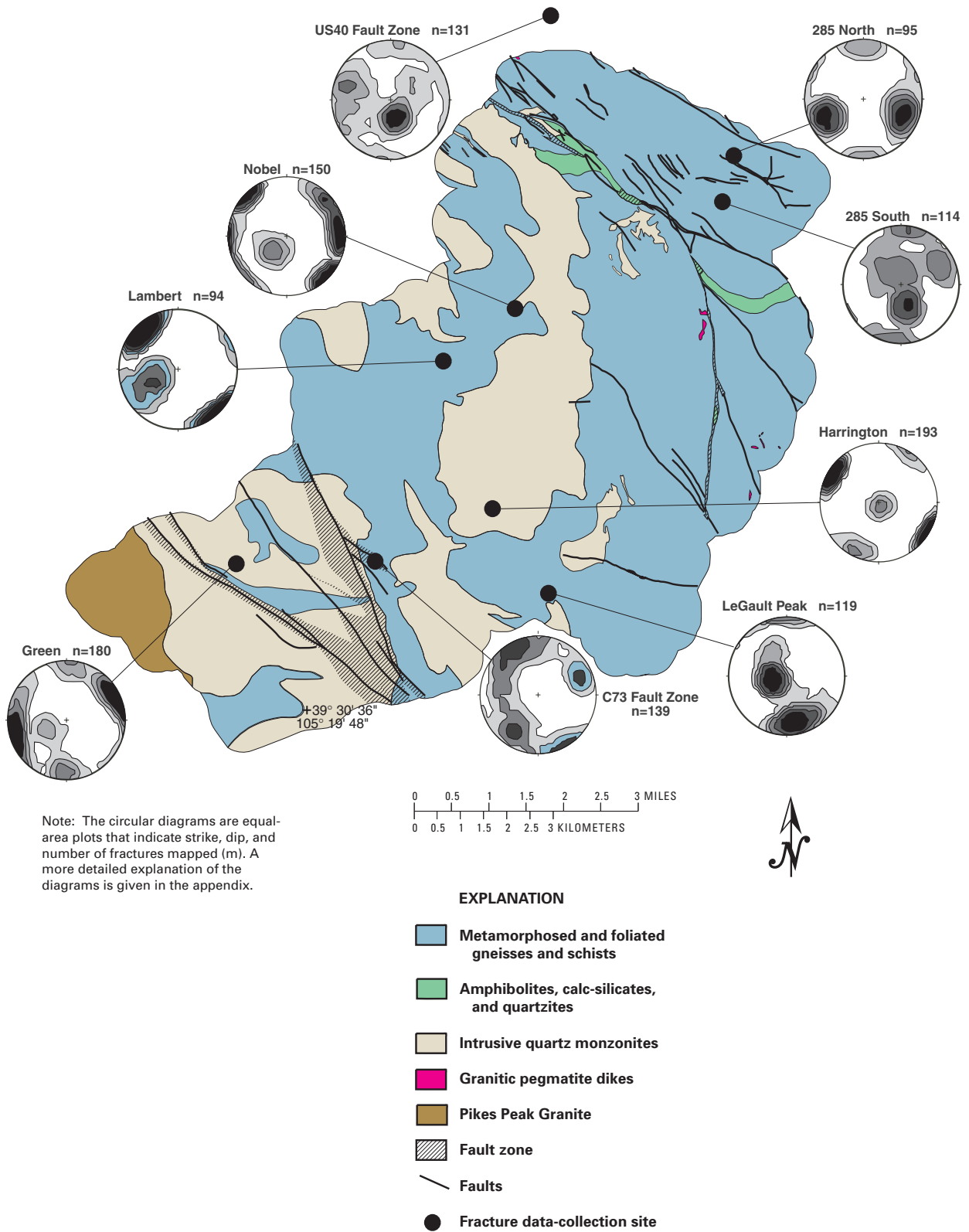


**Figure 3.** Simplified geologic map, locations of outcrops where fracture characteristics were measured or observed, and fracture-orientation data for measurements at each location.

**Table 1.** Individual rock types assigned to rock groups in the Turkey Creek watershed

[Individual rock types taken from the explanation in figure 2 are assigned to rock groups based on lithologic similarity, structural history, and geologic setting. The groups include (1) metamorphosed and foliated gneisses and schists; (1a) amphibolites, calc-silicates, and quartzites; (2) large-scale intrusive quartz monzonites found in plutons and consisting mostly of the Silver Plume Quartz Monzonite; (2a) Pikes Peak Granite and other granites; (2b) granitic pegmatites; and (3) major fault zones that cut all rock types. NP indicates rock types not present in the study area and Quaternary-age deposits have not been included. Y indicates Precambrian-age rocks that formed between 1.04 and 1.44 billion years ago, and X indicates rocks between 1.71 and 1.75 billion years old for this area. All other units are undated Precambrian-age rocks unless otherwise stated. The following is from Char, 2000, modified from Sheridan and others, 1972; Bryant and others, 1973; Scott, 1972; and Bryant, 1974]

Rock type name	Rock group assignment
Shonkinite	NP
Fountain Formation (Permian and Pennsylvanian-age sediments)	NP
Pikes Peak Granite	2a
Silver Plume Quartz Monzonite	2
Fine-grained porphyritic phase of Pikes Peak Granite	2a
Granitic rock	2a
Coarse-grained pegmatite	2b
Mafic granodiorite and quartz diorite	2
Gneissic granodiorite and quartz monzonite	1
Gneissic quartz monzonite	1
Migmatitic quartzo-feldspathic gneiss	1
Migmatite	1
Amphibolite, quartzite, marble, and associated rocks	1a
Amphibolite	1a
Biotite gneiss and associated rocks	1
Sillimanitic biotite gneiss containing garnet-bearing layers, and cordierite-feldspar-rich gneiss	1
Interlayered hornblende and calc-silicate gneiss and amphibolite	1a
Feldspar-rich gneiss	1
Garnet-mica gneiss	1
Well-foliated, medium-grained biotite-quartz monzonitic or granitic gneiss	1
Felsic gneiss	1
Rutile-bearing sillimanite quartzite	1a
Fault zone	3

The Colorado Rocky Mountain Front Range has a long and complex geologic history and associated brittle deformation. There are at least three generations of brittle deformation associated with the Precambrian rock in the watershed: (1) early Paleozoic-age burial and late Paleozoic-age Ancestral Rocky Mountain uplift, (2) mid- to late Mesozoic-age burial and late Mesozoic-age to early Cenozoic-age Laramide uplift, and (3) late Cenozoic-age volcanism, uplift, and possible extension (for example, Sonnenberg and Bolyard, 1997). This protracted geologic history and the response of the various rock types to deformation led to the complex joint (fractures with no shearing motion along them) and fault patterns that are observed today. The Turkey Creek watershed

represents a relatively undeformed portion of the Front Range relative to areas to the north in the Colorado Mineral Belt (Tweto and Sims, 1963).

Quaternary-age alluvium in the Turkey Creek watershed is sparse and is present primarily along stream channels and in open areas locally known as parks (fig. 2). The dominant soil types (stony loams to rock outcrops) are generally thin (about 2 to 3 ft thick), have generally low water availability, have moderate to high permeability, and are on moderate to steep slopes (U.S. Department of Agriculture, 1980). In addition, locally derived, very near-surface, bedrock weathering may be hydraulically significant. Thicker zones of weathered bedrock exist predominantly where there are coarse-grained intrusive rocks,



especially overlying the Pikes Peak Granite. Significant areas of weathered bedrock also occur where there are metamorphic rocks that are dominantly composed of hornblende and a variety of amphiboles. Field observations and anecdotal information from water-well drillers indicate that weathered bedrock is rare to absent except in the southwestern part of the watershed where the Pikes Peak Granite crops out (fig. 2). Weathering probably extends to depths of about 10 ft or less and is nonuniformly distributed where the Pikes Peak Granite crops out and in particular where it has been glaciated.

Surficial deposits of alluvium and soils are thin and not present everywhere in the Turkey Creek watershed; although the surficial deposits contain water, most wells in the watershed are completed in the crystalline bedrock and most water used for domestic supply in the watershed is withdrawn from the crystalline bedrock. The crystalline bedrock has very low primary, or intergranular, porosity; rather, open space that may contain water in the crystalline rocks consists mostly of fractures and fracture networks. The fractured bedrock aquifer system in the Turkey Creek watershed is the fractures and fracture networks in the crystalline rocks.

## DATA COLLECTION AND METHODS

Data used as part of this study are described in this section. Data collected in previous USGS studies and data compiled or collected by other agencies are referred to as “historical data,” and data collected as part of this study, beginning in 1998 and continuing through September 2001, are referred to as “contemporary data.” Some of the methods used in analyzing these data also are described in this section. Detailed descriptions of specialized methods used in developing estimates of fracture-network porosity, measurements of evapotranspiration, and characterization of spatial characteristics for some well-construction records are described in the Appendix. The preferred system of units for reporting in this report is the English inch-pound system; however, some data, such as those related to energy measures and rock fractures, are described in metric units as this is a standard and accepted practice.

## Historical Data

Much data for the Turkey Creek watershed collected as part of previous studies or maintained by agencies other than the USGS were used in this study. These data provide some descriptions of historical climatologic, streamflow, ground-water level, and water-quality conditions in or around the watershed. The data also include well-construction records available from the Colorado State Engineer’s Office (SEO) and miscellaneous data available from the Jefferson County Planning and Zoning Department including summaries of U.S. Census Bureau information, projections of population growth, locations of occupied households, some historical land-use classifications, and digital orthophoto imagery.

The Colorado Climate Center, in cooperation with the National Weather Service, maintains climatologic records for many locations in Colorado (Colorado Climate Center, 2002). Records for precipitation and daily air temperature extremes from three stations—Bailey (station 50454), Cheesman (station 51528), and Elk Creek (station 52633)—were used as part of this study (fig. 1). In addition, a detailed precipitation record covering more than 40 years (1956–99) was available from John and Marguerite Schoonhoven of Flying J Ranch (RG12 in table 2). Several other intermittent and short-term records of snowfall and temperature were available from various sources.

Historical records include those collected previous to this study and consist of data from two stream gages on Turkey Creek in the vicinity of the present gage (06710992, fig. 4). A summary for time-series data indicating periods of record for stream gages and other data is presented in table 2. Some historical records, from the late 1980’s, of surface-water discharge, or streamflow, in the Turkey Creek watershed are available from the Automatic Data Processing System (ADAPS) part of the National Water Inventory System (NWIS) (Bartholoma, 1997). NWIS is a computer system established by the USGS to manage and provide some analytical capabilities for a wide variety of hydrologic information; ADAPS addresses continuous records of many hydrologic data, including surface-water records. Additional historical records of streamflow from the 1940’s and 1950’s are not included in the NWIS but have been compiled in publications (U.S. Geological Survey, 1942–53).

**Table 2. List of sites with time-series records**

[Note: primary identifier, U.S. Geological Survey (USGS) station identification number or National Weather Service (NWS) station number; identifier type refers to source for identifier (1 - USGS, 2 - Colorado Climate Center, 3 - State Engineers Office); Local identifier, local identifier used by this study; Location, latitude and longitude in nad27; Elevation, feet above NGVD29; Type, defines type of data collected at site (1 - total daily precipitation [a - tipping bucket, b - weighing bucket], 2 - daily minimum and maximum air temperature, 3 - mean daily discharge, 4 - soil moisture, 5 - solar radiation, 6 - evapotranspiration, 7 - daily mean diversion, 8 - intermittent or monthly depth-to-water measurements, 9 - mean daily depth to water ); --, not applicable]

Identifier							
primary	type	local	Location	Elevation	Type	Period of record	Site name
DISCHARGE AND DIVERSIONS							
06710992	1	--	393703 1051324	6420	3	April 13, 2001 - continuing	Turkey Creek near Indian Hills
06710995	1	SWA01	393713 1051141	6040	3	April 1, 1998 - April 13, 2001	Turkey Creek at mouth of Canyon near Morrison
06711040	1	--	393827 1050934	5635	3	June 19, 1942 - September 30, 1953	Turkey Creek above Bear Creek Lake near Morrison
06711000	1	--	393809 1051003	--		April 25, 1986 - September 30, 1989	Turkey Creek near Morrison
393203105221600	1	STR-1	393203 1052216	9100	3	April 10, 2001 - August 1, 2001	North Turkey Creek upper tributary above Aspen Park
393210105205500	1	STR-2	393210 1052055	8435	3	April 10, 2001 - August 1, 2001	North Turkey Creek above Warhawk near Aspen Park
393141105200500	1	STR-3	393141 1052005	8350	3	April 17, 2001 - August 1, 2001	North Turkey Creek tributary above Aspen Park
393443105165800	1	STR-4	393443 1051658	7615	3	April 13, 2001 - August 1, 2001	North Turkey Creek tributary near Gartner Drive near Aspen Park
--	3	head 12	393714 1051155	6115	7	-- - --	Headgate Independent Highline # 12
--	3	head 27	393714 1051141	6015	7	-- - --	Headgate Bergen # 27
CLIMATOLOGIC							
393213105142100	1	RG1	393213 1051421	7460	1a	December 1, 1998 - September 30, 2001	RG1
393145105195900	1	RG2	393145 1051959	8250	1a	no record	RG2
393204105141700	1	RG3	393204 1051417	7900	1a	December 1, 1998 - September 30, 2001	RG3
393404105182701	1	RG4	393404 1051822	7820	1a	December 1, 1998 - September 30, 2001	RG4
393143105135600	1	RG5	393143 1051356	8480	1a	December 1, 1998 - September 30, 2001	RG5
393459105170300	1	RG6	393459 1051703	7560	1a	December 1, 1998 - September 30, 2001	RG6
393552105144201	1	RG7	393552 1051442	7480	1a	December 1, 1998 - September 30, 2001	RG7
393700105114500	1	RG8	393700 1051145	6040	1b,2	August 28, 1998 - September 30, 2001	RG8/AT1
393423105131000	1	RG9	393423 1051310	7160	1b	September 23, 1998 - September 30, 2001	RG9
393249105181900	1	RG10	393248 1051819	8240	1b	February 2, 1999 - September 30, 2001	RG10
393340105201500	1	RG11	393340 1052015	8180	1b	November 25, 1998 - November 23, 2001	RG11
--	1	RG12	393237 1051912	7980	1,2	January 1, 1956 - December 30, 1999	RG12
50454	1	RG13	392421 1052822	7730	11,2	August 1, 1948 - December 31, 1997	Bailey
51520	2	RG14	391313 1051640	6890	11,2	August 1, 1948 - June 30, 2000	Cheesman
52633	2	RG15	392953 1052000	8440	11,2	August 1, 1948 - September 30, 1951	Elk Creek
--	2	RG16	393227 1051925	8180	1a,2,4,5,6	February 3, 1999 - December 31, 2001	RG16/ ET Forest site/ ET Tower
--	2	RG17	393429 1051638	7770	1a,2,4,5,6	June 2, 2000 - December 31, 2001	RG17/ ET Meadow site
--	2	RG18	393429 1051638	7770	1b	December 6, 2000 - September 30, 2001	RG18/ ET Forest site
--	2	AT2	393104 1052109	9760	2	April 1, 2001 - September 30, 2001	Elk Creek Fire Station at Conifer Mountain
--	2	AT3	393304 1051621	8200	2	March 23, 2001 - September 30, 2001	North Meyer Ranch Park
--	2	AT4	393223 1051624	8200	2	March 23, 2001 - September 30, 2001	South Meyer Ranch Park
DEPTH TO WATER							
393821105161001	1	MH1	393820 1051612	7310	8	September 5, 1973 - February 14, 1983	MH1
					9	August 25, 1998 - continuing	
					9	May 23, 2001 - September 30, 2001	
393604105132100	1	MH2	393604 1051321	6900	8	November 4, 1998 - continuing	MH2
393513105181300	1	MH3	393513 1051813	7751	8	July 9, 1998 - continuing	MH3
393459105165701	1	MH4	393459 1051657	7672	8	December 3, 1998 - continuing	MH4
393350105184401	1	MH5	393350 1051844	7900	8	September 5, 1973 - February 14, 1983	MH5
					9	August 25, 1998 - continuing	
					9	May 23, 2001 - September 30, 2001	
393348105171400	1	MH6.1	393348 1051714	8375	8	December 3, 1998 - continuing	MH6.1
393344105171400	1	MH6.2	393344 1051714	8352	8	December 3, 1998 - continuing	MH6.2
393342105171500	1	MH6.3	393342 1051715	8340	8	December 3, 1998 - continuing	MH6.3
39333210515 800	1	MH7	393332 1051508	8337	8	December 3, 1998 - continuing	MH7
393301105150201	1	MH8	393301 1051532	8050	8	September 6, 1973 - February 14, 1983	MH8
					9	July 9, 1998 - continuing	
					9	May 23, 2001 - September 30, 2001	
393121105110600	1	MH9	393121 1051106	6720	8	September 6, 1973 - February 14, 1983	MH9
					9	August 25, 1998 - September 30, 2001	
392958105164601	1	MH10	392958 1051646	7950	8	September 6, 1973 - February 14, 1983	MH10
					9	August 25, 1998 - September 30, 2001	
393112105182100	1	MH11	393112 1051821	8477	8	June 18, 1998 - continuing	MH11
393143105195400	1	MH12	393143 1051954	8187	8	July 10, 1998 - continuing	MH12
393717105145300	1	MH13	393717 1051453	7279	8	May 11, 1999 - continuing	MH13

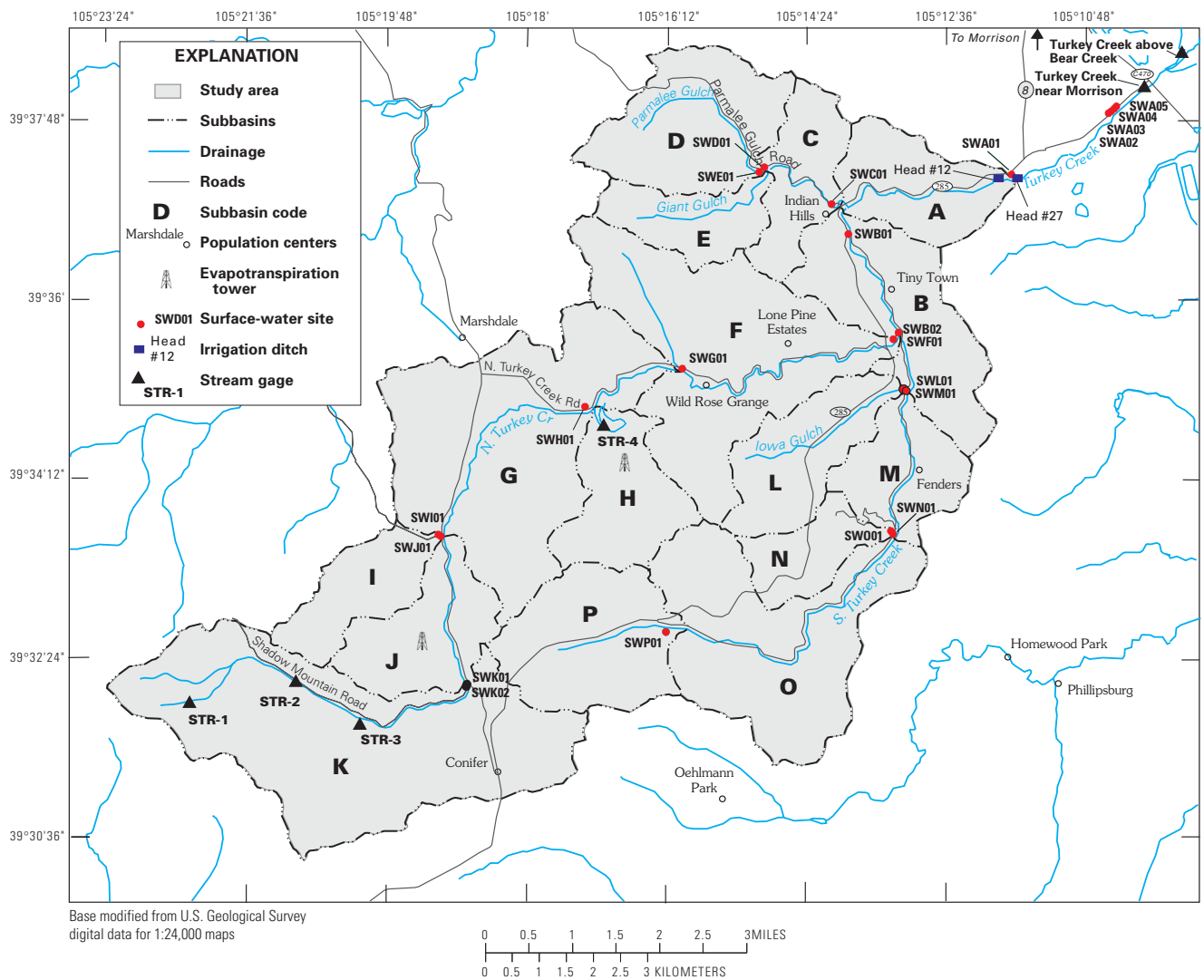


**Figure 4.** Locations of surface-water streamflow measurement and sampling sites, stream gages, and irrigation ditches.

Two stream gages on Turkey Creek were operated by the USGS at various times previous to this study. Station 06711040, Turkey Creek above Bear Creek Lake near Morrison, about 1.5 mi downstream from the present gage (station 06710992) (fig. 4), has data available from April 25, 1986, through September 30, 1989. Station 06711000, Turkey Creek near Morrison, about 1 mi downstream from the present gage, has data available from June 19, 1942, through September 30, 1953. Diversions from Turkey Creek upstream from these stations complicate streamflow records. Although streamflow records at these stations have an acceptable level of accuracy, they are not representative of stream regulation that occurs upstream from the gages. Regulation activity

typically consists of diversions. The water diverted from streams is not measured at the gages; consequently, the gage record is “low biased,” or consistently less than the sum of measured streamflow and the diversion, during times of diversion. Regulation also may include addition of water to streams. Records for diversions from the Independent Highline and Bergen ditches (fig. 4) are available from the SEO; other records from potential additional diversions or additions are not available.

The SEO is responsible for issuing permits for well construction in Colorado. As part of the permitting process, many well-construction details are obtained by the SEO and retained in their files. Many of these data, such as legal description, drillers’ logs,

and well-completion diagrams, are only available in paper format or scanned images of original paper copies. However, some data are available electronically as digital records. The SEO has about 3,300 digital well records with construction details on file for the Turkey Creek watershed. About 1,100 of those wells, referred to in this report as “permitted wells,” have defined locations that are shown in figure 5. The digital data describe reported well yield, total depth, and depth to water.

Water-quality data from previous studies were available for use in this study. Most of these data were collected in the 1970’s as part of the work by Hofstra and Hall (1975a) and Hall and others (1981). Bruce and McMahon (1997) also collected water-quality data

from a number of wells in Front Range settings, a few of which are in the watershed. In addition, Bruce and McMahon (1997) and Stevens and others (1997) collected water-quality data from wells completed in fractured rocks in other Front Range areas that can be compared to data collected during this study. All of these data include analyses for many water-quality properties and constituents addressed by this study as well as other constituents that are useful to this study. The locations for samples collected during previous studies in the Turkey Creek watershed are shown in figure 6. Univariate statistics for water-quality properties and constituents including major ions and some nutrients collected in previous studies are listed in table 3.

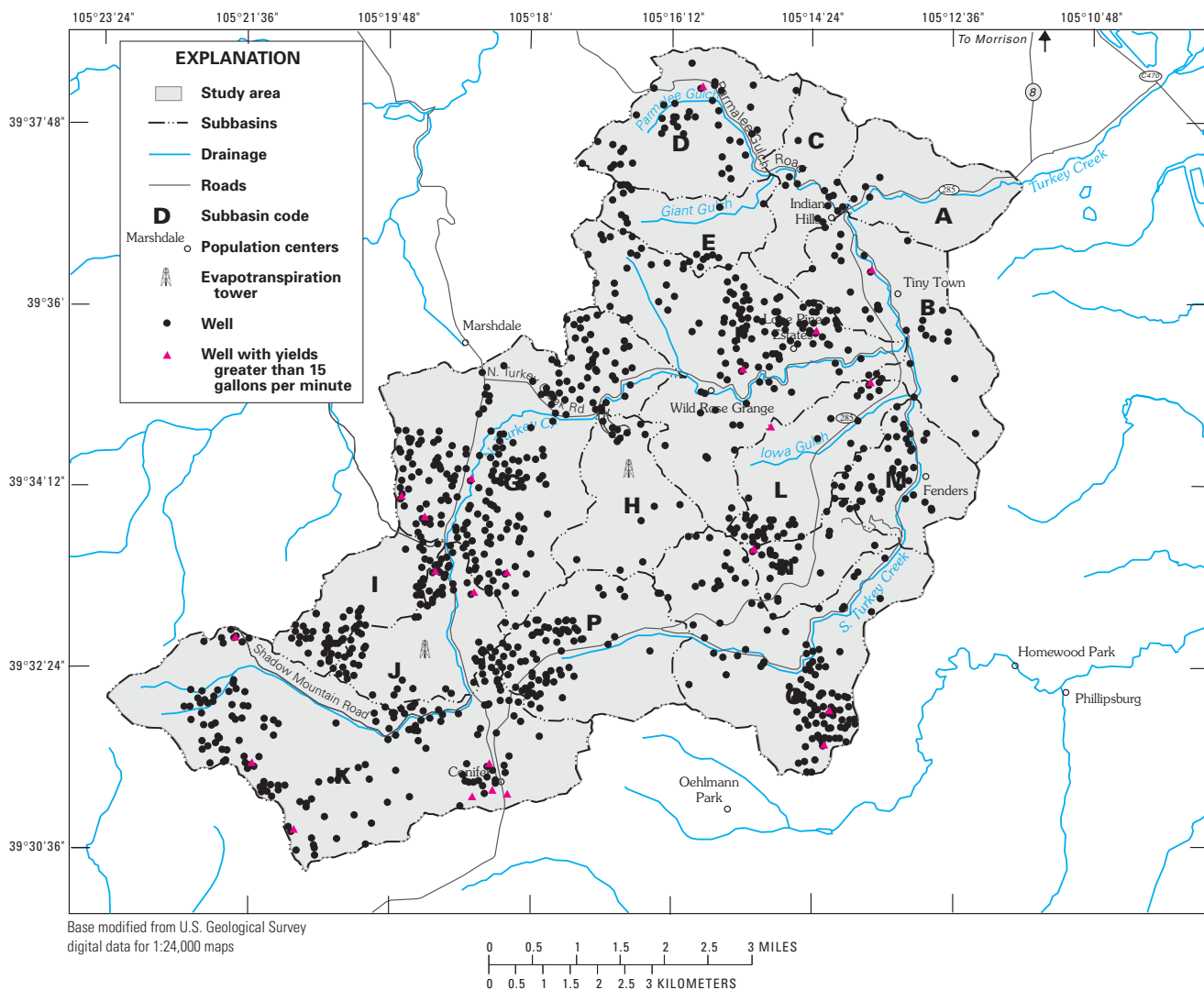


**Figure 5.** Locations of permitted wells from the State Engineers Office.

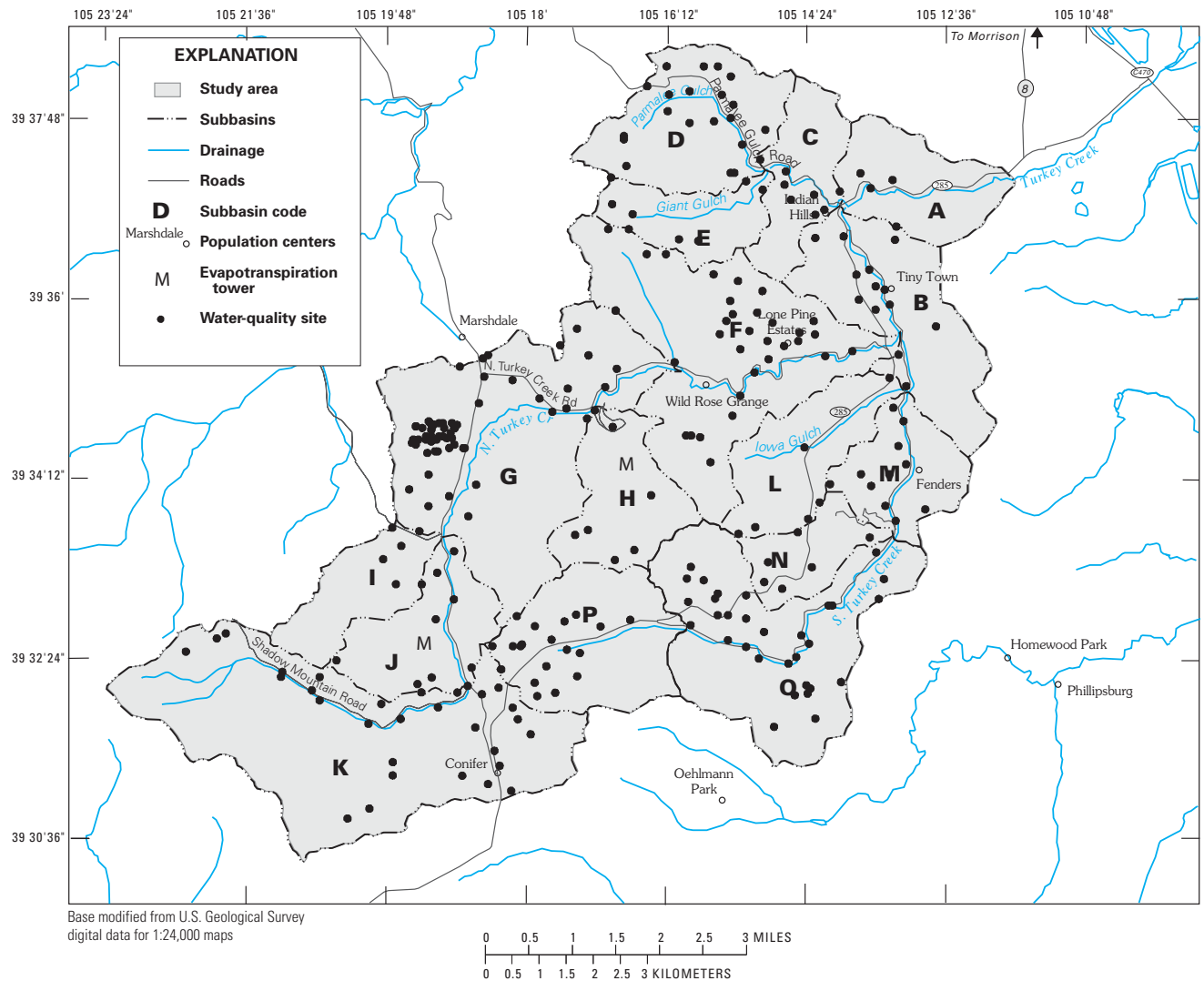


**Figure 6.** Spatial distribution of water-quality samples collected in previous studies in the Turkey Creek watershed.

## Contemporary Data

Many types of data were collected as part of this study, beginning in 1998 and continuing through September 2001, to describe fracture characteristics, climate, evapotranspiration, streamflow, ground-water level, and ground- and surface-water quality in the vicinity of the Turkey Creek watershed. The general nature of these contemporary data is described in this section.

## Fracture Characteristics

One goal of this study is to identify and quantify the major parameters that control the hydraulics of ground-water flow at the watershed scale and thus

better determine how much ground water can be transmitted to and stored within the complex fractured bedrock aquifer system in the Turkey Creek watershed. Some major questions are: (1) how do fracture intensity and orientation control fracture-network porosity (indicator of potential storage), (2) how does fracture porosity vary within individual lithologies, and (3) because distinct fracture networks are associated with distinct geologic structures (for example, faults and folds), how do fracture-network parameters that translate into hydraulic heterogeneity vary among different types of structures and how might they vary between the same type of structure in different lithologies? One way of approaching these questions is to collect and analyze fracture data and construct

**Table 3.** Univariate statistics for water-quality properties and constituents collected in previous studies

[Note: Detection, results greater than method reporting limit (rpl); Censoreds, results less than method reporting limit; Q1, concentration at the 25th percentile; Q3, concentration at the 75th percentile; Min, minimum; Max, maximum; N, number of samples; Percent < rpl, percentage of samples with concentration less than the reporting limit; na, not applicable; mg/L, milligrams per liter;  $\mu$ S, microsiemens per centimeter at 25° Celsius]

Variable	Detections							Censoreds			Percent < rpl
	Mean	Median	Q1	Q3	Min	Max	N	Mean	Median	N	
Specific conductance ( $\mu$ S/cm)	278.32	250.00	185.00	333.75	32.70	950.00	316	na	na	na	na
Hardness, total (mg/L)	109.83	89.00	51.00	160.00	22.00	380.00	65	na	na	na	na
Calcium, total [mg/L]	31.12	25.00	15.00	38.50	6.60	130.00	65	na	na	na	na
Magnesium, total [mg/L]	7.85	6.20	3.55	10.10	1.00	24.00	65	na	na	na	na
Sodium, total [mg/L]	19.50	11.00	6.80	13.50	2.90	120.00	65	na	na	na	na
Potassium, total [mg/L]	2.03	1.50	1.00	2.20	0.20	25.00	284	na	na	na	na
Alkalinity (mg/L)	111.75	89.00	46.94	145.50	13.00	425.00	62	na	na	na	na
Sulfate (mg/L)	13.39	10.00	5.40	14.00	1.20	90.00	65	na	na	na	na
Chloride (mg/L)	9.26	4.40	2.10	13.00	0.40	64.00	313	na	na	na	na
Fluoride (mg/L)	0.66	0.50	0.30	0.70	0.10	2.90	65	na	na	na	na
Nitrate/Nitrite, as N [mg/L]	2.03	0.50	0.11	1.90	0.01	36.00	299	na	na	na	na
Phosphorus, total [mg/L]	0.04	0.03	0.02	0.04	0.01	1.30	209	na	na	na	na

computer models of fracture networks present in natural outcrop exposures. The following section discusses how this was accomplished in the Turkey Creek watershed.

### Outcrop Selection

Color aerial photographs (at a scale of about 1:12,000) were initially used to identify exposures of the dominant rock groups (described in the “Geologic Framework” section). Field inspection narrowed the range of suitable sites. Final outcrop selection also was based on how representative a given outcrop was of its rock group (that is, that the structures and lithologies were similar at the outcrop scale to what was observed for most outcrops in the watershed). Nine outcrop localities were studied in detail (fig. 3), and four others were studied for supplemental data and observation. The amount of data collected at each outcrop varied depending on outcrop size, quality of exposure, and physical accessibility. About 100 or more fractures were measured at each locality, and more than 10,000 fracture attributes were measured in total. Outcrops at least 100 ft long and with at least two near-orthogonal faces were sought. By taking measurements on two near-orthogonal faces, fractures that were sub-parallel to one face were captured on the second face, which helps to minimize orientation bias from random sampling of outcrop faces (see Appendix for details).

### Methods of Fracture Measurement

Fracture data were collected along representative scanlines in each outcrop. A scanline is a graduated tape, or other marker, stretched across an outcrop face: fracture properties are measured along the scanline from beginning to end. The properties measured for each fracture that intersects the scanline include the following: position (from which fracture spacing and intensity are derived, as described in the Appendix), orientation (the strike and dip), trace length (typically not the actual diameter of the fracture but only the portion of it that intersects the outcrop face), termination (how the fracture tips end), an estimate of aperture size, degree and type of mineralization, shape, and roughness; also any indicators of timing relationships (for example, crosscutting and offset of other fracture sets) were recorded (Caine, 2001).

### Climatologic Data

Seven tipping-bucket rain gages were operated by the USGS throughout the watershed beginning in the fall of 1998 (RG1–RG7; fig. 7 and table 2), and four weighing-bucket rain gages also were operated (RG8–RG11; fig. 7 and table 2). In addition, RG16 and RG17 were established at sites of evapotranspiration measurements; records from RG16 are actually a composite of results from both a tipping- and a weighing-bucket rain gage, and records from RG17 are from a tipping bucket. The tipping- and

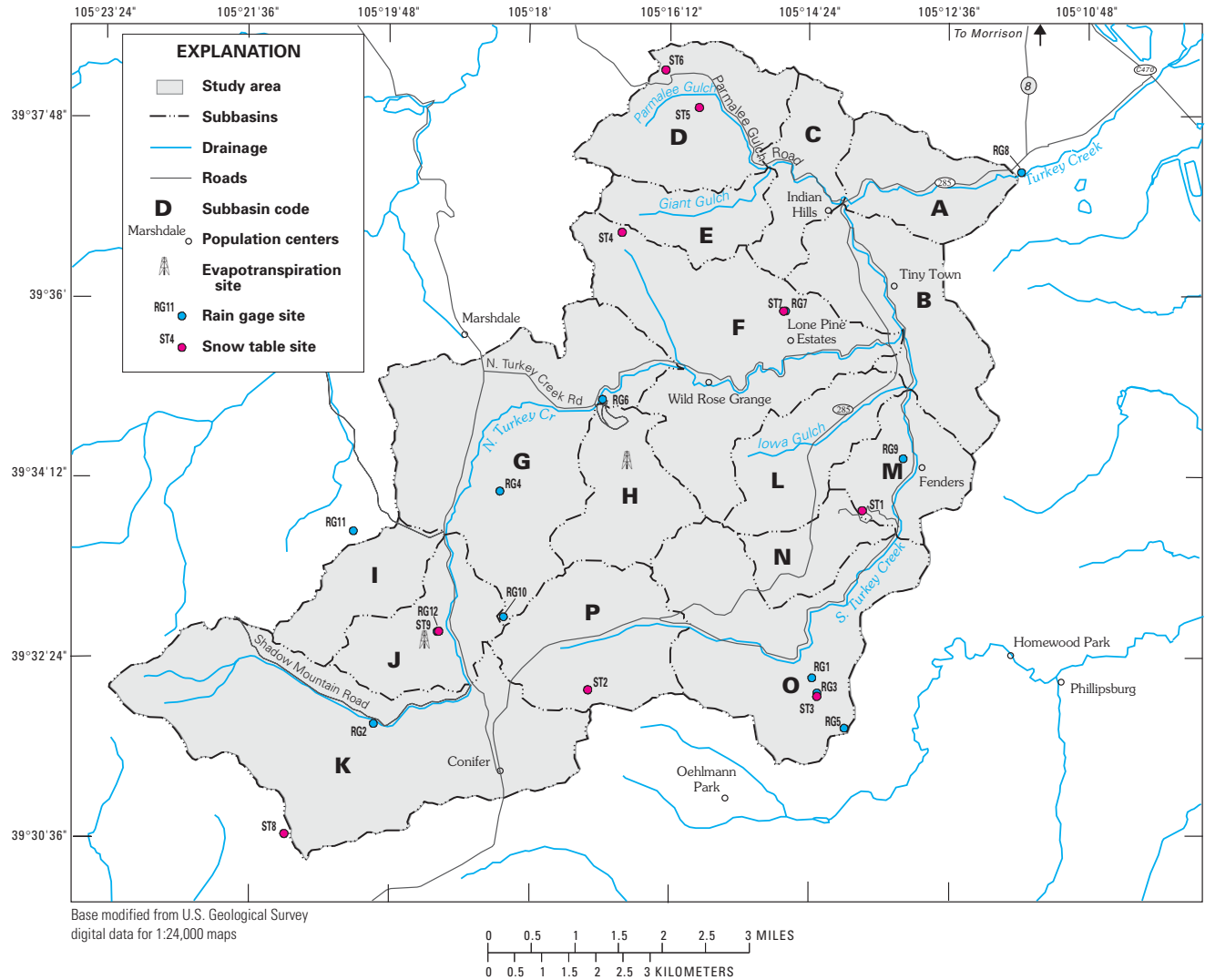


**Figure 7.** Location of climatologic monitoring sites.

weighing-bucket gages were used to develop daily records of precipitation in the watershed. In addition to these daily records, intermittent records of snowfall and corresponding water equivalency were maintained at snow table sites by several homeowners (fig. 7). Additional climatic data were collected at evapotranspiration sites. Also, in the spring of 2001, four air-temperature sites were established in the watershed (AT1–4; table 2, one of the air temperature sites is collocated with RG8).

Evapotranspiration (*ET*) is the transport of water from the surface of the Earth to the atmosphere, and involves a change in phase, from liquid to gas. *ET* is the sum of evaporation from wet surfaces (leaves, wet

soils and rock, and surface-water bodies, for example), sublimation from snow or ice, and transpiration, which is water evaporated from plant stomates. Stomates are microscopic holes connecting the surface of a leaf or needle to its interior cells. The primary purpose of stomates is to allow carbon dioxide ( $\text{CO}_2$ ) from the atmosphere to diffuse into the plant, where it is used for growth. Transpiration is fundamentally the same physical process as evaporation. Plants do not pump water out through stomates, they simply make liquid water available to the sub-stomatal cavities, where it is lost through the stomates in the process of obtaining  $\text{CO}_2$ . Mean *ET* over land is about 62 percent of precipitation worldwide (Brutsaert, 1982). The ratio

of  $ET$  to precipitation tends to be greater in arid climates and smaller in humid climates. The ratio of transpiration to evaporation (plus sublimation) generally increases as the amount of vegetation increases. In most regions, transpiration is much greater than evaporation on an annual basis.

The latent heat of vaporization of water ( $L$ ) is the amount of energy needed to evaporate a unit amount of water. Because  $L$  is relatively large ( $2,450 \text{ joules g}^{-1}$  at  $70^\circ\text{F}$ ),  $ET$  is an important link between the water balance and the energy balance of a surface. In most climatic settings, a fairly large portion of the net energy received by the land surface as sunlight is transferred to the atmosphere through the evaporation of water. The energy balance of a vegetated surface, in terms of watts per square meter, can be written as:

$$R_n - G - \Delta S = H + LE \quad (1)$$

where

- $R_n$  is net radiation,
- $G$  is soil heat flux,
- $\Delta S$  is the time rate of change in heat stored in the vegetation canopy,
- $H$  is sensible heat flux, and
- $LE$  is latent heat flux.

The left-hand side of this equation is the available energy, and the right-hand side is the turbulent flux. These fluxes are shown schematically with their typical positive daytime directions in figure 8. Net radiation,  $R_n$ , is equal to incoming short-wave and long-wave radiation minus outgoing short-wave and long-wave radiation. The effect of net radiation is to heat the surface warmer than both the overlying air and the subsurface soils. Soil heat flux,  $G$ , is the heat energy that moves from the surface into the subsurface soil by conduction. Sensible heat flux,  $H$ , is the heat energy that moves from the surface into the overlying air due to the temperature difference between them. Latent heat flux,  $LE$ , is the latent energy that moves from the surface into the overlying air as evaporation. Here,  $L$  is the latent heat of vaporization, defined above, and  $E$  is the mass flux of water vapor in grams per square meter per second, so that the product of  $L$  and  $E$  ( $LE$ ) is an energy flux in watts per square meter (a watt is one joule per second). Because  $L$  is roughly a constant (it varies only slightly with temperature), it is the constant of proportionality between the mass and energy fluxes associated with the evaporation of water. (The symbols  $ET$  and  $E$  are conceptually identical, referring to the mass flux of evaporating water. In this report,  $E$  is used for 30-min fluxes, in grams per square meter per second, and  $ET$  is used for longer intervals, converted into inches per day or year,

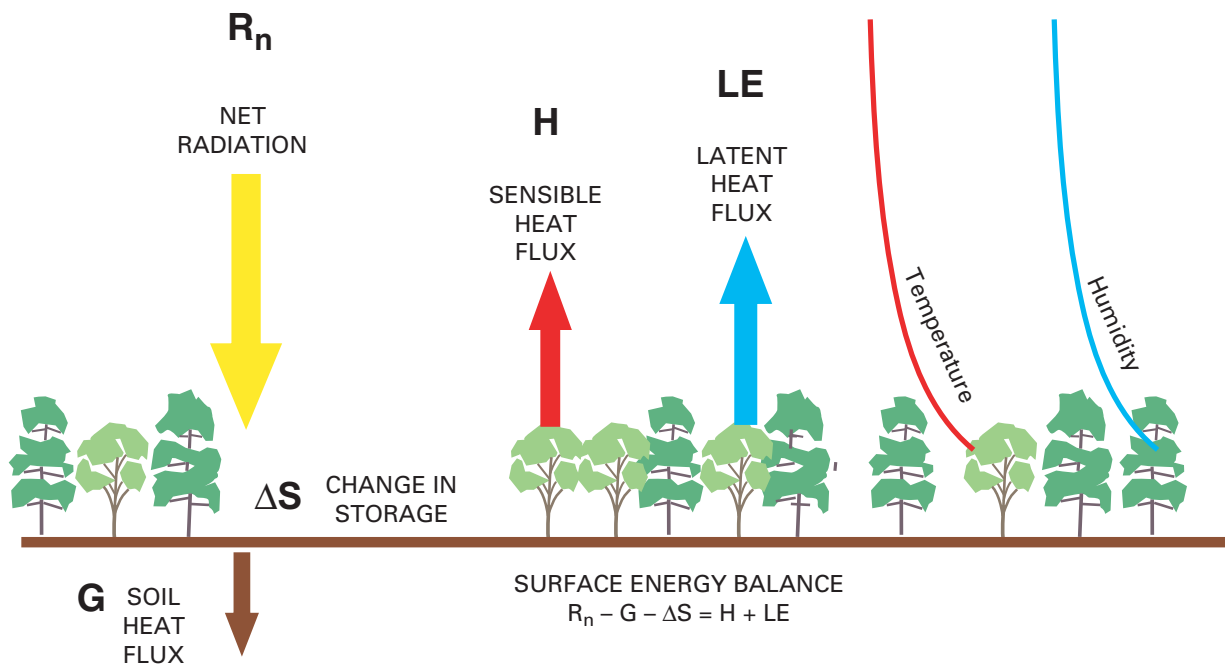


Figure 8. Schematic of the energy balance of a vegetated surface.



over the study surface). Both  $H$  and  $LE$  occur through turbulent eddy transport, a combination of convectively and mechanically generated turbulence. As water availability of a vegetated surface decreases, less of the turbulent flux occurs as  $LE$  and more occurs as  $H$ . The storage term,  $\Delta S$ , is the change in heat energy stored in the plant canopy during the measurement period due to a change in its temperature. It is usually much smaller than the other terms in equation 1. During typical daytime conditions, the major terms all have positive values and move in the directions shown in figure 8. At night, typically  $R_n$ ,  $G$ , and  $H$  reverse direction (and have negative values), and  $LE$  is approximately zero.

Detailed  $ET$  data were collected at two sites within the watershed: a lodgepole forest site and a grassland meadow site. Two different micrometeorological methods were used at the two sites, primarily because of equipment availability. The eddy-correlation (EC) method (Swinbank, 1951) was used at the forest site, and the Bowen-ratio (BR) method (Bowen, 1926) was used at the meadow site.

Extrapolation of  $ET$  measurements to other parts of the basin was attempted using the sap-flow method (Granier, 1985), a less expensive and more portable method than either EC or BR. Sap-flow sensors were installed at the forest site during March 2000 to measure the rate of water flow in the tree trunks. The intent was to then install additional sap-flow sensors at other sites in the watershed to develop a relation between  $ET$  at the forest site and  $ET$  at other sites. The sap-flow sensors did not work properly, and they produced anomalous data. Consequently, only limited quantitative sap-flow data were recovered, but the sensors did provide fairly reliable estimates of the onset and cessation of transpiration by the lodgepole pine trees at the forest site.

The forest site is collocated with RG16 (fig. 7, table 2) in a lodgepole forest at an elevation of 8,180 ft. Sensors used to collect data were located on and around a 60-ft-tall, triangular steel lattice-work tower (Rohn 45G) of the type used to support antennae. Observations at the site indicate that the mean height of the forest is 39 ft, and the forest canopy cover was estimated to be 60–70 percent. The forest extends for at least 0.25 mi in all directions except to the southwest. The forest is typical of lodgepole stands in the watershed. Slope and aspect of the land surface at the site are  $3.75^\circ$  and N14°E, respectively. Soil at the site is a fine to medium sand, about 9 inches deep,

underlain by decomposed granite. Tree roots extend into the granite to a depth of about 2 ft, although fine roots may extend deeper.

Data were measured at the forest site by using electronic sensors, and data summaries (means, covariances, standard deviations, vector sums) were stored digitally at 30-minute intervals using four automatic data loggers. The loggers are designated “eddy-correlation (EC),” “meteorological (MT),” “energy-balance (EB),” and “sap flow (SF)” (table 4). Eddy-correlation sensors were sampled every 0.125 second; all other sensors were sampled every 10 seconds. Data summaries were transferred to a storage module, a floppy disc, and a computer at monthly intervals. Eddy-correlation data collection began on day of year (DOY) 34 (February 3), 1999 at 4 p.m.  $ET$  values for DOY’s 1 through 34, 1999, were estimated to be 0.01 inch per day, which is roughly equal to the mean  $ET$  during the same DOY’s in 2000 and 2001. This estimate was made to facilitate computation of a 1999 yearly total  $ET$  value. Collection of meteorological and energy-balance data began on DOY 140 (May 20), 1999, at 7:30 p.m., but the initial data stored on the MT data logger were accidentally overwritten, so those data began on DOY 149 (May 29), 1999, at 7:00 a.m. Soil moisture values prior to DOY 149 were estimated to facilitate subsequent water-balance computations. Sap-flow data began on DOY 88 (March 28), 2000. Results are reported on data collected at this site from the above times through DOY 365 (December 31), 2001, at 12:00 p.m. Sensor types and heights, measured variables, and data-logger assignments are listed in table 4. A photograph of the eddy-correlation evapotranspiration tower installation is shown in figure 9.

The meadow site is collocated with rain gage RG17 (fig. 7, table 2) in a native grass meadow at an elevation of 7,770 ft. This site is about 3.25 mi northeast of the forest site. Sensors used to collect data were located on or around a 6-ft tripod. Average height of grass in the meadow was about 6 inches. The tripod was located near the middle of the meadow, which is about 1.2 mi long by 0.2 mi wide, with the long dimension trending north-northwest to south-southeast. Most of the grass in the meadow is typical of that found elsewhere in the watershed; the grass is not exceptionally well watered and vigorous such as low-lying meadow grasses along flood plains of the major creeks; nor is it overly dry, such as the grass in the high meadows in the watershed. A small,

**Table 4.** Sensor type, data loggers, sensor heights, and measured variables at forest site

[EC, eddy correlation; MT, meteorological; EB, energy balance; SF, sap flow; TDR, time-domain reflectometry; negative heights are depths below land surface; parenthetical numbers refer to number of sensors; ft, feet)]

Sensor type (number of sensors)	Data logger	Sensor height (ft)	Measured variables
Sonic anemometer	EC	57.1	Orthogonal windspeed components, air temperature
Krypton hygrometer	EC	57.1	Vapor density fluctuations
Thermistor	EC	4.92	Data logger temperature
Temperature-humidity probe	MT	51.8	Air temperature, relative humidity
Infrared thermometer	MT	50.5	Leaf (needle) surface temperature
Cup anemometer	MT	56.1	Windspeed
Wind vane	MT	56.1	Wind direction
Tipping-bucket rain gage	MT	33.1	Rainfall
Leaf wetness sensor	MT	13.3	Presence of water on leaves (needles)
Thermistor	MT	-0.49	Soil temperature
Thermistor	MT	-1.15	Soil temperature
TDR Probe	MT	-0.16	Soil moisture
TDR Probe	MT	-0.75	Soil moisture
Net radiometer	EB	53.5	Net radiation
Pyranometer	EB	54.1	Solar radiation
Thermocouples (4)	EB	12.8 to 18.0	Bole temperature
Soil heat flux plates (3)	EB	-0.26	Soil heat flux at 3.15 inches depth
Thermocouples (12)	EB	0 to -0.26	Soil temperature in top 3.15 inches of soil
Sap flow sensors (8)	SF	4.59	Sap velocity

intermittent creek runs south to north near the east edge of the meadow, about 400 ft east of the tripod. The grass within about 30 ft of the creek (the riparian zone) was much more lush and green than the rest of the meadow during much of the growing season. Slope and aspect of the land surface at the site are about 7° and N50°E, respectively. Soil at the site is a silty loam at least 2 ft deep, underlain by decomposed granite. Grass roots probably extend about 10 inches below land surface.

Data measurement, storage, and transport at the meadow site were similar to those operations at the forest site. Sensors were sampled every 10 seconds, and data summaries were stored digitally at either 15- or 30-minute intervals, all on one data logger. Collection of Bowen-ratio and associated data began on DOY 154 (June 2), 2000, at 6:30 p.m. Results are reported on data collected from this time through DOY 365 (December 31), 2001, at 12:00 p.m. Sensor types and heights and measured variables are listed in table 5. A photograph of the Bowen-ratio evapotranspiration tripod installation is shown in figure 10.

Precipitation was measured at both *ET* sites using tipping-bucket rain gages (RG16 at the forest site, RG17 at the meadow site, table 2); however, these gages provide less than ideal measurements of snowfall for two reasons. First, the snowfall usually is not measured when it falls but rather when it melts. Second, snowfall accumulations greater than about 3 inches in depth probably overtop the gage and are undermeasured. Therefore, snowfall at both sites was estimated using two weighing-bucket precipitation gages. The first weighing-bucket gage (RG11, table 2, fig. 7) was located about 1.4 mi northwest of the forest site. Data collection at this gage began on November 25, 1998, well before data collection began at the forest site. Snowfall amounts from RG11 were multiplied by an adjustment factor to account for differences in measured precipitation between the RG11 site and the forest site. The factor was determined by comparing rainfall data from both sites collected between DOY 134 (May 14), 2001, and DOY 327 (November 23), 2001. During this calibration period, both gages were functioning reliably and no overtopping occurred. Running totals of the two gages during this period were highly correlated

( $r^2 = 0.9978$ , standard error = 0.151 inch). An adjustment factor of 1.03 was computed as the ratio of the RG16 total to the RG11 total during the calibration period. This relation was used to estimate snowfall at the forest site during 1999 and 2000. On December 6, 2000, the second rain gage, a weighing-bucket gage, (RG18, table 2) was collocated with RG16 at the forest site to measure snowfall at that site directly. A comparison between RG18 and RG16 during the 2001 calibration period indicated an adjustment factor for RG18 of 1.15 ( $r^2 = 0.9991$ , standard error = 0.101 inch). This factor was unexpectedly larger than 1.00, considering

that RG16 and RG18 were separated by only about 200 ft and both gages were calibrated prior to installation. Inspection of the data revealed that RG18, a previously used weighing-bucket gage, chronically undermeasured small rainfalls (less than about 0.25 inch) but accurately measured larger rainfalls (greater than about 0.40 inch). Slightly excessive friction in the linkage mechanism could account for this bias. Because the standard error between RG18 and RG16 (0.101 inch) was significantly smaller than between RG11 and RG16 (0.151 inch), data from RG18 were used to estimate snowfall at the forest site during



**Figure 9.** Eddy-correlation evapotranspiration tower at forest site.

2001 by using the adjustment factor of 1.15. Comparisons also were made between the meadow site tipping-bucket gage (RG17) and the two weighing-bucket gages (RG11 and RG18). RG17 was more highly correlated with RG11 ( $r^2 = 0.9972$ , standard error = 0.172 inch) than with RG18 ( $r^2 = 0.9965$ , standard error = 0.189 inch), so RG11 data were used to estimate snowfall at the meadow site during 2000 and 2001 by using an adjustment factor of 1.003.

**Table 5.** Sensor type, heights, and measured variables at meadow site

[Negative heights are depths below land surface; parenthetical numbers refer to number of sensors; ft, feet)

Sensor type (number of sensors)	Sensor height (ft)	Measured variables
Net radiometer #1	4.66	Net radiation (level)
Net radiometer #2	4.79	Net radiation (normal to land surface)
Pyranometer	5.25	Solar radiation
Cup anemometer	5.74	Windspeed
Wind vane	5.74	Wind direction
Leaf wetness sensor	4.17	Presence of water on leaves
Temperature-humidity probe	6.52	Air temperature, relative humidity, upper
Temperature-humidity probe	3.48	Air temperature, relative humidity, lower
Tipping-bucket rain gage	1.41	Rainfall
Soil heat flux plates (3)	-0.16	Soil heat flux at 1.97 inches depth
Thermocouples (12)	0 to -0.16	Soil temperature in top 1.97 inches of soil
Thermistor	0.98	Data logger temperature

### Surface-Water Data

Contemporary records of streamflow associated with this study include data from stream gages on Turkey Creek in the vicinity of the present gage, short-term records from stream gages on tributaries to Turkey Creek, miscellaneous measurements of streamflow associated with water-quality sampling, and synoptic measurements of streamflow. All these data are available in the NWIS database.

Two stream gages on Turkey Creek were operated during this study (fig. 4). The present stream gage, station 06710992, Turkey Creek near Indian Hills, has data available beginning April 13, 2001. The present gage replaces station 06710995 (shown

as SWA01 in fig. 4), Turkey Creek at mouth of canyon near Morrison, Colorado (operated from April 1, 1998, through April 13, 2001), which was discontinued due to complications related to streamflow diversions and local anomalous conditions at the gage described in the “Surface-Water Conditions” section. Records for station 06710995 are affected by diversions from the Independent Highline ditch; in addition, records from 06710995 are estimated for April 15, 2000, to June 1, 2000. Additional short-term records of streamflow in the Turkey Creek watershed from four tributaries for the spring of 2001 are discussed in the “Surface-Water Conditions” section.

In addition to records of streamflow from the stream gages described above, miscellaneous measurements of streamflow were made when surface-water samples were collected in water year 1999; locations and identifiers for these miscellaneous measurements are in figure 4 and table 6. Additional synoptic measurements of streamflow were made periodically during the summer of 2001 at as many as 29 sites. This includes sites only used for synoptic measurements (SN sites in table 6) and some additional sites that, along with results of synoptic measurements, are discussed in the “Surface-Water Conditions” and “Runoff Modeling” sections.

### Ground-Water Data

Ground-water data were collected as part of this study in addition to historical water-level data collected in the 1970’s and well-construction data available from the SEO. These additional data include time-series water-level data and a fall 2001 synoptic measurement of water levels in a network of wells.

Water levels were measured monthly, by volunteers, at 15 monitoring wells distributed in and near the watershed beginning about 1999 (locations, fig. 11). These wells are no longer used by homeowners for various reasons and were volunteered to the study as reliable indicators of static water levels in parts of the watershed. Of these wells, five are USGS monitoring wells constructed in the 1970’s (local identifiers MH1, MH5, MH8, MH9, and MH10) completed in bedrock and previously sampled for selected water-quality parameters and water levels (Hofstra and Hall, 1975a; 1975b). All of these water-level data are available from the USGS NWIS database. Three of the non-USGS wells are pre-1950, shallow, hand-dug wells (local identifiers MH2, MH12, and MH13). The remaining wells are



**Figure 10.** Bowen-ratio evapotranspiration tripod at meadow site.

completed at various depths. Table 7 lists well-construction information available for these monthly water-level monitoring wells. Beginning May 2001 and through September 2001, time-series water-level data, at a time step of 60 minutes, were collected at a subset of 3 of the 15 monthly water-level monitoring wells (local identifiers MH1, MH5, and MH8).

Contemporary water levels were measured at 131 wells during September 24–October 4, 2001. Most of these measurements were made in domestic wells currently in use. The measuring devices were disinfected and rinsed between measurements. Information about domestic water usage on the day of

measurement was recorded if available. Locations of these wells are shown in figure 11, and the results of the measurements are listed in the Appendix (table A4).

### **Water-Quality Data**

Water-quality data describing water-quality properties and concentrations of constituents in surface water and ground water were collected at about quarterly intervals for 1 year (water year 1999), beginning in fall 1998, at 22 surface-water sites and at 110 wells and springs and in the watershed. USGS

**Table 6.** Site identifiers and selected characteristics for sites of surface-water-quality samples, short-term streamflow records, and synoptic streamflow measurements in the Turkey Creek watershed, Jefferson County, Colorado, 1998–2001

[Note: Local identifier (Surface-water sampling sites), SWlnn where l = character designating subbasin (fig. 4) and n is a sequential number for surface-water sites in the designated subbasin; Local identifier (synoptic measurement sites), SNGGnn where GG indicates geology and nn is a sequential number for synoptic measurement sites in the given geology; USGS identifier (synoptic measurement sites) indicate latitude and longitude of synoptic measurement site; Contributing drainage area, area in square miles; --, no data]

Local identifier	USGS identifier	Contributing drainage area	Site name
SURFACE-WATER SAMPLING AND MISCELLANEOUS STREAMFLOW MEASUREMENT SITES			
SWA01	06710995	47.42	Turkey Creek at mouth of canyon, near Morrison
SWA02	393753105102701	--	Turkey Creek above pipe above Hwy C-470 near Morrison
SWA03	393753105102700	--	Inflow pipe to Turkey Creek above C-470 near Morrison
SWA04	393755105102500	--	Turkey Creek below pipe, above C-470, near Morrison
SWA05	393756105102300	50.09	Turkey Creek above Hwy C-470, near Morrison
SWB01	393639105135000	39.63	Turkey Creek above Parmalee Gulch at Indian Hills
SWB02	393540105131100	13.32	South Turkey Creek at mouth near Indian Hills
SWC01	393657105140300	5.66	Parmalee Gulch above mouth at Indian Hills
SWD01	393719105145500	2.84	Parmalee Gulch above Giant Drive at Indian Hills
SWE01	393714105151000	1.33	Giant Gulch at mouth at Indian Hills
SWF01	393536105131500	24.56	North Turkey Creek at mouth near Indian Hills
SWG01	393518105155700	20.57	North Turkey Creek near Wild Rose Grange near Indian Hills
SHW01	393455105171200	1.92	North Turkey Creek tributary near Danks Dr near Indian Hills
SWI01	393338105190600	1.47	North Turkey Creek tributary at Blue Creek Rd near Aspen Park
SWJ01	393337105190400	9.48	North Turkey Creek above Blue Creek Rd trb near Aspen Park
SWK01	393207105184400	4.32	North Turkey Creek above Shadow Mountain Dr above Aspen Park
SWK02	393206105184100	3.18	North Turkey Creek tributary at Shadow Mountain Drive above Aspen Park
SWL01	393506105130700	2.00	Iowa Gulch at mouth near Indian Hills
SWM01	393505105130500	10.21	South Turkey Creek above Iowa Gulch near Indian Hills
SWN01	393339105131500	1.10	South Turkey Creek tributary above Flint Lane near Indian Hills
SWO01	393339105131400	7.47	South Turkey Creek above Flint Ln near Indian Hills
SWP01	393246105155200	2.68	South Turkey Creek above Meyer Rnch Pk near Aspen Park
SHORT-TERM STREAMFLOW RECORD SITES			
STR-1	393203105221600	0.27	North Turkey Creek upper tributary near Aspen Park (Pikes Peak Granite)
STR-2	393210105205500	2.23	North Turkey Creek tributary above Warhawk Road near Aspen Park (fault-zone rocks)
STR-3	393141105200500	0.96	North Turkey Creek tributary near Aspen Park (intrusive rocks)
STR-4	393443105165800	1.10	North Turkey Creek tributary near Gartner Drive near Aspen Park (intrusive rocks)
SYNOPTIC STREAMFLOW MEASUREMENT SITES			
SNDIV	393714 1051155	--	Diversion from Turkey Creek near Willow Cr subdivision
SNCG1	393202 1052218	0.27	Upper tributary to North Turkey Creek above Aspen Park
SNCG2	393213 1052209	0.27	North tributary to North Turkey Creek above Aspen Park
SNFZ1	393210 1051658	2.33	North Turkey Creek above Warhawk Rd near Aspen Park
SNFZ2	393114 1051835	1.72	Tributary to North Turkey Creek tributary at Conifer High School
SNGN6	393529 1051305	0.69	Tributary to South Turkey Creek at West Ranch near Tiny Town
SNGN9	393242 1051553	2.90	Tributary to South Turkey Creek below Meyer Ranch near Aspen Park
SNGN10	393658 1051413	0.41	South Tributary to Parmalee Gulch near US 285
SNSP1	393151 1051815	0.70	Tributary to North Turkey Creek at Light Lane near Aspen Park
SNSP2	393141 1052005	0.96	Tributary to North Turkey Creek above Aspen Park
SNSP4	393443 1051658	1.00	Tributary to North Turkey Creek near Gartner Dr n Aspen Park
SNQA2	393453 1051737	0.65	Tributary to North Turkey Creek near Danks Drive
SNQS1	393417 1051838	0.46	Tributary to North Turkey Creek on Grizzly Drive
SNQS2	393435 1051845	0.37	Tributary to North Turkey Creek near Red Fox
SNSG3	393815 1051426	0.41	Tributary to North Turkey Creek near Lone Pine Estates
SNSG4	393716 1051454	1.34	Giant Gulch at mouth

station numbers, local site identifiers, and selected characteristics for surface-water and ground-water sites that were sampled are listed in table 6 and table 8, respectively. These data reside in the USGS Water-Quality System of NWIS (Garcia and others, 1997). The locations of sampling sites are shown in figure 4

for surface water and figure 12 for ground water. In most cases, USGS station numbers consist of latitude (6 digits), longitude (7 digits), and a 2-digit sequential identifier appended into a unique 15-digit number for each site. Other USGS station numbers are 8-digit downstream-order numbers that indicate the major

river basin (Turkey Creek is part of the Missouri River Basin, which is drainage basin number 06) and a number indicating that site's downstream order in relation to other sites in the drainage (6 digits). Local site identification numbers were typically assigned on the basis of 16 subwatersheds identified by topographic boundaries, in alphabetical sequence (A–P), starting at the mouth of the watershed. Surface-water sites are prefixed SW and ground-water sites are prefixed GW. The samples were collected according to applicable protocols described in the National Field Manual for the Collection of Water-Quality Data (U.S. Geological Survey, 1997–present). Hundreds of quality-control samples were collected as part of these sampling activities; the results of the quality-control samples are

described in the Appendix and listed in tables A1–A3. Table 9 lists water-quality properties and constituents included in the analyses.

A limited number of additional miscellaneous samples were collected in water years 2000 and 2001 following the initial study sampling period in water year 1999. Included in the miscellaneous sampling are samples collected for tritium analysis in November 2000, samples collected for a suite of organic compounds associated with wastewater compound in April and September 2001, and samples collected concurrently with the wastewater-compound samples for analysis of major ions and nutrients. Results for selected major ions (fluoride, bromide) and nitrate plus nitrite are reported for samples

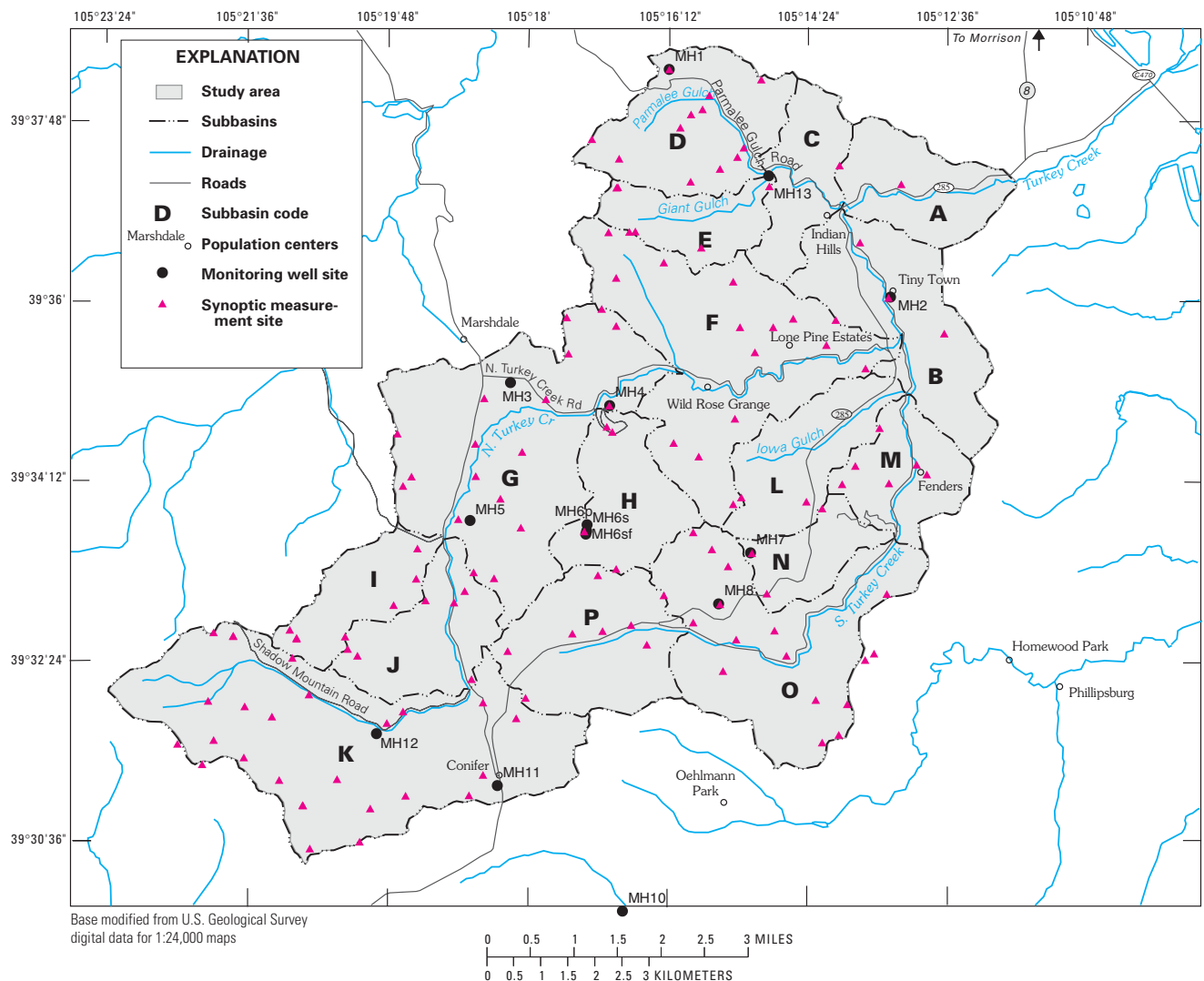


Figure 11. Locations of water-level monitoring wells.

**Table 7. Well-construction details and miscellaneous data for ground-water level monitoring wells in the Turkey Creek watershed, Jefferson County, Colorado, 1998–2001**

[ID, identifier; OB, overburden thickness; TPerf, top depth of perforation below land surface; Bperf, bottom depth of perforation below land surface; TD, total depth of well; gpm, gallons per minute; SWL, static water level; MP, measuring point for water levels in feet above land surface; Meta, metamorphic; SC, specific conductance; Temp, water temperature; Ave. WL Feb, average water level for month of February; nd, not determined;  $\mu\text{S}/\text{cm}$ , microsiemens per centimeter at 25° Celsius; NGVD29, National Geodetic Vertical Datum 1929]

Local ID	Permit number or USGS NWIS ID	Permit date	Latitude	Longitude	OB (inches)	Well diameter (inches)	Casing type	TPerf (feet)	BPerf (feet)	TD (feet)	Reported yield (gpm)
MH1	SC00507006CDD	6/21/73	393820	1051612	10	6	steel	nd	22	180	0.2
MH2	No permit-Hand dug	nd	393604	1051320	0	36	rock	nd	nd	nd	nd
MH3	59454	4/16/74	393513	1051813	nd	nd	nd	nd	nd	150	11
MH4	31708	5/25/76	393459	1051657	0	nd	nd	80	200	200	2
MH5	SC00607102BBD	6/21/73	393350	1051844	5	6	steel	nd	23	140	0.352
MH6.1	67101BAC	nd	393348	1051714	1	nd	nd	nd	nd	nd	nd
MH6.2	14341	1/26/63	393344	1051714	1	nd	nd	nd	nd	82	1
MH6.3	73389	6/01/25	393342	1051715	0	nd	nd	nd	nd	100	15
MH7	184948	12/19/94	393332	1051508	5	6	steel/pvc	225	505	505	50
MH8	SC00607007AAA	7/31/73	393301	1051532	5	6	steel	nd	23	70	6.8
MH9	SC00607013CCC	8/02/73	393120	1051106	10	6	steel	nd	18	160	0.443
MH10	SC00607125DAA	6/22/73	392958	1051646	40	6	steel	nd	43	220	0.091
MH11	3672	5/24/64	393112	1051821	nd	nd	nd	74	209	227	5
MH12	No permit-Hand dug	nd	393143	1051954	nd	36	rock	nd	nd	nd	nd
MH13	No permit-Hand dug	nd	393717	1051453	nd	36	rock	nd	nd	nd	nd

Local ID	SWL (feet)	Water level Date	MP (feet)	Elevation (ft NGVD29)	subbasin	Rock type	SC ( $\mu\text{S}/\text{cm}$ )	Temp (deg F)	Date	Ave. WL Feb (feet) 1999 and 2000	1973 - 1983
MH1	18.24	12/11/73	1.2	7,310	D	Meta	390	9.5	12/11/73	18.2	18.3
MH2	nd	nd	1.0	6,900	B	Meta	nd	nd	nd	13.9	nd
MH3	40	4/16/74	0.5	7,751	G	Meta	nd	nd	nd	9.30	nd
MH4	25	nd	0.0	7,672	G	Meta	nd	nd	nd	95.9	nd
MH5	28.14	12/11/73	2.0	7,900	G	Meta	170	7.0	12/11/73	30.8	31.4
MH6.1	nd	nd	0.5	8,375	H	Igneous	nd	nd	nd	8.40	nd
MH6.2	10	1/26/63	0.0	8,352	H	Igneous	nd	nd	nd	8.51	nd
MH6.3	nd	6/1/25	0.2	8,340	H	Igneous	nd	nd	nd	23.8	nd
MH7	25	1/13/97	1.17	8,337	N	Meta	nd	nd	nd	61.2	nd
MH8	12.45	12/12/73	1.3	8,050	O	Meta	160	8.5	11/6/73	15.1	11.7
MH9	15.97	12/10/73	1.33	6,720	O	Meta	305	8.0	11/6/73	17.4	15.6
MH10	22.14	12/12/73	1.5	7,950	K	Igneous	355	5.5	12/12/73	21.8	21.8
MH11	30	5/24/64	1.5	8,477	K	Meta	nd	nd	nd	19.3	nd
MH12	nd	nd	2.5	8,187	K	Igneous	nd	nd	nd	7.65	nd
MH13	nd	nd	2.5	7,279	E	Igneous	nd	nd	nd	9.40	nd

collected concurrently with the April 2001 wastewater-compound samples. The major ion sampling was a part of a larger quarterly sampling effort conducted by Jefferson County Health Department personnel at selected wells, in cooperation with Colorado Department of Public Health and Environment. Local identifiers for sites sampled and analyses completed at each site are listed in table 10.

Tritium concentrations in the watershed were evaluated on the basis of 24 ground-water environmental samples, and 5 duplicate samples were collected in 1-L glass bottles for tritium analysis during November 2000. Zero head-space in sample bottles was maintained and no additional filtration or preservation was done in the field. Ground-water samples for tritium analysis were collected by Jefferson County Health Department personnel from

outside spigots supplied by domestic wells. Bottles were sent by Jefferson County Health Department personnel to the Environmental Isotope Laboratory, University of Waterloo, in Ontario, Canada, for analysis of tritium content (Roy Laws, Jefferson County Health Department, oral commun., October 2001).

The occurrence of compounds indicative of human wastewater in the watershed was evaluated on the basis of wastewater-compound samples collected in April 2001 (eight ground water, four surface water, and two field blanks) and September 2001 (three surface water and one field blank). Quality-assurance samples associated with the wastewater-compound analyses included three field blanks, three laboratory blanks, and three laboratory spikes. Ground-water samples for wastewater-compound analysis were collected from outside spigots supplied from domestic



**Table 8. Site identifiers and selected characteristics for ground-water-quality sampling sites in the Turkey Creek watershed, Jefferson County, Colorado, 1998–2000**

[Note: SEO, State Engineers Office; Yield, well yield in gallons per minute as reported to State Engineers Office; Date of measurement, in month/day/year, refers to depth to water measurement; all depths reported in feet below land surface; --, not available; \*, spring; Elevation, elevation in feet above sea level;\*\* well sampled weekly for specific conductance in fall 2000 and spring 2001]

Local identifier	USGS identifier	SEO permit number	Elevation	Total depth	Depth to screen		Yield	Depth to water	Date of measurement
					Top	Bottom			
GWA01**	393713105131401	97069	6585	540	--	--	15	150	5/ 1/78
GWA02**	393712105131900	42209	6630	280	--	--	0	0	8/ 4/70
GWA03*	393733105111700	--	7556	0	--	--	0	--	--
GWB01	393602105133100	77536	6955	350	--	--	2.5	46	6/12/92
GWB02**	393604105132200	164834	6887	420	--	--	6.3	6	10/30/92
GWC01	393705105141100	61643	--	100	--	--	3.5	40	8/29/72
GWC02**	393703105145100	187422	6278	45	--	--	15	--	--
GWC99	393810105141900	141992	7794	250	--	--	30	80	9/17/85
GWD01	393758105163600	44798	7565	125	--	--	10	45	5/15/57
GWD02	393757105163400	46328	7738	318	--	--	1	32	6/17/71
GWD04**	393813105150100	153536	7550	266	--	--	1.47	28	--
GWD05	393812105145300	--	7698	254	--	--	--	--	--
GWD06	393815105152500	--	7430	--	--	--	--	--	--
GWD07	393742105153700	--	7259	--	--	--	--	--	--
GWD08	393746105153000	--	7230	--	--	--	--	--	--
GWE01	393711105151000	63369	7154	363	--	--	3	44	9/25/72
GWE03	393709105145300	68842	6957	150	25	145	15	15	5/17/73
GWF01	393528105151600	--	7458	270	--	--	3	60	--
GWF02	393532105150500	65593	7437	280	180	280	6	65	2/26/73
GWF03	393554105142100	89809	7494	340	--	--	2	105	9/ 3/77
GWF04	393553105142100	84734	7416	340	--	--	3	110	9/24/76
GWF05	393549105142200	81233	7498	360	--	--	5	107	11/ 3/75
GWF06**	393552105144200	--	7373	200	--	--	3	32	--
GWF08	393556105144600	--	7505	270	--	--	--	--	--
GWF09	393552105143600	45921	7430	255	--	--	2.5	37	6/17/71
GWF10**	393614105151800	129807	8213	325	--	--	4	50	5/ 3/83
GWF11**	393518105150200	58049	7376	300	240	300	6	101	9/19/73
GWF12	393546105141000	81747	7158	200	--	--	36	25	5/19/76
GWF13	393437105160700	109067	7727	--	--	--	--	--	--
GWF14	393551105144700	151655	7430	563	30	290	10	79	9/15/88
GWF15**	393640105164400	58531	7960	170	--	--	5	70	6/ 1/72
GWG01**	393308105181500	--	8094	130	--	--	--	--	--
GWG02	393404105182200	26910	7951	127	--	--	16	--	4/25/66
GWG03	393310105183200	--	8047	--	--	--	--	--	--
GWG04	393421105184700	--	7758	--	--	--	--	--	10/23/78
GWG05	393426105194300	98471	8196	240	--	--	2.5	40	3/ 7/79
GWG06	393344105191600	89565	7869	175	--	--	3	50	6/15/77
GWG07	393544105174100	--	8188	--	--	--	--	--	8/16/58
GWG08	393458105170000	--	7697	--	--	--	--	--	--
GWG09	393505105170400	188660	7620	260	--	--	10	60	9/19/95
GWG10	393316105181400	--	8295	--	--	--	--	--	--
GWG11	393459105165700	31703	7733	645	--	--	3.5	200	--
GWG12	393351105184500	97386	7908	625	--	--	2.5	280	6/ 6/78
GWG13	393444105173700	--	7820	--	--	--	--	--	--
GWH01**	393449105170100	31496	7571	160	--	--	1.5	30	7/14/67
GWH02	393449105164800	8596	7772	575	380	495	1	200	12/20/75
GWH03**	393444105165500	107430	7741	400	--	--	--	--	--
GWI01	393242105202000	83451	8564	220	--	--	6	20	5/24/76
GWI02	393237105204600	79402	8590	123	43	123	12	48	11/14/75
GWI03	393334105192500	15137	7920	118	--	--	21	40	5/ 9/63
GWI04	393300105194400	93546	8068	143	--	--	6	35	--
GWI05	393340105195000	--	8053	--	--	--	--	--	--
GWI06	393334105195100	144213	8101	243	123	223	7.5	40	8/13/86
GWI07	393241105203900	172590	8572	277	--	--	10	30	9/30/93
GWI08	393235105204300	103219	--	--	--	--	--	--	--
GWJ01**	393224105251600	181194	8689	600	--	--	4.25	315	8/25/97
GWJ02**	393230105201000	94815	8500	175	100	175	4	100	11/28/77
GWJ03	393234105201800	109522	8641	305	165	305	5	60	9/12/79
GWJ04	393242105201000	79785	8465	500	380	500	0.75	175	8/17/75
GWJ06	393301105185700	23678	7920	25	--	--	11	--	5/ 7/65

**Table 8. Site identifiers and selected characteristics for ground-water-quality sampling sites in the Turkey Creek watershed, Jefferson County, Colorado, 1998–2000—Continued**

[Note: SEO, State Engineers Office; Yield, well yield in gallons per minute as reported to State Engineers Office; Date of measurement, in month/day/year, refers to depth to water measurement; all depths reported in feet below land surface; --, not available; \*, spring; Elevation, elevation in feet above sea level;\*\* well sampled weekly for specific conductance in fall 2000 and spring 2001]

Local identifier	USGS identifier	SEO permit number	Elevation	Total depth	Depth to screen		Yield	Depth to water	Date of measurement
					Top	Bottom			
GWJ07	393259105185700	--	7918	--	--	--	--	--	--
GWJ08	393311105184100	--	8059	--	--	--	--	--	--
GWJ09	393308105184900	118007	7987	242	142	242	21.5	84	11/27/81
GWJ10	393314105190200	--	--	--	--	--	--	--	--
GWK01	393154105220100	187230	9143	300	180	280	60	80	11/11/96
GWK02	393209105220600	97263	8938	300	200	300	3	50	5/ 5/78
GWK03	393208105221600	89745	9129	320	--	--	15	81	7/22/77
GWK04**	393151105220800	187230	9227	300	--	--	60	51	2/13/97
GWK05	393237105222900	170503	9915	542	--	--	3.6	192	10/ 4/95
GWK06	393103105184800	--	8502	210	--	--	--	160	--
GWK07	393151105192200	79825	8171	280	--	--	0.5	36	6/29/77
GWK08	393206105204800	153657	8402	15	--	--	--	--	--
GWK09	393243105214500	31423	8827	220	--	--	3	100	7/ 6/67
GWK10	393153105192400	194248	8168	26	--	--	15	0	--
GWK11	393153105192401	194248	8196	80	--	--	70	8	1/24/97
GWL01	393352105150000	176233	8258	810	600	810	1.5	700	1/19/94
GWM02	393418105131000	12868	7159	350	--	--	15	100	2/14/85
GWM03	393413105132200	--	7254	--	--	--	--	--	--
GWM04	393413105135800	102558	7452	300	--	--	1	25	10/11/78
GWM05	393424105134800	115646	7442	305	145	305	12	40	8/19/80
GWM06**	393423105130400	59071	7086	54	--	--	5	--	9/23/56
GWM07**	393401105124600	107190	7278	500	--	--	0	0	9/19/79
GWM08	393400105125900	49818	7255	283	43	283	0.6	14	3/26/72
GWM09*	393426105130000	--	7102	0	--	--	--	--	--
GWM10	393457105131600	156284	7007	605	160	605	4	40	12/ 8/89
GWM11	392936105231600	--	--	--	--	--	--	--	--
GWN01**	393308105145500	102180	7888	280	--	--	7.5	40	9/26/79
GWN02	393342105131800	21039	--	90	50	90	3	25	8/12/64
GWN03	393337105150700	96531	--	245	--	--	6	140	2/25/78
GWN04	393331105145100	193271	--	405	200	400	18	80	3/15/96
GWN99	393341105131500	--	7178	--	--	--	--	--	--
GWO02**	393252105154800	44362	7911	288	--	--	1.25	10	2/ 9/71
GWO03	393233105152400	121662	7933	0	--	----	--	--	--
GWO04	393238105152000	69768	7760	144	44	144	1.25	35	9/11/73
GWO05	393245105145000	--	7925	--	--	--	--	--	--
GWO06	393231105144000	75027	7839	325	100	325	2	60	6/26/74
GWO07	393206105141800	67433	8023	245	165	245	10	175	2/21/73
GWO08	393226105151600	22265	7879	316	--	--	1	6	11/ 2/64
GWO09	393139105141200	64435	8398	195	45	195	1.5	80	2/ 8/73
GWO10**	393115105141100	41782	8149	75	30	70	3	60	8/15/70
GWO11	393144105135600	119397	8517	575	475	575	15	100	4/27/83
GWO12**	393122105142100	--	8490	--	--	--	--	--	--
GWO13	393236105142900	192230	8652	400	280	380	0.25	50	11/23/97
GWP01	393245105175800	187284	7900	600	--	--	0.48	41	1/23/97
GWP02	393249105174600	--	8384	475	--	--	3	--	--
GWP03	393227105181600	136487	8238	350	--	--	--	--	--
GWP04**	393204105180200	191850	8290	377	--	--	3.5	100	4/19/96
GWP05**	393244105172600	58806	8218	320	--	--	1	200	7/11/73
GWP99	393237105162900	172122	7977	190	--	--	1.5	150	--
GWX01	393031105211000	153691	9396	520	400	500	1.25	100	4/29/89

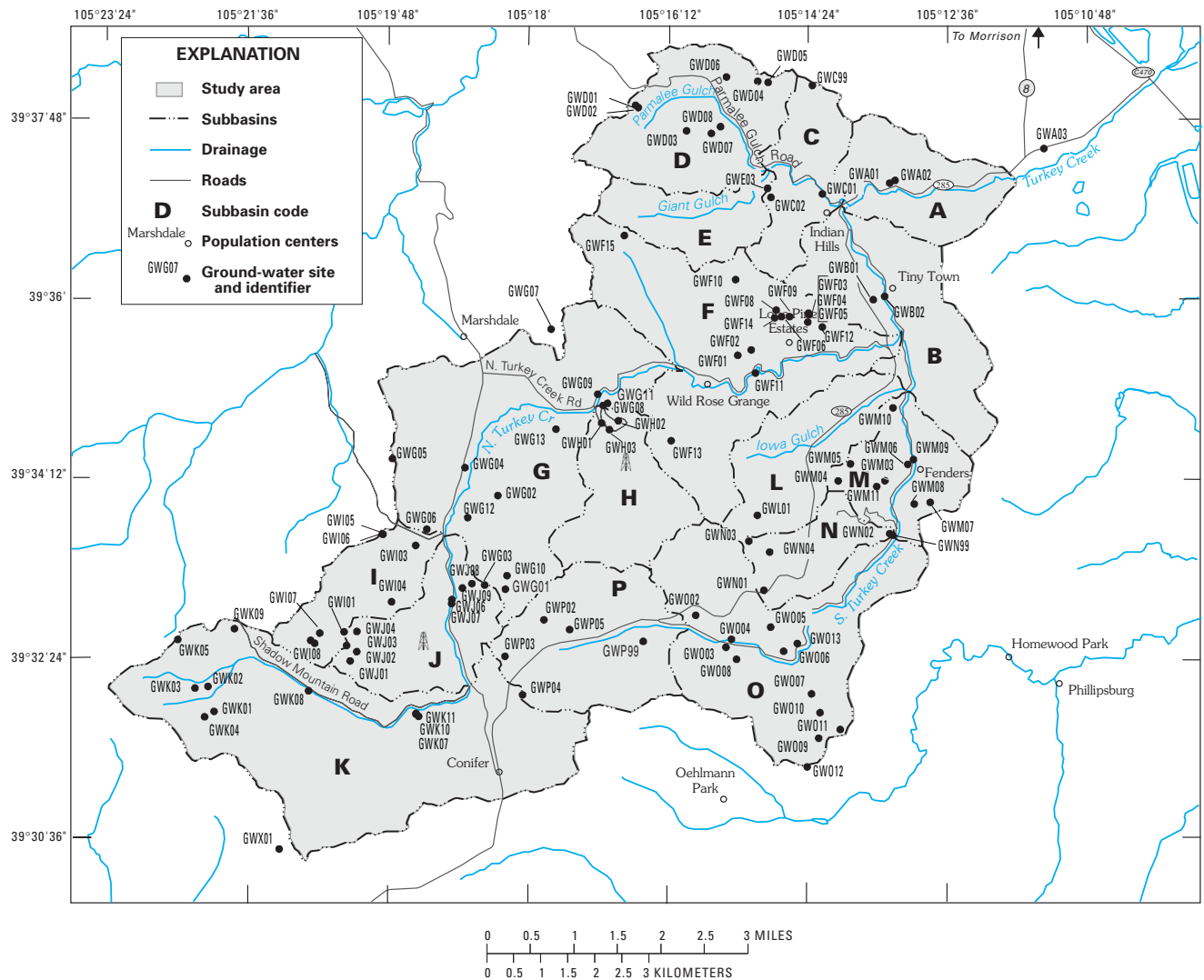


**Figure 12.** Location of ground-water sampling sites.

wells by Jefferson County Health Department personnel concurrently with inorganic samples. All surface-water sample bottles were filled by the dip method by USGS personnel. Wastewater samples were transported to the USGS National Water Quality Laboratory (NWQL) in Denver, Colo., for custom gas chromatograph analysis.

Major ion and nutrient samples were collected with the wastewater compound samples by using the same USGS protocols used in the water year 1999 sampling. Analytical determinations also were made at the U.S. Environmental Protection Agency Region VII laboratory except for low-level bromide determinations, which were made at the NWQL.

## Runoff Modeling Methods

Runoff modeling was used in this study to help estimate the amount of precipitation received by the Turkey Creek watershed that recharges the ground-water system, to characterize how much of the precipitation leaves the watershed as evapotranspiration or components of streamflow, and to develop estimates of water-balance terms. The runoff model selected for use in this study is the Precipitation-Runoff Modeling System (PRMS) (Leavesley and others, 1983) as implemented by the Modular Modeling System (MMS) (Leavesley and others, 1996). PRMS is a modularly designed, distributed-parameter,

**Table 9. Water-quality properties and constituents included in analyses in water year 1999**

[Note: cfs, cubic feet per second;  $\mu\text{S}/\text{cm}$ , microsiemens per centimeter at 25° Celsius; mg/L, milligrams per liter;  $\mu\text{g}/\text{L}$ , micrograms per liter; --, not applicable; °C, degrees Celsius]

USGS parameter code	Water-quality property or constituent	Reporting units	USGS parameter code	Water-quality property or constituent	Reporting units
PHYSICAL PROPERTIES			MINOR ELEMENTS		
00061	Discharge	cfs	01106	Aluminum (dissolved)	$\mu\text{g}/\text{L}$
00095	Specific conductance	$\text{uS}/\text{cm}$ at 25°C	01105	Aluminum (total)	$\mu\text{g}/\text{L}$
00400	pH	standard units	01095	Antimony (dissolved)	$\mu\text{g}/\text{L}$
00010	Temperature	degrees Celsius	01097	Antimony (total)	$\mu\text{g}/\text{L}$
00300	Dissolved oxygen	mg/L	01000	Arsenic (dissolved)	$\mu\text{g}/\text{L}$
00900	Hardness as $\text{CaCO}_3$ , total	mg/L	01002	Arsenic (total)	$\mu\text{g}/\text{L}$
MAJOR IONS			01005	Barium (dissolved)	$\mu\text{g}/\text{L}$
00915	Calcium, dissolved	mg/L	01007	Barium (total)	$\mu\text{g}/\text{L}$
00916	Calcium, total	mg/L	01010	Beryllium (dissolved)	$\mu\text{g}/\text{L}$
00925	Magnesium, dissolved	mg/L	01012	Beryllium (total)	$\mu\text{g}/\text{L}$
00927	Magnesium, total	mg/L	01020	Boron (dissolved)	$\mu\text{g}/\text{L}$
00930	Sodium, dissolved	mg/L	01022	Boron (total)	$\mu\text{g}/\text{L}$
00929	Sodium, total	mg/L	01025	Cadmium (dissolved)	$\mu\text{g}/\text{L}$
00935	Potassium, dissolved	mg/L	01027	Cadmium (total)	$\mu\text{g}/\text{L}$
00937	Potassium, total	mg/L	01030	Chromium (dissolved)	$\mu\text{g}/\text{L}$
00410	Alkalinity, total	mg/L	01034	Chromium (total)	$\mu\text{g}/\text{L}$
00945	Sulfate	mg/L	01035	Cobalt (dissolved)	$\mu\text{g}/\text{L}$
00940	Chloride	mg/L	01037	Cobalt (total)	$\mu\text{g}/\text{L}$
00950	Fluoride	mg/L	01040	Copper (dissolved)	$\mu\text{g}/\text{L}$
01140	Silicon, dissolved	mg/L	01042	Copper (total)	$\mu\text{g}/\text{L}$
01142	Silicon, total	mg/L	01046	Iron (dissolved)	$\mu\text{g}/\text{L}$
NUTRIENTS			01045	Iron (total)	$\mu\text{g}/\text{L}$
00680	Total organic carbon	mg/L	01049	Lead (dissolved)	$\mu\text{g}/\text{L}$
00610	Ammonia (as N)	mg/L	01051	Lead (total)	$\mu\text{g}/\text{L}$
00630	Nitrate/Nitrite (as N)	mg/L	01056	Manganese (dissolved)	$\mu\text{g}/\text{L}$
00613	Nitrite	mg/L	01055	Manganese (total)	$\mu\text{g}/\text{L}$
00665	Phosphorus, total	mg/L	01060	Molybdenum (dissolved)	$\mu\text{g}/\text{L}$
BACTERIOLOGICAL			01062	Molybdenum (total)	$\mu\text{g}/\text{L}$
--	E. coli	--	01065	Nickel (dissolved)	$\mu\text{g}/\text{L}$
--	Total coliform	--	01067	Nickel (total)	$\mu\text{g}/\text{L}$
			01145	Selenium (dissolved)	$\mu\text{g}/\text{L}$
			01147	Selenium (total)	$\mu\text{g}/\text{L}$
			01075	Silver (dissolved)	$\mu\text{g}/\text{L}$
			01077	Silver (total)	$\mu\text{g}/\text{L}$
			01057	Thallium (dissolved)	$\mu\text{g}/\text{L}$
			01059	Thallium (total)	$\mu\text{g}/\text{L}$
			01150	Titanium (dissolved)	$\mu\text{g}/\text{L}$
			01152	Titanium (total)	$\mu\text{g}/\text{L}$
			01085	Vanadium (dissolved)	$\mu\text{g}/\text{L}$
			01087	Vanadium (total)	$\mu\text{g}/\text{L}$
			01090	Zinc (dissolved)	$\mu\text{g}/\text{L}$
			01092	Zinc (total)	$\mu\text{g}/\text{L}$

physically based, deterministic model that characterizes the many physical processes involved in watershed runoff. MMS provides a computer environment that, among other capabilities, implements PRMS and many pre- and post-processing capabilities that facilitate watershed analyses.

For runoff modeling discussions in this report, the term “water balance” is used to indicate a description of the fate of precipitation in the watershed. A water balance is an accounting of system inputs and outputs that typically is balanced by a change in storage term and expressed as equation 2:

$$\Delta S = P - ET - Q \quad (2)$$

where

- $P$  is precipitation falling on the watershed,
- $ET$  is evapotranspiration leaving the watershed,
- $Q$  is streamflow leaving the watershed, and
- $\Delta S$  is change in watershed storage.

In this formulation, change in storage includes changes in the amount of ground water in the watershed and changes in the amount of soil moisture in the watershed.

A principal advantage of using a model such as PRMS is that values for all water-balance terms are typically calculated by the model. The general form for a water-balance equation used in equation 2 is, indeed, general. That is, each of the terms represented

in the equation could be expressed in terms of additional variables; for example, as described in the “Watershed Characterization Using the Precipitation-Runoff Modeling System” section, there are several components to streamflow and  $Q$  could be expressed as the sum of overland flow, interflow, and base flow.

It is convenient to describe water balances in terms of depth, in inches, over the area of consideration, and this is the convention that will be used in discussion of modeling results in this report. For example, 0.75 inch of precipitation for the watershed indicates a layer of water 0.75 inch deep over the

entire watershed. The watershed area associated with reported depths (47.2 mi<sup>2</sup> or 30,208 acres) is required to convert to the volume of acre-feet (1,888).

### General Characteristics of the Precipitation-Runoff Modeling System

The distributed nature of PRMS allows evaluation of hydrologic processes at watershed and intrawatershed scales. The ability to model intrawatershed areas allows users to derive estimates of hydrologic conditions for areas defined on the basis of watershed knowledge. Typically, users define units within the

**Table 10.** Miscellaneous data collected in water year 2001, including analysis results for bromide, selected inorganic ions, wastewater compounds, and tritium

[--, no data; <, less than; >, greater than; tritium, in tritium units; bromide, chloride, fluoride, and nitrite plus nitrate as nitrogen, in milligrams per liter; chloride/bromide ratio, dimensionless; MRL, method reporting limit; estimated wastewater detections are values between the instrument detection level under ideal conditions and the method reporting limit; blanks, quality assurance samples]

Local site identifier	Date (month/day/year)	Bromide	Chloride	Fluoride	Nitrite plus nitrate	Chloride/bromide ratio	Wastewater-compound detections above MRL	Estimated wastewater-compound detections	Tritium sample date (month/year)	Tritium (in tritium units)
GWA01	04/10/01	0.0232	1.29	0.4	0.69	56	--	--	11/00	14.3
GWA02	04/10/01	0.0356	3.38	3.14	1.22	95	--	--	11/00	6.2
GWB01	04/10/01	--	165	<0.2	10.3	--	--	--	11/00	17.1
GWB02	04/10/01	0.0271	3.16	1.12	<0.05	117	0	0	11/00	4.6
GWB03	04/12/01	<0.01	1.15	<0.2	0.13	>115	--	--	11/00	12.2
GWC02	04/09/01	0.062	39	0.38	9.91	629	0	0	11/00	19.5
GWD04	04/12/01	0.0252	3.57	0.23	1.69	142	--	--	11/00	14.5
GWF10	04/10/01	0.0346	6.02	1.29	0.11	174	--	--	11/00	15.9
GWF11	04/10/01	0.0435	9.03	2.26	0.57	208	--	--	11/00	8.3
GWF15	04/10/01	0.0112	14.4	0.25	0.23	1286	--	--	11/00	13.1
GWG01	04/10/01	0.0156	0.74	1.13	<0.05	47	--	--	11/00	11.1
GWH01	04/09/01	0.1063	21.1	0.47	2.17	198	0	0	11/00	19.7
GWH03	04/09/01	0.0714	60.5	0.42	1.71	847	1	2	11/00	13.3
GWJ01	04/09/01	<0.01	1.41	<0.2	0.61	>141	--	--	11/00	33.2
GWJ02	04/09/01	--	1.38	0.26	0.57	--	--	--	11/00	ruined cell
GWK04	04/09/01	0.0119	3.82	2.35	0.81	321	--	--	11/00	13.7
GWM06	04/09/01	0.1367	134	<0.2	8.84	980	0	0	11/00	12
GWM07	04/10/01	0.3594	5.48	0.34	2.16	15	--	--	11/00	20.6
GWN01	04/09/01	0.029	5.38	1.58	0.28	186	--	--	11/00	8.9
GWO02	04/09/01	0.169	62.2	1.92	<0.05	368	--	--	11/00	2.3
GWO10	04/10/01	0.0314	111	<0.2	6.53	3535	0	0	11/00	12.3
GWO12	04/09/01	0.1058	102	<0.2	3.41	964	--	--	11/00	12
GWP04	04/10/01	0.0305	4.77	0.22	1.45	156	0	0	11/00	18.9
GWP05	04/10/01	0.0611	55.6	0.33	3.06	910	0	5	11/00	22.2
SWD01	04/09/01	--	119	<0.2	0.98	--	0	1	11/00	--
SWE01	04/10/01	0.0348	68.6	0.28	0.33	1971	0	1	11/00	--
SWH01	04/09/01	0.0837	31.9	0.29	0.15	381	0	0	11/00	--
SWH01	04/09/01	0.1031	32	0.28	0.16	310	blank	blank	11/00	--
SWL01	04/09/01	0.3131	138	0.21	<0.05	441	1	2	11/00	--

watershed that have a unique set of physical characteristics that dictate hydrologic response. In this report, the finest unit of delineation will be referred to, individually, as a “hydrologic response unit (HRU).” Each HRU supplies water to the subsurface in the form of downward-percolating soil-water excess, which is referred to as “*I*” in the evapotranspiration discussions. The soil-water excess is routed to interflow and base-flow reservoirs that are the source for interflow and base flow. Together, interflow and base flow account for ground-water contributions to streamflow. Interflow is relatively dynamic and occurs in direct response to precipitation, whereas base flow is relatively steady and may sustain streamflow through rainless periods.

In general, surface or near-surface processes such as interception, snowpack accounting, overland flow, infiltration, and evapotranspiration take place at the HRU scale, and interflow and base-flow accounting takes place at their respective subsurface reservoir scales. In this study, HRU’s were defined on the basis of slope and aspect by using automated procedures developed by the USGS (Viger and others, 1998; Viger, 1998). Interflow and base-flow reservoirs are interlinked and can be referred to collectively as subsurface reservoirs. The subsurface reservoirs represent ground water that is associated with streamflow, which is a portion of all the ground water in the watershed. In the watershed characterization developed in this study, the subsurface reservoirs have a one-to-one relation with each other and were defined on the basis of geology and streamflow measurements. In this study, the subsurface reservoirs do not have a one-to-one relation with HRU’s, and there are typically several HRU’s associated with each interflow and base-flow reservoir. The methods and rationale used for schematization of HRU’s and interflow and base-flow reservoirs in the Turkey Creek watershed are discussed in the “Runoff Modeling” section.

The physically based nature of PRMS allows simulation of physical processes involved in watershed runoff. Processes are represented with algorithms that describe known physical laws or empirical relationships that have some physical interpretation based on measurable watershed characteristics. The individual terms in algorithms that require input from model users can be referred to as “input parameters.” For simulation of the Turkey Creek watershed, values for many input parameters, especially those that are related to physical characteristics of the basin, were estimated using parameterization routines described by Leavesley and others (1983) and Wolock (1997) that are implemented by Viger and others (1998).

## **Watershed Characterization Using the Precipitation-Runoff Modeling System**

A brief introduction to PRMS watershed characterization is included here in order to provide readers with information about the nature of PRMS and to establish a context for terminology used in later discussions of runoff modeling. Readers in need of a more rigorous description of the intricacies of PRMS are referred to in Leavesley and others (1983).

The general schematization shown in figure 13 indicates many physical processes in a watershed that are characterized by PRMS. There are literally hundreds of PRMS system variables associated with the PRMS characterization of watershed processes, and figure 13 is a simplified yet effective schematization of the general watershed system that PRMS emulates. PRMS system variables that describe physical conditions such as soil moisture, ground water associated with streamflow, components of streamflow, and many other watershed conditions are sometimes referred to as “state variables” because they indicate status of various watershed conditions. In this report, PRMS simulations result in values for state variables on a daily basis.

The general schematization in figure 13 also indicates the way system inputs are used in model algorithms to determine system outputs. The figure depicts subsurface reservoirs for interflow and base-flow processes; these reservoirs are defined for accounting purposes. Readers should be careful not to assume that there are rigidly designed reservoirs in the subsurface of the watershed. Rather, there are certain subsurface processes, such as interflow and base flow, that are conceptualized and accounted for differently; the so-called reservoirs are designated to facilitate the associated accounting.

System inputs consist of daily precipitation, which describes the amount of water put into the system, and daily temperature extremes, which are used to define energy terms. System outputs consist of values for all state variables. Some of the most important state variables for this study are the three components of streamflow (overland flow, interflow, and base flow), evapotranspiration, and the contents of the subsurface reservoirs.

An additional state variable referred to as “*GSNK*” (ground-water sink) also is important to results presented in this report. *GSNK* is the amount of water that is removed from the base-flow reservoir

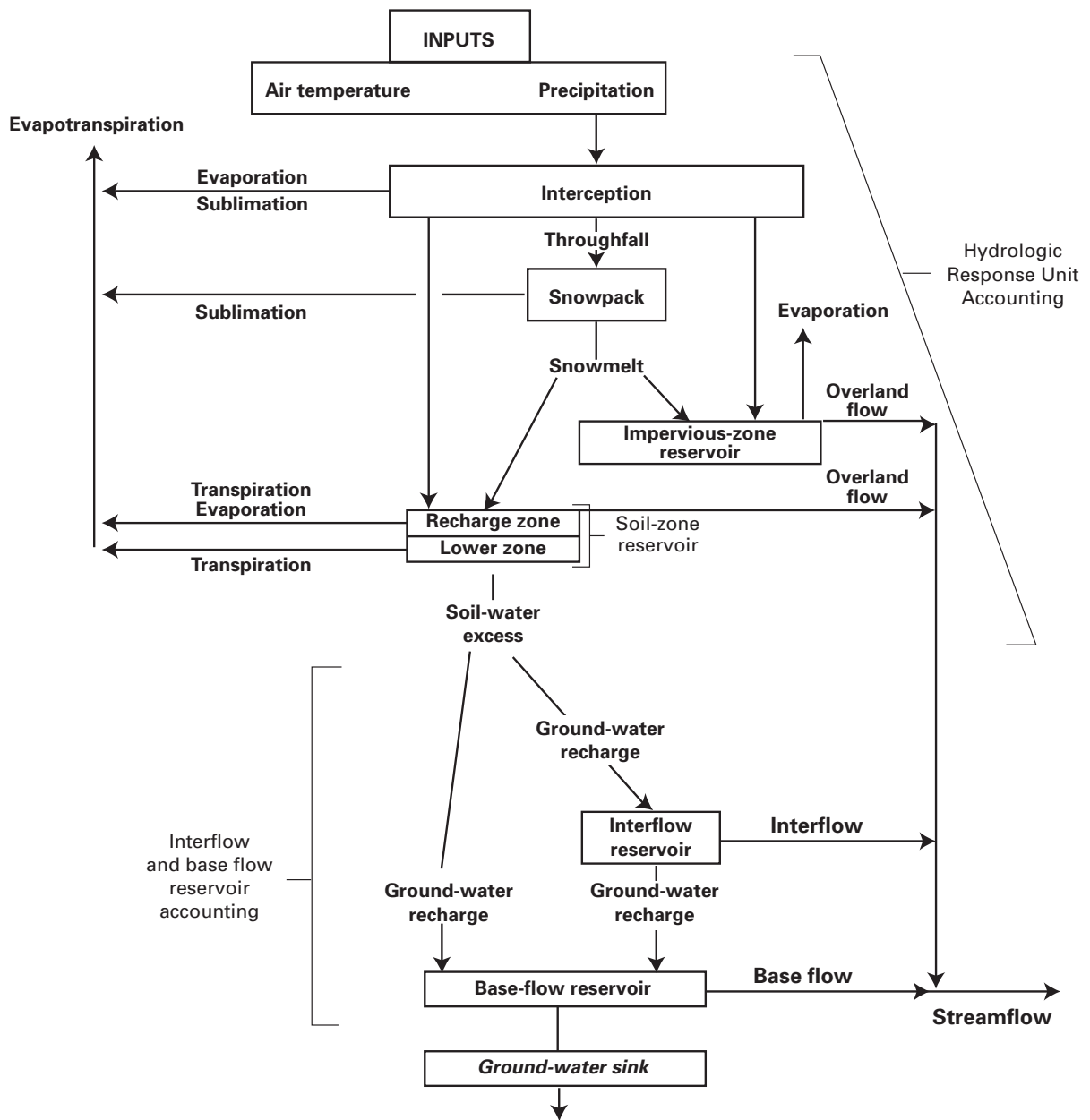


**Figure 13.** Schematic diagram of selected physical processes characterized by Precipitation-Runoff Modeling System.

and cannot drain, by gravity, to local streams in the watershed. Conceptually, this water may be associated with underflow, which is ground water that leaves the watershed by means other than streamflow or evapotranspiration, or long-term storage.

In this report, the terms of greatest interest are those associated with inputs and outputs to the ground-water system. By using the framework of physical processes described above, an equation that describes ground water associated with base flow can be developed as follows:

$$\Delta BFR = GWI - BF - GSNK \quad (3)$$

where

$\Delta BFR$  is change in the contents of the base-flow reservoir,

$GWI$  is ground-water recharge to the base-flow reservoir,

$BF$  is base flow, and

$GSNK$  is ground water that is lost from the base-flow reservoir.

A similar equation can be used for interflow. The terms in equation 3 will be discussed in more detail in the “Runoff Modeling” section.

## HYDROLOGIC CONDITIONS

Hydrologic conditions in the watershed are characterized on the basis of contemporary data collected as part of this study; contemporary conditions are compared to historical conditions when possible. The hydrologic conditions described in this section include evapotranspiration and surface- and ground-water conditions including water quality. Descriptions of evapotranspiration in the watershed are developed on the basis of sophisticated techniques described in the Appendix. Evapotranspiration measurements reduce the need to use less accurate estimates of evapotranspiration when developing water balances.

### Evapotranspiration

*ET* results and analyses are presented in terms of calendar year (January 1 to December 31) rather than water year (October 1 to September 30) for two reasons. First, the annual cycle of *ET* tends to be in phase with the calendar year, peaking near midsummer and reaching a minimum near midwinter. Therefore, the bulk of the flux occurs near the middle of the year and divisions between years occur at times of low flux. Second, because data collection began in early 1999, the use of calendar years provides three full years of data (including the estimate of *ET* for January 1999), whereas only two full water years of data were collected. The calendar-year summaries presented in this section related to *ET* should not be used in conjunction with water-year summaries presented elsewhere in this report.

### Forest Site Results

Daily totals of *ET* at the forest site are shown for all 3 years in figure 14. Daily totals of precipitation and daily means of soil moisture are shown in figure 15. Soil moisture is computed as the mean of soil moisture measurements made at 0.16-ft and 0.75-ft depths (table 4). Daily means of solar radiation are shown in figure 16.

Evaporation of water requires both energy and water availability. A general pattern of greater *ET* values from midspring to the end of summer and smaller values the rest of the year can be seen during all 3 years (fig. 14). The overall pattern is somewhat similar to the annual trend in solar radiation (fig. 16). Solar radiation is the ultimate source of virtually all energy used for *ET*, and this general similarity illustrates the control of solar radiation on *ET*. A rather smooth sinusoidal curve can be imagined that passes through all the greatest values of solar radiation in figure 16, corresponding to clear-sky conditions. The clear-sky value changes by a factor of about 3.8 during the course of a year, caused by the tilt of the Earth’s axis. This seasonal variation in the maximum amount of energy available at the Earth’s surface is one of the main drivers of seasonal changes in *ET*. In addition, the effect of extremely overcast days on *ET* can be seen by noting numerous 1- to 3-day periods when solar radiation is very small (say, less than one-third of the clear-sky value) and corresponding decreases in *ET* are evident.

In the context of *ET*, water availability refers to the presence of liquid or solid water near the Earth’s surface in locations where it can readily evaporate or sublimate into the atmosphere. At the forest site, available water is delivered as precipitation (rain or snow) or dew and resides as soil moisture, snowpack, or interception. Soil moisture is the water held in the spaces between soil particles and can contribute to transpiration or evaporation. Snowpack accumulates on the land surface during the winter and evaporates or sublimates slowly during that time. Interception is precipitation or dewfall that lodges in the vegetation canopy and evaporates or sublimates directly without reaching the land surface.

The influence of soil moisture on *ET* can be seen by comparing figures 14 and 15. Soil moisture increases immediately following large rainfall as the water soaks into the soil and then decreases slowly and asymptotically as the soil dries (fig. 15). The variability in soil moisture is reflected in the time series of *ET* as a modulation of the annual pattern set by solar radiation. Typically, this modulation occurs on a time scale of one to several weeks. For example, periods of high soil moisture and *ET* occurred during DOY’s 169–180 and 219–230 in 1999, and DOY’s 179–186 and 230–258 in 2000. Conversely, dry soils reduced *ET* rates during DOY’s 160–167 and 223–229 in 2000 even though solar radiation was near normal (fig. 16B).



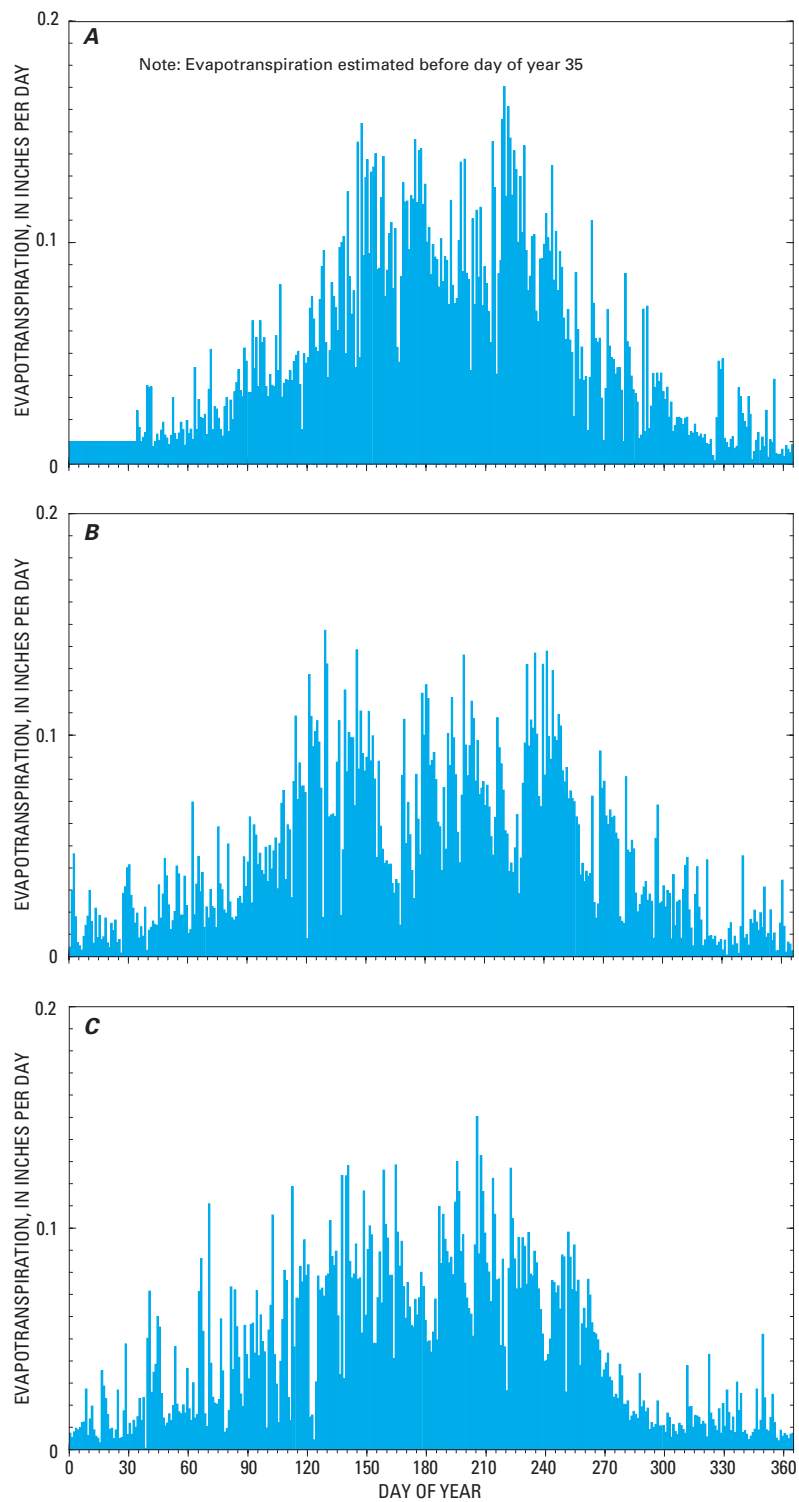


**Figure 14.** Daily evapotranspiration at forest site during (A) 1999, (B) 2000, and (C) 2001.

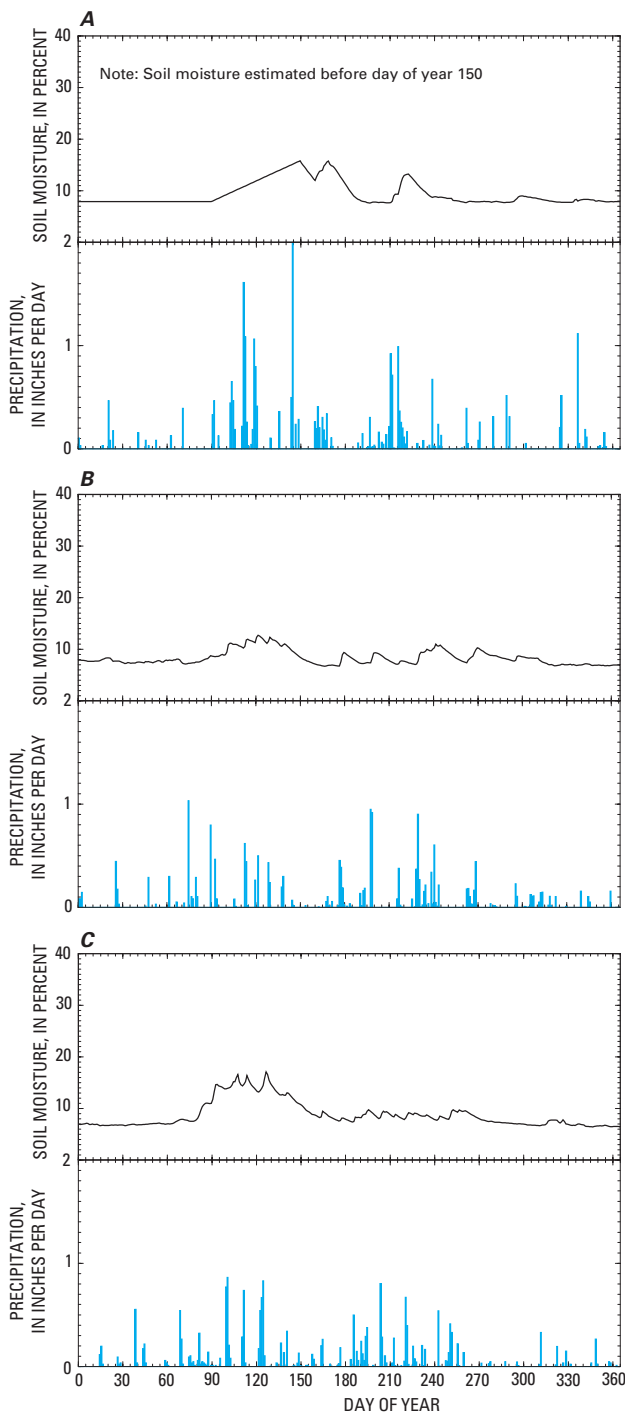


**Figure 15.** Daily precipitation and daily mean soil moisture at forest site during (A) 1999, (B) 2000, and (C) 2001.

Soil moisture also affects *ET* on a seasonal time scale. In a forest setting, soil moisture has a greater influence on transpiration than on evaporation from the soil surface. In general, soil moisture is greater during spring, summer, and early fall than during late fall and winter. Sap-flow measurements indicated

that the lodgepole transpiration season lasted from about DOY 99 (April 8) to DOY 286 (October 12) in 2000, and from DOY 108 (April 18) to DOY 271 (September 28) in 2001. The correspondence of the greater soil-moisture levels with the transpiration season of the trees exerts a seasonal influence on *ET* through water availability. This influence accentuates the seasonal control of solar radiation on *ET*. Whereas mean solar radiation varies seasonally by a factor of about 3.5 (fig. 16), mean *ET* varies seasonally by a factor of about 10 (fig. 14) as a result of the additional soil-moisture influence.

The influence of rainfall interception on *ET* can be seen by comparing figures 14 and 15. This relation is relatively subtle because the rainfall interception capacity of the forest is probably 0.1 to 0.2 inch (Rutter and others, 1975; Calder, 1977); however, single days of relatively high *ET* often occur on or immediately following days of rainfall. Interception increases *ET* because the water is directly exposed to the passing air and to solar radiation. Examples of high *ET* days associated with rainfall are DOY's 148, 244, and 264 in 1999, DOY's 115, 130, and 200 in 2000, and DOY's 113, 165, and 206 in 2001. Interception also was responsible for many other days of high *ET* during the study. The timing of interception relative to solar radiation also strongly influences *ET*. Rain that falls at night, followed by a clear day, produces the greatest values of *ET*, whereas little *ET* may occur during several rainy days in a row because the evaporation process during the rainy period is energy limited.

The influence of snowfall interception on *ET* is somewhat more apparent than rainfall interception, because the snowfall interception capacity is greater than that for rain. Snow interception capacity is probably about 4 inches of snow (Lundberg, 1993), which is equivalent to 0.4 inch of water at a water density of 10 percent. If the snow remains in the tree canopy, it can boost *ET* noticeably for several days after a snowfall. For example, high *ET* rates associated with snowfalls occurred on DOY's 327–330 and 338–344 in 1999, DOY's 2–4 and 28–33 in 2000, and DOY's 17–20 and 40–47 in 2001. These events maintained elevated *ET* rates for 3 to 8 days following snowfall. Often, however, the snow unloads from the canopy to the ground before it fully evaporates or sublimates. This can be caused by high wind, temperature, solar radiation, or a combination of these factors. Examples of short-term elevated *ET* following snowfall occurred on DOY's 64 and 356 in 1999, DOY's 63, 81, and 342 in 2000, and DOY's 29 and 323 in 2001.

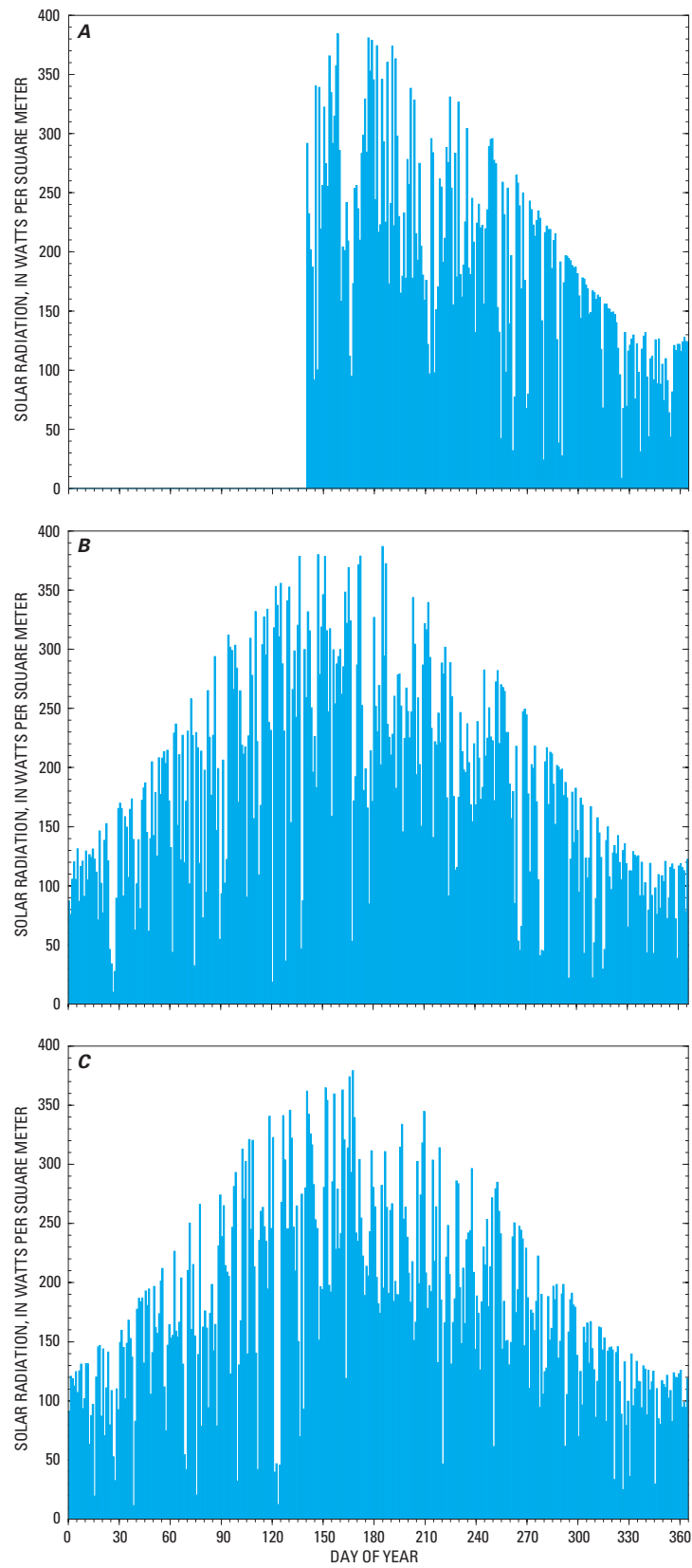


**Figure 16.** Daily mean solar radiation at forest site during (A) 1999, (B) 2000, and (C) 2001.

Using data collected during this study, a water balance was computed for the vegetated surface at the forest site. A layer was established, extending from just above the plant canopy to just below the root zone. Accounting for all inputs, outputs, and changes in storage in the layer during some time period, the balance can be written as:

$$P - ET - I - O = \Delta C + \Delta SP + \Delta SM \quad (4)$$

where

$P$  is precipitation,

$ET$  is evapotranspiration,

$I$  is soil-water excess that percolates downward and is referred to as infiltration in  $ET$  discussions in this report,

$O$  is overland flow,

$\Delta C$  is change in canopy storage,

$\Delta SP$  is change in snowpack storage, and

$\Delta SM$  is change in soil moisture storage.

$I$  is the amount of water that infiltrates out of the bottom of the layer, below the root zone. This is the water that has the potential to become recharge to the ground-water system.  $O$  is water that moves as sheet-flow over the land surface into a stream during and after precipitation. Because of the relatively permeable sandy soils, the organic litter mat on the forest floor, the gentle slope, and the low rainfall intensities at this site, it is estimated that overland flow was negligible at this site during the study period ( $O = 0$ ).  $\Delta C$  is the change in

the amount of water stored in the vegetation canopy (either liquid or solid) during the time period.  $\Delta SP$  is the change in the amount of water stored in the snowpack on the land surface during the time period. Annual values of  $\Delta C$  and  $\Delta SP$  were calculated using observations of canopy and snowpack storage made during site visits on December 30, 1998, December 23, 1999, January 3, 2001, and January 2, 2002. Observations of storage on these dates were adjusted by measured  $ET$  and  $P$  between these dates and the end of the year (midnight, December 31) to obtain year-end values. Canopy storage (and therefore  $\Delta C$ ) at year end was zero for all 4 years. Snowpack storage was calculated by multiplying an estimated snow depth by an estimated water density in the snowpack, and  $\Delta SP$  was computed by difference. Year-end values of soil-moisture storage were computed by multiplying soil moisture measured at midnight on December 31 (mean of -0.16 ft and -0.75 ft readings, table 4) by a rooting depth. Based on observations of uprooted lodgepole trees near the tower, the rooting depth is estimated to be 2 ft. The rooting depth may be underestimated because uprooted (toppled) trees tend to leave the smaller, deeper roots in the ground and only the larger, shallower roots are observable in the toppled tree-root mass. Using a deeper rooting depth was considered unjustifiable, however, because the deepest soil-moisture sensor was located at a depth of 0.75 ft. Annual values of  $\Delta SM$  were computed by difference. Equation 4 was then used to solve for annual values of  $I$ . Annual values of all terms in equation 4 are presented in table 11.

**Table 11.** Climatic and water balance summary for calendar years 1999, 2000, 2001, and 3-year mean, at forest site

[--, not applicable; \*, value estimated using partial-year data, adjusted using a ratio determined from 2000 and 2001 data; infiltration calculated using equation 4]

Term	1999	2000	2001	3-year mean	Percentage of 3-year mean precipitation
Precipitation (inches)	26.43	18.17	19.20	21.27	100
Evapotranspiration (inches)	18.73	17.34	16.83	17.63	82.9
Change in canopy storage (inches)	0.00	0.00	0.00	0.00	0.0
Change in snowpack storage (inches)	0.55	-0.74	-0.30	-0.16	-0.8
Change in soil moisture storage (inches)	0.00	-0.23	-0.11	-0.11	-0.5
Infiltration (inches)	7.15	1.80	2.78	3.91	18.4
Mean air temperature (°F)	43.82	43.69	43.76	43.76	--
Mean soil moisture (percent)	9.35	8.31	8.76	8.81	--
Mean solar radiation (watts per square meter)	194.0*	185.1	180.3	186.5	--

Precipitation,  $P$ , was much more variable than  $ET$  during the 3 years of study (table 11). Annual  $P$  varied by 8.26 inches and annual  $ET$  varied by 1.90 inches: a ratio of 4.3 to 1. At a site with a deep water table, where  $ET$  from ground water cannot occur, a positive correlation between  $ET$  and  $P$  would be expected because the water needed for  $ET$  to occur is derived primarily from  $P$  (eq. 4, table 11). At this site,  $ET$  tended to reflect the annual value of  $P$  ( $r = 0.93$ ; however, with only three data points,  $r$  has little significance), but not consistently. A comparison of 2000 and 2001 shows that  $ET$  was less in 2001 even though  $P$  and mean soil moisture (table 11) were greater. Because energy also is needed for  $ET$ , the smaller  $ET$  value in 2001 probably was caused by the smaller value of solar radiation that year (table 11). Air temperature appears not to be a factor in the 2000–2001  $ET$  comparison (table 11). Overall,  $ET$  was 82.9 percent of  $P$  during the 3 years of study at this site.

Infiltration,  $I$ , was quite variable during the 3 years of study (table 11).  $I$  decreased from 7.15 inches in 1999, a wet year, to 1.80 inches in 2000, a dry year. This large contrast (a ratio of 4 to 1) was caused primarily by the large percentage of  $P$  that is removed by  $ET$ , combined with the relatively constant nature of  $ET$  from year to year.  $I$  can be thought of as an upper limit on the amount of water that reaches the water table (recharge) beneath the forest site. Although this water infiltrates below the root zone, some of it may resurface as spring discharge, for example, at the site of temporary perched water tables, considering the complex structure of the weathered granite regolith underlying the site. The 3 years of study illustrate quite well that at a semiarid upland site, the water potentially available for recharge is small and quite sensitive to the variability in  $P$  from year to year. Overall,  $I$  was 18.4 percent of  $P$  during the 3 years of study at this site.

A rough estimate of long-term mean infiltration at the forest site can be made by relating  $I$  to  $P$ . Annual values of  $I$  and  $P$  are plotted in figure 17. The three points are nearly collinear ( $r^2 = 0.997$ ), indicating that at this site, annual  $I$  might be predicted somewhat reliably as a function of annual  $P$ . The best fit line shown in figure 17 is described by the equation:

$$I = 0.633P - 9.55 \quad (5)$$

where  $I$  is infiltration and  $P$  is precipitation, both in inches per year. The mean  $P$  for 1951–80 at this site is estimated to be 19.0 inches based on data from the

Colorado Climate Center (1984). Inserting this estimate of long-term  $P$  into equation 5 yields an estimate of 2.47 inches (13.0 percent of  $P$ ) of long-term mean infiltration at this site. Although the three points in figure 17 are nearly collinear, they constitute a very small data set. Therefore, equation 5 should be used only as a guideline because other years may plot farther from the line. Probably the greatest source of variability in the relation between  $I$  and  $P$  is the timing of  $P$ . In general, fewer and larger precipitation events (especially events that occur in the spring or fall) produce more  $I$  than the same amount of precipitation spread out over a greater number of small events. Overwhelming the root zone with water from large events causes infiltration below the root zone by gravity flow, whereas smaller, more frequent additions of water can be absorbed by the soil and held in place, ultimately to be discharged as  $ET$ .

Equation 5 also can be used to estimate the effects of very dry years on infiltration. As seen in figure 17, the equation predicts zero  $I$  at an annual  $P$  of about 15 inches. Use of equation 5 in this way is even more tentative than for predicting long-term mean  $I$  because in addition to the variability mentioned previously, factors related to extrapolation arise. Beyond the range of  $P$  measured in this study, the relation between  $I$  and  $P$  is completely untested. For example, as  $P$  decreases below about 17 inches,  $I$  may plot above the projected line, asymptotically approaching zero as  $P$  approaches zero (dotted line in figure 17). However, figure 17 indicates that during very dry years when  $P$  is 15 inches or less,  $I$  is likely to be very small, probably less than 1 inch, at this site.

Equation 4 also was used to calculate  $I$  on a daily basis. The daily values were summed to calculate a cumulative value,  $\Sigma I$ , during the course of a year, in order to learn more about the timing of  $I$  (fig. 18). To accomplish this, an assumption was made about  $\Delta C$  and  $\Delta SP$  because these were not measured on a daily basis. Daily values of both terms were set equal to the annual values divided by the number of days in the year. This treatment introduces transient errors in the time series of  $\Sigma I$ , but these errors cancel by the end of the year. For example, a 10-inch snowfall with a water density of 10 percent will cause an immediate apparent increase in  $\Sigma I$  of 1 inch of water (assuming that  $ET$ ,  $O$ , and  $\Delta SM$  all equal 0); however, during the following days, as the snow evaporates, sublimates, or melts, the value of  $\Sigma I$  gradually decreases to a more realistic value. This process creates a sawtooth pattern in the wintertime series of  $\Sigma I$  characterized by a steep

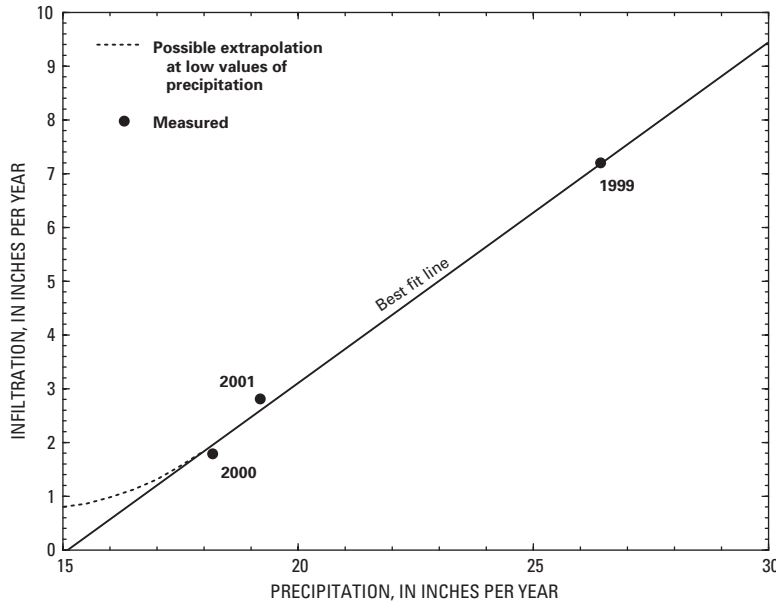


**Figure 17.** Annual precipitation and infiltration at forest site during the study period.

increase followed by a slower, asymptotic decrease. Daily values of  $\Delta SM$  were calculated using midnight measurements of soil moisture (table 4), multiplied by a rooting depth. The two soil-moisture sensors were located under the edge of a tree crown and may not be a good indication of the site-mean soil moisture at all times (Nnyamah and Black, 1977), although their long-term values probably are indicative of the site mean. In addition, the rooting depth, as noted above, may be underestimated. The effect of these two potential sampling errors is similar to that of  $\Delta C$  and  $\Delta SM$  on the calculation of  $\Sigma I$ , causing a sawtooth pattern during the warmer months. Finally,  $SM$  was estimated during early 1999 (fig. 15A), which introduces further sawtooth artifacts but again has very little effect on the final value of  $\Sigma I$  (winter soil moisture typically is low and relatively constant; see fig. 15). The sawtooth artifacts in figure 18 largely can be removed by computing a 30-day running mean of  $\Sigma I$ , shown as a dotted line in figure 18. Use of the running mean, however, does not remove the longer term storage artifacts and probably underestimates the rapidity of the infiltration events. As a result of storage artifacts, only the larger changes in  $\Sigma I$  (fig. 18) are meaningful. In particular, gradual decreases in  $\Sigma I$  (implying upward movement of water into the root zone) for extended periods primarily are caused by measurement errors in  $\Delta SM$  and represent periods of little or no infiltration.

The 30-day running mean of  $\Sigma I$  during 1999 reveals that  $I$  tends to be episodic, occurring primarily in the spring and secondarily in the fall (fig. 18A). The largest single  $I$  event occurred between about DOY's 103 and 145 of 1999. During this period, 10.4 inches of  $P$  fell, mostly in four large multiday events (fig. 15A), and about 6 inches of  $I$  occurred. Transpiration probably began for the year during this period (it began on DOY 99 in 2000 and DOY 108 in 2001) but remained at a low level during most of the period (fig. 14A). This sequence indicates that  $I$  occurs most effectively when storms are large and closely spaced in time and  $ET$  is small. These conditions all contribute to exceeding the water-holding capacity of the root zone and to causing  $I$ . Because  $ET$  depletes the root-zone soil moisture between storms, low  $ET$  rates and short periods between storms maintain high soil-moisture levels, reducing the amount of additional storage available. A steady rainfall for several days is particularly effective at causing  $I$  because root-zone storage is maintained virtually full, routing all new  $P$  directly to  $I$ . Events of about 2 inches of water separated by only a few days seem to be sufficient to cause substantial springtime  $I$  at this site. During the summer of 1999, two large rainfall events totaling 4.0 inches occurred in quick succession (about DOY's 210–222; fig. 15A) but caused little  $I$  (fig. 18A).  $ET$  levels were high between days of rainfall during this period and tended to keep the root zone relatively dry between the

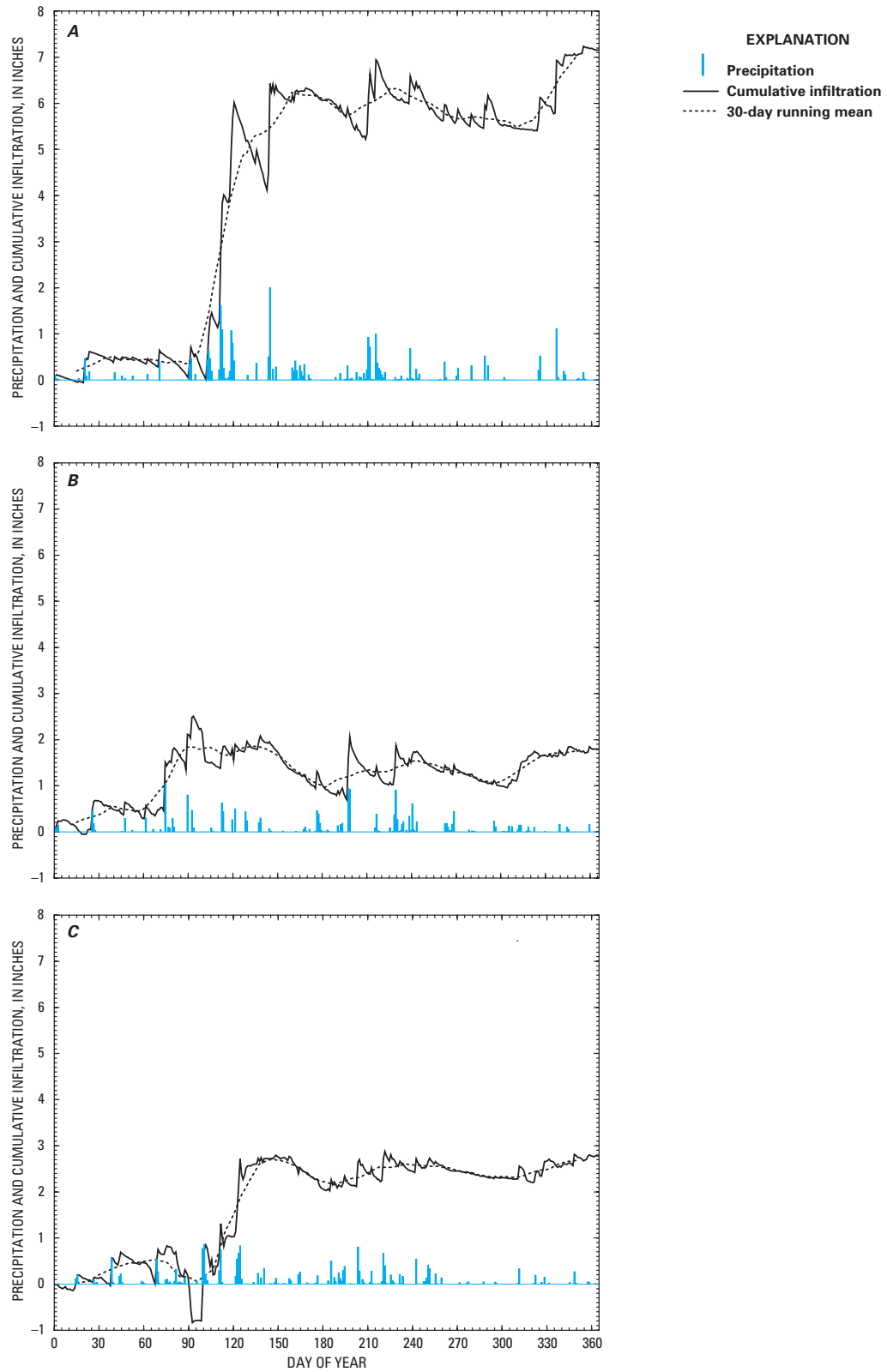


**Figure 18.** Daily precipitation and cumulative infiltration at forest site during (A) 1999, (B) 2000, and (C) 2001.

events. Only very large, successive rainfalls during the summer are likely to cause substantial *I*. In the fall of 1999, three early snowfalls that subsequently melted (DOY's 325–338; figure 15A) were sufficient to cause a significant amount of *I*. Even though these snowfalls totaled only 2.2 inches of water, *I* occurred primarily because transpiration had long since ceased for the year.

The large springtime pulse of *I* that occurred during 1999 at the forest site is not nearly as evident during 2000 or 2001. The dry spring of 2000 was notably lacking in *P*, and the storms generally lasted only 1 or 2 days (fig. 15B). The conditions needed to exceed the water-holding capacity of the root zone were seldom met, and only about 1.3 inches of *I* occurred (fig. 18B). Precipitation during the spring of 2001 shared elements with both of the previous years. Three multiday springtime storms occurred in 2001 (DOY's 100–126) that were similar in timing and duration to those in 1999 but totaled only 5.3 inches (fig. 15C). The resulting 2.4 inches of *I* (fig. 18C) was greater than in 2000 but much less than the 1999 value. A small amount of *I* appears to have occurred in the fall of 2000 and 2001 (figs. 18B and 18C), but the apparent increases in  $\Sigma I$  may just be storage-term artifacts caused by the accumulation of snowpack during this time.

In summary, during the 3-year study period at the forest site, mean annual values of precipitation (*P*), evapotranspiration (*ET*), and infiltration (*I*) were 21.27 inches, 17.63 inches, and 3.91 inches, respectively. *ET* was 82.9 percent of *P*, whereas *I* was only 18.4 percent of *P*. *ET* was positively correlated with *P* but was much less variable. As a result, *I* was quite variable because *I* is largely determined by the difference between *P* and *ET*. The 3 years spanned a relatively wide range of water availability, from slightly drier than average to very wet. For the 3 years of study, *I* was very nearly a linear function of *P*. Long-term mean *P* at this site is estimated to be 19.0 inches, yielding a long-term mean estimate for *I* of about 2.47 inches. A daily water balance revealed that *I* overwhelmingly occurs in the spring, when *ET* is still small. The amount of *I* depends on both the amount and timing of *P*. A few large storms occurring in quick succession effectively cause *I*, whereas many smaller events tend to be absorbed in the root zone and lost to *ET*. *I* also occurred in the fall after transpiration had ceased for the year, but to a lesser degree than in the

spring. Very little *I* occurred during the summer, even during relatively large storms. At these times, higher *ET* rates apparently removed soil moisture at a sufficient rate that the root zone did not exceed its water-holding capacity.

### Meadow Site and Comparison to Forest Site

Daily totals of *ET* at the meadow site and forest site are shown for 2000 and 2001 in figure 19. Daily totals of precipitation at the meadow site and daily means of soil moisture at the meadow and forest sites are shown in figure 20. Soil moisture was an integrated measurement over the 0- to 1-ft depth at the meadow site (table 5). Daily mean values of solar radiation are shown in figure 21.

Although a general similarity can be seen between the annual patterns of *ET* at the forest and meadow sites, significant differences also are apparent at various times of the year (fig. 19). The meadow soil was wetter than the forest soil year round, especially during the growing season (fig. 20), even though the two sites received equal *P* during the one full calendar year of comparison, 2001 (table 12). The meadow soil is finer grained than the forest soil and tends to hold more of the infiltrating water close to the surface. Therefore, water availability is less limiting at the meadow site, and *ET* depends more on the energy input. For example, the greatest *ET* values at the meadow site occurred during late spring (about DOY's 151–169) in 2001 (fig. 19B). The pattern of *ET* bears little resemblance to the pattern of soil moisture during this period, which decreased from about 27 percent to about 17 percent (fig. 20B). However, the pattern of *ET* is very similar to the pattern of solar radiation (fig. 21B), which also was peaking during this period. Although soil moisture was decreasing rapidly, it was in ample supply and therefore *ET* was energy limited. Further, soil moisture at this site peaked in early spring of 2001 (about DOY's 91–151, fig. 20B) before the peak *ET* (about DOY's 151–169). During the soil-moisture peak *ET* was well below its peak value (fig. 19B) and again was highly correlated with and limited by solar radiation (fig. 21B). Soil moisture was not always plentiful at the meadow site, however. The steady decrease in *ET* rates from about DOY's 209–230 in 2000 is related to the severe drop in soil moisture during that time, not to the amount of solar radiation.



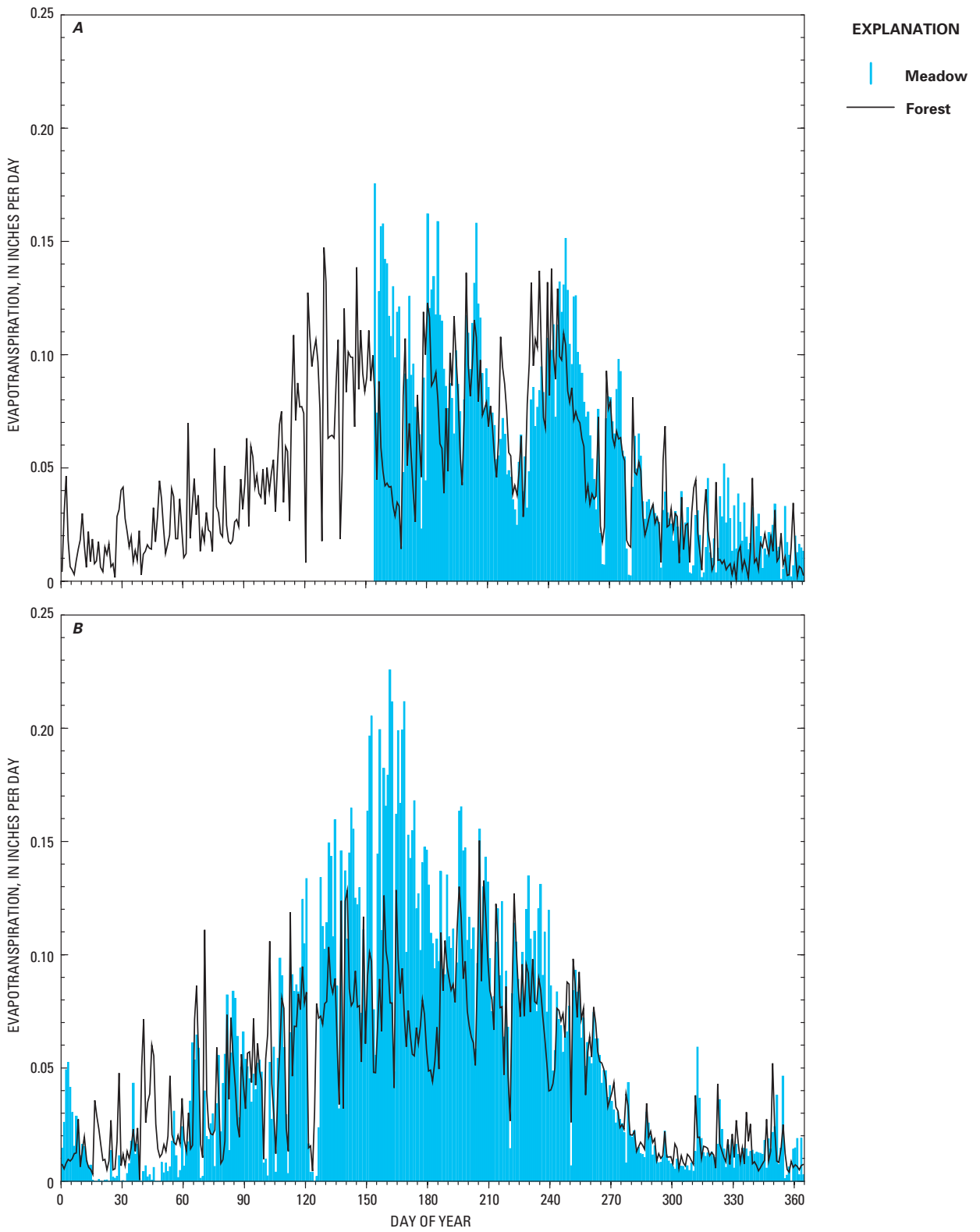


**Figure 19.** Daily evapotranspiration at meadow and forest sites during (A) 2000 and (B) 2001.

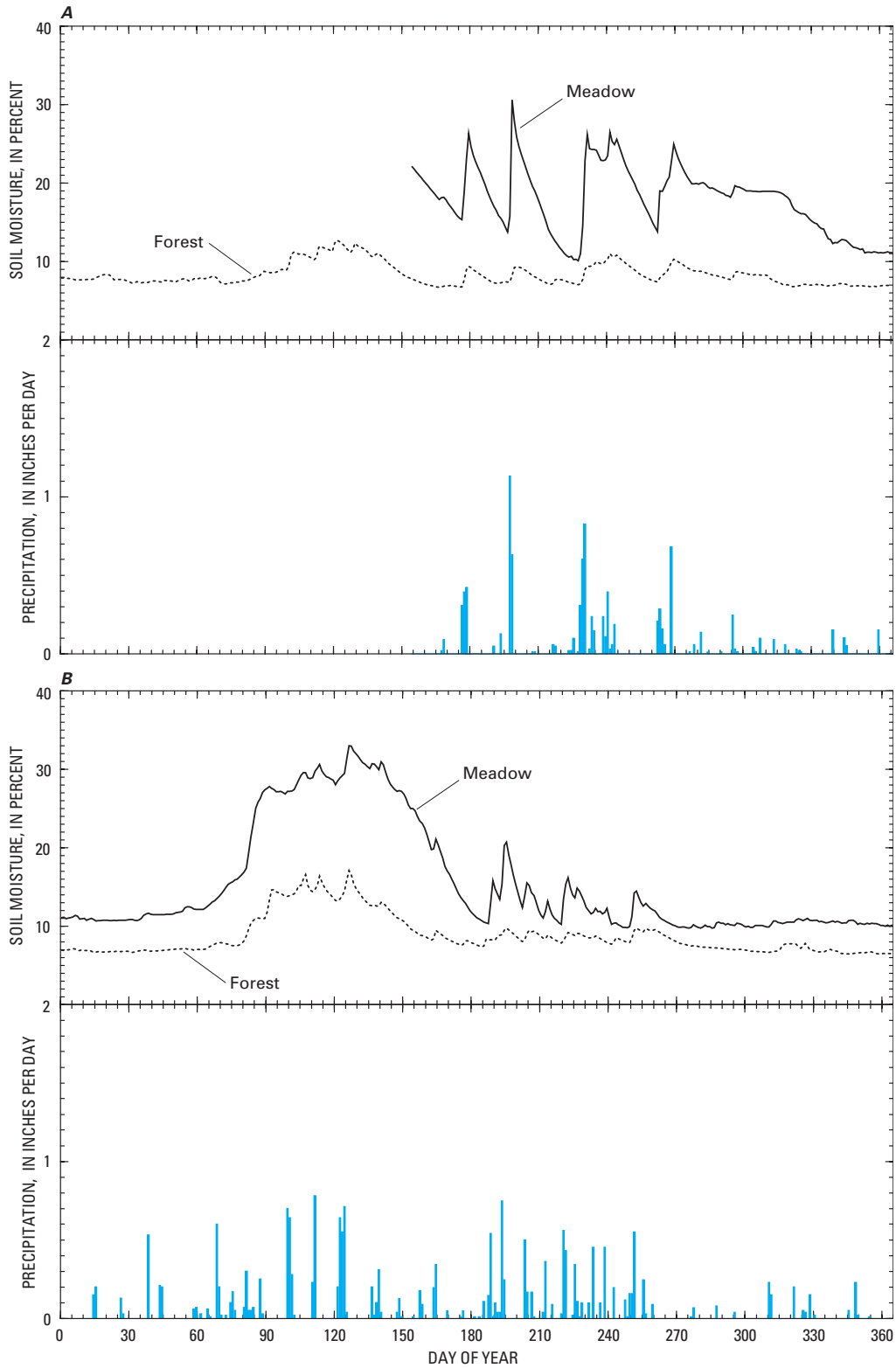


**Figure 20.** Daily precipitation at meadow site, and daily mean soil moisture at meadow and forest sites during (A) 2000 and (B) 2001.

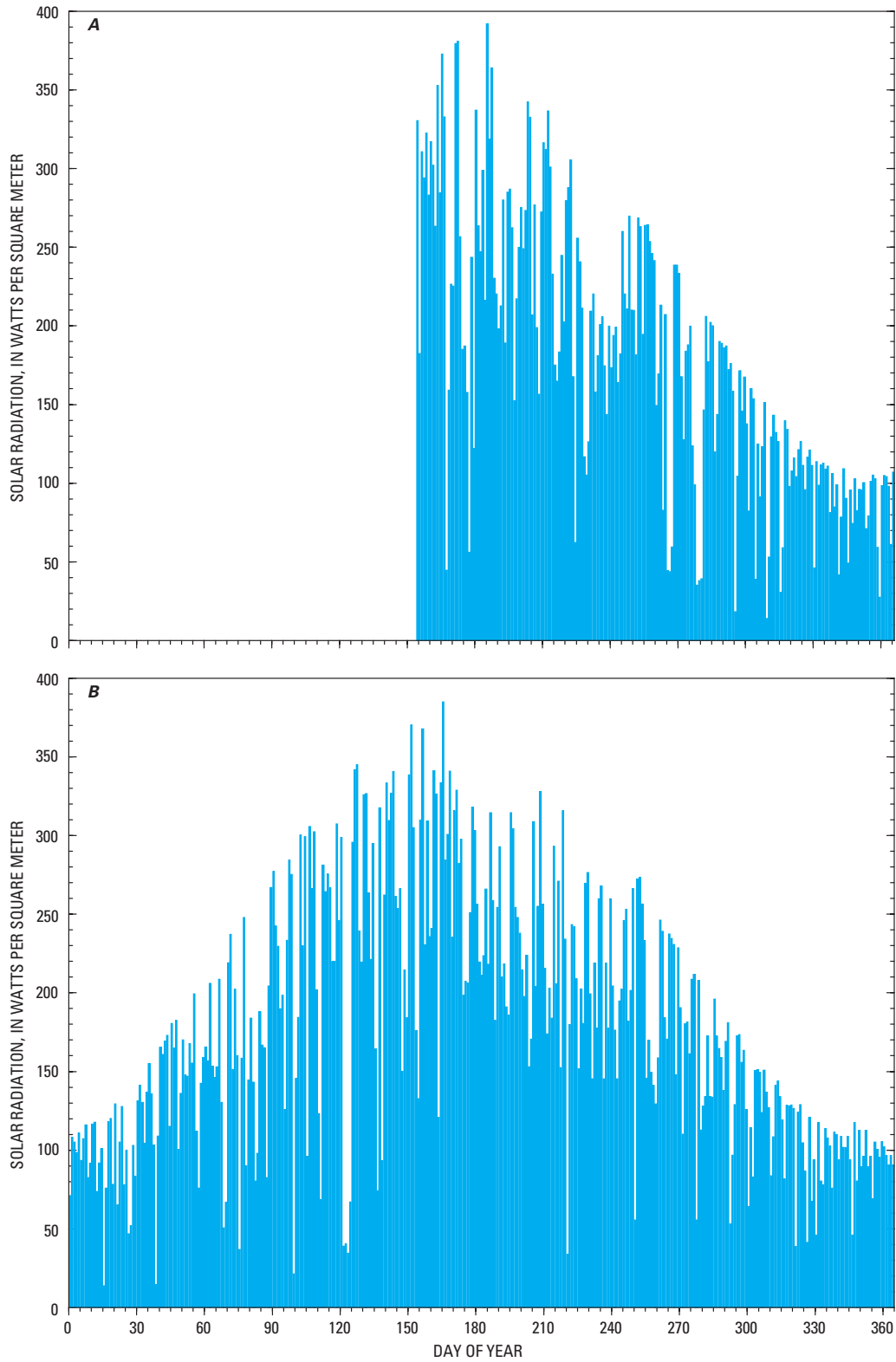


**Figure 21.** Daily mean solar radiation at meadow site during (A) 2000 and (B) 2001.

**Table 12.** Climatic and water balance summary for calendar year 2001 at meadow and forest sites

[Infiltration calculated using equation 4]

Site	Meadow	Forest
Precipitation (inches)	19.20	19.20
Evapotranspiration (inches)	20.56	16.83
Change in canopy storage (inches)	0.00	0.00
Change in snowpack storage (inches)	0.21	-0.30
Change in soil moisture storage (inches)	-0.14	-0.11
Infiltration (inches)	-1.43	2.78
Mean air temperature (°F)	41.95	43.76
Mean soil moisture (percent)	15.41	8.76
Mean solar radiation (watts per square meter)	176.38	180.3

During the growing seasons a number of short-term differences in *ET* between the two sites occur (fig. 19). The largest differences occurred when meadow *ET* rates exceeded forest *ET* rates, as on DOY's 155–167, 171–175, 181–191, and 246–263 in 2000 (fig. 19A), and DOY's 128–136, 142–148, 151–163, 165–186, and 196–203 in 2001 (fig. 19B). Every one of these periods began shortly after a rainfall, corresponded to a drying trend in soil moisture (or dry-down) at both sites, and ended just before the beginning of another rainfall (figs. 15, 20). (Technically, the first period in 2000, represented by DOY's 155–167, probably began on DOY 140 [fig. 15B], but data collection at the meadow site began on DOY 155). In general, dry-downs with greater ratios of meadow to forest soil moisture were typified by greater ratios of meadow to forest *ET*. However, this proportion was not always preserved and probably was modified somewhat by phenological differences between the meadow grasses and the forest lodgepole pines. Nonetheless, this set of dry-downs clearly illustrates that *ET* at the forest site is more sensitive to soil moisture than is *ET* at the meadow site. Differences in interception also caused short-term contrasts in growing-season *ET* rates between the two sites. Because the forest interception capacity is much greater than that of the meadow, forest *ET* rates typically were greater than meadow *ET* rates during or one day after days of rainfall. If rainfall occurred over several days, forest *ET* rates generally exceeded meadow *ET* rates for the whole period. Forest *ET* rates exceeded meadow *ET* rates due to interception on DOY's 178–180, 193–194, 217–219, and 230–236 in 2000 (fig. 19A) and DOY's 125–127 and 249–252 in 2001 (fig. 19B). Most of the significant differences

between forest and meadow growing-season *ET* rates during the study can be explained in terms of soil-moisture differences during dry-downs and differences in interception. The combination of these two influences tends to produce an alternating pattern during the growing season: greater *ET* at the forest during and just after rainfall, followed by greater *ET* at the meadow during the intervening dry-down (figs. 15, 19, 20).

During the nongrowing season, the relative evaporation (or sublimation) rates at the meadow and forest depend mostly on the amount of snow stored in the forest canopy and the amount of snowpack at both sites. Snow (or rain) stored in the forest canopy is most available for evaporation, followed by snowpack in the meadow, followed by snowpack on the forest floor. However, the interplay between these three sources is complex. The potential for meadow snowpack to evaporate depends on the percentage of snowpack cover in the meadow and the amount of snow in the forest canopy around the meadow. The reason is that snow is highly reflective, so that net radiation over a complete snowpack in winter usually is very near zero. For evaporation to take place, dark surfaces are needed to absorb solar radiation and convert this energy into heat, which is then used for evaporation. If the snowpack in the meadow is patchy, the bare patches absorb the sunlight and transfer the energy to the nearby snow patches (small-scale advection). If the forest canopy surrounding the meadow is snow-free, the trees absorb the sunlight and the energy can be advected over the meadow for evaporation there (large-scale advection). Evaporation of snow (or rain) stored in a tree canopy is always high because even at maximum snow capacity, dark fronds are partially exposed and promote small-scale advection. Small-scale advection is much more efficient than large-scale advection and will dominate if the two are in competition. Therefore, if snow is stored in the forest canopy surrounding the meadow, evaporation of the canopy snow will take precedence over evaporation of a full meadow snowpack. If the meadow snowpack is patchy and snow is stored in the surrounding forest canopy, the two evaporation rates may be similar. A patchy meadow snowpack surrounded by a snow-free forest canopy evaporates quickly because both small- and large-scale advection take place. Snowpack on the forest floor evaporates slowly because the trees shade the snowpack. The heat generated by the dark canopy moves upward into the atmosphere more easily than downward, effectively insulating the snowpack from the energy source.

The principles outlined in the previous paragraph explain most of the relative trends in *ET* seen at the forest and meadow sites during the nongrowing season (fig. 19). *ET* rates during much of this time were roughly equal, resulting from (a) a patchy meadow snowpack combined with moderate forest canopy storage, (b) a very patchy (nearly bare) meadow snowpack combined with an empty forest canopy but snow on the forest floor, or (c) no snow present at either site. These three conditions correspond to high, medium, and low rates at both sites. Interspersed among these periods of general similarity are periods when the two rates differed significantly. Some periods are very short and some are longer, but all tend to occur in response to snowfalls. Virtually all snowfalls initially boost the forest *ET* above meadow *ET* for a day or two, while the canopy snow evaporates rapidly by small-scale advection, as on DOY's 311–313, 317–318, 323, and 360–361 in 2000, and DOY's 101–104, 312, 323, and 350 in 2001. If snowfalls are small, these short bursts of forest *ET* usually deplete the canopy storage and are followed by relatively greater meadow *ET* for a short time. In this case, the meadow snowpack evaporates by a combination of large- and small-scale advection, as on DOY 319 in 2000 and DOY's 313–315, 324–326, and 352 in 2001. For larger snowfalls, or snowfalls in quick succession, the course that the relative *ET* rates take after the first day or two of relatively high forest *ET* mostly depends on the fate of the snow in the forest canopy. If the snow remains in the canopy, forest *ET* tends to be greater than meadow *ET*. However, in this foothills setting, snow often unloads from the canopy and falls to the ground before evaporating, as a result of high winds, temperature, solar radiation, or a combination of these. In this case, forest *ET* suddenly drops because the snow is shaded, the energy received by the forest is redirected to meadows by large-scale advection, and meadow *ET* rates can exceed forest *ET* rates. Two examples of snow remaining in the forest canopy for extended periods occurred on DOY's 17–33 and DOY's 40–54 in 2001. Forest *ET* was relatively high during these periods, and meadow *ET* was near zero. Examples of *ET* patterns resulting from large-scale advection occurred on DOY's 325–339 in 2000, DOY 362 in 2000 to DOY 6 in 2001, and DOY's 360–362 in 2001. Meadow *ET* significantly exceeded forest *ET* during these periods.

A water balance was computed for the meadow site 2001 calendar year using equation 4 and is compared to the forest site in table 12. *I* at the meadow

site was –1.43 inches for the year, indicating a net movement of water upward into the root zone and then into the atmosphere at the meadow site. *ET* exceeded *P* by 1.36 inches (table 12), which accounted for most of the upward movement. Differences in soil moisture probably account for the differences in *ET* between the meadow and forest sites. On average, soil moisture at the meadow site was 76 percent greater than soil moisture at the forest site (table 12), and during the growing season, it was often 100–200 percent greater (fig. 20). In contrast, mean values of solar radiation and temperature at the meadow were both lower than at the forest during 2001 (table 12) and probably did not contribute to the greater *ET* rates. As mentioned previously, the meadow grass appeared to be not overly lush, except for the grasses in the riparian zone of an intermittent stream that runs roughly south to north near the east edge of the meadow. Because the meadow slopes at about 7° down to the stream, water-table depth is expected to be deeper to the west side of the meadow and shallower to the east, approaching land surface near the stream at times when the stream is flowing. The capillary fringe thickness in the fine-grained meadow soil probably is in the range of 2–5 ft (Fetter, 1980, p. 80), creating a zone of water that is available for *ET* 2–5 ft above the water table. Therefore, water probably was amply supplied to the grass roots in a relatively large zone surrounding the stream. The *ET* station was roughly centered in the meadow. Bowen-ratio measurements are a weighted mean of *ET* rates from a source area, at this site extending about 400–500 ft upwind from the sensors. For easterly wind directions, the source area included the lush grasses in the riparian zone and parts of the meadow with shallow water-table depths. Conversely, for westerly wind directions, the source area included parts of the meadow with deeper water-table depths. An analysis of wind direction, windspeed, and *ET* indicated that 67 percent of the measured *ET* occurred during times of easterly winds (azimuth 345°–165°). Therefore, the mean *ET* measured at this site was significantly influenced by the greater *ET* rates that occurred in the riparian zone and in the shallow water table parts of the meadow. This site was selected to represent average grassland conditions in the watershed, but the measurements probably reflect somewhat wetter than average conditions because of the prevailing easterly winds at the site. Although the *ET* measurements indicate the site is a discharge area (*ET* is greater than *P*), the upper part of this meadow likely contributes to recharge while the lower part, near the stream, is a discharge area.

In summary, *ET* at the meadow site was significantly greater than *ET* at the forest site during the 1-year, 7-month period of comparative measurements. During one full calendar year (2001), meadow *ET* was 22 percent greater than forest *ET*, even though precipitation at the two sites was equal. During the growing season, interception contributed to greater *ET* rates at the forest site for short periods of time after rainfall events. However, this effect was minor compared to the greater meadow *ET* during interstorm dry-downs, when soil moisture at the forest site became limiting. Wintertime evaporation at the two sites was roughly equal, tending to be greater at the forest when intercepted snow was held in the canopy and greater at the meadow when the forest canopy was snow-free. Average soil moisture at the meadow was 76 percent greater than at the forest and often was 100–200 percent greater during the growing season. The greater soil moisture at the meadow resulted from the finer grained soil at that site and probably accounted for a large part of the difference in *ET* rates between the two sites. An intermittent stream and its associated lush riparian grasses, however, also affected the *ET* measurements at the meadow site more strongly than was anticipated because of the prevailing wind direction. As a result, the *ET* rates measured at this site probably are somewhat greater than *ET* rates from typical upland grasslands in the watershed.

## Surface-Water Conditions

Records of streamflow in Turkey Creek near the mouth of the watershed describe surface-water conditions for the entire watershed. Intrawatershed records of streamflow describe the spatial variations in watershed-scale surface-water conditions.

### Watershed Conditions

Streamflow hydrographs for four stream gages in the Turkey Creek watershed indicate an annual cycle dominated by direct runoff in the spring, usually March through May or June (fig. 22). Direct runoff is runoff that occurs in direct response to precipitation or snowmelt or both. In many years, a second period of direct runoff caused by thunderstorms occurs in the summer months. Direct runoff consists of overland flow and interflow. Records indicate that the magnitude of spring runoff ranges from daily mean peaks of less than 50 ft<sup>3</sup>/s to more than 200 ft<sup>3</sup>/s; instantaneous

flows can be greater than 1,000 ft<sup>3</sup>/s. The peak daily mean streamflow that was measured during spring runoff in 1949 is 208 ft<sup>3</sup>/s, or about 4.5 ft<sup>3</sup>/s/mi<sup>2</sup> (table 13).

Spring hydrographs in the Turkey Creek watershed are typically asymmetrical and have a strong positive skew (fewer days with high flows than low flows). Asymmetrical hydrographs can be characterized with the term “flashy,” indicating that streamflow quickly rises from low levels to peaks that are short lived and then recedes. The hydrographs have a rising limb that rises abruptly and linearly increases to a sharp peak and a falling limb that recedes more slowly than the rising limb and is curvilinear. As direct runoff attenuates, the hydrograph slope may become nearly flat, indicating a transition from interflow to base flow. The duration of spring runoff in Turkey Creek depends on the size of the snowpack and amount of spring precipitation. If the snowpack is widespread and more than a few inches thick, the spring runoff can easily persist for weeks.

The Turkey Creek watershed also experiences direct runoff as a result of local convective thunderstorms. Thunderstorm hydrographs sometimes punctuate the spring runoff hydrograph, as in May–June of 1999, and thunderstorms sometimes occur after the spring runoff hydrograph has completed its recession, as in July–August of 1999 (fig. 22). In either case, thunderstorm hydrographs have the same distinctive asymmetrical shape as spring hydrographs; however, their duration is typically much shorter. Although the largest peaks do occur from thunderstorms, in general, thunderstorms result in daily mean peaks of tens of cubic feet per second, or a fraction of typical spring peaks. Direct runoff from individual storms in the Turkey Creek watershed rarely persists for more than a few days and often lasts only hours.

As indicated previously, the principal components of direct runoff are overland flow and interflow. Interflow consists of water delivered to streams from the subsurface in direct response to precipitation or snowmelt or both. Intuitively, interflow is associated with the soil zone, where intergranular porosity is likely to establish hydraulic characteristics capable of supporting the rapid movement of water (Hewlett, 1961). In this report, the soil zone includes the transition from soil to indurated crystalline rock. The transition from the soil zone to the underlying crystalline rock is sharp in some places. In other places, however, it is gradational and consists of a weathered section of

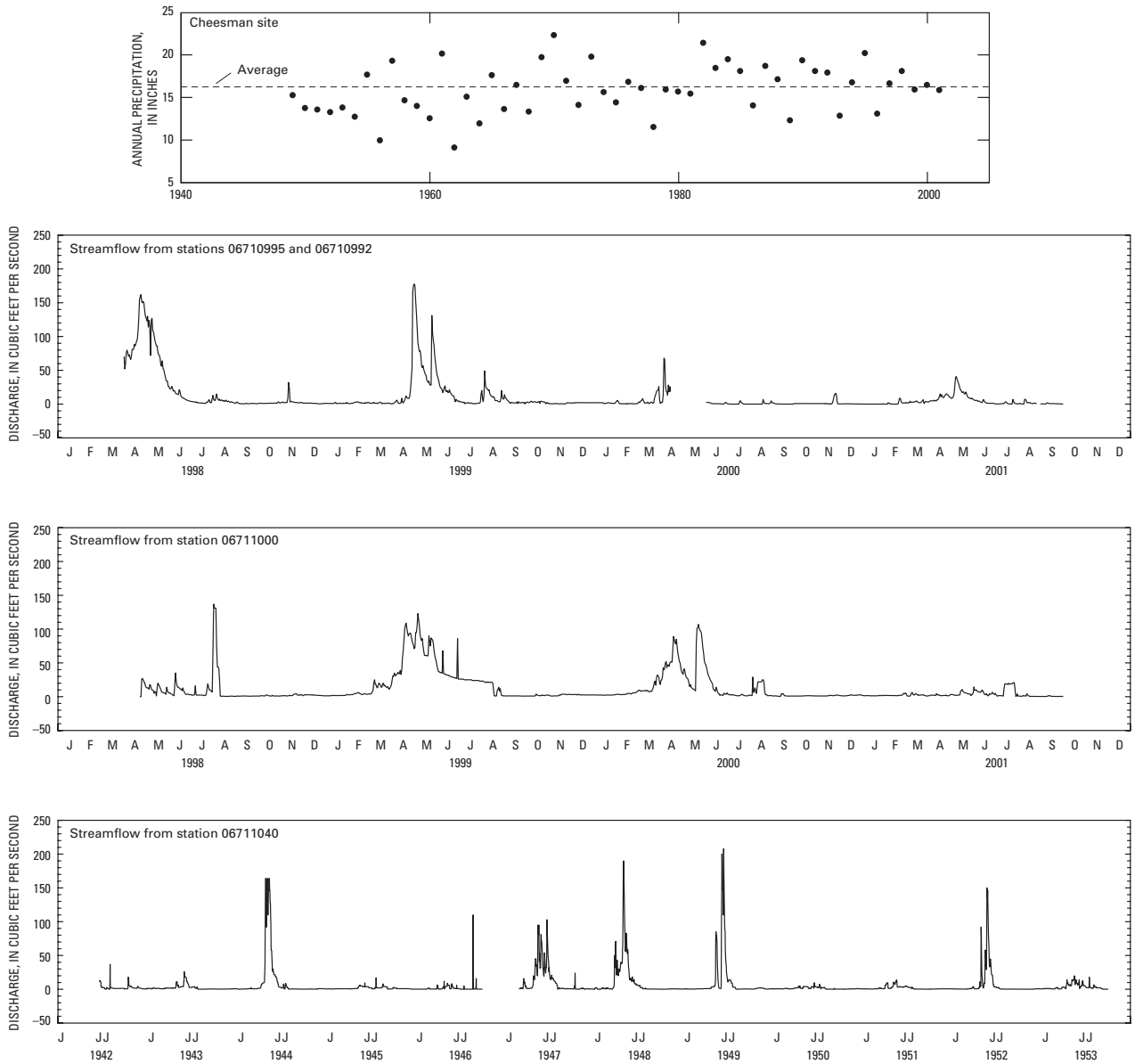


**Figure 22.** Streamflow hydrographs for the three stream gages on Turkey Creek and annual precipitation at the Cheesman site.

rock that is loose, coarse, and generally believed to be comparable to or greater than the soil zone in thickness. The bedrock surface also is commonly the site of low-angle stress-relief fractures. The soil zone and transitional weathered-bedrock zone mantle the crystalline rock surface and have a configuration that is very similar to the watershed topography. Intergranular porosity exists in the soil and weathered bedrock zones, which are collectively referred to as “regolith” in this report. The differences between the intergranular porosity present in the soil and transition zones

compared to the fracture porosity in the crystalline rock also provide a physical basis for definition of a preferential flow path along their interface.

In general, overland flow is a very quick and short-lived component of direct runoff. Interflow is usually a much larger component of the direct-runoff hydrograph than overland flow because most precipitation or snowmelt infiltrates into the subsurface (Hewlett, 1961). Because interflow emanates from the subsurface and moves through a porous medium rather than over the land surface, it moves more slowly than

overland flow. This difference in rate of movement is a principal contributor to the curvilinear nature of the recession typical of the falling limb for asymmetrical hydrographs.

Between periods of direct runoff, streamflow in the Turkey Creek watershed may be sustained at relatively steady and low levels of base flow that emanates from ground water. Streams that have sustained streamflow through relatively long rainless periods are referred to as “well sustained.” For well-sustained streams, base flows may vary seasonally but are typically steadier than variations in the components of direct runoff.

If streamflow is not sustained through relatively long rainless periods, streams become dry and are referred to as “poorly sustained” or “intermittent.” Streams may go dry because there is little ground-water recharge in their contributing drainage area or because any ground-water recharge that does occur is quickly transmitted to streamflow. The presence of base flow in streams indicates that local ground-water levels are high enough to support streamflow. The absence of base flow in the watershed does not indicate that all ground water has drained from the watershed; however, it does indicate that local ground-water levels are below the streambed.

About 65 days of zero flow, or about 5 percent of the period of record (April 1998 to April 2001), are reported for station 06710995 (table 13). During periods reported as zero streamflow in the summer of 2000, the stream was observed to be flowing a short distance both upstream and downstream from the stream gage, indicating the presence of anomalous conditions with a low bias at the gage site. The anomalous conditions are most likely related to the proximity of a major geologic contact that acts as a local streamflow sink. Records from other Turkey Creek stream gages in the vicinity of the canyon mouth, representing 16 years of measurements, indicate very few days of zero streamflow in the watershed (table 13). Compositing all streamflow records available for Turkey Creek in the vicinity of station 06710995 provides 6,506 days of streamflow record (table 13) that contains 86 days of zero streamflow, which is only about 1.3 percent of the composited record and only 21 days more than the number of days with zero streamflow in the relatively short record from 06710995.

Based on reported data, annual streamflow in Turkey Creek, reported as a depth of water over the entire watershed, ranges from as little as 0.39 inch to as much as 5.83 inches (table 14). Daily mean

streamflow is rarely greater than 100 ft<sup>3</sup>/s (less than between 1 and 2 percent of the time; table 13); however, it is frequently less than about 1 ft<sup>3</sup>/s (40 percent of all mean daily flows are less than 0.92 ft<sup>3</sup>/s; table 13).

Although the series of annual watershed streamflow values for Turkey Creek is incomplete, the series of annual precipitation data from Cheesman Reservoir (fig. 1) is complete for water years 1949 through 2001 (table 14) and can be used to characterize climatic conditions for the past several decades in the vicinity of the Turkey Creek watershed. Precipitation records from Cheesman Reservoir, which have an annual water-year average of 16.49 (table 14), are probably biased low compared to precipitation records from the Turkey Creek watershed, which have an estimated annual average of about 18 inches based on information compiled by the Colorado Climate Center (1984). At Cheesman Reservoir, for the 22-year period of water years 1980 through 2001, all but 7 years exceeded the 1949 through 2001 annual mean precipitation, indicating that conditions have been relatively wet during the past two decades. However, the Cheesman precipitation data also include relatively dry years, many of which are in the 1950's and 1960's and, in general, describe a normally distributed series of data. The Cheesman data set covers 53 years and is a more robust representation of natural climatologic conditions for the area compared to the approximately 3-year set of contemporary data collected as part of this study.

### Intrawatershed Conditions

Intrawatershed surface-water conditions help describe spatial variability of hydrologic processes in the Turkey Creek watershed and are especially useful for characterizing base-flow conditions in the four rock groups as described in the “Interflow and Base-Flow Reservoir Delineation and Parameterization” section. The intrawatershed records of streamflow are sometimes referred to as “short-term records” because they were operated only from April 2001 through July 2001. Each intrawatershed record indicates the integrated effect of all hydrologic processes occurring within its contributing drainage area. The four short-term records of streamflow (locations shown in fig. 23) were collected primarily to describe differences in base-flow rates in the watershed. Streamflow records, normalized for contributing drainage area (table 15), from the four sites are shown in figure 24 and can be used to make observations concerning the variability of base-flow rates in the watershed.



**Table 13.** Streamflow statistics for Turkey Creek

[Composite, all records of streamflow on Turkey Creek; Percent, percentage of time given streamflow, in cubic feet per second, was equaled or exceeded]

Univariate statistics				
Station	Mean	Minimum	Maximum	Days of record
06710992	5.54	0.11	41.00	171
06710995	10.97	0.00	177.75	1109
06711000	5.75	0.00	208.00	3971
06711040	11.94	0.32	137.00	1255
Composite	7.83	0.00	208.00	6506

Duration statistics					
Percent	Station and discharge				
	06710992	06710995	06711000	06711040	Composite
99.	0.13	0.00	0.09	0.34	0.01
98.	0.15	0.00	0.09	0.41	0.08
95.	0.20	0.01	0.19	0.68	0.19
90.	0.25	0.14	0.24	0.90	0.26
85.	0.32	0.42	0.28	1.09	0.33
80.	0.42	0.60	0.33	1.26	0.39
75.	0.56	0.77	0.37	1.44	0.49
70.	0.70	0.94	0.42	1.66	0.63
65.	0.84	1.14	0.51	1.91	0.78
60.	0.99	1.36	0.62	2.16	0.92
55.	1.25	1.59	0.74	2.46	1.11
50.	1.53	1.87	0.86	2.83	1.34
45.	2.06	2.14	0.99	3.20	1.62
40.	3.09	2.51	1.25	3.72	1.98
35.	4.88	3.04	1.53	4.98	2.39
30.	6.74	3.65	2.00	7.71	3.05
25.	8.59	4.96	2.65	11.95	3.94
20.	10.44	7.75	3.63	19.09	5.41
15.	12.56	15.78	5.09	24.91	10.23
10.	16.08	27.55	10.39	35.50	19.25
5.	21.61	76.91	27.23	65.49	41.76
2.	32.74	122.05	72.78	92.69	90.13
1.	37.87	149.77	114.52	108.17	122.34

The recessions, or hydrograph slopes after the peaks from spring runoff, have the typical falling-limb curvilinear shape (better seen in fig. 24B) from about May 9 to about June 13. The change in slope after about June 13 indicates the beginning of streamflow dominated by base flow. The portion of the hydrographs from about June 13 through about July 11 appears to consist almost entirely of base flow and indicates differences in base-flow contributions to streamflow. After about July 11, direct runoff from thunderstorms increased streamflow above base-flow levels at the four short-term sites.

The slope of the hydrographs during the June 13 through July 11 period indicates the rate at which ground water drains from the system to supply base flow to streams. The hydrographs for STR-1, STR-2, and STR-3 indicate about the same rate during the nearly 4-week period (fig. 24A). The hydrograph for STR-4, however, spans nearly three

log cycles and shows zero streamflow (plotted as 0.0001 ft<sup>3</sup>/s) several times during the period, indicating that at times there is no water to sustain streamflow.

In order to help assess the occurrence of base flow in other areas of the watershed, synoptic measurements of streamflow were made at several sites (fig. 23 and table 15). The measurements were made in a short period of time (4–6 hours) to minimize the influence of changing conditions. The results of these measurements, together with those from the short-term sites, indicate that on a unit area basis, two general base-flow conditions characterize the watershed. The first and more prevalent condition is that of base-flow rates of about thousandths of cubic feet per second per square mile, or less. This first category is representative of much of the watershed and includes many sites where zero streamflow was measured on July 6, 2001. The second category, which appears to be restricted mostly to the southwest part of the watershed, is that of base-flow rates of hundredths or even tenths of cubic feet per second per square mile. Measurements at sites SNCG1, SNCG2, SNFZ1, SNFZ2, and SNSP2 consistently fall into this category based on measurements made in the summer and fall of 2001.

The synoptic measurements also help to document two other important conditions in the Turkey Creek watershed. The measurements made at sites SNSP3 and SNQA2 are on the same tributary to North Turkey Creek upstream and downstream from a tens-of-acres area containing alluvial-fill deposits. The measurements made at these sites indicate that alluvial areas can, at times, store ground water and sustain streamflow.

The series of seven synoptic measurements of upstream diversions from Turkey Creek made at the Independent Highline ditch (upstream from station 06710995 and referred to as DIV in table 15), station 06710995, and station 06710992 can be used to evaluate how records from station 06710995 represent ground-water discharge conditions. For synoptic measurements made during periods of base flow at nearly the same times, the sum of measurements from the Independent Highline and station 06710995 should be about equal to the measurement at station 06710992, assuming that there are no losses or gains in the relatively short intervening stream reach between the two stream gages. The mean ratio between the sum and streamflow at station 06710992 is 0.93 for the seven sets of measurements and indicates that there is about a 7-percent loss between the two stations. Because of the observations of

**Table 14.** Measured precipitation and streamflow in and near the Turkey Creek watershed

[Note: Water year, one year period beginning in October and ending in September; Precipitation is from Cheesman (Colorado Climate Center, 2002); all measurements in inches; Min, minimum; Max, maximum, Var, variance; --, no data]

Sorted by water year						Sorted by measured precipitation					
Water year	Precipitation	Streamflow				Water year	Precipitation	Streamflow			
		Station 06710992	Station 06710995	Station 06711000	Station 06711040			Station 06710992	Station 06710995	Station 06711000	Station 06711040
1943	--	--	--	0.75	--	1943	--	--	--	0.75	--
1944	--	--	--	3.55	--	1944	--	--	--	3.55	--
1945	--	--	--	0.45	--	1945	--	--	--	0.45	--
1946	--	--	--	0.39	--	1946	--	--	--	0.39	--
1947	--	--	--	2.94	--	1947	--	--	--	2.94	--
1948	--	--	--	3.23	--	1948	--	--	--	3.23	--
1949	15.85	--	--	2.90	--	1962	9.47	--	--	--	--
1950	14.28	--	--	0.60	--	1956	10.31	--	--	--	--
1951	14.10	--	--	0.55	--	1978	11.97	--	--	--	--
1952	13.73	--	--	1.98	--	1964	12.40	--	--	--	--
1953	14.35	--	--	0.78	--	1989	12.76	--	--	--	0.58
1954	13.18	--	--	--	--	1960	13.00	--	--	--	--
1955	18.29	--	--	--	--	1954	13.18	--	--	--	--
1956	10.31	--	--	--	--	1993	13.35	--	--	--	--
1957	19.98	--	--	--	--	1996	13.57	--	--	--	--
1958	15.17	--	--	--	--	1952	13.73	--	--	1.98	--
1959	14.50	--	--	--	--	1968	13.85	--	--	--	--
1960	13.00	--	--	--	--	1951	14.10	--	--	0.55	--
1961	20.87	--	--	--	--	1966	14.14	--	--	--	--
1962	9.47	--	--	--	--	1950	14.28	--	--	0.60	--
1963	15.66	--	--	--	--	1953	14.35	--	--	0.78	--
1964	12.40	--	--	--	--	1959	14.50	--	--	--	--
1965	18.28	--	--	--	--	1986	14.57	--	--	--	--
1966	14.14	--	--	--	--	1972	14.62	--	--	--	--
1967	17.08	--	--	--	--	1975	14.97	--	--	--	--
1968	13.85	--	--	--	--	1958	15.17	--	--	--	--
1969	20.42	--	--	--	--	1963	15.66	--	--	--	--
1970	23.15	--	--	--	--	1949	15.85	--	--	2.90	--
1971	17.59	--	--	--	--	1981	15.99	--	--	--	--
1972	14.62	--	--	--	--	1974	16.21	--	--	--	--
1973	20.53	--	--	--	--	1980	16.25	--	--	--	--
1974	16.21	--	--	--	--	1979	16.48	--	--	--	--
1975	14.97	--	--	--	--	1999	16.51	--	3.29	--	--
1976	17.46	--	--	--	--	1977	16.67	--	--	--	--
1977	16.67	--	--	--	--	2001	16.41	--	0.86	--	--
1978	11.97	--	--	--	--	2000	17.07	--	0.96	--	--
1979	16.48	--	--	--	--	1967	17.08	--	--	--	--
1980	16.25	--	--	--	--	1997	17.25	--	--	--	--
1981	15.99	--	--	--	--	1994	17.36	--	--	--	--
1982	22.16	--	--	--	--	1976	17.46	--	--	--	--
1983	19.13	--	--	--	--	1971	17.59	--	--	--	--
1984	20.19	--	--	--	--	1988	17.73	--	--	--	3.54
1985	18.76	--	--	--	--	1965	18.28	--	--	--	--
1986	14.57	--	--	--	--	1955	18.29	--	--	--	--
1987	19.36	--	--	--	5.83	1992	18.58	--	--	--	--
1988	17.73	--	--	--	3.54	1985	18.76	--	--	--	--
1989	12.76	--	--	--	0.58	1998	18.76	--	--	--	--
1990	20.09	--	--	--	--	1991	18.77	--	--	--	--
1991	18.77	--	--	--	--	1983	19.13	--	--	--	--
1992	18.58	--	--	--	--	1987	19.36	--	--	--	5.83
1993	13.35	--	--	--	--	1957	19.98	--	--	--	--
1994	17.36	--	--	--	--	1990	20.09	--	--	--	--
1995	20.96	--	--	--	--	1984	20.19	--	--	--	--
1996	13.57	--	--	--	--	1969	20.42	--	--	--	--
1997	17.25	--	--	--	--	1973	20.53	--	--	--	--
1998	18.76	--	--	--	--	1961	20.87	--	--	--	--
1999	16.51	--	3.29	--	--	1995	20.96	--	--	--	--
2000	17.07	--	0.96	--	--	1982	22.16	--	--	--	--
2001	16.21	0.81	--	--	--	1970	23.15	--	--	--	--
Mean	16.49										
Min	9.47										
Max	23.15										
Var	8.95										

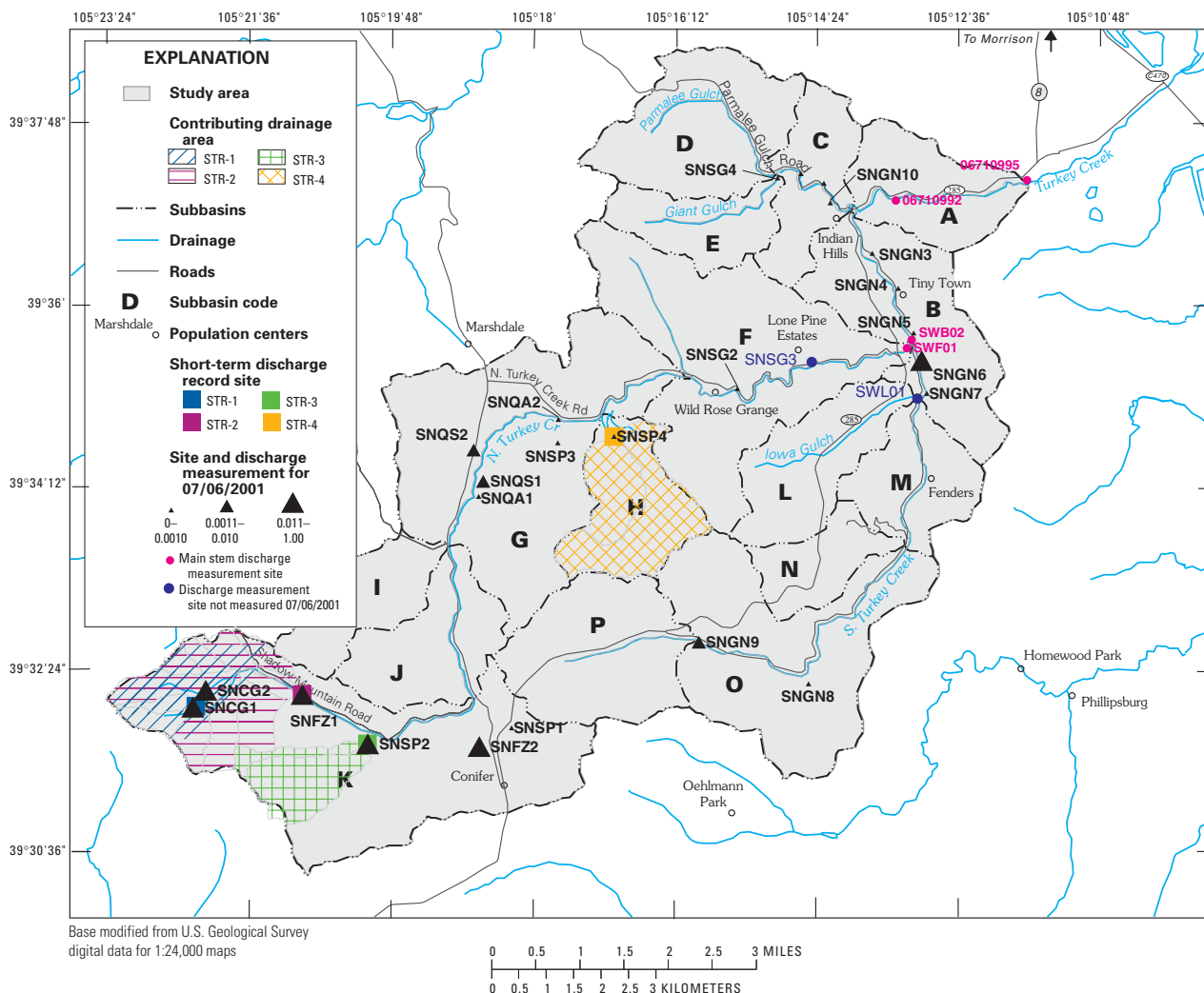


Figure 23. Locations of short-term record stream gages and sites of synoptic streamflow measurements.

streamflow near station 06710995 described in the “Watershed Conditions” section, it seems reasonable to conclude that the losses are occurring near station 06710995.

### Ground-Water Conditions

Ground-water conditions are described on the basis of time-series measurements of water levels in wells and a synoptic round of water-level measurements made in fall 2001. In addition, an analysis of SEO well-construction data is used to characterize ground-water conditions, especially reported well yields. In this report, the term “reported yield” is used to represent the estimated well yield, typically developed using undocumented techniques at the time of well construction, indicated in SEO records.

### Time-Series Water Levels

Figure 25 illustrates fluctuations in ground-water levels in monitoring wells in the Turkey Creek watershed. The first five sets of graphs in figure 25 illustrate historical (left graph) and contemporary (right graph) ground-water levels at the same well. The remainder of the graphs illustrate fluctuations in contemporary ground-water levels measured as part of this study. Precipitation from the Cheesman climatologic site is shown across the top of the graph for historical water-level comparisons and from a variety of local rain gages for contemporary water-level comparisons.

Ground-water levels fluctuate seasonally in the monitoring wells; the highest water levels correlate directly with snowmelt and precipitation and indicate the effects from recharge. After the seasonal highs, water levels recede at a relatively constant rate during

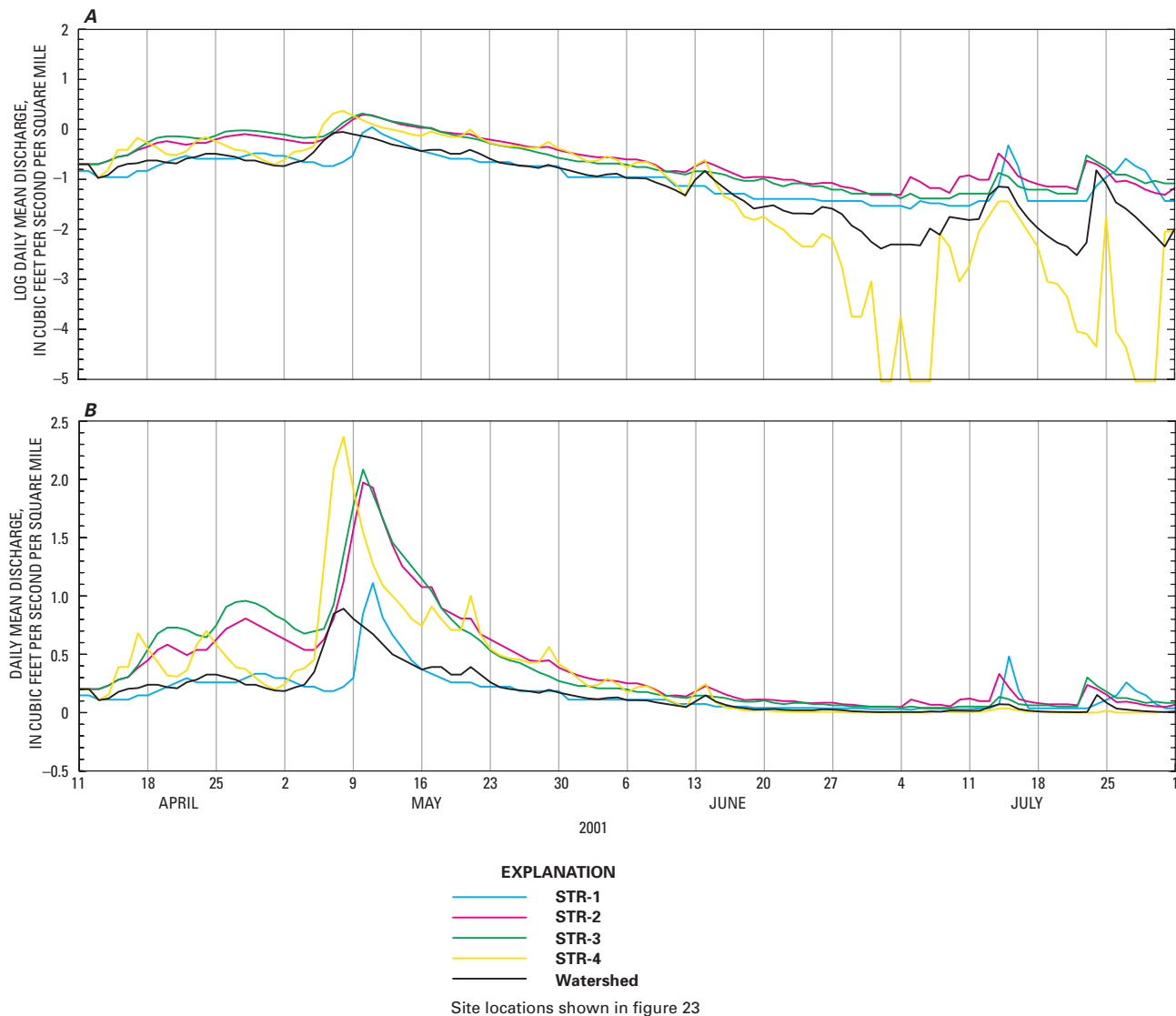


**Figure 24.** Hydrographs from short-term records of streamflow (A, log; B, arithmetic).

rainless periods until additional recharge occurs. This pattern is most readily seen in the contemporary ground-water levels where snowmelt and the accumulation of precipitation from March through May 1999 are accompanied by the highest recorded water levels in almost all of the monitoring wells (fig. 25). Precipitation in July and August 1999 is correlated with a slight rise in water levels in most wells. Precipitation was less in 2000 and 2001 than in 1999, but rises in ground-water levels in 2000 and 2001 still can be associated with precipitation events. The time lag between precipitation and rise in water levels may be as much as an effect of measurement frequency, which is daily for

precipitation and monthly for water levels, as it is of recharge rate (fig. 25). Contemporary water levels in most of the monitoring wells have fluctuated from 3 to 20 ft. Water levels fluctuated about 80 ft in MH4 and about 50 ft in MH7.

Historical ground-water levels also appear to correlate with precipitation events and had large fluctuations over time (fig. 25). In the early 1970's, water levels were measured more frequently than in the late 1970's through 1980's; therefore, the earlier part of the hydrograph shows more seasonal variability. In general, the hydrographs indicate an overall decrease in water levels occurred at MH1, MH5, and MH9 from

1974 through 1983. Contemporary water levels (1998–2001) at these three wells are similar to water levels measured 1974–83. However, the decrease does not continue at the same rate into the contemporary 1999–2000 period, possibly the result of a change in climatic conditions. Water levels at MH10 appear to be relatively stable through time. MH8 shows a slight decrease in water level (about 4 ft) from the 1970’s through 2000. The annual low (lowest ground-water elevation, generally occurring during fall or winter months when ground-water recharge is minimal or nonexistent) for MH1, MH5, MH8, MH9, and MH10 for the contemporary period are comparable to annual lows measured 1974–83, but these wells represent only a fraction of the Turkey Creek watershed.

Continuous water-level measurements were collected at three monitoring wells (MH1, MH5, and MH8) from May to October of 2001 and are shown in figure 25. Water levels in MH1 and MH8 are more directly affected by smaller amounts of precipitation than the water level at MH5. Precipitation of approximately 0.5 inch on August 8 resulted in a water-level rise that peaked near August 13 in MH1 and on August 10 in MH8. There was no apparent water-level rise in MH5 from the same precipitation event. Precipitation of approximately 0.9 inch on September 7 resulted in an increase of about 0.2 ft over 2 days in MH8, while only a very small or no water-level rise occurred in MH1 and MH5.

**Table 15.** Synoptic measurements of streamflow made at rock group sites and surface-water sampling sites

[Local identifier; 8 U.S. Geological Survey digit station number, or a 2 to 4 character prefix to a sequential number indicating geology of contributing drainage area (SP for intrusive, GN for metamorphic, FZ for fault zone, CG for Pikes Peak Granite, QA or alluvium, QS for alluvium and intrusive, and SG for intrusive and metamorphic), additional local identifiers indicate Independent Highline ditch (DIV), the sum of DIV and station 06710995 (TOT), the ratio of TOT and 06710992 (RATIO), sites that were part of the surface-water sampling network (characters 1 and 2 = SW); cda, contributing drainage area, in square miles; cfs, discharge in cubic feet per second; cfsm, unit area discharge in cubic feet per second per square mile; --, no data]

Local identifier	Date of measurement in month, day, 2-digit year format																
	070601			092001			102501			110201		110601		110901		111301	
	cda	cfs	cfsm	cfs	cfsm	cfs	cfsm	cfs	cfsm	cfs	cfsm	cfs	cfsm	cfs	cfsm	cfs	cfsm
SNCG1	0.27	0.009	0.0333	0.007	0.0259	0.0024	0.0089	--	--	--	--	--	--	--	--	--	--
SNCG2	0.27	0.040	0.1481	0.030	0.1111	0.013	0.0481	--	--	--	--	--	--	--	--	--	--
SNFPZ1	2.33	0.196	0.0841	0.162	0.0695	0.111	0.0476	--	--	--	--	--	--	--	--	--	--
SNFPZ2	1.72	0.097	0.0564	0.040	0.0233	0.030	0.0174	--	--	--	--	--	--	--	--	--	--
SNGN1	--	0.000	0.000	--	--	--	--	--	--	--	--	--	--	--	--	--	--
SNGN2	--	0.000	0.000	--	--	--	--	--	--	--	--	--	--	--	--	--	--
SNGN3	--	0.000	0.000	--	--	--	--	--	--	--	--	--	--	--	--	--	--
SNGN4	--	0.000	0.000	--	--	--	--	--	--	--	--	--	--	--	--	--	--
SNGN5	--	0.000	0.000	--	--	--	--	--	--	--	--	--	--	--	--	--	--
SNGN6	0.69	0.119	0.1725	0.0025	0.0036	0.001	0.0014	--	--	--	--	--	--	--	--	--	--
SNGN7	--	0.000	0.000	--	--	--	--	--	--	--	--	--	--	--	--	--	--
SNGN8	--	0.000	0.000	--	--	--	--	--	--	--	--	--	--	--	--	--	--
SNGN9	2.90	0.007	0.0024	0.030	0.0103	0.017	0.0059	--	--	--	--	--	--	--	--	--	--
SNGN10	0.41	0.0003	0.0007	0.0017	0.0041	0.0011	0.0027	--	--	--	--	--	--	--	--	--	--
SNSP1	0.70	0.000	0.000	0.000	0.000	0.000	0.000	--	--	--	--	--	--	--	--	--	--
SNSP2	0.96	0.068	0.0708	0.045	0.0469	0.035	0.0365	--	--	--	--	--	--	--	--	--	--
SNSP3	--	0.000	0.000	--	--	--	--	--	--	--	--	--	--	--	--	--	--
SNSP4	1.00	0.001	0.0010	0.0002	0.0002	0.0045	0.0045	--	--	--	--	--	--	--	--	--	--
SNQA1	--	0.000	0.000	--	--	--	--	--	--	--	--	--	--	--	--	--	--
SNQA2	0.65	0.0005	0.0008	0.000	0.000	0.0001	0.0002	--	--	--	--	--	--	--	--	--	--
SNQS1	0.46	0.0041	0.0089	0.000	0.000	0.000	0.000	--	--	--	--	--	--	--	--	--	--
SNQS2	0.37	0.0024	0.0065	0.0029	0.0078	0.0041	0.0127	--	--	--	--	--	--	--	--	--	--
SNSG3	0.41	--	--	0.000	0.000	0.0004	0.0010	--	--	--	--	--	--	--	--	--	--
SNSG4	1.34	0.0013	0.0010	0.000	0.000	0.000	0.000	--	--	--	--	--	--	--	--	--	--
DIV	--	0.160	--	0.470	--	0.423	--	0.380	--	0.513	--	0.423	--	0.876	--	--	--
TOT	--	0.160	0.0034	0.586	0.0124	0.480	0.0102	0.393	0.0083	0.596	0.0126	0.458	0.0097	0.921	0.0195	--	--
RATIO	--	0.76	0.74	1.11	1.07	1.23	1.18	0.86	0.83	0.91	0.88	0.68	0.66	0.99	0.97	--	--
SWF01	24.56	0.230	0.0094	0.540	0.0220	0.354	0.0140	--	--	--	--	--	--	--	--	--	--
SWB02	13.32	0.076	0.0057	0.083	0.0062	0.051	0.0038	--	--	--	--	--	--	--	--	--	--
SWL01	2.00	--	--	--	--	0.017	0.0085	--	--	--	--	--	--	--	--	--	--
06710992	45.80	0.210	0.0046	0.530	0.0116	0.390	0.0085	0.456	0.0100	0.657	0.0143	0.670	0.0146	0.927	0.0202	--	--
06710995	47.42	0.000	--	0.116	--	0.057	--	0.013	--	0.083	--	0.035	--	0.045	--	--	--

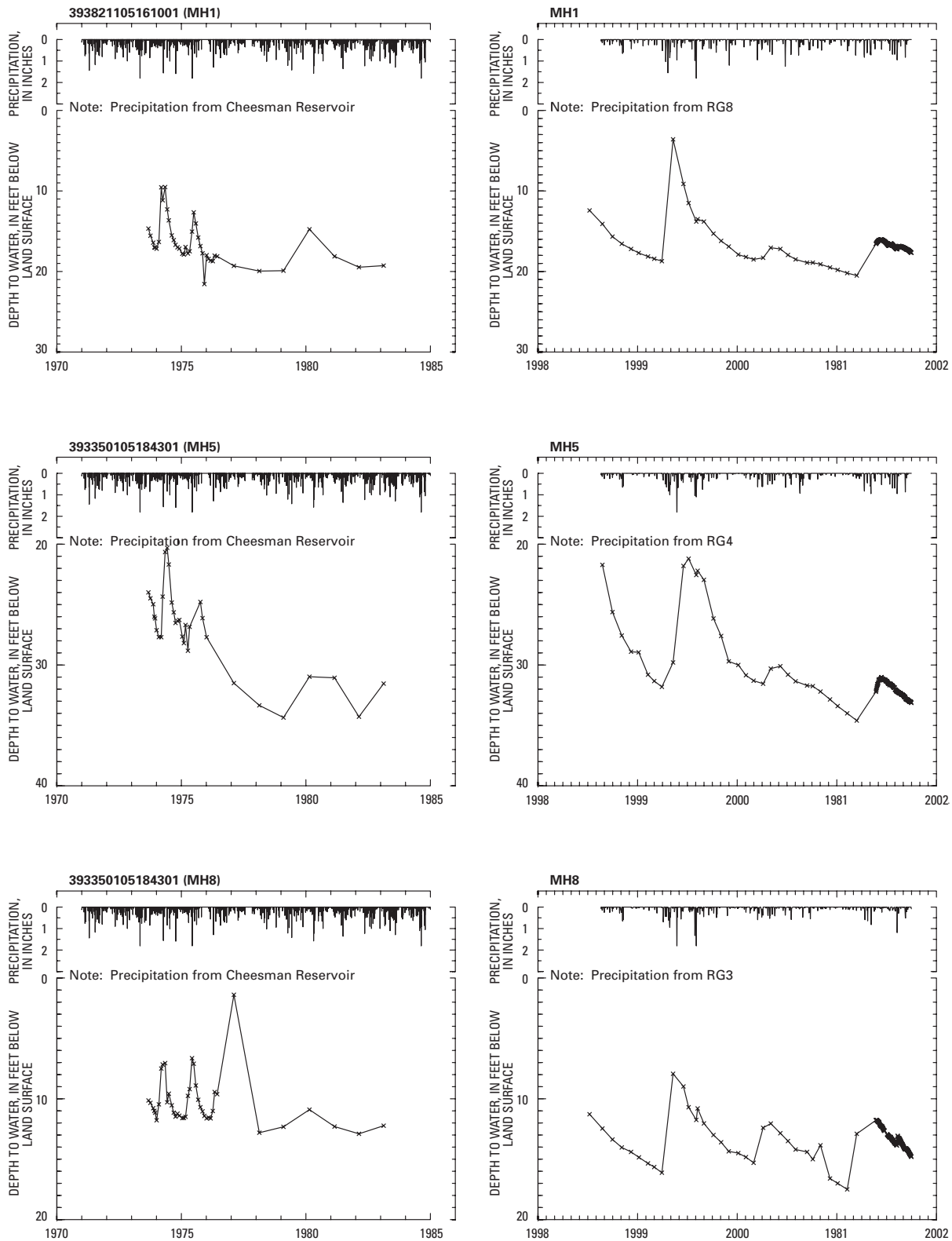
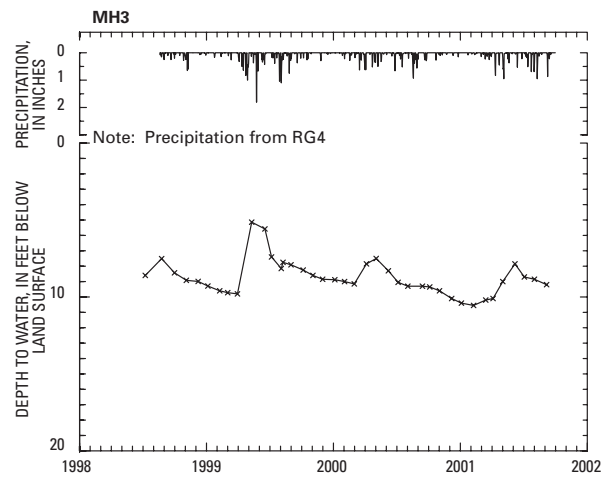
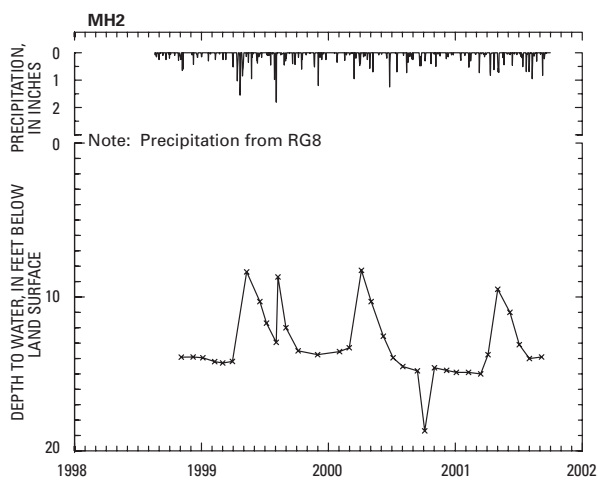
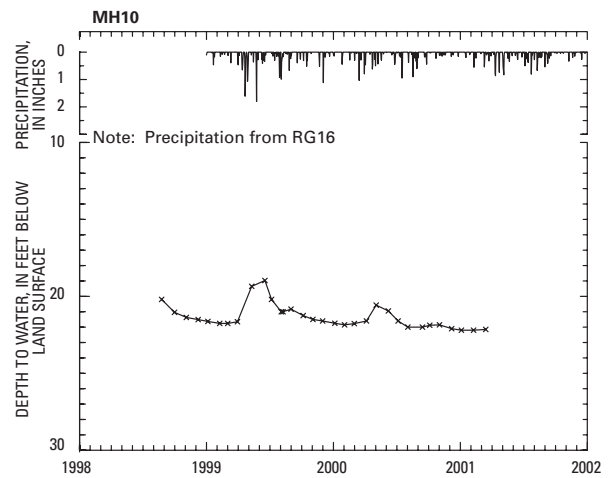
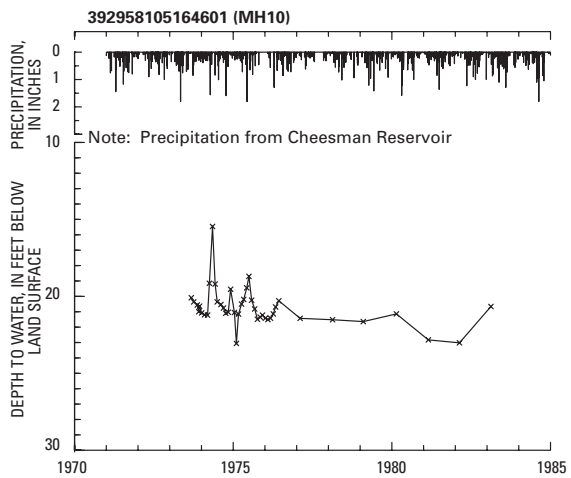
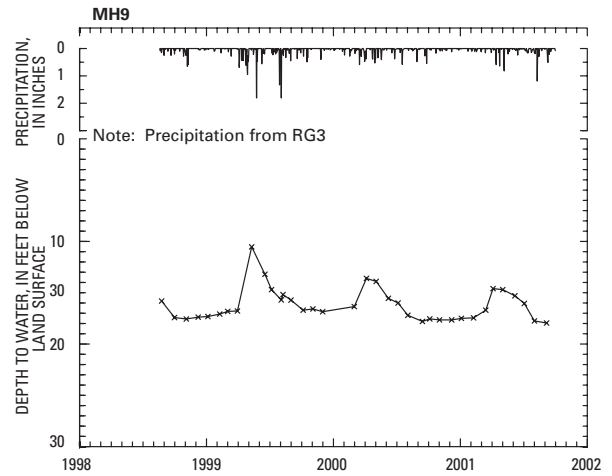
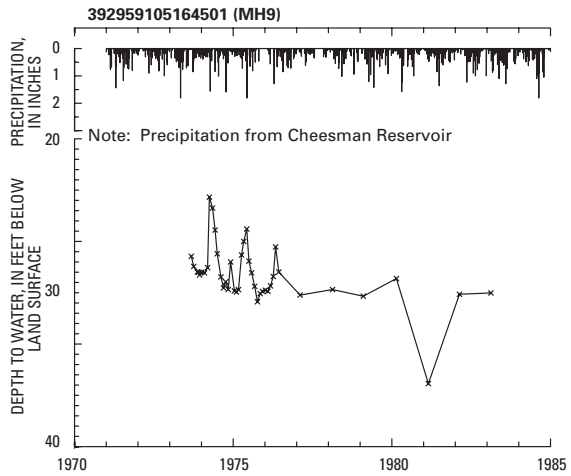
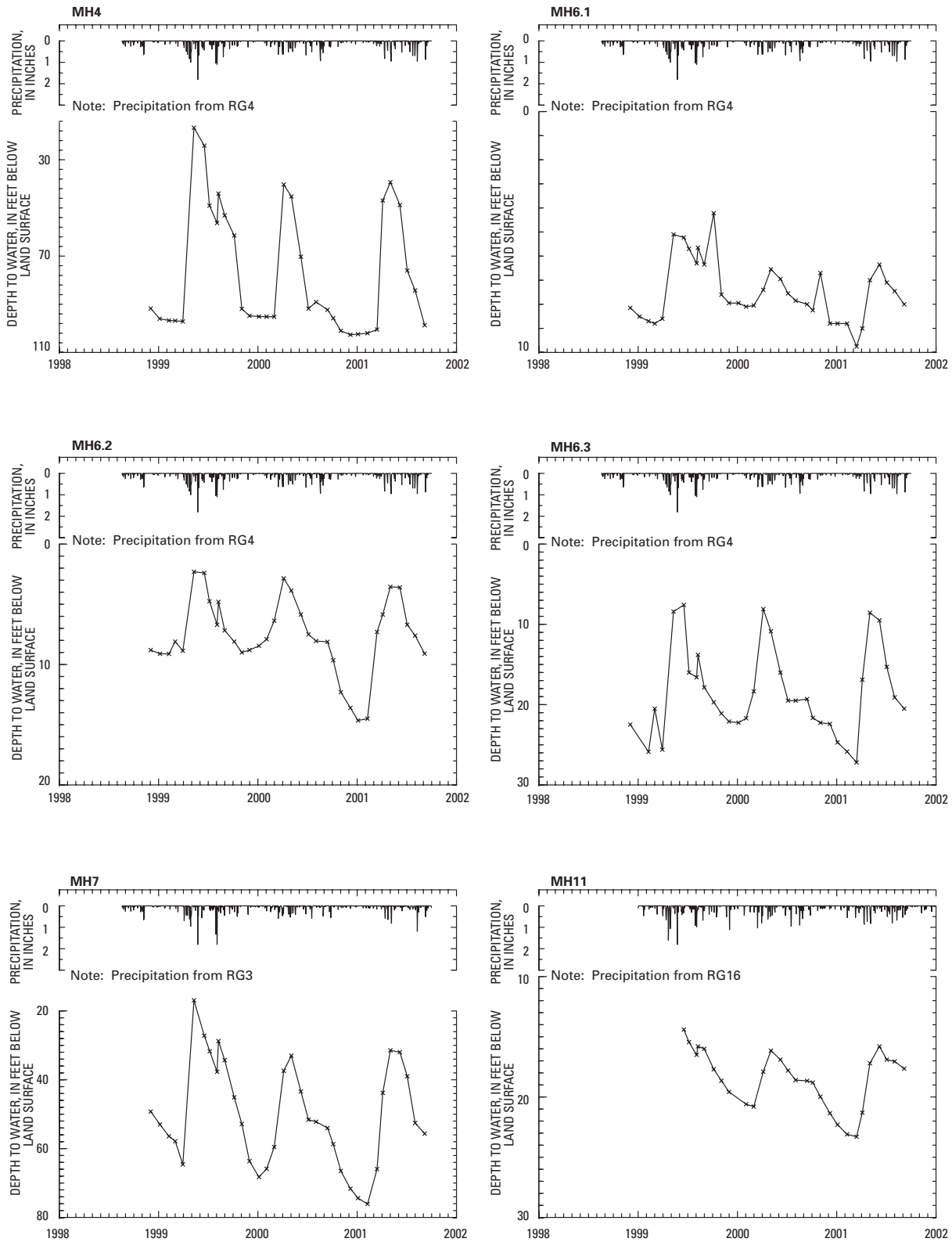


Figure 25. Ground-water fluctuations in water-level monitoring wells.



**Figure 25.** Ground-water fluctuations in water-level monitoring wells—Continued.



**Figure 25.** Ground-water fluctuations in water-level monitoring wells—Continued.



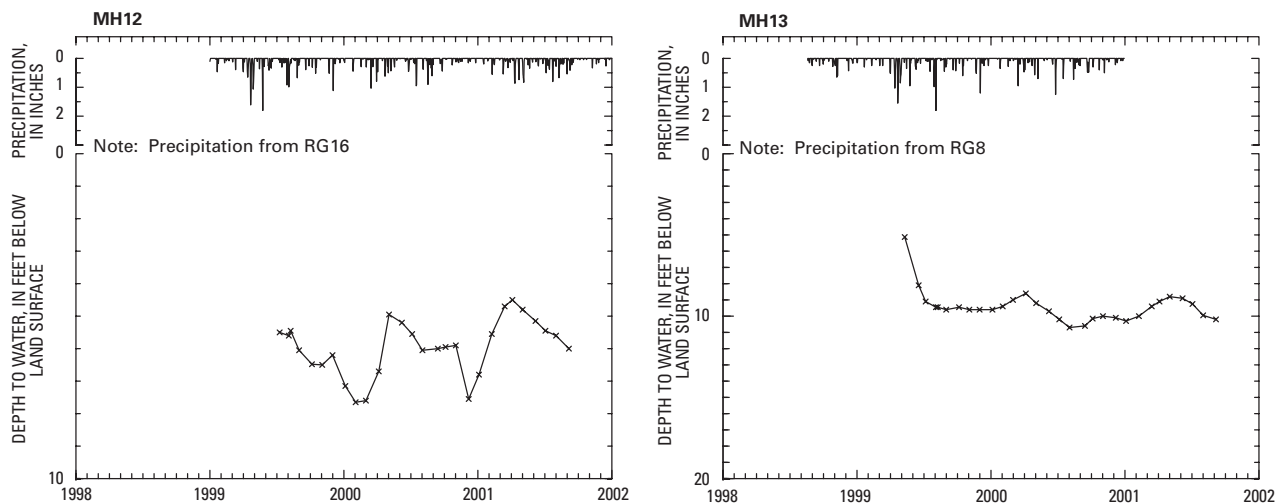


Figure 25. Ground-water fluctuations in water-level monitoring wells—Continued.

### Synoptic Water Levels

Synoptic measurements of depth to water were obtained September 24–October 4, 2001. Measurements were made at wells identified in a spatial analysis of depth-to-water data from the SEO. Variogram analysis was performed to estimate range; the method of variogram analyses is discussed in the Appendix. As a result of the variogram analysis, a grid of square cells, with dimensions of about 0.5 mi by 0.5 mi, was created over the watershed with the goal of finding one candidate well for water-level measurement in each cell; wells that had reported total depths of less than 75 ft were not included. The mean and median depth to water in each cell was calculated from the SEO data. First priority was given to wells that had previously been sampled as a part of this study. Next priority was given to wells from the SEO database that had a depths to water nearest the mean or, if skewed, median depth to water for that cell. Jefferson County personnel contacted each well owner to gain permission to make depth-to-water measurements. A few wells also were added to the network during field activities, usually in areas that had not been represented in the defined network because the well owner could not be reached by phone. The network established in this exercise has the potential of becoming a regularly visited water-level monitoring network that could be used to evaluate ground-water conditions over the long term.

Measurements from the network described above were used to construct the water-table map shown in figure 26, and the depth-to-water contour map shown in figure 27. Well locations were determined in the field by Global Positioning System (GPS) equipment. Measured, and presumed, static depth-to-water level measurements from 134 wells were subtracted from land-surface elevations estimated from a topographic map. The resulting ground-water elevations were plotted and, assuming homogeneous and isotropic conditions, contoured to construct a water-table map (fig. 26). In a similar manner, depth-to-water measurements were plotted and contoured to construct a depth-to-water contour map (fig. 27).

The water-table surface in figure 26 generally appears to be a continuous surface that approximates the topography of the watershed, indicating that ground water generally exists in an unconfined state. Water-table contours can indicate direction and relative rate of ground-water movement. For example, along the southwest edge of watershed, the water-table contours indicate that ground-water flow is from the southwestern boundary of the watershed, perpendicular to the water-table contours, to the northeast toward North Turkey Creek (fig. 26). Throughout the Turkey Creek watershed, these inferred flow directions are important for determining general direction and rate of movement of ground water in the crystalline rocks or to streamflow. In general, the water-table map indicates that ground water moves from high to low topographic areas. There

are no obvious differences in the water table due to bedrock geology or environmental conditions at the current spatial resolution.

The depth-to-water map in figure 27 indicates that there are some areas of the watershed where depths to water are generally less than 50 ft; the mean depth to water is about 105 ft. The map also indicates that there are some areas where depths to water are greater than 300 feet; in general, areas of the largest depths to water are where local relief is greatest. Some areas of the watershed are not contoured because they are outside the extent of the computer-generated grid shown in the figure 27, which represents the geometric extent of the well network.

### Analysis of State Engineer Well-Construction Data

Univariate statistics for all available well-construction data were prepared to summarize well characteristics in the watershed (table 16). Variogram analysis was used to evaluate spatial relations of reported well yields in the watershed.

#### Univariate Statistics

Univariate statistics for well-construction details indicate a mean reported yield of 5.56 gallons per minute (gal/min) and a median of 4 gal/min. The statistics also indicate that the distribution of reported yields is somewhat skewed as a result of a few reports

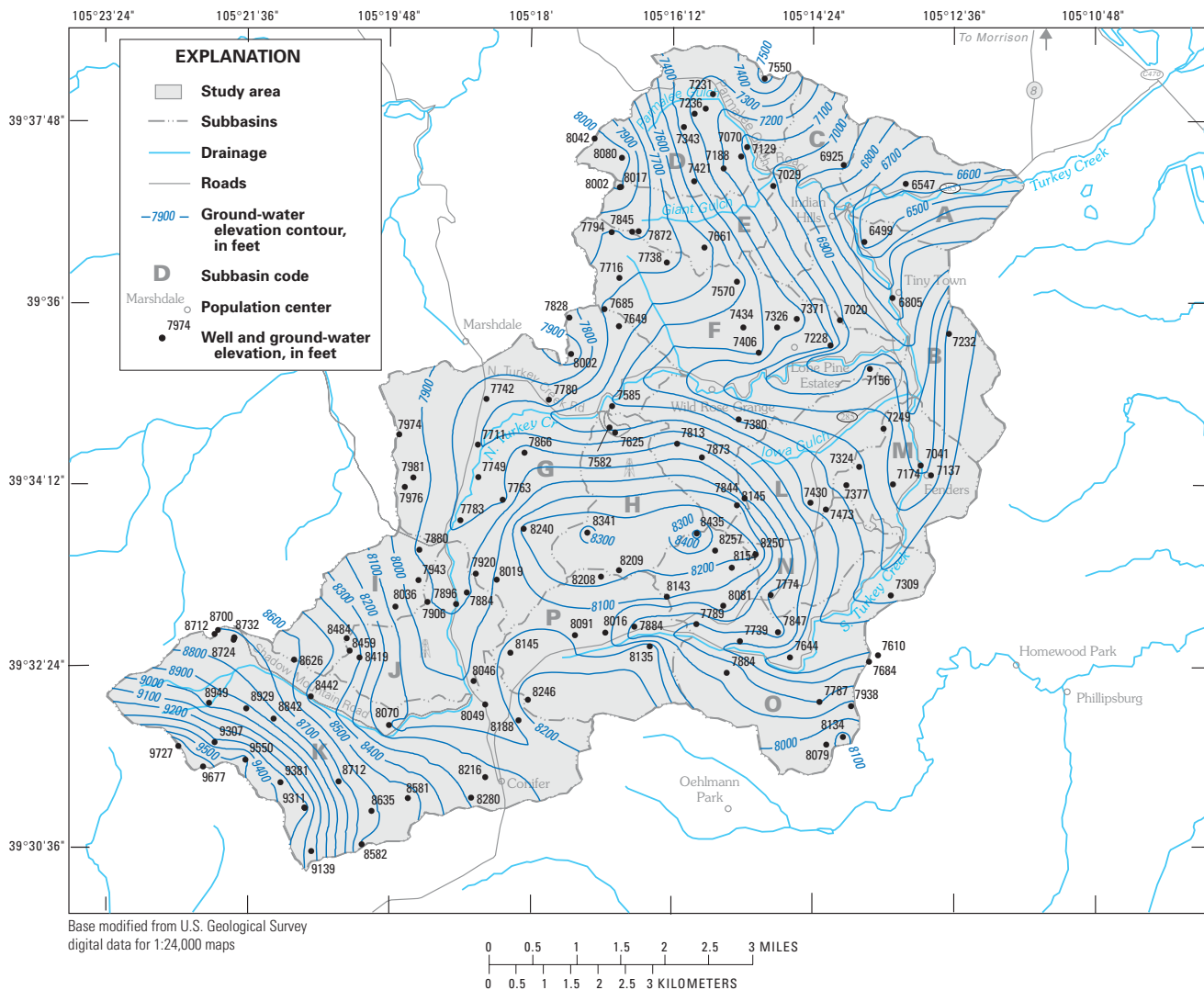
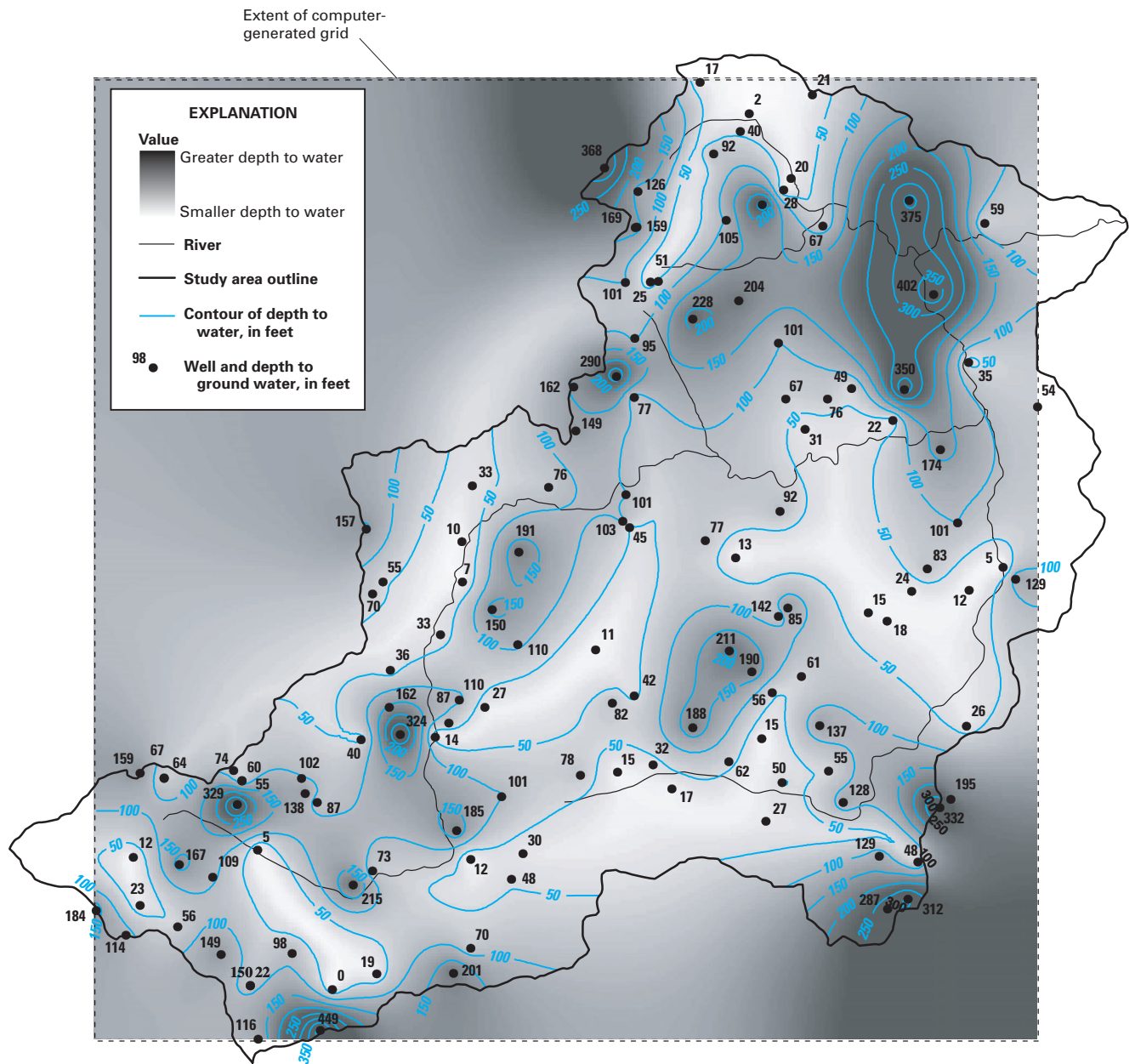


Figure 26. Ground-water table in the Turkey Creek watershed, September 2001.



**Figure 27.** Contours of depth to ground water for September 2001.

of relatively high yield wells. Wells with reported yields in the range of greater than 15 to 50 gal/min represent about the upper 1.5 percent of the distribution and were defined as “reported high-yield wells” for the purposes of this study. The locations for these 23 reported high-yield wells are shown in figure 5.

Eight of the 14 rock types listed in table 1 had well-construction data available for fewer than 15 wells. By aggregating individual rock types into the

four groups identified in the “Geologic Framework” section—metamorphic, intrusive, fault zone, and Pikes Peak Granite—the rock group statistics become more robust. Table 17 compares depth to water, well depth, and water-table elevation among the rock groups. Wells completed in metamorphic and intrusive rocks had water levels at about the same depth (means of about 88.65 and about 93.35 ft below land surface, respectively) which was about 16 to 22 ft deeper than

**Table 16.** Univariate statistics and correlations for well-construction characteristics

[Note: yield, reported well yield in gallons per minute; td, total well depth, in feet below land surface; dtw, depth to water in feet below land surface; prfln, casing perforation length, in feet; tperf, depth to top of perforated length, in feet below land surface; bperf, depth to bottom of perforated length, in feet below land surface; Stddev, standard deviation; Q1, 25th percentile; Q3, 75th percentile; Min, minimum; Max, maximum; N, number of cases; --, not applicable]

Univariate statistics								
Variable	Mean	Median	Stddev	Q1	Q3	Min	Max	N
yield	5.56	4	5.37	2	7	0.06	50	1109
td	340.19	305	164.12	225	425	6	902	1116
dtw	89.13	70	75.62	40	108	1	519	1075
prfln	154.04	100	107.44	100	200	4	663	631
tperf	219.91	195	147.35	105	300	9	820	631
bperf	373.95	350	165.35	260	477	55	900	631

Pearson correlations						
Variable	tperf	bperf	prfln	yield	td	dtw
tperf	1.00000	0.76962	-0.18742	-0.05043	0.76338	0.54985
bperf	--	1.00000	0.48294	-0.10946	0.98141	0.56203
prfln	--	--	1.00000	-0.09924	0.46291	0.11056
yield	--	--	--	1.00000	-0.12423	-0.12020
td	--	--	--	--	1.00000	0.56226
dtw	--	--	--	--	--	1.00000

Valid cases = 626      Missing cases = 490

water levels in wells completed in the Pikes Peak Granite (mean of 72.7 ft below land surface) or fault-zone rocks (mean of 70.9 ft below land surface). Total well depth for wells completed in fault-zone rocks (293 ft below land surface) are shallower on average than for wells completed in the other rock groups. Water-table elevation also differs by rock group, with highest elevations in the Pikes Peak Granite and lowest elevations in the metamorphic rocks.

Because reported well yields are probably the best index of aquifer characteristics available in the well-construction details, and because a goal of this study is to identify any spatial patterns in aquifer characteristics, univariate statistics also were prepared for reported well yields, rock types, and rock groups (table 18). Uncertainty associated with the reported well yields results from use of several undocumented methods for determining the reported yield during a period of nearly five decades.

The rock-group statistics indicate some variation in means for reported well yields, but the differences are not large and do not, by themselves, provide a basis for defining differences in aquifer characteristics. The combination of the highest mean for reported yield and a variance that is much higher than the

variance for other rock groups, however, indicates that the fault-zone rock group is capable of yielding relatively large amounts of water compared to other rock groups. The Pikes Peak Granite is similar, at least in mean, to the fault-zone rocks for reported well yields.

Results in table 18 also include information describing reported well yields through time that, for wells with a reported date of construction, indicate the number of wells drilled per decade is, in general, increasing. There was a large increase in the population and the number of buildings in the watershed in the 1970's and smaller increases in the 1980's and 1990's. Substantial increases in the reported number of wells drilled between the 1960's and 1970's are likely a result, at least in part, of widespread acceptance of record-keeping practices. It is clear, however, that there are many more wells in the watershed today (2001) than there were in the 1950's, or even the 1970's.

Figure 28 provides a graphical summary of well construction, reported well yields, and well depths. Reported well depths have increased with time. The graph of reported well yield and well depth in figure 28 indicates there is no strong relation between well yield and well depth in the Turkey Creek watershed.

### Variogram Analysis

The variogram analysis, which is similar to work by Drew and others (1999), consisted of preparing a variogram surface map for all reported yields. The process of constructing a variogram surface map is described in the Appendix. The analysis was done for two sets of reported well yields: first, for all reported yields and second, for all reported yields except the arbitrarily defined reported high-yield wells (reported yields greater than 15 gal/min).

Some basic spatial relations were simply evaluated as a preliminary step to the variogram analysis to determine if conditions of spatial stationarity were acceptable. For the purposes of this study stationarity can be described as a condition of no large spatial trends in the reported well yields. The spatial-trend evaluations used as part of this study, simple linear regression of reported yields relative to spatial coordinates and an initial inspection of computed variogram, indicated stationary data.

**Table 17.** Descriptive statistics for selected physical characteristics of permitted wells from the State Engineers Office, by rock group

[NGVD29, Nation Geodetic Vertical Datum 1929; NA indicates number of wells with records of total depth but no record of depth to water]

	Intrusive	Metamorphic	Fault zone	Pikes Peak Granite
	<b>Depth to water (feet)</b>			
Mean	93.35	88.65	70.92	72.69
Minimum	1.00	4.00	5.00	20.00
Maximum	410.00	519.00	300.00	170.00
Standard deviation	76.42	76.46	59.95	43.77
25th percentile	40.00	40.00	40.00	41.75
50th percentile	71.00	70.00	50.00	66.50
75th percentile	120.00	105.75	85.00	85.75
Number of wells	315	741	44	16
NA	11	23	7	0
	<b>Well depth (feet)</b>			
Mean	349.42	339.45	293.25	322.19
Minimum	10.00	6.00	10.00	120.00
Maximum	900.00	902.00	660.00	710.00
Standard deviation	160.90	165.78	163.54	138.51
25th percentile	250.00	221.00	183.75	250.00
50th percentile	320.00	305.00	265.00	301.00
75th percentile	441.00	425.00	388.75	340.00
Number of wells	315	741	44	16
NA	0	0	0	0
	<b>Water-table elevation (feet above NGVD29)</b>			
Mean	8225.67	7759.55	8134.40	9169.65
Minimum	6589.52	6464.88	6878.16	8918.32
Maximum	9731.76	9482.48	8754.32	9528.40
Standard deviation	639.93	426.14	396.88	175.30
25th percentile	7868.72	7448.06	8098.32	9061.00
50th percentile	8159.00	7796.56	8242.64	9156.12
75th percentile	8564.08	8039.28	8301.68	9212.70
Number of wells	315	741	44	16
NA	11	23	7	0

**Table 18.** Univariate statistics for reported well yields by rock type and group and through time

[Note: Category, except for ALL, which refers to all rock types together, refers to rock types defined in table 1, or rock groups defined in "Geologic Framework" section; N, number of cases; --, not applicable; <, before]

Category	Mean	Variance	Median	Skewness	Minimum	Maximum	N
ALL	5.56	28.86	4.00	2.83	0.06	50.00	1109
By rock type							
GMG	15.00	--	15.00	--	15.00	15.00	1
P	10.50	0.50	10.50	0.00	10.00	11.00	2
XGNM	4.50	24.50	4.50	0.00	1.00	8.00	2
FG	4.53	10.84	3.55	0.42	2.00	9.00	4
XGQG	1.93	1.47	1.40	0.78	1.00	4.00	10
FGU	2.88	2.52	3.00	-0.26	0.25	5.00	12
XHCS	2.56	2.57	2.25	0.33	0.75	5.00	12
XMGD	3.67	9.16	2.50	1.17	1.00	11.00	14
YPP	6.91	21.86	5.00	0.77	1.00	15.00	15
FLTZN	7.33	83.88	4.00	2.78	0.75	50.00	43
XF	4.47	14.34	3.00	1.60	0.06	15.00	44
XB	5.41	25.08	3.50	2.01	0.20	30.00	163
YSP	5.60	29.18	4.00	3.25	0.40	50.00	285
XM	5.70	28.11	4.00	2.46	0.20	50.00	450
By rock group							
METAMORPHIC	5.51	26.12	4.00	2.38	0.06	50.00	677
INTRUSIVE	5.39	27.90	4.00	3.30	0.40	50.00	309
FAULT ZONE	7.33	83.88	4.00	2.78	0.75	50.00	43
PIKES PEAK GRANITE	6.91	21.86	5.00	0.77	1.00	15.00	15
All rock types in time							
1950 - < 1960	2.00	--	2.00	--	2.00	2.00	1
1960 - < 1970	2.80	3.70	2.00	0.73	1.00	6.00	5
1970 - < 1980	5.46	24.17	3.40	1.67	0.25	30.00	191
1980 - < 1990	7.03	51.75	5.00	2.65	0.06	50.00	133
1990 - < 1998	5.98	36.28	4.00	3.34	0.25	50.00	296

The results of the variogram analysis provide two principal findings (fig. 29). The first finding is that there is a substantial contrast in the variogram surface map prepared using all reported yields and the map prepared using all but the reported high-yield wells. The variogram surface map prepared with all but the reported high-yield wells (fig. 29A) consists of mostly uniformly colored cells and has a relatively uniform appearance, indicating that there is a relatively constant amount of variability in reported well yields in the Turkey Creek watershed regardless of the well spacing. When the reported high-yield wells are included, the variogram surface map consists of mostly blue with some bright (yellow and red) cells, indicating relatively higher amounts of variability with increasing well spacings (fig. 29B).

The observed differences described in the previous paragraph correspond to a conceptual model in which there is a relatively uniform background condition, or fabric, that is accented with local deviations

caused by wells with reported yields greater than 15 gal/min. In a practical sense, this indicates that there can be variability at very short spacings—that is, two wells located very close to each other will not necessarily have the same yield. This condition appears to be relatively constant over the entire watershed; however, a relatively persistent presence, which can be thought of as a larger fabric, of higher yield wells exists.

The second finding has to do with directional characteristics of the variogram surface maps. Each map, but in particular the map including reported high-yield wells (on the basis of a general cluster of lighter colored blocks has a tendency to indicate from low to high contrast in the northwest-to-southeast direction. In effect, this is the orientation of the so-called larger fabric. The northwest-to-southeast direction corresponds with the orientation of structural fabric described in the "Geologic Framework" section and indicates that high-yield features may align themselves with this fabric.

## Water-Quality Characteristics in the Turkey Creek Watershed

General water quality is described in this report with univariate statistics, Stiff and trilinear diagrams (Hem, 1985), maps of areal distribution of selected constituents, and comparison of sample results with applicable State (Colorado Department of Public Health and Environment, 1998) and Federal (U.S. Environmental Protection Agency, 1996) water-quality standards. Also presented are additional discussions of tritium results, chloride/bromide ratios, wastewater-compound analyses, mass balances of chloride sources, and seasonality of specific conductance.

### General Water-Quality Characteristics

Statistical summaries of quarterly ground-water and surface-water samples collected in the Turkey Creek watershed are shown in table 19 and table 20. Censored values in table 19 and table 20 are those concentrations that are less than reporting levels for the laboratory.

The Stiff diagrams in figure 30 of composite ground water and composite surface water illustrate that the general chemical composition of water in Turkey Creek watershed is calcium bicarbonate type water. This is consistent with other studies that have reported on the chemical composition of water from crystalline

rocks along the Front Range (Bruce and McMahon, 1997). A feature of the Stiff diagram for composite surface water is a stronger chloride component than in the Stiff diagram for composite ground water, which indicates that chloride concentrations from surface-water samples were, in general, elevated compared to chloride concentrations in samples of ground water. In fact, calcium-chloride type water similar to the diagram shown for GWO10 was observed in both ground and surface water; however, the chloride component was more pronounced in surface-water samples.

Trilinear diagrams are plots of relative major-ion composition that represent the chemical signature of the major-ion concentrations of a water sample as a single point on a diagram. Waters with different major-ion chemistry plot in different locations on the diagram, allowing clusters of points to be interpreted as being distinct. A trilinear diagram indicating results for all ground-water and surface-water samples collected for this study is shown in figure 31. Similar to the Stiff diagrams for composite ground water and surface water, the trilinear diagram indicates that the most common anion differences between ground-water and surface-water major-ion chemistry are the presence of more chloride, less bicarbonate, and less sulfate in surface-water samples. For cations, the pattern in the trilinear diagram shows somewhat more sodium and less calcium in most surface-water samples than in most ground-water samples.

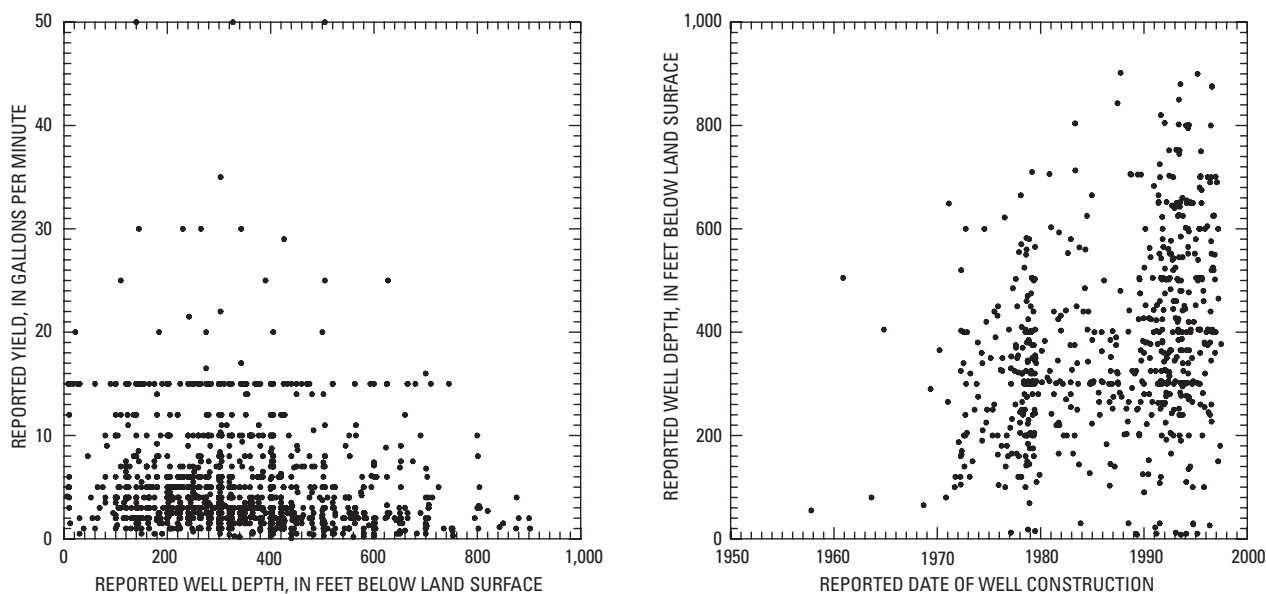
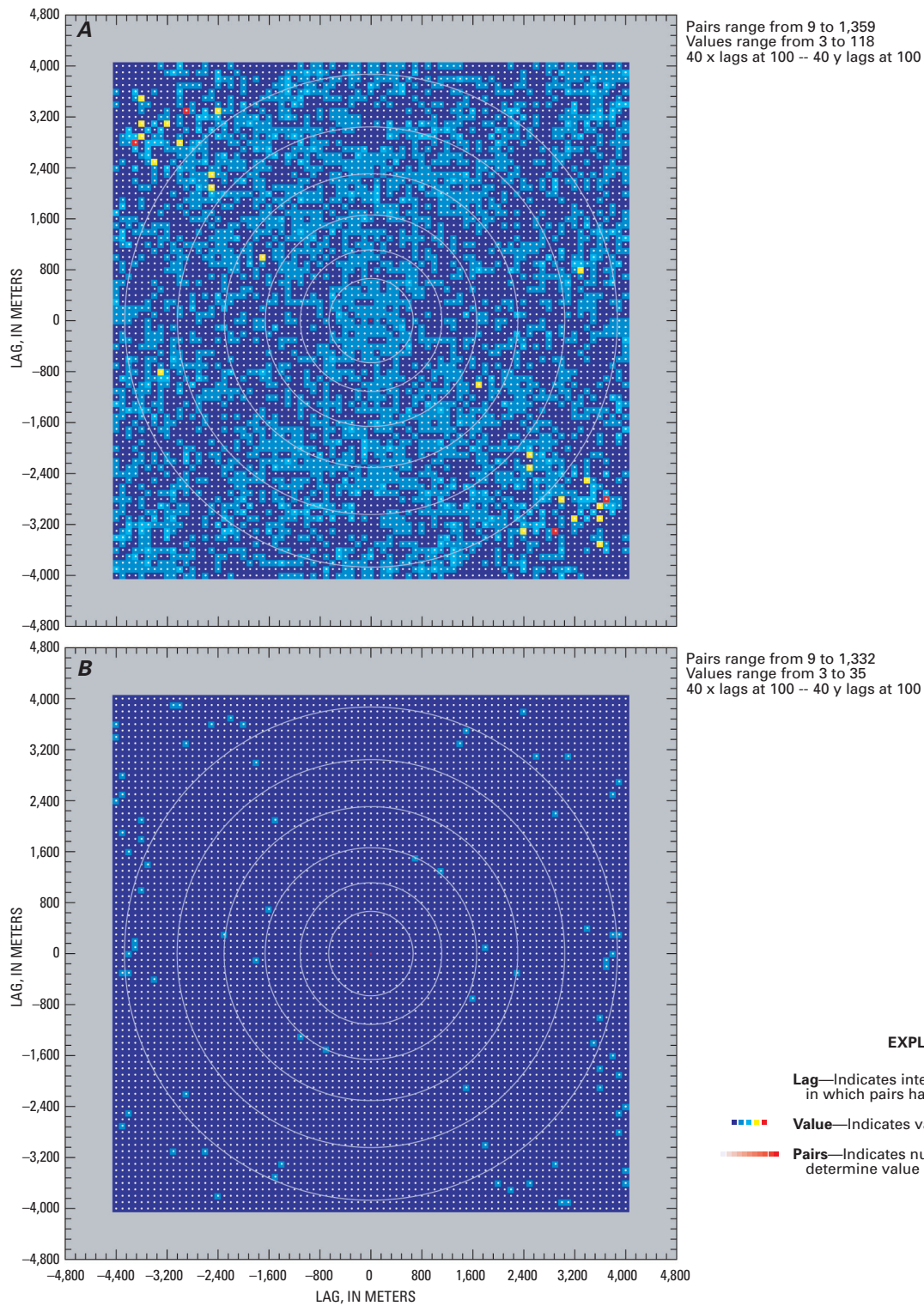


Figure 28. Well yield and total depth for State Engineers Office permitted wells.



**Figure 29.** Variogram surface maps.



**Table 19. Univariate statistics for water-quality properties and constituents in selected ground-water samples collected September 1998 through November 1999**

[Note: Q1, concentration at the 25th percentile; Q3, concentration at the 75th percentile; Min, minimum; Max, maximum; N, number of samples; Percent < rpl, percentage of samples with concentration less than the reporting level; NPDWS, National Primary Drinking Water Standards, or MCL, Maximum Contaminant Level established by the U.S. Environmental Protection Agency (1999); NSDWS, National Secondary Drinking Water Standards, established by the U.S. Environmental Protection Agency (1991); --, not applicable; Exceptions, number of samples that exceeded the relevant regulation;  $\mu$ s, microsiemens; cm, centimeter; mg/L, milligrams per liter;  $\mu$ g/L, micrograms per liter; °C, degrees Celsius; N, nitrogen]

Property or constituent	Detections										Censored values					Excep- tions
	Mean	Median	Q1	Q3	Min	Max	N	Mean	Median	N < rpl	NPDWS	Excep- tions	NSDWS			
Specific conductance ( $\mu$ s/cm at 25°C)	330.36	313.00	199.00	414.00	22.00	1090.00	363	--	--	0	--	--	--			
pH (standard units)	7.07	7.05	6.63	7.53	5.18	8.47	358	--	--	0	--	--	6.5-8.5			
Temperature (Degrees Celsius)	9.14	9.00	7.80	10.20	2.70	19.30	365	--	--	0	--	--	--			
Dissolved oxygen (mg/L)	3.75	3.29	1.87	5.61	0.03	10.50	358	--	--	0	--	--	--			
Hardness, total	136.61	120.00	82.00	180.00	0.16	550.00	269	--	--	0	--	--	--			
Calcium, dissolved (mg/L)	39.20	36.30	22.60	52.31	0.10	146.00	269	0.01	0.01	1	0.37	--	--			
Calcium, total (mg/L)	39.75	40.30	24.02	51.60	3.98	77.40	22	--	--	0	--	--	--			
Magnesium, dissolved (mg/L)	9.41	7.90	4.96	12.71	0.04	46.00	270	--	--	0	--	--	--			
Magnesium, total (mg/L)	9.61	8.54	6.01	14.40	0.85	19.90	22	--	--	0	--	--	--			
Sodium, dissolved (mg/L)	15.94	11.30	8.86	17.83	3.49	116.34	270	--	--	0	--	--	--			
Sodium, total (mg/L)	15.22	11.10	8.47	16.85	5.87	50.40	22	--	--	0	--	--	--			
Potassium, dissolved (mg/L)	1.93	1.73	1.10	2.68	0.26	6.26	142	2.00	2.00	59	29.35	--	--			
Potassium, total (mg/L)	2.91	2.55	2.27	3.28	2.18	4.64	7	2.00	2.00	15	68.18	--	--			
Alkalinity, total (mg/L)	118.15	120.00	80.00	160.00	7.12	270.00	273	5.00	5.00	3	1.09	--	--			
Sulfate (mg/L)	22.05	11.80	7.00	18.00	1.00	2500.00	273	1.00	1.00	3	1.09	--	250			
Chloride (mg/L)	24.95	6.78	3.05	36.30	0.50	230.00	269	0.50	0.50	6	2.18	--	250			
Fluoride (mg/L)	0.88	0.62	0.39	1.11	0.15	4.70	242	0.27	0.20	34	12.32	4.00	3			
Silicon, dissolved (mg/L)	10.17	9.80	8.20	11.50	4.30	16.10	93	--	--	0	--	--	--			
Silicon, total (mg/L)	8.70	8.70	--	--	8.70	8.70	1	--	--	0	--	--	--			
Total organic carbon (mg/L)	3.02	2.50	1.80	3.72	1.00	11.20	110	0.06	0.05	346	75.88	--	--			
Ammonia, as N (mg/L)	0.10	0.10	0.08	0.11	0.05	0.12	8	0.06	0.05	346	97.74	--	--			
Nitrate/Nitrite, as N (mg/L)	2.26	1.02	0.40	2.67	0.05	18.50	309	0.05	0.05	45	12.71	10.0	14			
Nitrite (mg/L)	--	--	--	--	--	--	0	0.20	0.20	13	--	1.00	0			
Phosphorus, total (mg/L)	0.10	0.06	0.03	0.11	0.02	0.71	64	0.03	0.02	291	81.97	--	--			
Aluminum, dissolved ( $\mu$ g/L)	54.33	47.00	28.50	80.50	12.00	118.00	6	25.37	40.00	164	96.47	--	--			
Aluminum, total ( $\mu$ g/L)	266.12	98.50	52.50	622.00	41.00	797.00	8	40.00	40.00	14	63.64	--	200			
Antimony, dissolved ( $\mu$ g/L)	4.60	5.00	3.90	6.00	0.60	6.00	6	1.97	0.60	257	97.72	--	--			
Antimony, total ( $\mu$ g/L)	--	--	--	--	--	--	0	0.60	0.60	23	--	6.00	0			
Arsenic, dissolved ( $\mu$ g/L)	1.25	1.10	1.00	1.65	1.00	1.80	4	1.02	1.00	259	98.48	--	--			
Arsenic, total ( $\mu$ g/L)	--	--	--	--	--	--	0	1.00	1.00	10	--	5.00	0			
Barium, dissolved ( $\mu$ g/L)	67.62	46.60	19.00	84.25	1.00	638.00	160	1.00	1.00	10	5.88	--	--			
Barium, total ( $\mu$ g/L)	88.91	63.00	21.75	101.25	1.00	604.00	22	--	--	0	--	200	2			
Beryllium, dissolved ( $\mu$ g/L)	0.62	0.50	0.40	0.90	0.30	1.00	5	0.61	1.00	165	97.06	--	--			
Beryllium, total ( $\mu$ g/L)	--	--	--	--	--	--	0	1.00	1.00	22	--	4.00	0			
Boron, dissolved ( $\mu$ g/L)	29.33	13.00	9.00	36.50	7.00	155.00	109	7.67	8.00	61	35.88	--	--			
Boron, total ( $\mu$ g/L)	27.44	16.50	10.00	32.50	7.00	156.00	18	7.00	7.00	4	18.18	--	--			
Cadmium, dissolved ( $\mu$ g/L)	0.23	0.20	0.20	0.30	0.20	0.30	3	0.47	0.60	260	98.86	--	--			
Cadmium, total ( $\mu$ g/L)	--	--	--	--	--	--	0	0.60	0.60	23	--	5.00	0			
Chromium, dissolved ( $\mu$ g/L)	1.57	1.60	1.20	1.90	1.20	1.90	3	0.74	0.80	260	98.86	--	--			
Chromium, total ( $\mu$ g/L)	1.60	1.60	--	--	1.60	1.60	1	4.56	7.00	132	99.25	100	0			

Cobalt, dissolved (µg/L)	0.61	0.40	0.30	0.50	0.30	7.00	38	4.56	7.00	132	77.65	--	--
Cobalt, total (µg/L)	7.00	7.00	7.00	7.00	7.00	7.00	3	7.00	7.00	19	86.36	--	--

**Table 19. Univariate statistics for water-quality properties and constituents in selected ground-water samples collected September 1998 through November 1999—Continued**

[Note: Q1, concentration at the 25th percentile; Q3, concentration at the 75th percentile; Min, minimum; Max, maximum; N, number of samples; Percent < rpl, percentage of samples with concentration less than the reporting level; NPDWS, National Primary Drinking Water Standards, or MCL, Maximum Contaminant Level established by the U.S. Environmental Protection Agency (1999); NSDWS, National Secondary Drinking Water Standards, established by the U.S. Environmental Protection Agency (1991); --, not applicable; Exceptions, number of samples that exceeded the relevant regulation; µs, microsiemens; cm, centimeter; mg/L, milligrams per liter; µg/L, micrograms per liter; °C, degrees Celsius; N, nitrogen]

Variable	Detections										Censored values				Excep- tions	Excep- tions
	Mean	Median	Q1	Q3	Min	Max	N	Mean	Median	N	Percent < rpl	NPDWS	Excep- tions	NSDWS		
Copper, dissolved (µg/L)	57.50	27.00	12.00	71.00	0.60	549.40	251	1.42	2.00	12	4.56	--	--	--	--	
Copper, total (µg/L)	30.67	20.60	7.30	34.80	0.70	239.00	23	--	--	0	--	1300	0	1000	0	
Iron, dissolved (µg/L)	27.96	10.00	7.00	25.00	4.00	389.00	47	4.57	5.00	123	72.35	--	--	--	--	
Iron, total (µg/L)	4580.75	13.50	6.00	252.25	5.00	69430.00	16	5.00	5.00	6	27.27	--	--	300	4	
Lead, dissolved (µg/L)	1.34	1.05	0.80	1.70	0.60	4.60	80	0.98	0.60	183	69.58	--	--	--	--	
Lead, total (µg/L)	2.24	2.80	0.85	3.35	0.80	3.60	5	0.60	0.60	18	78.26	15.0	0	--	--	
Manganese, dissolved (µg/L)	20.53	2.30	1.00	12.00	0.30	286.00	125	0.72	1.00	45	26.47	--	--	--	--	
Manganese, total (µg/L)	53.68	6.00	1.00	31.00	1.00	446.00	19	6.08	9.00	104	84.55	--	--	50.0	3	
Molybdenum, dissolved (µg/L)	13.04	10.75	3.40	21.70	1.20	50.00	66	6.08	9.00	104	61.18	--	--	--	--	
Molybdenum, total (µg/L)	21.00	18.00	16.00	27.50	16.00	30.00	5	9.00	9.00	17	77.27	--	--	--	--	
Nickel, dissolved (µg/L)	0.93	0.80	0.50	1.10	0.40	3.40	38	7.23	11.00	132	77.65	--	--	--	--	
Nickel, total (µg/L)	--	--	--	--	--	--	0	11.00	11.00	22	--	--	--	--	--	
Selenium, dissolved (µg/L)	2.99	2.00	1.35	3.55	1.00	11.40	25	1.00	1.00	238	90.49	--	--	--	--	
Selenium, total (µg/L)	2.80	2.80	--	--	2.50	3.10	2	1.00	1.00	21	91.30	50.0	0	--	--	
Silver, dissolved (µg/L)	--	--	--	--	--	--	0	0.39	0.20	263	--	--	--	--	--	
Silver, total (µg/L)	--	--	--	--	--	--	0	0.20	0.20	23	--	--	--	100	0	
Thallium, dissolved (µg/L)	--	--	--	--	--	--	0	1.70	0.60	263	--	--	--	--	--	
Thallium, total (µg/L)	--	--	--	--	--	--	0	1.00	1.00	168	--	2.00	0	--	--	
Titanium, dissolved (µg/L)	1.50	1.50	--	--	1.00	2.00	2	1.00	1.00	168	98.82	--	--	--	--	
Titanium, total (µg/L)	6.00	6.00	--	--	2.00	10.00	2	1.00	1.00	20	90.91	--	--	--	--	
Vanadium, dissolved (µg/L)	0.96	0.80	0.50	1.33	0.50	2.60	30	4.45	7.00	140	82.35	--	--	--	--	
Vanadium, total (µg/L)	--	--	--	--	--	--	0	7.00	7.00	22	--	--	--	--	--	
Zinc, dissolved (µg/L)	169.68	13.00	7.00	64.50	2.50	4763.00	135	3.37	4.00	35	20.59	--	--	--	--	
Zinc, total (µg/L)	297.21	15.00	5.00	323.00	4.00	2908.00	19	-0.01	-0.01	1	5.00	--	--	5000	0	

**Table 20. Univariate statistics for water-quality properties and constituents in selected surface-water samples collected September 1998 through November 1999**

[Note: Q1, concentration at the 25th percentile; Q3, concentration at the 75th percentile; Min, minimum; Max, maximum; N, number of samples; Percent < rpl, percent of samples with concentration less than the reporting level; -- not applicable; In-stream standards as defined by Colorado Department of Public Health and Environment, 2000; \*, a maximum C-degree increase over a 4-hour period is acceptable; \*\*, several censored values at < .2 may include values greater than the in-stream standard; µs, microsiemens; cm, centimeter, mg/L, milligrams per liter; µg/L, micrograms per liter; °C, degrees Celsius; N, nitrogen]

Variable	Detections											Censored values						In-stream standards		
	Mean	Median	Q1	Q3	Min	Max	N	Mean	Median	N	Percent < rpl	Acute	Excep- tions	Chronic	Excep- tions					
Discharge (in cfs)	1.56	0.33	0.14	0.96	0.01	14.60	71	--	--	0	--	--	--	--	--					
Specific conductance (in µs/cm)	596.22	457.00	293.75	652.50	106.00	2270.00	78	--	--	0	--	--	--	--	--					
pH (in standard units)	8.00	7.99	7.80	8.21	7.11	8.70	78	--	--	0	--	--	6.5-9	0						
Temperature (in degrees Celsius)	9.47	10.60	5.10	14.00	0.30	20.30	79	--	--	0	--	--	20*	1						
Dissolved oxygen (in mg/L)	9.02	8.75	7.90	10.62	3.01	14.40	58	--	--	0	--	--	6.0	4						
Hardness (total)	242.09	150.00	81.75	245.00	25.00	1300.00	56	--	--	0	--	--	--	--	--					
Calcium (dissolved) [in mg/L]	71.73	41.79	23.62	66.53	7.01	464.00	56	--	--	0	--	--	--	--	--					
Calcium (total) [in mg/L]	73.61	42.20	24.80	72.77	7.10	460.00	53	--	--	0	--	--	--	--	--					
Magnesium (dissolved) [in mg/L]	15.62	10.36	5.76	19.35	1.83	66.40	56	--	--	0	--	--	--	--	--					
Magnesium (total) [in mg/L]	16.38	10.96	6.34	20.00	1.91	70.98	53	--	--	0	--	--	--	--	--					
Sodium (dissolved) [in mg/L]	35.74	27.50	20.55	39.83	6.13	162.99	56	--	--	0	--	--	--	--	--					
Sodium (total) [in mg/L]	37.15	27.30	21.00	39.35	6.07	174.22	53	--	--	0	--	--	--	--	--					
Potassium (dissolved) [in mg/L]	3.15	2.81	2.43	3.51	0.91	8.00	34	2.00	2.00	7	17.07	--	--	--	--					
Potassium (total) [in mg/L]	3.73	3.35	2.68	4.00	0.90	11.00	50	2.00	2.00	3	5.66	--	--	--	--					
Alkalinity (total) [in mg/L]	115.21	98.50	66.35	160.00	24.80	330.00	58	--	--	0	--	--	--	--	--					
Sulfate (in mg/L)	70.63	12.65	9.00	20.77	2.50	1100.00	58	--	--	0	--	--	--	--	--					
Chloride (in mg/L)	78.89	64.50	34.33	96.40	5.41	390.00	58	--	--	0	--	--	--	--	--					
Fluoride (in mg/L)	0.51	0.46	0.37	0.55	0.13	2.70	55	2.00	0.50	3	5.17	--	--	--	--					
Silicon (dissolved) [in mg/L]	7.43	7.25	6.62	8.15	6.20	9.10	20	--	--	0	--	--	--	--	--					
Silicon (total) [in mg/L]	8.19	8.00	7.00	8.60	6.90	12.80	17	--	--	0	--	--	--	--	--					
Total organic carbon	4.77	4.30	3.40	6.18	0.35	13.80	76	0.06	0.05	76	50.00	--	--	--	--					
Ammonia (as N) [in mg/L]	0.06	0.06	--	--	0.06	0.07	2	0.06	0.05	76	97.44	0.43	1	0.02	1					
Nitrate/Nitrite (as N) [in mg/L]	0.52	0.36	0.12	0.87	0.05	1.47	47	0.05	0.05	31	39.74	--	--	--	--					
Nitrite (in mg/L)	--	--	--	--	--	--	0	0.20	0.20	10	--	--	--	--	--					
Phosphorus (total) [in mg/L]	0.04	0.04	0.03	0.05	0.02	0.15	33	0.03	0.02	45	57.69	--	--	--	--					
Aluminum (dissolved) [in µg/L]	130.75	122.00	88.75	181.50	87.00	192.00	4	27.81	40.00	32	88.89	750	1	87	1					
Aluminum (total) [in µg/L]	364.62	113.00	72.50	208.50	34.00	4048.00	29	40.00	40.00	4	12.12	--	--	--	--					
Antimony (dissolved) [in µg/L]	--	--	--	--	--	--	0	1.86	0.60	56	--	--	--	--	--					
Antimony (total) [in µg/L]	2.85	2.85	--	--	0.70	5.00	2	1.98	0.60	48	96.00	--	--	--	--					
Arsenic (dissolved) [in µg/L]	1.08	1.05	1.00	1.15	1.00	1.30	6	1.00	1.00	50	89.29	340	0	150	0					
Arsenic (total) [in µg/L]	1.70	1.70	--	--	1.00	2.40	2	--	--	0	--	--	--	--	--					
Barium (dissolved) [in µg/L]	94.99	83.35	43.88	149.15	14.50	210.00	36	--	--	0	--	--	--	--	--					
Barium (total) [in µg/L]	104.82	96.50	46.50	155.70	13.40	238.00	33	--	--	0	--	--	--	--	--					
Beryllium (dissolved) [in µg/L]	2.10	2.10	--	--	2.10	2.10	1	0.66	1.00	35	97.22	--	--	--	--					
Beryllium (total) [in µg/L]	1.00	1.00	--	--	1.00	1.00	1	0.62	1.00	32	96.97	--	--	--	--					
Boron (dissolved) [in µg/L]	41.21	27.00	18.75	52.00	11.00	156.00	34	8.00	8.00	2	5.56	--	--	--	--					
Boron (total) [in µg/L]	50.88	37.00	27.50	65.00	11.00	166.00	33	--	--	0	--	--	--	--	--					

Cadmium (dissolved) [in µg/L]	0.20	0.20	--	--	0.20	0.20	1	0.49	0.60	55	98.21	5.86	0	2.77	0
Cadmium (total) [in µg/L]	0.33	0.20	0.20	0.60	0.20	0.60	3	0.49	0.60	47	94.00	--	--	--	--
Chromium (dissolved) [in µg/L]	--	--	--	--	--	--	0	0.76	0.80	56	--	722	0	93.7	0
Chromium (total) [in µg/L]	1.90	1.15	2.30	0.90	4.70	9	4.77	7.00	30	76.92	--	--	--	--	--
Cobalt (dissolved) [in µg/L]	0.45	0.35	0.60	0.30	0.90	6	4.77	7.00	30	83.33	--	--	--	--	--
Cobalt (total) [in µg/L]	0.38	0.40	0.30	0.45	0.30	0.50	5	4.37	7.00	28	84.85	--	--	--	--

**Table 20. Univariate statistics for water-quality properties and constituents in selected surface-water samples collected September 1998 through November 1999—Continued**

Note: Q1, concentration at the 25th percentile; Q3, concentration at the 75th percentile; Min, minimum; Max, maximum; N, number of samples; Percent < rpl, percent of samples with concentration less than the reporting level; -- not applicable; In-stream standards as defined by Colorado Department of Public Health and Environment, 2000; \*, a maximum C-degree increase over a 4-hour period is acceptable; \*\*, several censored values at < .2 may include values greater than the in-stream standard; µs, microsiemens; cm, centimeter, mg/L, milligrams per liter; °C, degrees Celsius; N, nitrogen]

Variable	Detections											Censored values					In-stream standards				
	Mean	Median	Q1	Q3	Min	Max	N	Mean	Median	N	Percent < rpl	Acute	Excep- tions	Chronic	Excep- tions						
Copper (dissolved) [in µg/L]	1.54	1.00	0.70	1.35	0.60	10.90	25	1.32	2.00	31	55.36	17.7	0	11.5	0						
Copper (total) [in µg/L]	2.38	1.60	1.20	2.00	0.70	12.60	35	2.00	2.00	15	30.00	--	--	--	--						
Iron (dissolved) [in µg/L]	64.47	32.00	16.75	62.75	9.00	393.00	34	5.00	5.00	2	5.56	--	--	--	--						
Iron (total) [in µg/L]	494.74	269.00	170.00	451.00	45.00	2973.00	31	4.50	4.50	2	6.06	--	--	1000	2						
Lead (dissolved) [in µg/L]	5.82	1.35	0.75	12.85	0.60	23.30	10	0.85	0.60	46	82.14	88.8	0	3.46	0						
Lead (total) [in µg/L]	2.13	1.10	0.70	4.60	0.70	4.60	3	0.60	0.60	31	91.18	--	--	--	--						
Manganese (dissolved) [in µg/L]	76.06	30.00	17.60	112.10	1.20	345.00	35	1.00	1.00	1	2.78	3280	0	1810	0						
Manganese (total) [in µg/L]	91.40	33.40	22.30	137.80	3.00	424.00	31	5.71	9.00	34	52.31	--	--	--	--						
Molybdenum (dissolved) [in µg/L]	1.30	1.30	--	--	1.00	1.60	2	5.71	9.00	34	94.44	--	--	--	--						
Molybdenum (total) [in µg/L]	1.43	1.20	1.20	1.90	1.20	1.90	3	5.53	9.00	30	90.91	--	--	--	--						
Nickel (dissolved) [in µg/L]	0.91	0.75	0.62	1.35	0.40	1.50	8	7.97	11.00	28	77.78	599	0	65.6	0						
Nickel (total) [in µg/L]	0.54	0.40	0.40	0.75	0.40	1.00	5	6.84	11.00	28	84.85	--	--	--	--						
Selenium (dissolved) [in µg/L]	1.82	1.80	1.55	2.10	1.50	2.10	5	1.00	1.00	51	91.07	18.4	0	4.6	0						
Selenium (total) [in µg/L]	1.95	1.45	1.15	3.25	1.10	3.80	4	1.00	1.00	46	92.00	--	--	--	--						
Silver (dissolved) [in µg/L]	0.80	0.80	--	--	0.80	0.80	1	0.36	0.20	55	98.21	3.42	0	0.54	0						
Silver (total) [in µg/L]	1.00	1.00	--	--	1.00	1.00	1	0.38	0.20	49	98.00	--	--	--	--						
Thallium (dissolved) [in µg/L]	--	--	--	--	--	--	0	1.57	0.60	56	--	--	--	15	0						
Thallium (total) [in µg/L]	4.67	4.00	4.00	6.00	4.00	6.00	3	1.00	1.00	35	92.11	--	--	--	--						
Titanium (dissolved) [in µg/L]	2.00	2.00	--	--	2.00	2.00	1	1.00	1.00	35	97.22	--	--	--	--						
Titanium (total) [in µg/L]	12.11	2.91	1.51	6.00	1.24	90.00	19	1.00	1.00	14	42.42	--	--	--	--						
Vanadium (dissolved) [in µg/L]	3.18	0.60	0.50	4.60	0.50	14.00	9	5.07	7.00	27	75.00	--	--	--	--						
Vanadium (total) [in µg/L]	3.70	3.10	0.60	4.90	0.50	11.00	7	4.50	7.00	26	78.79	--	--	--	--						
Zinc (dissolved) [in µg/L]	4.78	4.00	4.00	5.93	2.20	10.20	16	3.10	4.00	20	55.56	150	0	151	0						
Zinc (total) [in µg/L]	8.77	7.00	5.00	10.35	3.50	23.00	21	--	--	0	--	--	--	--	--						

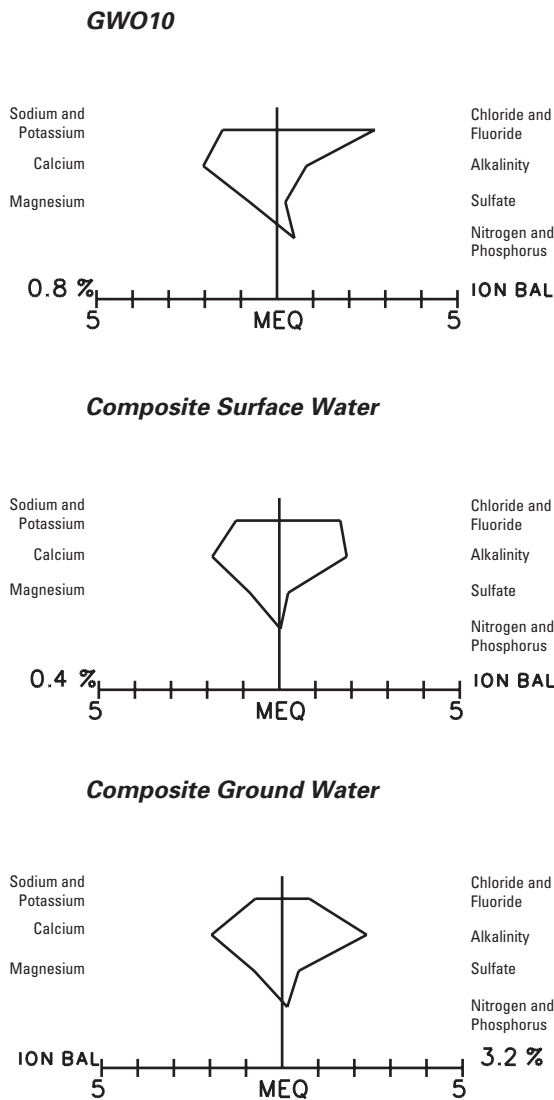


**Figure 30.** Stiff diagrams of selected water-quality constituents in the Turkey Creek watershed.

Spatial differences in water quality can be characterized with plots of constituent ranges on maps of the watershed (figs. 32–35). Those constituents potentially associated with individual sewage-disposal system (ISDS) effluent are of greatest interest. Specific conductance, chloride, nitrate plus nitrite, and boron are associated with septic-tank effluent, and spatial concentration patterns could indicate ISDS influence. Specific conductance is an indicator of dissolved solids. Chloride in effluent is related to human consumption of salt and chlorine-based home products. Nitrate is an end-member product of nitrification of organic and ammonia nitrogen in human and animal waste. Boron is present in the waste from laundry and other cleaning products.

In the specific-conductance map (fig. 32), few patterns are evident. Although there is variation in specific conductance, high and low values are relatively evenly distributed across the watershed. An exception is an area of lower specific-conductance values that can be seen in ground water in the south-western part of the watershed in subwatersheds I, J, and K. When median values of concentration for water from the Pikes Peak Granite and water from a group of all other rock types are compared using the Wilcoxon rank-sum test (Helsel and Hirsch, 1992), differences in specific conductance, as well as all the major cations, chloride, sulfate, and nitrate plus nitrite all are significant at the 99.9 percent level ( $p < 0.001$ ). Overall, specific conductance ranged from 22 to 1,090  $\mu\text{S}/\text{cm}$  in ground water and 106 to 2,270  $\mu\text{S}/\text{cm}$  in surface water. In general, the results of samples collected in this study indicate that surface water is slightly more concentrated than ground water.

Pearson correlation coefficient is a measure of the linear relation between two variables. A value of “zero” indicates no correlation and a value of “one” indicates a perfect linear relation. In dilute waters, quasilinear relations between specific conductance and major ions are expected due to consistent inputs of solutes derived from rock-weathering reactions (Drever, 1988; Morgan, 2000). A lack of good correlation may indicate a more complex geochemical evolution or additional sources of solutes. Water from chloride-poor rock might be expected to have a poor correlation of chloride with dissolved solids because chloride is derived from precipitation and not from the fractured rock. Sources of chloride such as ISDS’s and road salt also would tend to complicate correlation unless chloride concentrations were high enough to control overall dissolved-solids concentration.

In the Turkey Creek watershed, major ions are positively correlated with specific conductance in both ground and surface water. Except for calcium and chloride, Pearson correlation coefficients are larger in surface-water samples than in ground-water samples. In ground-water samples, the correlation of specific conductance and nitrate plus nitrite was stronger than the specific-conductance correlations with sodium, potassium, sulfate, and silica. A simple ground-water system, based primarily on rock contact time and not influenced by the addition of solutes, might be expected to display stronger correlation coefficients than those reported here. Correlations of specific conductance with possible ISDS-related constituents

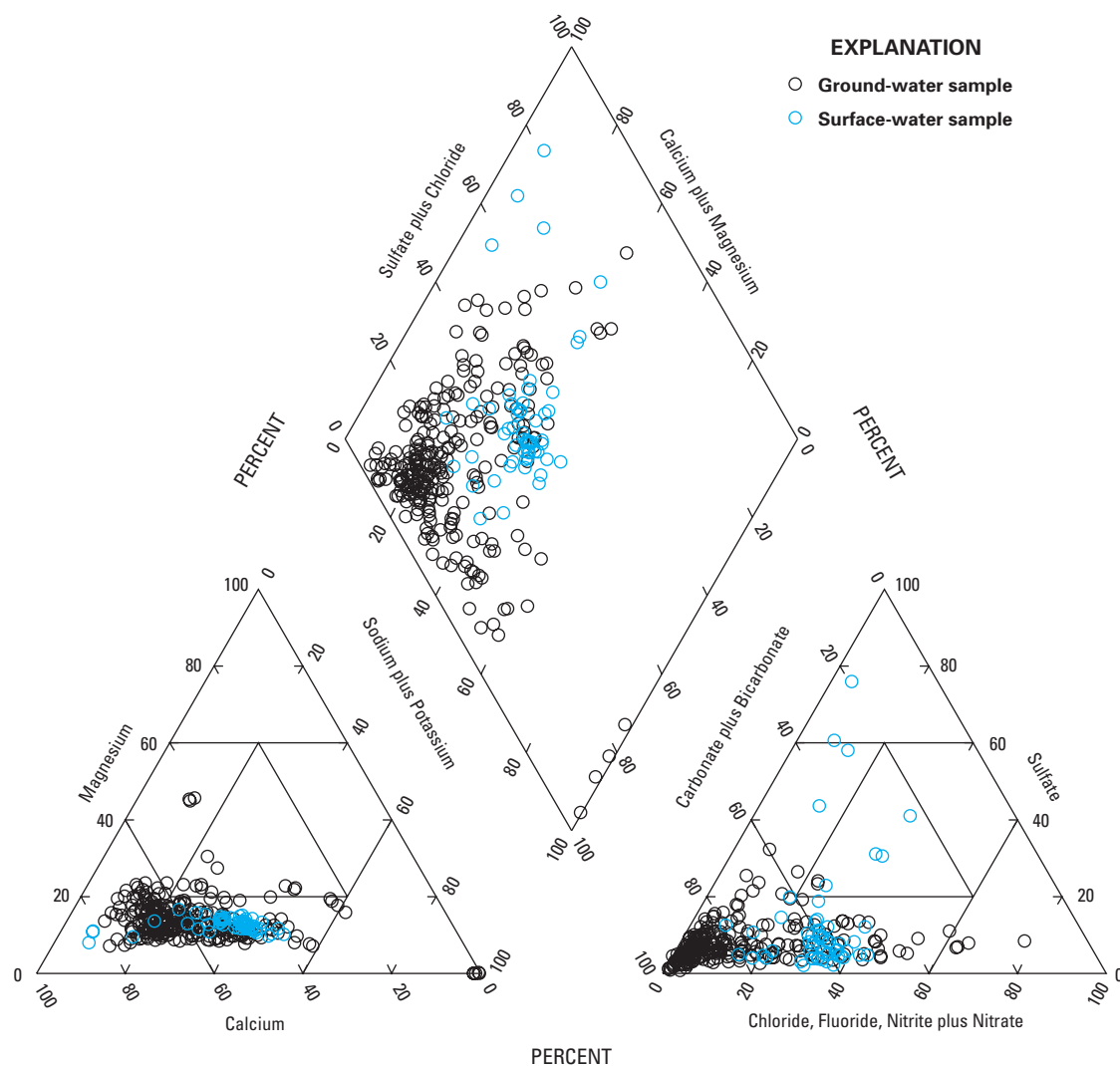


**Figure 31.** Trilinear diagram of quarterly ground-water and surface-water samples collected in the Turkey Creek watershed.

were moderately strong to weak: chloride, 0.73 and 0.78; nitrate plus nitrite, 0.34 and 0.61; boron, 0.87 and 0.4 in surface-water and ground-water samples, respectively.

Chloride concentrations ranged from 5.41 to 390 mg/L in surface-water samples (table 20) and from 0.5 to 230 mg/L in ground-water samples in the watershed (table 19). The distribution of moderate concentrations (greater than 5 mg/L, less than or equal to 35 mg/L) and high concentrations (greater than 35 mg/L) shows no particular pattern (fig. 33). Lower concentrations of chloride were found in the area of low specific conductance in the southwestern part of the watershed. Correlations of chloride with possible

ISDS-related constituents were weak: nitrate plus nitrite, 0.25 and 0.45; boron, 0.44, and 0.31 in surface-water and ground-water samples, respectively.

The map of nitrate plus nitrite as nitrogen concentrations (fig. 34) shows low and moderate nitrate plus nitrite concentrations distributed throughout the watershed. Median concentrations of nitrate plus nitrite in ground water (1.0 mg/L) were higher than those in surface water (0.52 mg/L). Lower nitrate plus nitrite concentrations in surface water may be due in part to seasonal biological consumption. A few relatively high concentrations (greater than 10 mg/L) were measured in ground-water samples from subbasins C and D, based on sampling results

from fall 1999; however, relatively high nitrate plus nitrite concentrations are not limited to subbasins C and D as results from other sampling rounds indicated relatively high concentrations for nitrate plus nitrite as nitrogen at other locations. Correlation of nitrate plus nitrite concentrations with boron were weak: boron, 0.39 and 0.20 in surface-water and ground-water samples, respectively.

The map of boron concentrations (fig. 35) indicates a weak spatial trend of increasing boron concentration from west to east in ground water and upstream to downstream in surface water. Flynn and Barber (2000) reported that background concentrations of boron in ground and surface waters of the Colorado

Front Range are in the range of 10 to 40 micrograms per liter ( $\mu\text{g/L}$ ). In Turkey Creek ground-water samples, 86 percent of boron concentrations were less than 40  $\mu\text{g/L}$ ; the maximum was 155  $\mu\text{g/L}$ . In Turkey Creek surface-water samples, 69 percent of boron concentrations were less than 40  $\mu\text{g/L}$ ; the maximum was 156  $\mu\text{g/L}$ . The median boron concentration in surface water (27  $\mu\text{g/L}$ ) was higher than the median concentration in ground water (13  $\mu\text{g/L}$ ).

Where applicable, concentrations in ground water were compared to U.S. Environmental Protection Agency National Primary Drinking Water Standards (NPDWS) (U.S. Environmental Protection Agency, 1999) and National Secondary Drinking Water

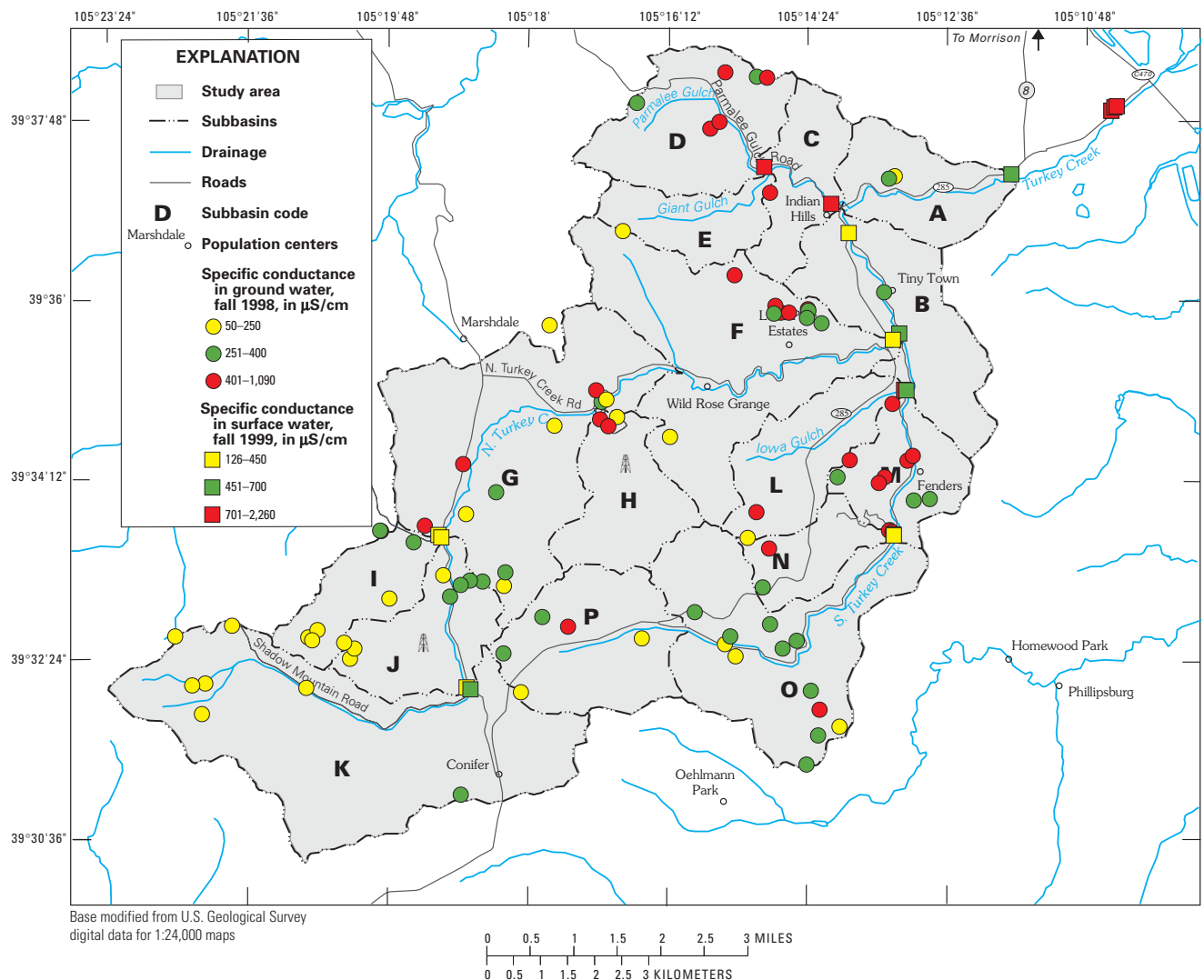


**Figure 32.** Specific-conductance measurements in ground- and surface-water samples.

Standards (NSDWS) (U.S. Environmental Protection Agency, 1991) given in table 19. Comparison of surface-water concentrations to Colorado In-Stream Standards (Colorado Department of Public Health and Environment, 2000) is given in table 20. Concentrations in ground-water samples (table 19) occasionally exceeded NPDWS for fluoride (1.1 percent), nitrate plus nitrite (4.51 percent), and total barium (9.10 percent). NSDWS, which mostly refer to taste or esthetic properties, were not met for pH (17.6 percent), sulfate (0.37 percent), total aluminum (13.6 percent), total iron (18.2 percent), and dissolved manganese (2.4 percent). Concentrations in only a few surface-water samples (table 20) exceeded standards for pH, dissolved oxygen, ammonia, dissolved aluminum, and total iron.

### Comparison to Historical Water-Quality Data

Contemporary ground-water quality data collected in Turkey Creek watershed from 1998 through 1999 were compared to historical data collected from 1972 through 1975. The Wilcoxon rank-sum test was used to test for differences in the median values and concentrations for the two time periods. Significantly (p-value less than 0.10, or 90-percent confidence) higher values and concentrations in the 1998–99 data were identified for specific conductance ( $p = <0.0001$ ), calcium ( $p = 0.0023$ ), magnesium ( $p = 0.0464$ ), sodium ( $p = 0.0882$ ), chloride ( $p = <0.0001$ ), and nitrate plus nitrite ( $p = 0.0286$ ). Although the contemporary data were collected from a network of wells (fig. 12) that is different than the network of wells for the historical data

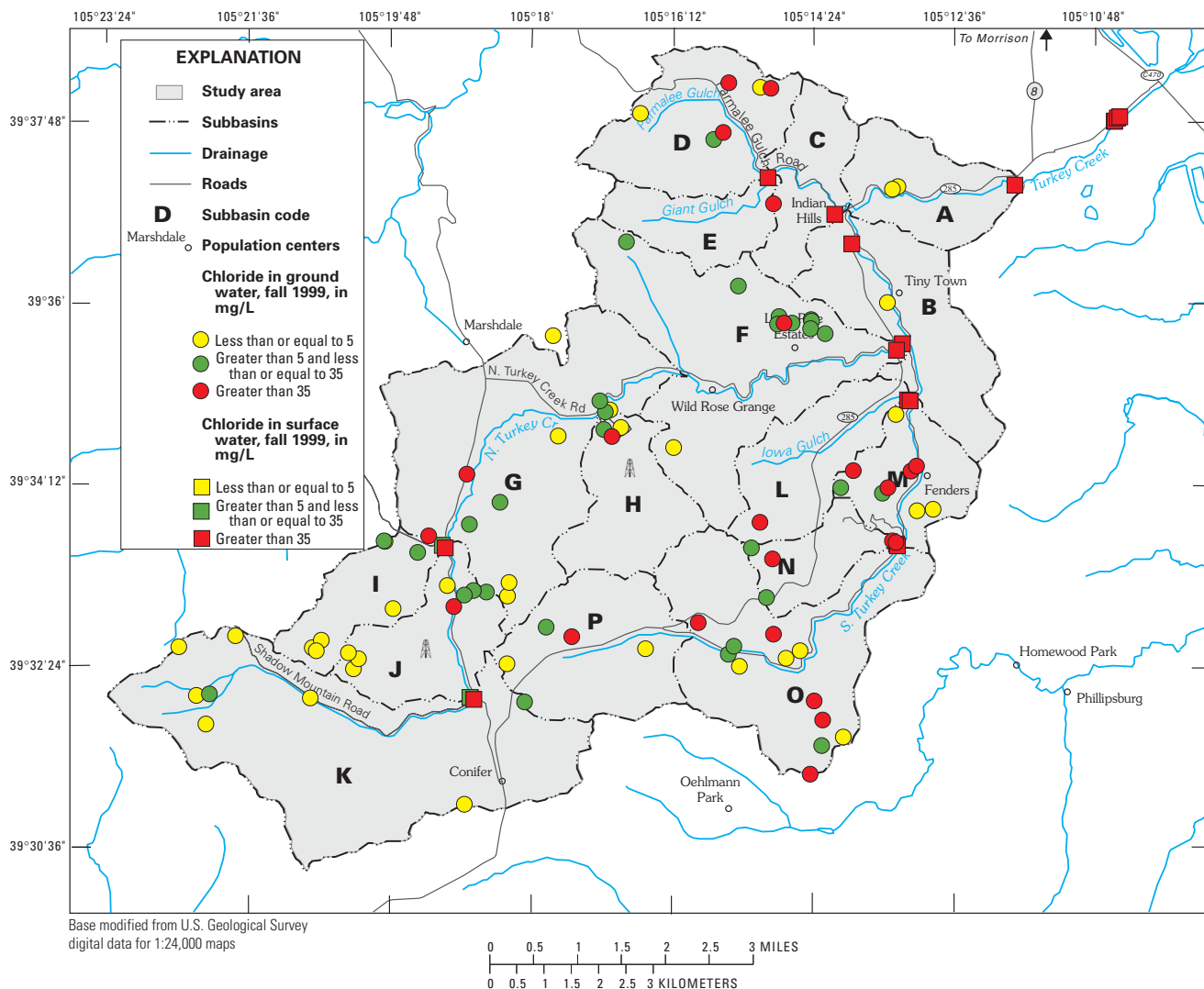


Figure 33. Concentrations of chloride in ground- and surface-water samples.



(fig. 6), both networks are widespread throughout the watershed, and the statistical differences for concentrations can be used to infer that water withdrawn from wells in Turkey Creek watershed is becoming more concentrated in dissolved solids and some major ions, and that nitrate plus nitrite concentrations have increased.

### Tritium

Tritium is an isotope of hydrogen with low natural background concentrations (about 8 tritium units [TU]) and short half-life (12.43 years). Tritium was released into the atmosphere in large quantities during above-ground testing of nuclear bombs primarily during the late 1950's and early 1960's. Tritium can be

useful in making gross estimates of the recharge dates of ground water (the time water was isolated from the atmosphere). Based on correlation and interpolation (Michel, 1989) using tritium concentrations at Albuquerque, New Mexico, the expected year 2000 tritium concentration in precipitation is approximately 10 plus or minus 4 TU (seasonal differences can account for much of the variation) (fig. 36). Samples with a tritium concentration well below 10 TU probably have a large component of pre-bomb water (pre-1952). Samples with concentrations substantially greater than current precipitation concentration are probably composed predominantly of water recharged during the 1960's. Intermediate concentrations are probably the result of mixtures of water of variable recharge dates.

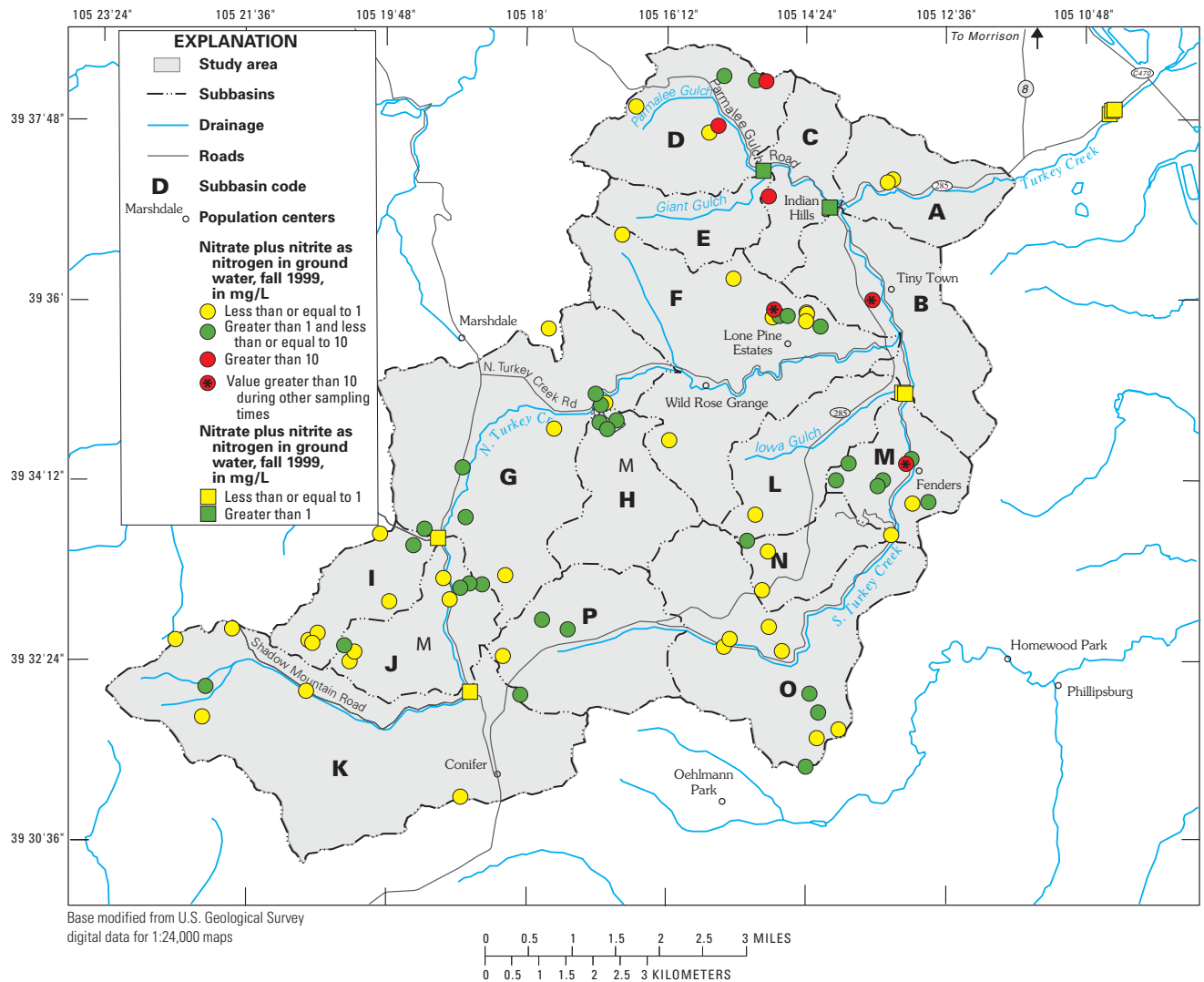


Figure 34. Concentrations of nitrate plus nitrite in ground- and surface-water sample.

The tritium samples collected in 24 selected wells in the Turkey Creek watershed (table 10) had concentrations that ranged from 2.3 to 33.2 TU. The median concentration was 13.3 TU. Two samples had tritium concentrations less than 5 TU, indicating water that has a component of pre-bomb recharge. Three sample concentrations were greater than 20 TU, indicating water with a component of recharge from the nuclear bomb testing era (1960's). These tritium results indicate that some water in the Turkey Creek watershed was recharged 30 to 40 years ago or longer. Most of the remaining samples (about 80 percent) are probably indicative of more recent recharge or some indeterminate mixture containing various amounts of pre-bomb, bomb era, and recent recharge.

### Chloride to Bromide Ratios

The April 2001 samples collected in 23 selected wells in the Turkey Creek watershed (table 10) were analyzed for bromide concentration in order to compute chloride to bromide ratios (Cl/Br). Chloride to bromide ratios can be used to distinguish sources of chloride in water. Both ions are considered to be mostly conservative during transport. Seawater and precipitation near coastal areas have a Cl/Br ratio of about 290, and precipitation in the Turkey Creek watershed probably has a Cl/Br ratio in the range of 40 to 75 (Davis and others, 2001).

Sources of bromide such as ethylene dibromide from historical use as a gasoline antiknock compound and from bromine-rich pesticides can cause ratios in

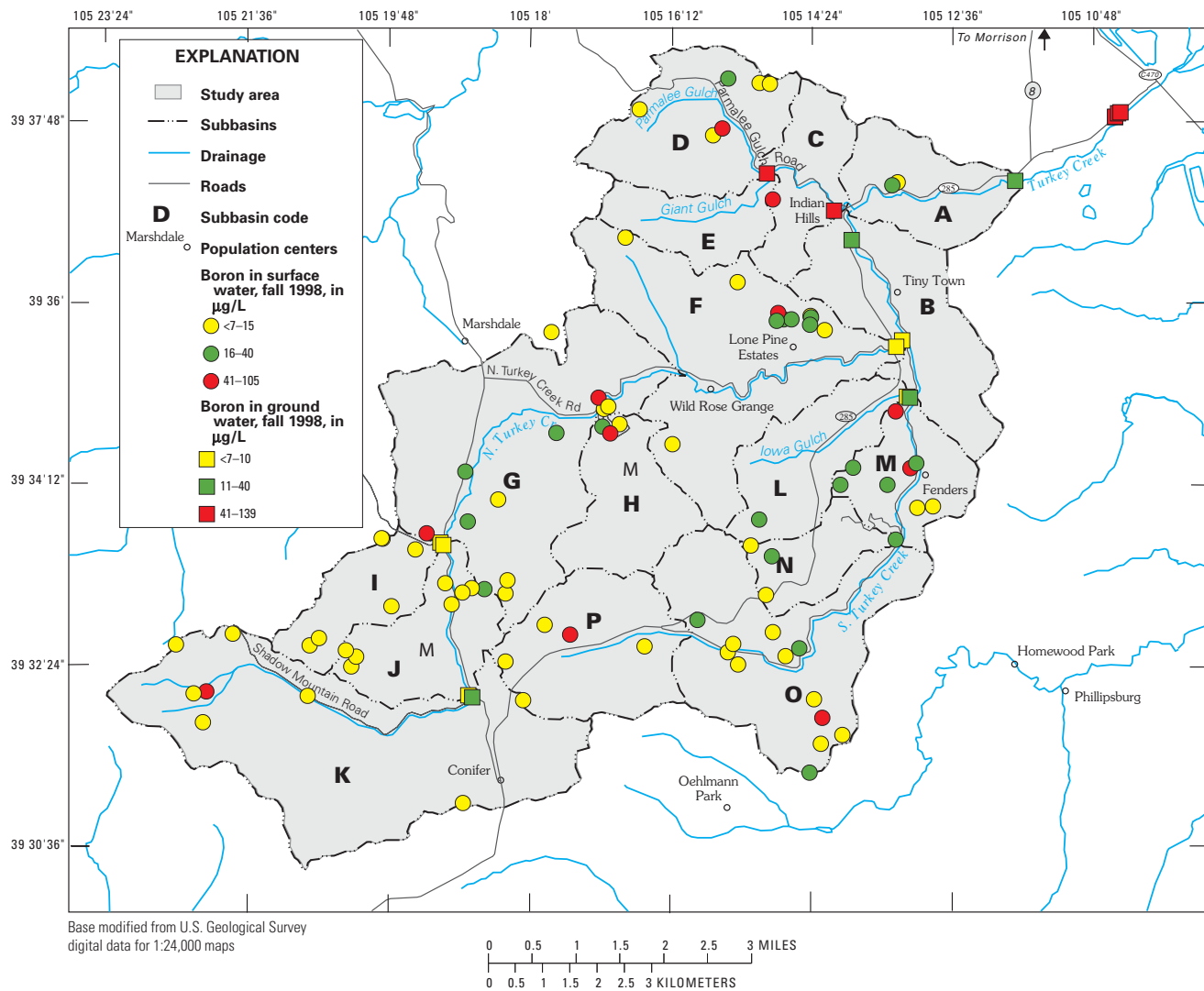
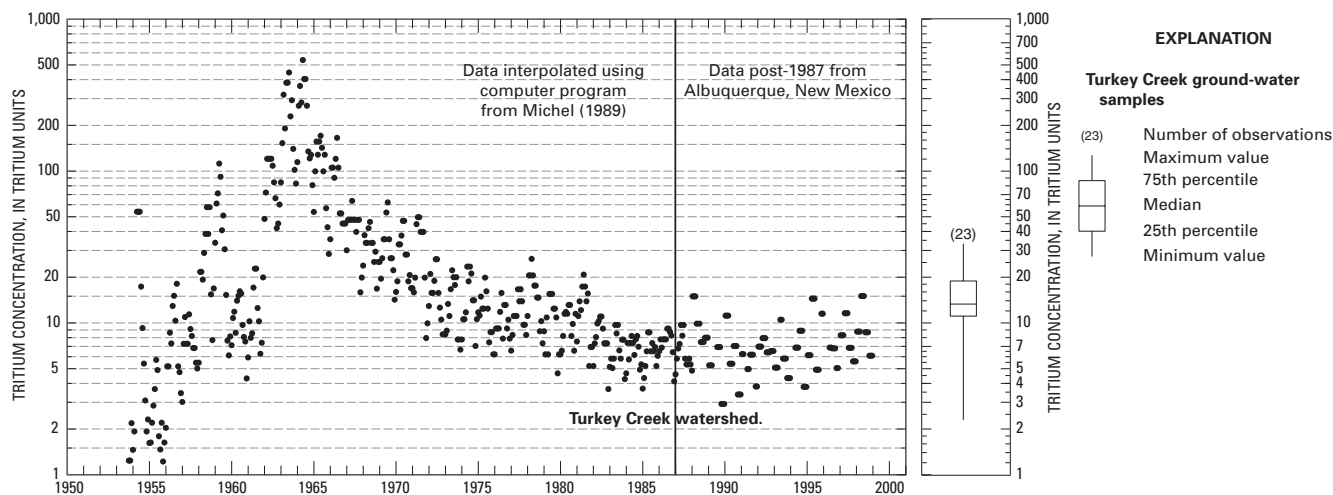


Figure 35. Concentrations of boron in ground- and surface-water samples.



**Figure 36.** Plot of tritium concentrations in precipitation interpolated to Turkey Creek watershed location and decayed to year 2000 values, and boxplot of tritium concentrations in selected water wells in the Turkey Creek watershed.

some hydrologic settings to be lower than in precipitation. Fractionation during crystallization of salt from solution lowers relative bromide content, causing high Cl/Br ratios (Ohio road salt Cl/Br = 8,000; Knuth and others, 1990). In water influenced by dissolution of evaporites, application of road salt, or treated sewage effluent, Cl/Br ratios are higher than 300 due to the addition of chloride from salt that is impoverished in associated bromide. Some studies have suggested that domestic wastewater, which includes ISDS effluent, has a Cl/Br ratio between 300 and 600 and road-salt-affected water a Cl/Br ratio between 1,000 and 10,000 (Vengosh and Pankratov, 1998; Davis and others, 1998; and Risch and Robinson, 2000); however, Granato and Smith (2000) documented treated sewage effluent with Cl/Br ratios greater than 2,000, a level that overlaps into reported ranges for road salt and introduces uncertainty in making distinctions between road salt and ISDS influence.

Turkey Creek watershed Cl/Br ratios ranged from 15 to 3,535 in ground water (median 192). Three ground-water samples had Cl/Br ratios less than 80, indicating Cl/Br ratios influenced by precipitation. Of the three, one had a ratio of 15, indicating a possible source of bromide. Surface-water Cl/Br ratios ranged from 310 to 1,971 (median 919). Chloride/bromide ratio was poorly correlated to chloride ( $r^2 = 0.05$ ), nitrate plus nitrite ( $r^2 = 0.03$ ), and tritium ( $r^2 = 0.16$ ) concentration. Nine of the ground-water samples and all three surface-water samples had Cl/Br ratios greater than 300, indicating an influence from a source of halite dissolution such as road salt or ISDS effluent,

or both. Without additional data that document Cl/Br ratios in ISDS effluent within the Turkey Creek watershed as unique and distinct from ratios resulting from road salt and other deicers/dust inhibitors (which are increasing in usage) used on roads, determining the precise source is not possible; however, Cl/Br ratios clearly indicate that surface water and most ground water sampled in the Turkey Creek watershed are affected by anthropogenic sources of chloride.

### Wastewater Compounds

Samples analyzed for wastewater compounds were collected in ground water and surface water to evaluate whether sources of human wastewater contaminants such as ISDS's could be affecting water quality. The types of wastewater compounds reported by the method include selected hormones, pesticides, fragrances and flavorings, flame retardants, fecal indicators, petroleum products, combustion products, nonionic detergent metabolites, food preservatives, and solvents. The analytical identification of these compounds is still being refined, and analytical recoveries of some compounds are poor (Steven Zaugg, U.S. Geological Survey National Water Quality Laboratory, oral commun., November 2001). Concentrations that are identified by the analyst but are less than the method reporting limit are reported as estimated. Compounds with poor analytical recoveries also are considered estimated. Contamination during sample collection and analysis is a risk, and little is known about the fate and transport of wastewater

compounds in the subsurface. Samples were collected in April 2001 (eight ground-water samples, four surface-water samples, and two field blanks) and September 2001 (three surface-water samples, one field blank). No samples of ISDS effluent were collected; however, the compounds reported by the method are known to occur in human wastewater effluent.

On the basis of concentrations reported in estimated ranges, April 2001 results from three of four surface-water samples indicated the presence of at least one wastewater compound, and results from two of eight ground-water samples indicated the presence of wastewater compounds (table 10). In September 2001, two of three surface-water samples had estimated concentrations. The compounds reported in analyses were cholesterol, beta-sitosterol, tributylphosphate, ethanol 2-butoxy-phosphate, skatol, phenol, tetrachloroethylene, bisphenol A, prometon, N,N-diethyltoluamide (DEET), benzophenone, tri(2-chloroethyl)phosphate, acetyl-hexamethyl-tetrahydro-naphthale (AHTN), and hexahydrohexamethyl-cyclopentabenzopyran (HHCB).

The sample results indicate that some wastewater compounds were present both in ground water and surface water in the Turkey Creek watershed. However, no more than a few compounds were present in any one particular sample (highest number of detections in a sample was five), little consistency among compounds detected was observed, and when detected, compounds generally were reported in trace amounts (most concentrations were estimated). Although the number of samples was small, the frequency of detections was higher among surface-water samples than ground-water samples.

### Chloride Sources

Chloride is a conservative anion present in trace amounts in precipitation. In watersheds such as Turkey Creek, rock weathering contributes negligible chloride to ground water because of a lack of chloride-bearing minerals in bedrock and soil materials. In these watersheds, the sources of chloride other than precipitation are anthropogenic, such as ISDS's and the application of salt and dust inhibitors to roads.

Assuming that chloride is conservatively transported through the watershed, that the concentration of chloride in precipitation and the amount of precipitation is known, and that evapotranspiration can be measured or estimated, a variant of the method described in Claassen and Halm (1996) can be used to estimate the expected base-flow (or ground-water) concentration of

chloride in the watershed. For the Turkey Creek watershed, a conservative estimate of chloride concentration in base flow was made by assuming that evapotranspiration was 90 percent of watershed mean precipitation and concentration of chloride in precipitation was about 0.09 mg/L (mean of the precipitation-weighted means over the period of record for five Colorado Front Range National Atmospheric Deposition Program stations [U.S. Geological Survey, 2001]). On the basis of these assumptions, a chloride concentration for ground water of about 0.9 mg/L was calculated. At the mouth of the canyon in September 1998 (at near base-flow conditions), chloride concentration in Turkey Creek was 127 mg/L. It is therefore unlikely that precipitation is the only source of chloride to the watershed. The median chloride concentration in ground water was about 6.8 mg/L, and the median concentration in surface water was 64 mg/L. This difference indicates that chloride may be transported preferentially along flow paths connected to surface water rather than flow paths connected to wells.

Salt applied to roads is one likely source of chloride enrichment in the watershed. The Colorado Department of Transportation applied an estimated mean of 250 tons of salt per year in the form of sand and salt mixture to U.S. Highway 285 from 1988 to 2000 (Chuck Loerwald, Colorado Department of Transportation, written commun., August 2000). Other unestimated sources of chloride are salt and magnesium chloride applied to roads and driveways by Jefferson County and private landowners. Known loads of chloride in road salt were compared to estimated loads of chloride transported in Turkey Creek at the mouth of the canyon. Using a natural log regression of flow and specific conductance and then linear regression of chloride to specific conductance resulted in estimates of chloride load (tons) and flow-weighted-mean concentrations in milligrams per liter for water years 1999 through 2001 as follows: 1999 = 400 tons, 36 mg/L; 2000 = 169 tons, 51 mg/L; 2001 = 168 tons, 52 mg/L. These estimates show that in 2000 and 2001 the chloride load is in the same range as a mean mass of chloride in road salt applied to U.S. Highway 285. In 1999, a high-flow year, the mean applications of road salt do not account for all the estimated chloride transported out of the watershed. Other sources of chloride such as ISDS's may be another cause of high chloride in streams. An unanswered question is why high concentrations of chloride found in surface-water base flow are rarely seen in the domestic wells sampled in the watershed.

## Seasonality of Specific Conductance

Seasonality of specific-conductance measurements in water wells and in streams could indicate source-water dynamics through the annual cycle and provide information about interactions between ground water and surface water. To assess seasonality of changes in specific conductance, additional non-USGS data were available for analysis. Samples for analysis of specific conductance were collected weekly by homeowners at 24 wells (24 wells in August through October 2000 [fall measurement] and 23 of the original 24 wells in March through June 2001 [spring measurement]) (231 wells listed in table 8 and locations shown in fig. 12 except GWB03, which is an undocumented location). Specific conductance was then measured by Jefferson County Health Department personnel who picked up the samples from the homeowners. Measurements of specific conductance in surface water were available from USGS measurements associated with gaging stations (approximately monthly, 1998–2001), from USGS measurements made during quarterly samples collected for this study (four values, 1998–99), and from data collected during monitoring of the reconstruction of U.S. Highway 285 through the Turkey Creek watershed (monthly, 1995–2000; data from Timothy D. Steele, Colorado Department of Transportation consultant, written commun., October, 2001).

Weekly specific-conductance measurements of samples from the 24 wells with both spring and fall measurements are plotted along with the following hydrologic variables: estimated watershed daily mean snowpack and precipitation, daily mean streamflow at Turkey Creek at mouth, and monthly water levels in two monitoring wells (MH2 and MH11) in figure 37. During the fall measurement period, samples from most wells showed little change in specific conductance. Samples from a few wells showed relatively minor increases and decreases in specific conductance by the end of August or early September. The changes were generally less than 25 percent, although samples from GWH03 had a relatively large decrease in specific conductance (from 538 to 358  $\mu\text{S}/\text{cm}$ ) and samples from GWO02 had a relatively large increase in specific conductance (from 214 to 430  $\mu\text{S}/\text{cm}$ ). Samples from GWN01 had the largest change in specific conductance (a decrease of 46 percent of the fall median value), but that change is a result of a single anomalous measurement.

During the spring measurement period, generally minor changes in specific conductance also were measured; however, the results of the spring measurements showed greater variability than the

fall measurements. Samples from six wells had changes during the spring measurement period that were larger than 50 percent of their spring period median, and samples from five of those wells (GWB03, GWF10, GWH03, GWO10, GWO12) showed a decrease in specific conductance during the spring melt. One of the largest changes (103 percent of the spring median), however, was in samples from well GWO02, which showed an increase in specific conductance from 367 to 943  $\mu\text{S}/\text{cm}$  during the spring melt. A seasonality of specific conductance in ground water could indicate dilute recharge, in response to precipitation, is entering the flow system connected to a well. The expected response is related to increases in water level in the well, such as that observed in several wells noted above. Samples from the well that showed increases in specific conductance during spring and fall (GWO02) may be the result of recharge even if the pattern does not fit the conceptual model of dilution. If seasonal recharge was rich in dissolved salt from road salt or other sources, an increase in specific conductance during the spring melt might result. However, because only two samples were collected at the GWO02 well for major ions, and neither sample was collected during spring melt, additional information is not available to verify the hypothesis that road salt is affecting the specific conductance in GWO10. Also, GWO02 had the lowest tritium concentration sampled, indicating a relatively large component of pre-bomb recharge. The majority of wells showed minor seasonal changes in specific conductance, providing little evidence that recently recharged (dilute) water was present, despite water-level fluctuations throughout the watershed that indicated seasonal influences on the depth of the water table.

Instantaneous specific-conductance measurements made in Turkey Creek (stations 06710992 and 06710995) (fig. 38) (data from USGS and Timothy D. Steele, Colorado Department of Transportation consultant, written commun., October 2001) and its tributaries indicate that specific conductance is inversely proportional to streamflow, and decreases in specific conductance occur during a spring high-flow period, responding to runoff of relatively dilute water. Base-flow specific-conductance values were high (more than 600  $\mu\text{S}/\text{cm}$ ) compared to specific conductance in ground water (median 313  $\mu\text{S}/\text{cm}$ , table 19). In fact, the highest specific-conductance value measured in Turkey Creek at the mouth (796  $\mu\text{S}/\text{cm}$ ) was greater than the 96th percentile of ground-water samples. Even at high streamflow, specific conductance in Turkey Creek was

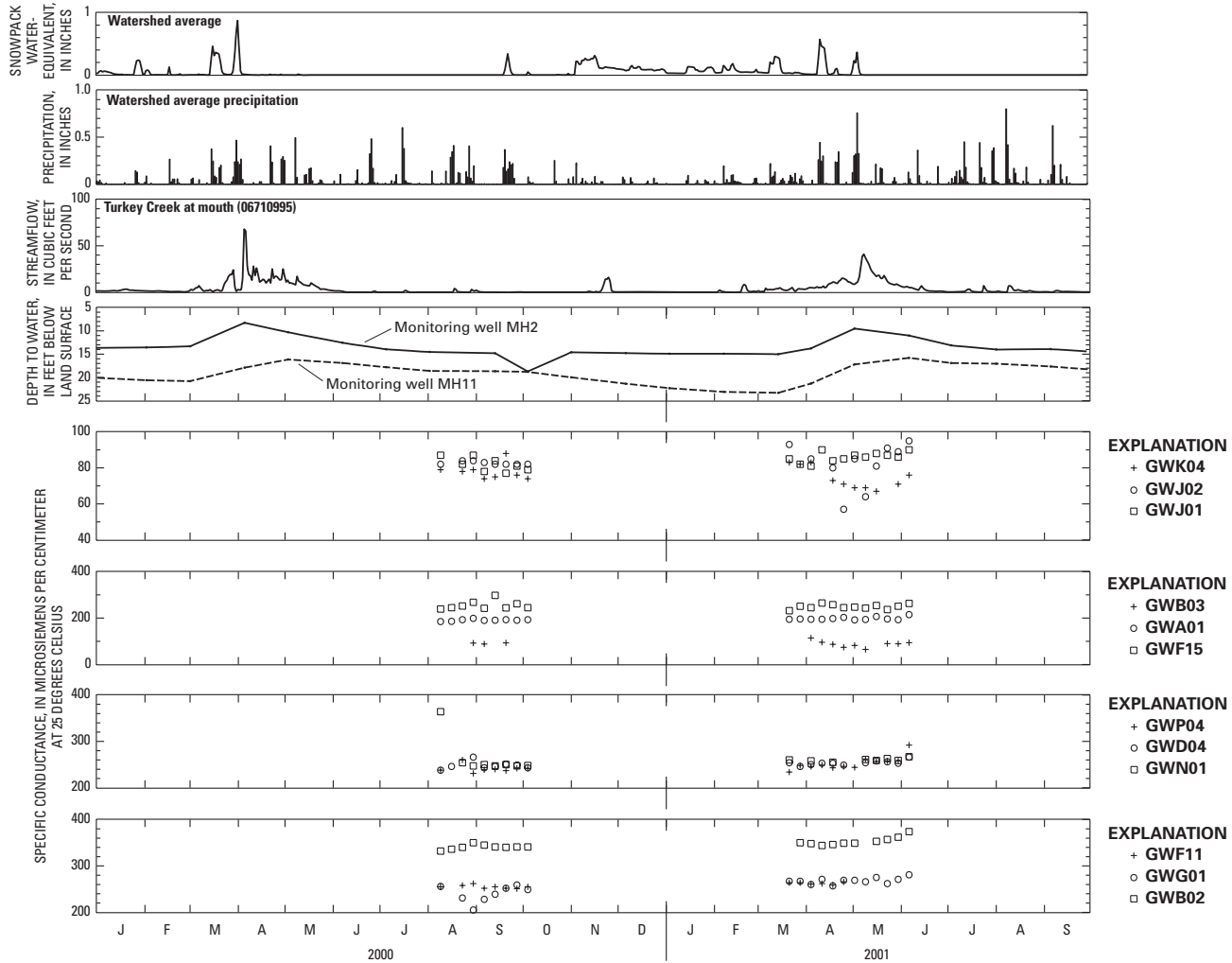


**Figure 37.** Time-series plot of Turkey Creek watershed hydrologic variables and seasonal specific-conductance measurements collected at selected wells in fall 2000 and spring 2001.

not observed at levels much below 200  $\mu\text{S}/\text{cm}$ , indicating a fairly strong dissolved-solids signal for a mountainous, crystalline rock, hydrogeologic setting.

There are six watersheds that have components of similar crystalline bedrock geology, contain similar elevation ranges as the Turkey Creek watershed, and have NWIS streamflow and specific-conductance data from sites along the eastern slope of the Rocky Mountains in Colorado. Detailed demographic data are not available for these sites, but in general they are less developed, in terms of population, than the Turkey Creek watershed. Site locations (A–G) are shown in figure 1 and summaries of specific-conductance data are listed in table 21. Although the Turkey Creek seasonal variation in specific conductance has a range as a percentage of median that is similar

to comparison sites (B–G in table 21), specific-conductance values are generally substantially higher than comparison sites (fig. 39). This indicates that water exiting the Turkey Creek watershed is more concentrated than water from the selected comparison sites in similar hydrologic settings.

The flow-weighted-mean specific conductance (FWMSC) computed from daily values predicted from a regression with streamflow is about 290  $\mu\text{S}/\text{cm}$  (period of 1999–2001 data for station 06710995), a value that represents the central tendency of specific conductance by streamflow volume, not time. If probable measurement and computational uncertainties are considered, the FWMSC is similar to median ground-water specific conductance.

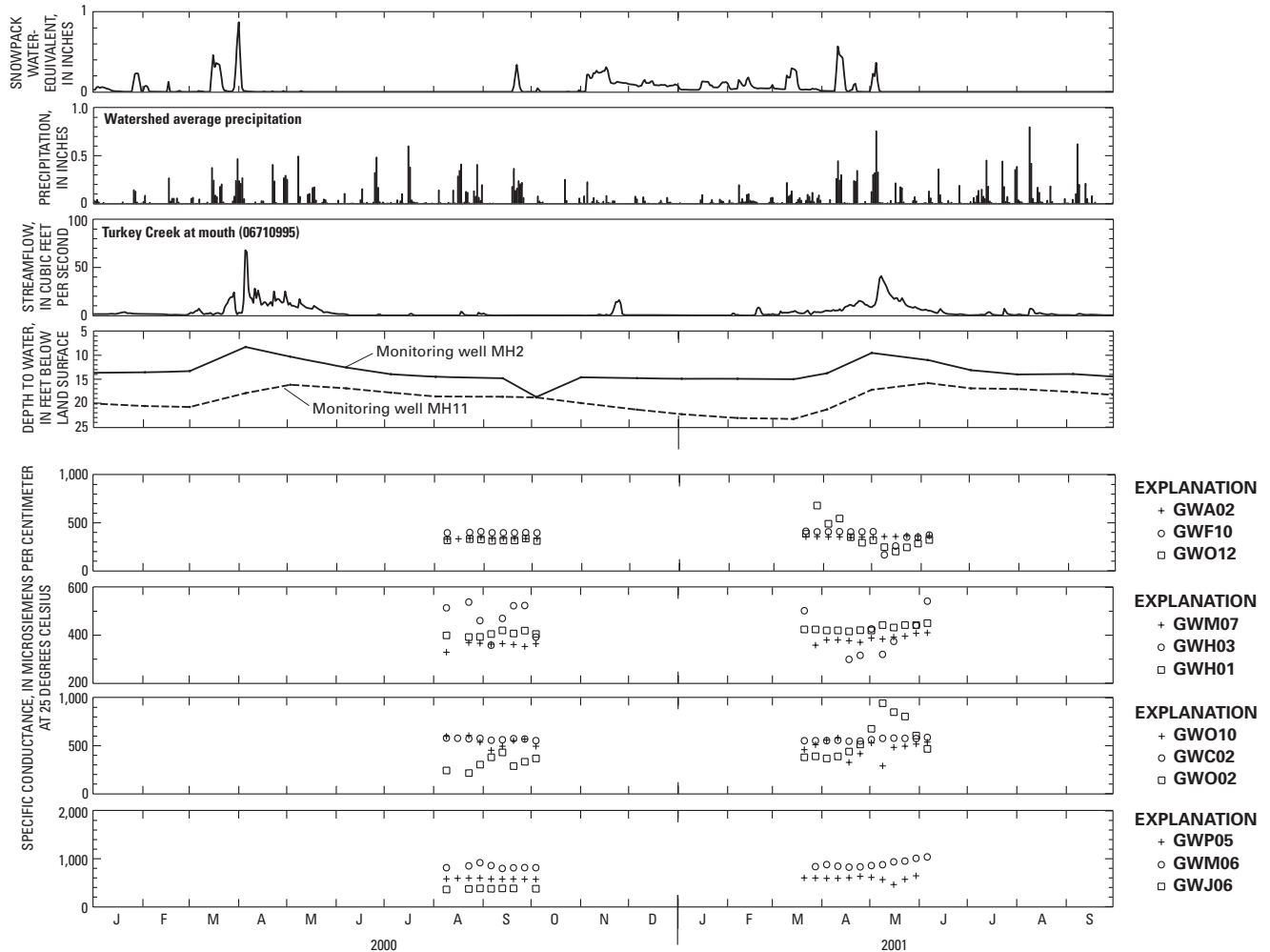


**Figure 37.** Time-series plot of Turkey Creek watershed hydrologic variables and seasonal specific-conductance measurements collected at selected wells in fall 2000 and spring 2001—Continued.

## ASSESSMENT OF WATER RESOURCES

An assessment of the water resources in the Turkey Creek watershed is presented in this section. Much of the assessment is based on the hydrologic conditions described in the preceding sections and a characterization of many of those conditions in a watershed model. The watershed model characterization permits quantified estimates of hydrologic conditions in time and space. The watershed model characterization provides simulated estimates for water-balance terms such as precipitation, evapotranspiration, soil moisture, overland flow, interflow, and base flow, as well as the contents of interflow and base-flow reservoirs. In addition, the estimates for water-balance terms help answer questions about the fate of water that percolates below the soil zone, or

soil-zone reservoir as depicted in figure 13. Although the watershed model does not characterize movement of water that is not associated with local streamflow, it does characterize the amount of water that is lost from base-flow reservoirs; the most likely fate of this water is underflow that is discharged from the watershed by means other than evapotranspiration or streamflow.

### Estimates of Potential Fracture-Network Porosity

In order to bracket the potential volume available for ground-water storage in the different rock-group fracture networks, estimates of potential porosity were calculated for each of the fracture-network models or realizations generated with software known as FracMan

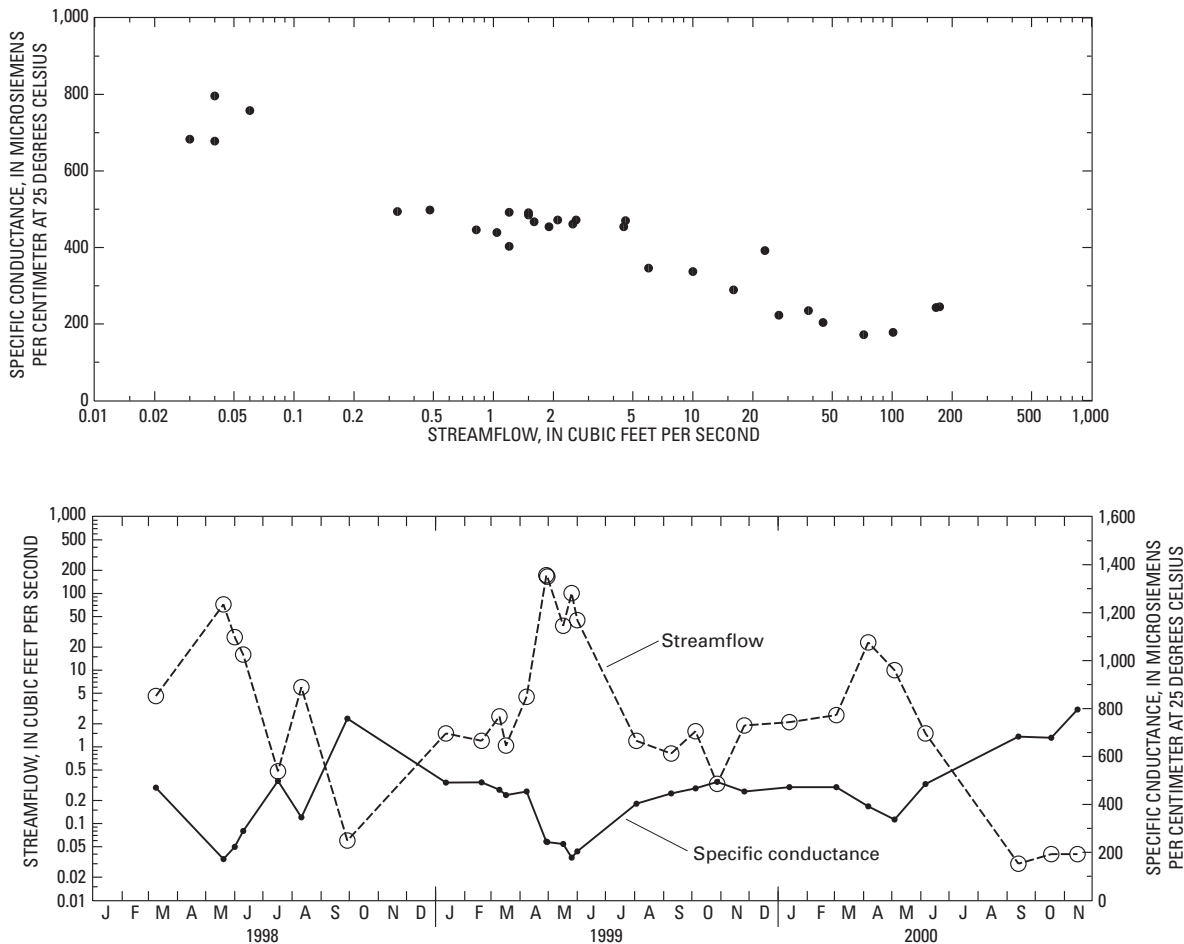


**Figure 38.** Correlation of specific conductance and streamflow and time-series plot showing seasonal variation of specific conductance and streamflow at Turkey Creek at mouth of canyon near Morrison.

(Dershowitz and others, 1996) that is briefly described in the Appendix. Potential porosity is defined here as a measure of fracture porosity based solely on simulation of geometric measures from outcrops (for example, fracture intensity, trace length). Potential porosity calculations assume that rock groupings, computed fracture-set statistics and intensities, reasonable estimates of aperture, and the scale of the model domains are all representative of near-surface field conditions. Potential porosity is not directly linked to hydraulic parameters from field measures such as pumping tests or analysis of water levels compared with precipitation and discharge over time. Rather, potential porosity is simply an estimate based on reasonable values for aperture and measured fracture intensities. Use of geometric fracture-network measurements to simulate hydraulic properties tends to result in overestimation. Simulation results, however, are based on measurements in the Turkey Creek watershed and provide a reasonable

set of estimated porosity values for the representative rock groups relative to one another. Additionally, as is described below, the fracture-network realizations also were conditioned by using transmissivities and apertures derived from previously completed aquifer tests and the cubic law, respectively (Tomusiak and others, 2000; Folger, 1995).

Ten calibrated fracture-network realizations were constructed with FracMan for the watershed at representative localities. Three realizations represent the intrusive rocks, four represent the metamorphic rocks, and three realizations represent the fault zones (as in Caine and Forster, 1999). Two of the realizations represent faulted metamorphic rock, and one represents faulted intrusive rock.

In each realization, the fracture apertures are initially set to a constant value and are correlated with transmissivity by using the cubic law (for example, Snow, 1968):



$$T_f = \frac{b^3}{12} \times \frac{\rho g}{\mu} \quad (6)$$

where

- $T_f$  is fracture transmissivity [ $L^2/T$ ],
- $b$  is aperture [ $L$ ],
- $\rho$  is the fluid density [ $M/L^3$ ],
- $g$  is the acceleration due to gravity [ $L/T^2$ ], and
- $\mu$  is the dynamic fluid viscosity [ $M/LT$ ]  
( $M = \text{mass}$ ,  $L = \text{length}$ ,  $T = \text{time}$ ).

In calculating fracture volume ( $V_f$ ) and total fracture porosity ( $n_p$ ), estimates of hydraulic aperture ( $b$ ), fracture intensity ( $P_{32}$ ), and domain volume ( $V_m$ ) are the only parameters needed.  $V_f$  and  $n_p$  are calculated using:

$$V_f = b \times P_{32} \times V_m \quad (7)$$

$$n_p = \frac{V_f}{V_m} \quad (8)$$

where

- $V_f$  and  $V_m$  have the dimensions of [ $L^3$ ],
- $b$  has the dimension of [ $L$ ], and
- $P_{32}$  has the dimension of [ $L^2/L^3$ ].

Two end-member cases and one intermediate case for constant aperture were used in the porosity calculations (1,000  $\mu\text{m}$  [or 1 mm], 100  $\mu\text{m}$ , and 10  $\mu\text{m}$ ). Although aperture distributions were not recorded in the field, except to note if the fractures were less than or greater than 1 mm, the chosen end members are assumed to be representative of field conditions. Simulations with all fractures having apertures of 1 mm may overestimate porosity, whereas simulations with all fractures having apertures of 10  $\mu\text{m}$  will likely underestimate porosity. The actual aperture distribution is likely between the end-member extremes for near-surface conditions (about 0 to 300 ft below land surface). The aperture estimates were compared to calculated hydraulic fracture apertures made by Folger (1995) in the intrusive rocks in the vicinity of Conifer, Colo. (fig. 1). Folger (1995) used the cubic law to calculate apertures from transmissivity values obtained from single-well, short-term aquifer pumping tests. Folger's calculated aperture estimates ranged between 60 and 570  $\mu\text{m}$ , which is well within the end-member estimates for the intrusive rocks (Folger, 1995, table 22). Even if these aperture estimates are reasonable, however, there is the random possibility that one very large fracture (for example, 5 mm) or a network of very small fractures (for example less than 1  $\mu\text{m}$ ) could completely disrupt porosity estimates. These random fractures could dominate the local flow and storage system,

**Table 21.** Specific-conductance data summary for Turkey Creek at mouth (site A) and eight comparison sites on the eastern slope of the Rocky Mountains in Colorado

[ID, identification number; specific conductance in microsiemens per centimeter at 25 degrees Celsius; drainage area in square miles; range percentage of median computed by dividing the difference between maximum and minimum by the median; most measurements collected on monthly basis associated with stream-gage operations]

Site letter in fig. 1	USGS station ID	Station name	Latitude (degrees, minutes, seconds)	Longitude (degrees, minutes, seconds)	Drainage area	Minimum	Median	Maximum	Range percentage of median
A	06710995	Turkey Creek at mouth of canyon near Morrison	39 37 13	105 11 41	47.4	172	454	796	137
B	07099050	Beaver Creek above upper Beaver Cemetery near Penrose	38 33 42	105 01 17	122	57	88	129	82
C	07105000	Bear Creek near Colorado Springs	38 49 21	104 53 17	6.89	70	91	147	85
D	07105490	Cheyenne Creek at Evans Ave at Colorado Springs	38 47 26	104 51 49	21.7	68	110	175	97
E	07105945	Rock Creek above Fort Carson Reservation	38 42 27	104 50 46	6.79	56	149	240	123
F	07107900	Greenhorn Creek near Rye	37 55 14	104 57 21	9.56	48	85	120	85
G	07108100	Graneros Creek near Rye	37 54 47	104 55 31	4.32	70	160	286	135

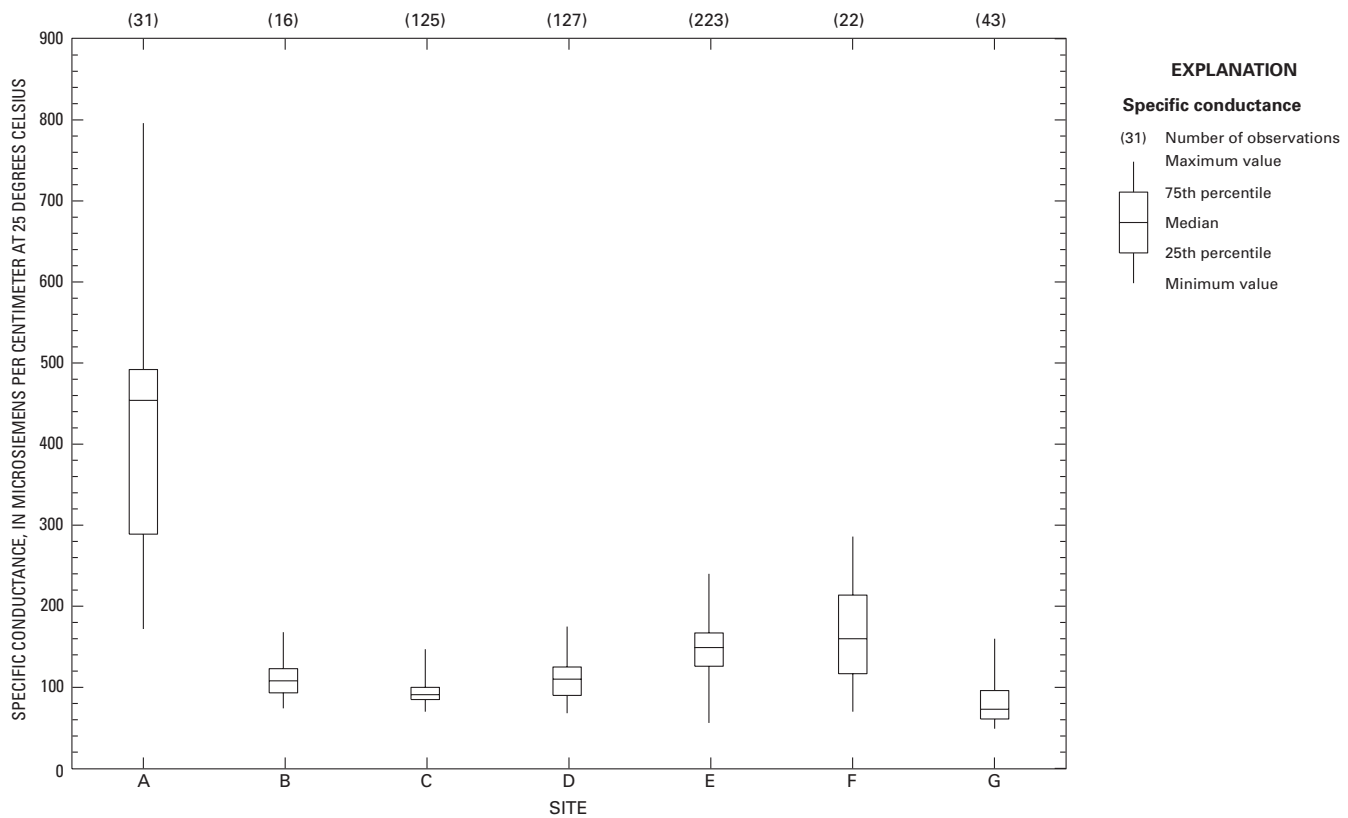


**Figure 39.** Boxplot showing distribution of specific conductance at Turkey Creek at mouth of canyon (site A) and six comparison sites.

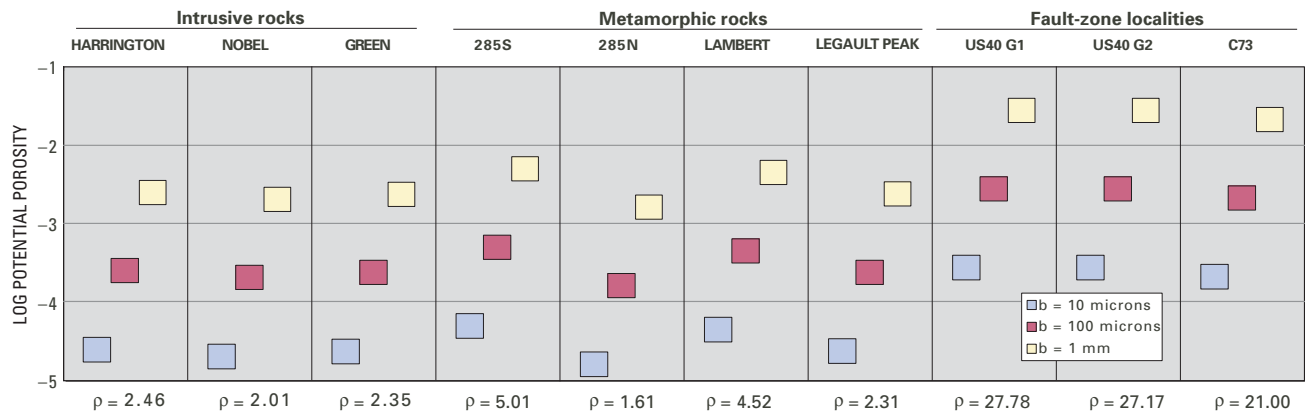
particularly when considering the heterogeneity of the fracture-intensity distributions and the realization that some near-surface fractures likely close down with depth. Regardless, these are reasonable estimates of aperture that are translated into potential porosities that might exist considering the lack of field observations and measurements of fracture-network properties with depth.

Figure 40 and table 23 are a compilation of the estimated fracture intensities and total potential porosities for each fracture-network realization using the end-member apertures. Calculated porosity estimates are shown for each lithology and their faulted equivalents (table 23). Although the calculated fracture-porosity values range over 4 orders of magnitude (from 0.0016 to 2.78 percent), the midrange (100  $\mu\text{m}$ ) constant aperture simulations produce porosity values from 0.016 percent to 0.051 percent for the nonfault-zone realizations and of approximately 0.27 percent for the fault-zone realizations (table 23). The intrusive-rock porosity shows little variation and ranges from 0.020 to

**Table 22.** Turkey Creek watershed hydrologic parameter estimates from previous work (Folger, 1995)

[m<sup>2</sup>/s, square meters per second;  $\mu\text{m}$ , micrometers; %, percentage; max, maximum; min, minimum]

Estimated transmissivities (m <sup>2</sup> /s)	Hydraulic aperture estimates ( $\mu\text{m}$ )	Porosity estimates (%)	
0.0000347	380	0.019	
0.0000694	240	0.012	
0.000127	110	0.006	
0.0000347	200	0.001	
0.000000810	190	0.057	
0.0000104	120	0.036	
0.00139	60	0.016	
0.00000231	100	0.003	
0.00000463	570		
0.00000926	360	0.057	max
0.0000231	160	0.001	min
0.0000810	300		
0.000162			
0.000174	570		max
0.000139	60		min
0.0000116			
0.00185			
0.00000810			
0.00000579			
0.00185			max
0.000000810			min



**Figure 40.** Plot of the log of total fracture model potential porosity for each locality ( $\rho$  = fracture intensity).

0.025 percent, whereas the metamorphic-rock porosity shows slightly greater variation ranging from 0.016 to 0.051 for the 100- $\mu$ m constant aperture simulations (fig. 40 and table 23). The fault-zone porosity values are relatively uniform within a single fault zone and from one fault zone to another, and the fault-zone porosity values are consistently one order of magnitude greater than the nonfault-zone porosity values. The calculated porosity values are well within the general values of porosity reported for crystalline rocks (Freeze and Cherry, 1979) and also within values estimated by Folger (1995).

In the Turkey Creek watershed, fracture porosity is a critical factor limiting water availability because it is, in general, extremely low. The estimated potential porosities for the rock groups are, on average, roughly two to three orders of magnitude lower than those in sedimentary rocks that typically have porosities of 5 to 25 percent (Freeze and Cherry, 1979). The actual amount of available ground water is a function of the distribution of porosity and other factors such as recharge and discharge rates from natural and human causes, saturated thickness, and the circulation depth of ground-water flow.

## Runoff Modeling

The watershed characterization presented in this section helps address some of the issues stated in the preceding “Estimates of Potential Fracture-Network Porosity” section. The simulated results provide temporal and spatial estimates of recharge.

The simulations also provide estimates of how much and how quickly recharge leaves the watershed as interflow and base flow and how much of the recharge percolates to deeper parts of the watershed and is not associated with local streamflow. Estimates for terms presented in this section can be compared to estimates of contemporary (2001) withdrawals made by domestic wells.

## Hydrologic Response Unit Delineation and Parameterization

Hydrologic Response Units (HRU’s) were delineated to provide a topography-based accounting framework for surface, or near-surface, processes related to evapotranspiration, soil moisture, snowpack, and percolation to deeper parts of the watershed system. All of these processes, to some extent, are influenced by topographic characteristics such as aspect and slope. As indicated in the “Runoff Modeling Methods” section, automated methods were used to delineate HRU’s in the Turkey Creek watershed. The methods implement a series of algorithms that have been developed to work with digital elevation model (DEM) data to define surfaces and their topographic characteristics within the watershed that border streams and conform to the watershed boundary (Jensen and Domingue, 1988). The number of HRU’s can be controlled to obtain a user-defined, acceptable level of resolution with respect to topographic features. The watershed was subdivided so that, on an HRU basis, values for slope and aspect were relatively representative of aspects for all points within the HRU. The result was 112 HRU’s with a mean area of 270.7 acres (fig. 41, table 24).

**Table 23. Turkey Creek watershed fracture-model potential porosity results**

[ $V_f$  = total fracture volume in cubic meters;  $n_p$  = total fracture porosity in model in percent;  $m^2/m^3$ , square meter per cubic meter;  $m^3$ , cubic meter,  $\mu m$ , micrometer  
MAX, maximum; MIN, minimum]

Location and model size	Model fracture density ( $m^2/m^3$ )	Model volume ( $m^3$ )	$V_f$			$n_p$		
			10 $\mu m$	100 $\mu m$	1mm	10 $\mu m$	100 $\mu m$	1mm
METAMORPHIC ROCKS								
285South								
2 m	5.10	8	0.000408	0.00408	0.0408	0.0051	0.051	0.51
5 m	5.10	125	0.00638	0.0638	0.638			
10 m	5.10	1000	0.0510	0.510	5.10			
15 m	5.10	3375	0.172	1.72	17.2			
285North								
2 m	1.607	8	0.000129	0.00129	0.0129	0.0016	0.0161	0.1607
5 m	1.607	125	0.00201	0.0201	0.201			
10 m	1.607	1000	0.0161	0.161	1.61			
15 m	1.607	3375	0.0542	0.542	5.42			
LAMBERT								
2 m	4.517	8	0.000361	0.00361	0.0361	0.0045	0.0452	0.4517
5 m	4.517	125	0.00565	0.0565	0.565			
10 m	4.517	1000	0.0452	0.452	4.52			
15 m	4.517	3375	0.152	1.52	15.2			
LEGAULT PEAK								
2 m	2.31	8	0.000185	0.00185	0.0185	0.0023	0.0231	0.231
5 m	2.31	125	0.00289	0.0289	0.289			
10 m	2.31	1000	0.0231	0.231	2.31			
15 m	2.31	3375	0.0780	0.780	7.80			
					AVERAGE	0.0034	0.0338	0.3384
					MAX	0.0051	0.051	0.51
					MIN	0.0016	0.0161	0.1607
INTRUSIVE ROCKS								
HARRINGTON								
2 m	2.46	8	0.000197	0.00197	0.0197	0.0025	0.0246	0.246
5 m	2.46	125	0.00308	0.0308	0.308			
10 m	2.46	1000	0.0246	0.246	2.46			
15 m	2.46	3375	0.0830	0.830	8.30			
NOBEL								
2 m	2.01	8	0.000161	0.00161	0.0161	0.0020	0.0201	0.201
5 m	2.01	125	0.00251	0.0251	0.251			
10 m	2.01	1000	0.0201	0.201	2.01			
15 m	2.01	3375	0.0678	0.678	6.78			
GREEN								
2 m	2.35	8	0.000188	0.00188	0.0188	0.0024	0.0235	0.235
5 m	2.35	125	0.00294	0.0294	0.294			
10 m	2.35	1000	0.0235	0.235	2.35			
15 m	2.35	3375	0.0793	0.793	7.93			
					AVERAGE	0.0023	0.0227	0.2273
					MAX	0.0025	0.0246	0.2460
					MIN	0.0020	0.0201	0.2010
FAULT ZONE ROCKS								
US40 FAULT ZONE GRID 1								
2 m	27.78	8	0.00222	0.0222	0.222	0.028	0.278	2.78
5 m	27.78	125	0.0347	0.347	3.47			
10 m	27.78	1000	0.278	2.78	27.8			
15 m	27.78	3375	0.938	9.38	93.8			
US40 FAULT ZONE GRID 2								
2 m	27.17	8	0.00217	0.0217	0.217	0.027	0.272	2.72
5 m	27.17	125	0.0340	0.340	3.40			
10 m	27.17	1000	0.272	2.72	27.2			
15 m	27.17	3375	0.917	9.17	91.7			
C73 FAULT ZONE								
2 m	21.00	8	0.00168	0.0168	0.168	0.021	0.210	2.10
5 m	21.00	125	0.0263	0.263	2.63			
10 m	21.00	1000	0.210	2.10	21.0			
15 m	21.00	3375	0.709	7.09	70.9			
					AVERAGE	0.0253	0.253	2.53
					MAX	0.028	0.278	2.78
					MIN	0.021	0.210	2.10

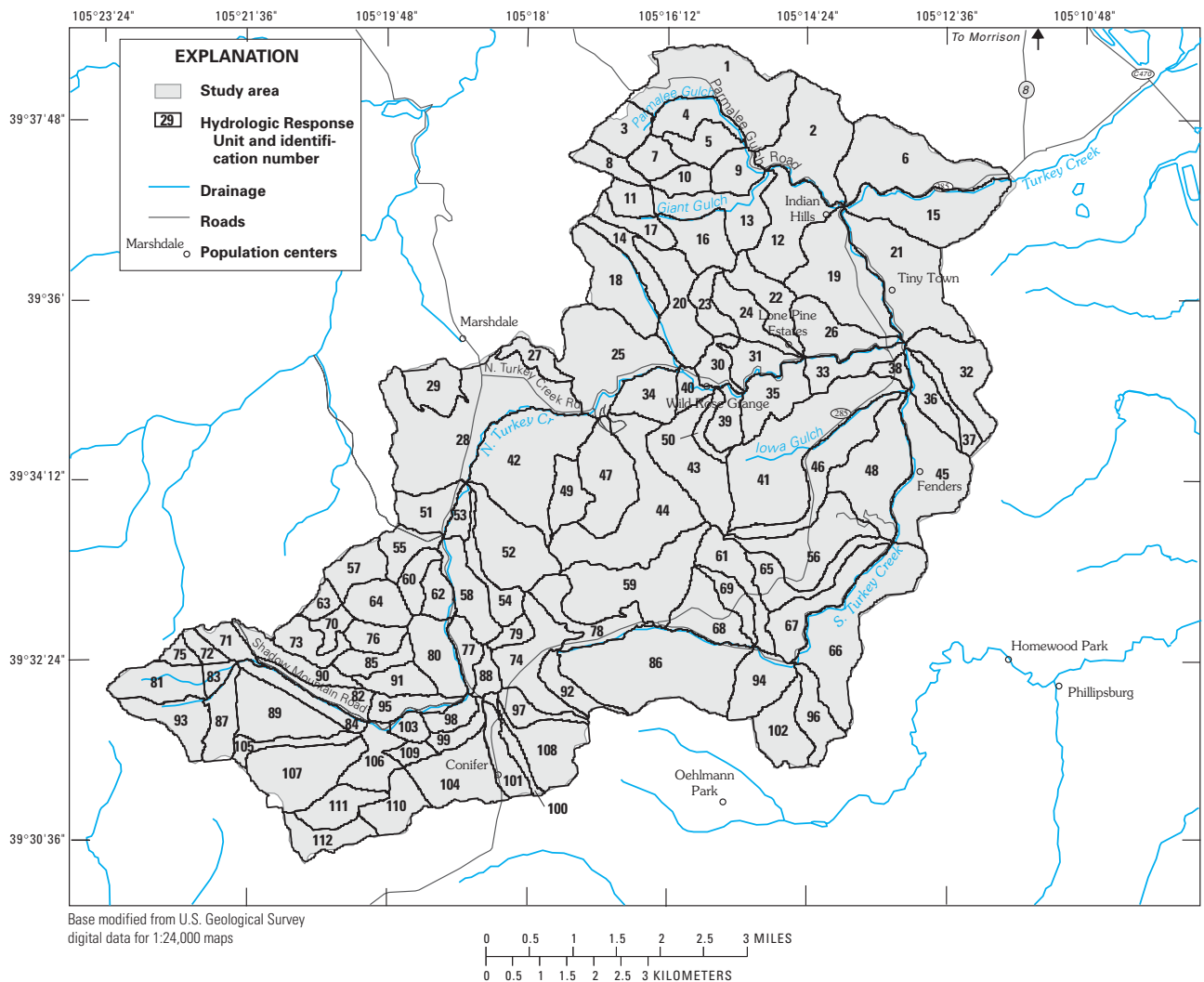


**Figure 41.** Hydrologic Response Units delineated for use with the Precipitation-Runoff Modeling System in the Turkey Creek watershed.

Precipitation-Runoff Modeling System (PRMS) input parameters related to soil characteristics were determined by using digital data available from the Soil Survey Geographic data base (SSURGO) (U.S. Department of Agriculture, 1995) and a local implementation (Viger, 1998) of algorithms developed by Wolock (1997). The algorithms assign values to PRMS input parameters related to soil properties such as thickness and water-holding capacities.

PRMS input parameters associated with vegetation were defined in terms of type and density (table 24). Vegetation types were defined as trees and grasses, and densities were determined using digital orthophoto imagery provided by Jefferson County. The original imagery, which has a grid resolution of 15 ft, was reclassified to a grid that matches the DEM (98.4 ft) and has values for percentage of trees

(R.M.T. Webb, U.S. Geological Survey, oral commun., 2001). Additional PRMS input parameters associated with vegetation such as seasonal interception rates were provided from other calibrations of PRMS in the mountainous areas of Colorado, as part of the methods implemented by Viger (1998).

Most of the remaining PRMS input parameters are related to processes describing movement of water from one part of the system to another (such as percolation from the soil zone to deeper parts of the watershed system), energy-budget processes that are related to evapotranspiration, precipitation phase assignment, or snowpack melt and accumulation. Initial values for input parameters associated with climatic processes also were obtained from other calibrations of PRMS in the mountainous areas of Colorado, as part of the methods implemented by Viger (1998).





## Interflow and Base-Flow Reservoir Delineation and Parameterization

The four rock groups—metamorphic, intrusive, fault zone, and Pikes Peak Granite—were fundamental to the process of defining the conceptual subsurface (interflow and base-flow) reservoirs used for accounting purposes by PRMS. These mappable rock groups were defined on the basis of differences in fracture or weathering characteristics with the underlying hypothesis that the level of fracturing or weathering is related to base-flow rates and to measurable differences in amount of ground water associated with streamflow. The short-term records of intrawatershed streamflow, described in the “Surface-Water Conditions” section, were established to measure such differences. The contributing drainage areas for the records of intrawatershed streamflow, which can be characterized in terms of hundreds of acres, define the resolution of knowledge concerning base-flow conditions established in this study.

Ideally, multiple streamflow records consisting of multiple years of record would be available for each rock group. Several factors, however, including but not limited to duration of the study, geographic constraints imposed by the mapped configuration of some rock groups, and logistical challenges associated with acquiring access to sites, influenced the availability of records. As a result, the short-term records were obtained in intrusive rocks (STR-3 and 4), faulted rocks (STR-2), and Pikes Peak Granite (STR-1) (table 2, table 6, fig. 23) but not metamorphic rocks. In addition, the intrawatershed records cover only about 4 months of streamflow; however, repetitive synoptic measurements of streamflow made throughout the watershed help offset these deficiencies. The synoptic measurements include results for all four rock groups.

Results from the short-term records of streamflow indicate two general and distinct conditions of base flow in the watershed. The first and most prevalent condition is base flow in streams that is poorly sustained. This first condition was observed in intrusive rocks at STR-4 and at many of the synoptic measurements in intrusive and metamorphic rocks. The synoptic measurements indicate that, in general, much of the watershed has poorly sustained streamflow. The second condition is base flow that supports streamflow at relatively steady rates. This condition was found in the Pikes Peak Granite (STR-1) and fault-zone rocks (STR-2). Well-sustained streamflow emanating from the fault-zone rocks fits well with the findings presented in the “Estimates of Potential

Fracture-Network Porosity” section. In addition, well-sustained streamflow emanating from Pikes Peak Granite fits well with the intuitive concept that the highly weathered Pikes Peak Granite may be capable of storing and slowly transmitting ground water to streams. However, well-sustained streamflow also was observed at STR-3, which drains intrusive rocks. Although the presence of well-sustained streamflow in some portions of the intrusive rocks does not support the hypothesis that the rock groups may uniquely influence ground-water conditions, the observed effect cannot be refuted on the basis of available records. One possible explanation for the well-sustained streamflow observed at STR-3 is that the geologic mapping, which is based mostly on rock composition, does not delineate fracture characteristics that transcend rock types.

On the basis of the rock group, and the streamflow records and synoptic measurements of streamflow described above, four conceptual interflow and base-flow reservoirs (fig. 42) were defined and used for accounting purposes in PRMS. Although the reservoirs are mappable and distinct from each other, they should not be considered distinct aquifers. Rather, each reservoir represents a part of a single aquifer system that behaves somewhat differently than the rest of the aquifer system. The watershed characterization implemented with PRMS facilitates quantitative descriptions of differences between base-flow reservoirs. Available records do not describe ground-water discharge conditions at a scale less than the contributing drainage areas for streamflow records, and there is no basis for undertaking detailed subsurface accounting at the HRU scale.

The subsurface reservoirs are referred to as “metamorphic,” “intrusive,” “fault zone,” and “Pikes Peak Granite.” The reservoirs generally conform to the mapped rock groups. The metamorphic-rock reservoir was characterized with the results of synoptic streamflow measurements and watershed records. The intrusive-rock reservoir was characterized with records from STR-4. The fault-zone reservoir was represented with records from STR-2. Because short-term records of streamflow from STR-3 indicate base-flow characteristics similar to fault-zone rocks (STR-2), they were grouped together to characterize the fault-zone reservoir. Two additional HRU’s, 32 and 37, also were added to the fault-zone reservoir on the basis of synoptic measurements of discharge (SNGN6, table 15). The Pike Peak Granite reservoir was characterized with records from STR-1. In addition, any



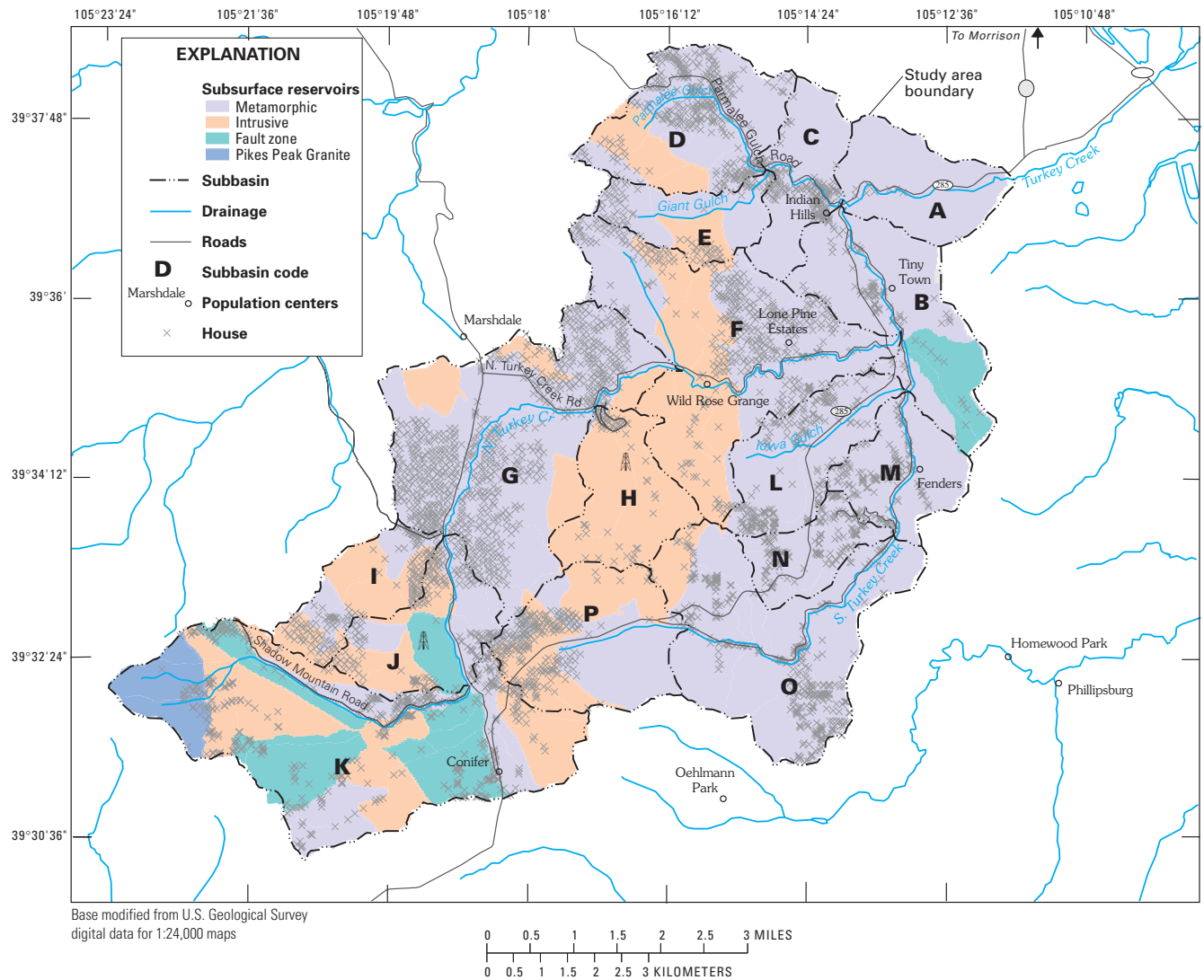


**Figure 42.** Interflow and base-flow reservoirs delineated for use with the Precipitation-Runoff Modeling System in the Turkey Creek watershed.

isolated occurrence of a rock group that was less than about 40 acres in area was considered to be homogeneous with respect to its surroundings. Interflow reservoirs were defined to be coincident with base-flow reservoirs and, therefore, occur as a paired member to each base-flow reservoir. Each interflow and base-flow reservoir pair is associated with multiple HRU's (table 24), and input to the base-flow reservoir is a combination of accretions from the soil moisture and interflow storage (fig. 13).

Initial input-parameter values for each interflow and base-flow reservoir were assigned on the basis of streamflow records, either from stream gages or synoptic measurements. Values for base-flow reservoir parameters that control the amount of water routed

to streamflow were assigned so that areas that have poorly sustained streamflow would deplete their storage at relatively fast rates compared to areas that have well-sustained streamflow (table 24).

#### **Distribution of Precipitation and Temperature Data**

Precipitation and temperature data are the starting point for PRMS simulations, and the model is sensitive to these data. Each HRU is associated with a measured record of precipitation and temperature from designated sources. The location, period of record, and type of instrumentation for precipitation records were considered as the records to be associated with HRU's were selected.

For PRMS calibration, only data collected in the Turkey Creek watershed were used. Because records from some rain gages did not cover the entire calibration period, and also because many rain gages had substantial periods of missing record, a subset of the 14 available watershed precipitation records (table 2) was used for PRMS calibration. Records that were not used directly in the calibration procedure were used indirectly to update other records according to proximity and the results of correlations among the gages (table 25). In general, records for tipping-bucket gages were preferred for summer periods, and records from weighing-bucket gages were preferred for winter periods. The rain gages selected for use in calibration (table 24) were associated with a number of HRU's using a combination of the Thiessen polygon method (Chow, 1964) and judgment. Monthly means for measured precipitation show considerable variation and generally do not correlate strongly with elevation (table 25).

Air-temperature records were available from both evapotranspiration sites, from RG12, and from four air-temperature monitors established in the spring of 2001 (table 2). None of these records covered the entire calibration period, and records from RG12

and the evapotranspiration tower, which are located close to each other, were composited to obtain a single record for use with the model. The simulated results provide temperature at the HRU scale on the basis of the input record, elevation, slope, and aspect. Records from the air-temperature monitors established in spring 2001 were used to calibrate simulated temperature.

### Model Calibration

Runoff models are typically calibrated to match observed (measured) data. In this study the principal calibration data consist of streamflow measured at stations 06710992 and 06710995 (SWA01, fig. 4). Streamflow measured at these sites represents the cumulative effect of all processes that generate streamflow in the watershed; that is to say, streamflow at these two stream gages is an integrated measurement of all watershed processes. For PRMS calibration, records of diversions to the Independent Highline ditch were added to streamflow records for 06710995.

Intrawatershed measurements of streamflow and point measurements of other processes that are related to hydrologic conditions have the potential to provide

**Table 25.** Monthly means and selected summary statistics for measured precipitation

[Note: Identifier refers to local identifier or summary statistic; na, not applicable; Corr, correlation coefficient between elevation and month mean; Rng/mn, range divided by mean; Elevation, elevation in feet above NVGD29]

Identifier	Elevation	January	February	March	April	May	June	July	August	September	October	November	December
RG1	7,460	0.29	0.46	1.10	5.41	3.30	2.62	3.42	4.30	0.82	0.95	0.41	0.42
RG3	7,900	0.34	0.48	1.15	4.67	3.46	1.81	2.81	4.45	0.83	1.17	0.49	0.35
RG4	7,820	0.27	0.46	1.11	4.92	4.40	2.40	3.00	3.75	0.95	0.97	2.76	0.25
RG5	8,480	0.14	0.13	0.30	3.23	2.66	2.24	3.04	3.57	0.85	1.29	0.36	0.28
RG6	7,560	0.26	0.12	0.29	3.92	3.12	2.14	2.37	3.42	1.13	0.88	0.43	0.17
RG7	7,480	0.32	0.37	1.00	4.57	2.72	1.94	2.43	2.93	1.07	1.07	0.35	0.51
RG8	6,040	0.56	0.38	1.40	4.82	1.63	1.77	1.54	3.53	1.01	1.16	1.86	1.48
RG9	7,160	0.70	0.23	1.39	4.49	2.06	1.09	1.79	3.39	1.28	0.90	1.54	0.59
RG10	8,240	na	0.34	0.38	8.62	2.10	5.13	0.89	na	na	na	na	na
RG11	8,180	0.85	0.32	1.20	5.65	2.10	1.94	1.95	2.40	0.89	0.88	1.44	1.38
RG12	8,200	0.31	0.54	1.00	1.30	2.46	2.54	3.37	3.30	1.81	1.09	0.68	0.32
RG13	7,730	0.39	0.60	1.34	1.96	2.31	1.87	2.83	2.67	1.40	1.28	0.69	0.59
RG14	6,890	0.44	0.65	1.32	1.80	2.19	1.82	2.88	2.61	1.20	1.16	0.74	0.60
RG15	8,440	0.62	0.77	1.38	2.77	2.55	2.86	3.05	1.49	0.71	0.52	0.60	0.28
RG16	8,200	0.83	0.33	1.20	4.83	2.77	1.41	2.86	3.29	0.92	1.15	0.70	1.87
Selected summary statistics													
Mean	na	0.45	0.41	1.04	4.20	2.66	2.24	2.55	3.22	1.06	1.03	0.93	0.65
Median	na	0.37	0.38	1.15	4.57	2.55	1.94	2.83	3.35	0.98	1.08	0.69	0.46
Minimum	na	0.14	0.12	0.29	1.30	1.63	1.09	0.89	1.49	0.71	0.52	0.35	0.17
Maximum	na	0.85	0.77	1.40	8.62	4.40	5.13	3.42	4.45	1.81	1.29	2.76	1.87
Range	na	0.71	0.65	1.11	7.32	2.77	4.04	2.53	2.96	1.10	0.77	2.41	1.70
Corr	na	-0.03	0.03	-0.34	-0.15	0.35	0.40	0.57	-0.21	-0.14	-0.20	-0.32	-0.22
Rng/mn	na	1.58	1.58	1.06	1.74	1.04	1.80	0.99	0.92	1.04	0.75	2.59	2.61

significant refinements to modeling that addresses spatial differences in hydrologic responses within the watershed. Multiple intrawatershed records also provide a mechanism to cross-reference simulated results within the watershed and develop a calibration that integrates estimates for all measured streamflow data. Intrawatershed records of streamflow were available from four sites (STR-1, 2, 3, and 4), and point measurements of evapotranspiration and soil moisture were available at two sites (RG16, in HRU 80; and RG17, in HRU 47) as described in the “Evapotranspiration” section. The intrawatershed records of streamflow were used to verify that simulated rates of base flow matched measured base flow. The point measurements of evapotranspiration were used to verify that simulated evapotranspiration volumes are similar to observed volumes.

PRMS provides a capability to evaluate parameter sensitivity that can be used as a guide to optimizing calibrations based on a user-specified objective function of differences between simulated and measured data (Troutman, 1985). The calibration developed in this study, however, was achieved by manually adjusting a relatively small number of input parameters to obtain a reasonable visual match between monthly and annual sums, as well as daily hydrographs of simulated and measured streamflow (Bevan, 1997). The principal parameters adjusted to achieve calibration are associated with soil-moisture accounting and routing water to and from interflow and base-flow reservoirs.

#### **Watershed Calibration Procedures**

The model was initially calibrated to measured streamflow for the watershed, and a satisfactory match between simulated and measured volumes was obtained. Because a goal of the study was to make estimates for ground-water conditions, which represent a subset of the entire watershed conditions, some preference was given to matching volumes, such as the amount of streamflow or evapotranspiration, during periods of months or years, over precisely matching hydrograph shape on a daily basis. A good volume match is very important to the assessment of water resources in the Turkey Creek watershed for several reasons, including the relatively small magnitude of watershed streamflow and the relatively large magnitude of evapotranspiration. The initial calibration was completed with minor adjustments made to optimize

the match between hydrographs of simulated and measured streamflow; however, the volume match was preserved as closely as possible.

Simulated evapotranspiration from the initial calibration was compared to measured evapotranspiration; the estimates were found to be biased low by about 20 percent. Low bias in simulated evapotranspiration led to high bias in simulated ground-water recharge. The simulated evapotranspiration, even though low biased, accounted for a large percentage of precipitation and appeared to be reasonable; the availability of evapotranspiration measurements guided calibration procedures to reduce the high bias present in simulated ground-water recharge.

Several methods, many involving energy terms, to improve the match between simulated and measured evapotranspiration were investigated. Soil moisture, however, was the single most important constraint to reducing the amount of bias in simulated evapotranspiration. To approach satisfactory matches between simulated and measured evapotranspiration, it was necessary to make upward adjustments to model parameters that control the amount of soil moisture available for evapotranspiration; these adjustments were made uniformly to all HRU's.

The results of adjustments made to reduce the low bias in simulated evapotranspiration were evaluated by comparing simulated results to measurements of evapotranspiration from the HRU's where evapotranspiration was measured (HRU 47 and HRU 80). The evapotranspiration measurements, although they do integrate effects over an area of perhaps a few acres, are essentially point measurements compared to HRU estimates, which (for the HRU's involved) have areas of hundreds of acres (table 24). Consequently, simulated results for HRU's 47 and 80 likely represent a different set of physical conditions than local conditions in the vicinity of evapotranspiration measurements.

The same point-versus-area considerations apply to measurements of soil moisture associated with the evapotranspiration measurement. These considerations appear to be particularly pertinent to comparisons of simulated and measured soil moisture in HRU 47 (“meadow site”) described in the “Evapotranspiration” section. Simulated results for soil moisture were comparable to the measurements at the meadow site only when upward adjustments to model parameters controlling the amount of water

available for evapotranspiration were so large that simulated streamflow in HRU 47 during periods of direct runoff was almost completely depleted. Streamflow records from STR-4, which includes HRU 47, however, indicate that direct runoff is common in HRU 47. This indication implies that soil moisture at the meadow site is not representative of the entirety of HRU 47 and supports the finding presented in the “Evapotranspiration” section that the supply of moisture available for evapotranspiration in the area of the evapotranspiration measurement was likely augmented by the locally shallow ground-water table. The results help to explain low-biased simulated evapotranspiration.

### **Intrawatershed Calibration Procedures**

Intrawatershed calibrations were made on the basis of streamflow records available from STR-1, 2, 3, and 4 and synoptic measurements of streamflow. Model parameters adjusted to achieve the calibration principally concerned interflow and base-flow accounting, although the maximum amount of water that can be transferred from soil moisture to ground water was decreased for fault-zone areas. As indicated in the “Surface-Water Conditions” section, short-term records of streamflow and synoptic streamflow measurements indicate well-sustained streamflow in some parts of the watershed and poorly sustained streamflow in other parts of the watershed. Water that has percolated to the conceptual base-flow reservoirs in PRMS is affected by the value of a base flow routing coefficient and the ground-water seepage coefficient; in both cases, higher values tend to deplete the reservoir rapidly, and lower values tend to allow water to accumulate in the reservoir. Relatively low values for the routing coefficient were selected in order to match measured streamflow emanating from the Pikes Peak Granite and fault-zone reservoirs (table 24). Conversely, relatively high values were selected to route water more rapidly from the metamorphic and intrusive reservoirs. Values for the seepage coefficient were set to prevent the amount of water in the base-flow reservoirs from producing simulated base-flow rates higher than measured base-flow rates.

Initial contents values for the base-flow reservoir also are an important part of the calibration. If these values are set too high, simulated base flow will be greater than measured base flow, or extremely low

streamflows, such as those observed in the intrusive-rock areas, will not be matched, or both. The contents of the base-flow reservoirs do not represent the total amount of ground water in the system; rather, the contents represent the amount of ground water available to support local streamflow.

### **Final Calibration**

The results of watershed and intrawatershed calibration procedures are shown in graphs and tables that compare simulated results to measured data. Hydrographs of simulated and measured streamflow (fig. 43) indicate that simulated results are an accurate representation of measured data. Simulated streamflow is higher than measured streamflow in the spring of 1999, a relatively wet period, and lower than measured streamflow in the spring of 2001, a relatively dry period; otherwise simulated streamflow closely matches measured streamflow; the mean of daily differences  $-0.0001$  inch (table 26). Hydrographs of intrawatershed simulated streamflow provide a reasonable characterization of diverse intrawatershed processes (fig. 44). Intrawatershed simulated evapotranspiration compares favorably to measurements at the forest site (table 26) but is lower than measured evapotranspiration at the meadow site due to local conditions discussed in the “Watershed Calibration Procedures” section.

The measured data used to develop the final calibration include some of the extremes that can be expected in climatic data for precipitation and air temperature. However, the calibration period is relatively short, beginning in 1999 and ending in fall 2001, and a longer period of record would provide a much better description of climatic variability in the watershed.

### **Contemporary Simulations**

Simulated results for some water-balance terms, by HRU, are shown in table 24. Additional water-balance summaries in table 27, table 28, and table 29 are more complete and include daily, monthly, and annual simulated hydrologic watershed and intrawatershed conditions, based on data collected as part of this study. Simulated results qualified with the term “watershed” indicate area-weighted results, either by HRU or subsurface reservoir, for the entire watershed.

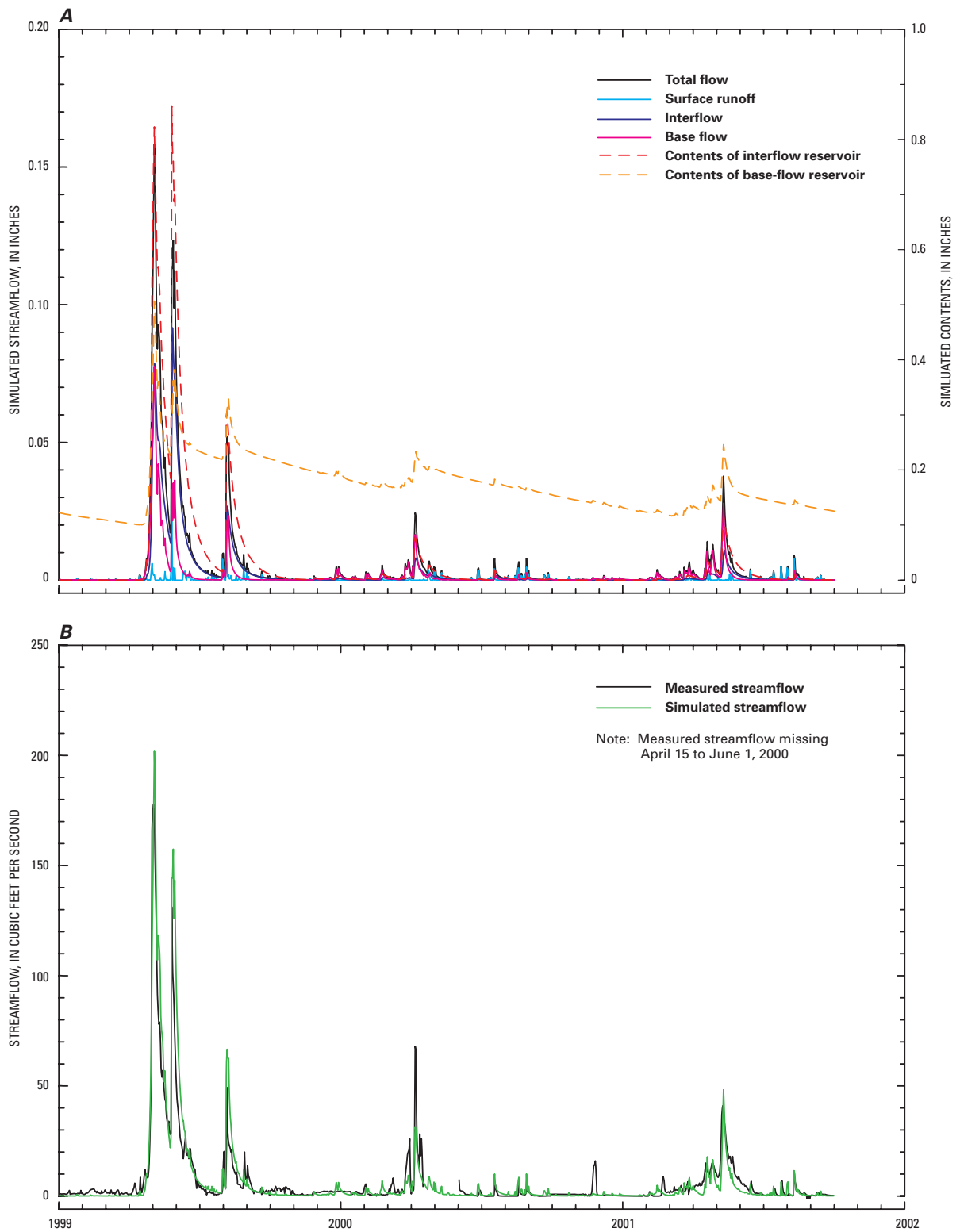


**Figure 43.** Watershed hydrographs of contemporary simulated and measured results.

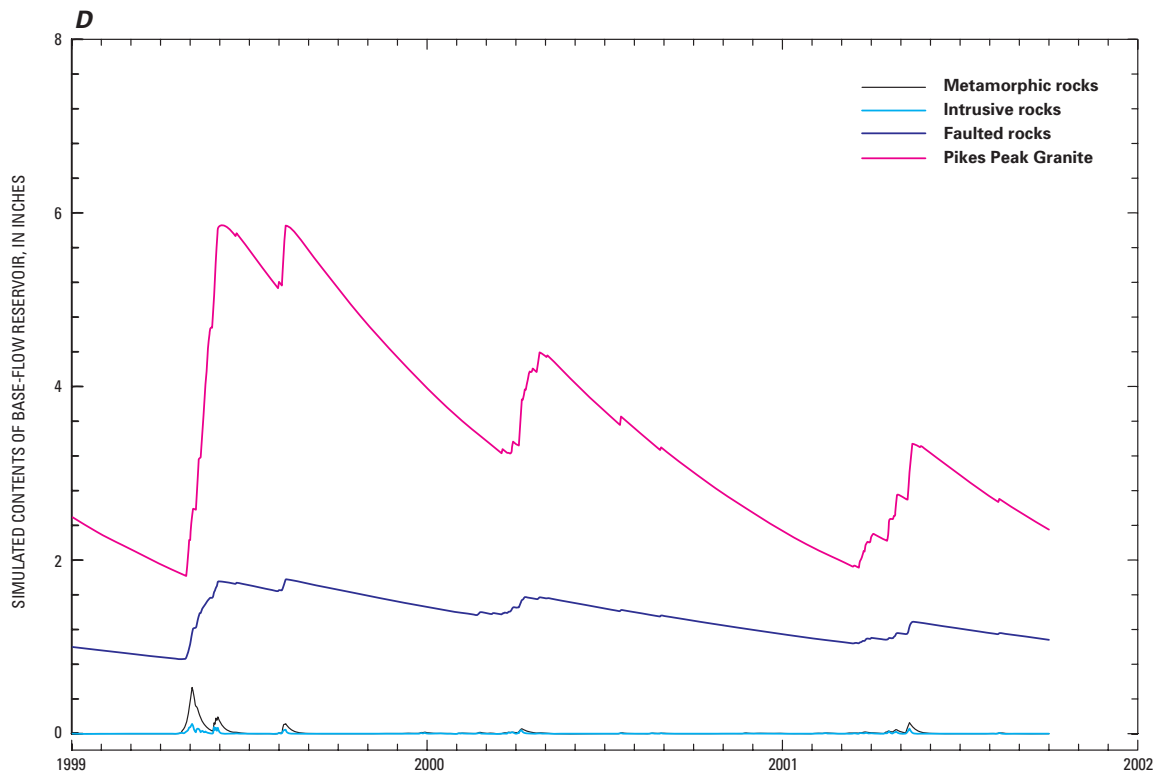
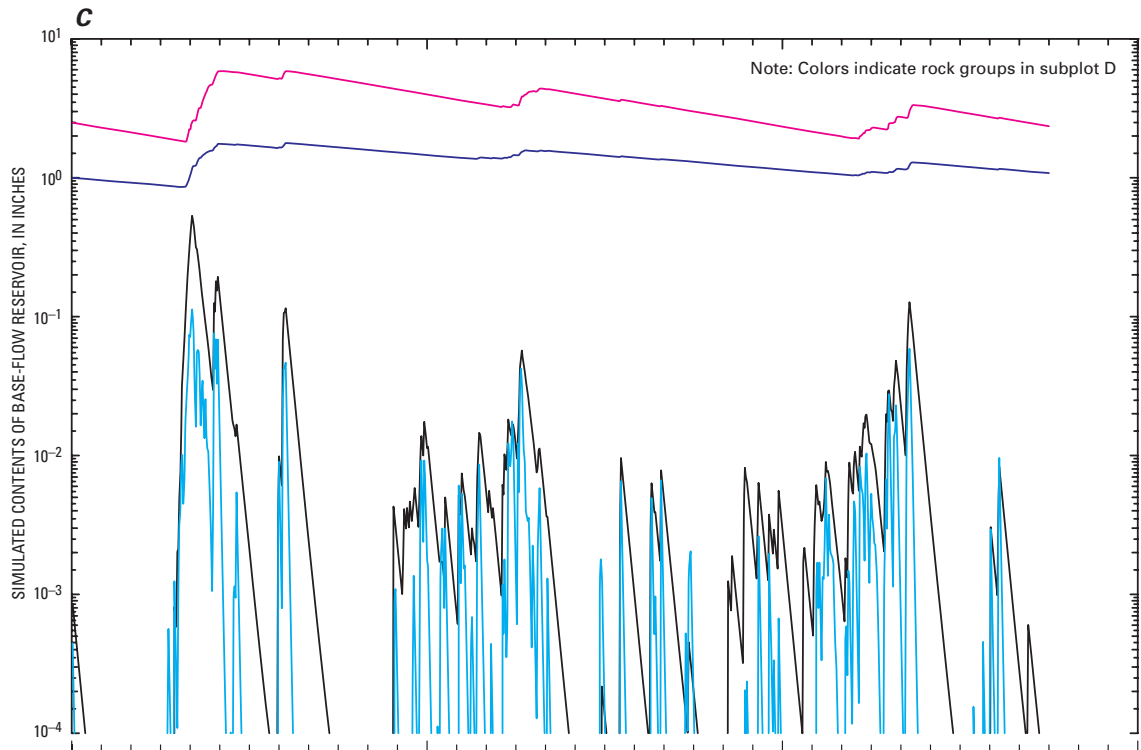


**Figure 43.** Watershed hydrographs of contemporary simulated and measured results—Continued.

**Table 26. Watershed and intrawatershed calibration statistics**

[All values except Nmiss are inches; Min, minimum; Max, maximum; Period, January 1, 1999 - September 30, 2001; WY, water year; Nmiss, number of missing days; ET, evapotranspiration; --, not applicable; <, less than]

Watershed streamflow						
	Mean	Median	Min	Max	Sum	
Simulated streamflow	0.0053	0.0005	0.0001	0.1568	5.09	
Measured streamflow	.0052	.0012	--	.1393	4.96	
Difference	-.0001	.0003	-.0553	.0407	.1315	
Intrawatershed streamflow						
Intrusive rocks						
Simulated streamflow	0.008	0.0013	<0.0001	0.092	0.879	
Measured streamflow	0.007	0.0045	<0.0001	0.054	0.822	
Difference	-0.001	0.0002	-0.0489	0.017	-0.059	
Fault-zone rocks						
Simulated streamflow	0.008	0.002	0.0007	0.061	0.924	
Measured streamflow	0.015	0.010	0.0019	0.076	1.712	
Difference	0.007	0.005	-0.0088	0.021	0.788	
Pikes Peak Granite						
Simulated streamflow	0.007	0.003	0.002	0.033	0.785	
Measured streamflow	0.006	0.004	0.001	0.042	0.707	
Difference	-0.001	-0.001	-0.026	0.016	-0.077	
Intrawatershed ET						
Calibration Period			WY1999			
	Mean	Sum	Nmiss	Mean	Sum	Nmiss
Measured forest ET	0.051	51.50	34	0.051	18.73	0
Simulated forest ET	0.051	51.12	0	0.047	17.15	0
Measured meadow ET	0.066	32.03	542	--	--	365
Simulated meadow ET	0.053	53.80	0	0.051	18.60	0
WY2000			WY2001			
Measured forest ET	0.047	17.34	0	0.057	15.43	0
Simulated forest ET	0.049	17.81	0	0.059	16.17	0
Measured meadow ET	0.060	12.82	154	0.070	19.20	0
Simulated meadow ET	0.047	17.46	0	0.065	17.73	0

Table 24 lists annual residuals between precipitation, evapotranspiration, and overland flow on an HRU basis. This residual was referred to as “infiltration (*I*)” in evapotranspiration discussions but is generally referred to here as “ground-water recharge.” Annual recharge is sometimes identified as a theoretical upper bound to water that might be safely available for withdrawal by wells, in part because it is often thought that recharge is a good surrogate for the amount of water that will be replaced on an annual basis. Ground-water recharge is only a portion of the total amount of ground water in the system. Ground-water recharge supplies interflow, base flow, and *GSNK*. Consequently, much ground-water recharge leaves the watershed as streamflow. If there were some mechanism to withdraw

the annual recharge as it occurred, then streamflow in the Turkey Creek watershed would consist only of overland flow. Interflow quickly leaves the watershed, whereas base flow typically persists for longer periods of time.

Simulated results for ground-water recharge, as used in this report and shown as “rsd” in table 24, varies considerably from HRU to HRU. HRU differences in ground-water recharge result from the physical characteristics of the watershed, the atmospheric energy conditions, and the availability of water, all of which are accounted for in the PRMS characterization of the watershed. During a wet period, such as the January through September portion of 1999, simulated results indicate that ground-water recharge is always

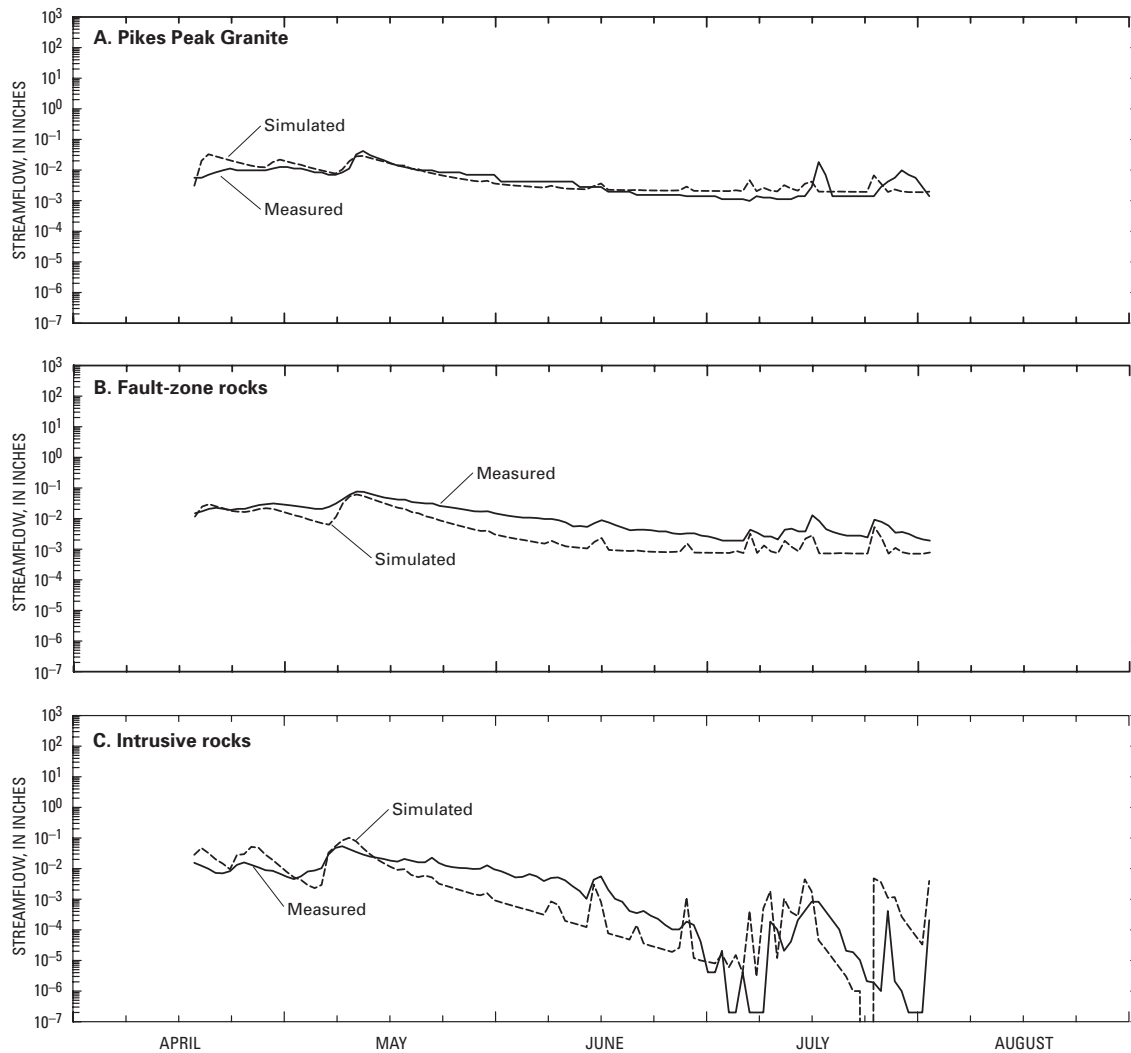


**Figure 44.** Intrawatershed hydrographs of contemporary simulated and measured results.

positive and, on a watershed scale, has a magnitude of 5.97 inches. For the same period, on an HRU scale, simulated results indicate ground-water recharge ranges from 2.76 inches to as much as 10.54 inches. However, during a relatively dry period, such as water year 2001, the results are strikingly different. In fact, during water year 2001, simulated results for the watershed indicate 0.39 inch, or about 6.5 percent of the 1999 value, of ground-water recharge; and at many HRU's the estimates are negative, indicating a condition in which evapotranspiration is depleting water in storage (as discussed in the "Evapotranspiration" section eq. 4). For these and other reasons, such as the fact that much ground-water recharge leaves the watershed as streamflow, annual estimates of ground-water recharge are

not the optimal predictor of ground-water availability, and it is desirable to have estimates that describe the status of water in the interflow and, particularly, base-flow reservoirs as characterized by PRMS.

Table 27 provides monthly and annual summary information for hydrologic conditions such as the amount of precipitation, evapotranspiration, soil moisture, the contents of interflow and base-flow reservoirs, GSNK, overland flow, interflow, and base flow. Most results listed in table 27 are totals for the period of evaluation; for instance, precipitation figures indicate a total amount of precipitation for the given month or year. Contents results (sm, bfr, ir in table 27), however, indicate the contents on the last day of the given month or year. The simulated results listed



**Table 27.** Monthly and annual summary statistics for contemporary simulations (January 1, 1999, through September 30, 2001) for the entire Turkey Creek watershed

[Year, water year (October through September) if month not given; Mo, month; all numbers other than dates in inches; Precip, total precipitation; ET, total evapotranspiration; sm, contents of soil-zone reservoir at end of given period; bfi, total water added to base-flow reservoir; bfr, contents of base flow reservoir at end of accounting period; bf, total base flow discharged to stream; gsnk, total water lost from base-flow reservoir that is not available to support local streamflow; ir, contents of interflow reservoir at end of the accounting period; if, total interflow; ovf, total overland flow; tf, total watershed flow]

Year	Mo	Precip	ET	sm	bfi	bfr	bf	gsnk	ir	if	ovf	tf
1999	1	0.5739	0.2149	0.4103	0.0000	0.1148	0.0027	0.0052	0.0000	0.0000	0.0008	0.0036
1999	2	0.2828	0.3735	0.3668	0.0000	0.1088	0.0017	0.0043	0.0000	0.0000	0.0007	0.0024
1999	3	0.4561	0.5550	0.2670	0.0000	0.1026	0.0018	0.0044	0.0000	0.0000	0.0008	0.0026
1999	4	6.9443	0.8300	3.9826	0.5410	0.3750	0.2116	0.0570	0.6542	0.1398	0.0157	0.3670
1999	5	4.0518	3.1074	3.5065	1.0510	0.3421	0.8591	0.2247	0.5581	1.4703	0.0428	2.3722
1999	6	1.7843	3.6532	1.6121	0.0140	0.2440	0.0768	0.0354	0.0685	0.4865	0.0153	0.5786
1999	7	2.6156	1.7375	2.4511	0.0116	0.2355	0.0086	0.0116	0.0221	0.0557	0.0170	0.0813
1999	8	4.0234	3.7386	2.2448	0.1713	0.2401	0.1238	0.0428	0.0459	0.2604	0.0368	0.4211
1999	9	1.0532	1.4890	1.8016	0.0001	0.2249	0.0049	0.0105	0.0093	0.0364	0.0059	0.0472
1999		21.7855	15.6991	1.8016	1.7890	0.2249	1.2910	0.3958	0.0093	2.4491	0.1359	3.8761
1999	10	1.0461	1.2213	1.6792	0.0000	0.2115	0.0037	0.0097	0.0019	0.0074	0.0024	0.0135
1999	11	0.6593	0.5881	1.7288	0.0039	0.2008	0.0052	0.0093	0.0019	0.0019	0.0013	0.0084
1999	12	1.0468	0.5194	2.0843	0.0404	0.1946	0.0314	0.0152	0.0063	0.0055	0.0014	0.0383
2000	1	0.4969	0.4532	1.8454	0.0105	0.1770	0.0166	0.0114	0.0009	0.0055	0.0002	0.0223
2000	2	0.6033	0.8462	1.9174	0.0416	0.1744	0.0308	0.0133	0.0062	0.0080	0.0028	0.0417
2000	3	2.4735	1.0712	2.4385	0.0792	0.1844	0.0518	0.0174	0.0096	0.0157	0.0018	0.0693
2000	4	2.2362	2.3592	2.6116	0.1622	0.2058	0.1098	0.0310	0.0169	0.1021	0.0094	0.2213
2000	5	1.4886	2.9785	1.3496	0.0036	0.1921	0.0076	0.0097	0.0026	0.0142	0.0089	0.0307
2000	6	1.5576	1.3943	1.5006	0.0017	0.1812	0.0046	0.0080	0.0011	0.0027	0.0093	0.0166
2000	7	1.5432	2.0604	0.9474	0.0119	0.1733	0.0103	0.0094	0.0047	0.0109	0.0096	0.0308
2000	8	3.4605	2.1231	2.2449	0.0145	0.1657	0.0127	0.0094	0.0019	0.0051	0.0232	0.0410
2000	9	1.4314	1.9466	1.7202	0.0023	0.1547	0.0062	0.0073	0.0006	0.0017	0.0066	0.0145
2000		18.0434	17.5615	1.7202	0.3716	0.1547	0.2906	0.1513	0.0006	0.1807	0.0770	0.5483
2000	10	0.5499	0.9592	1.2887	0.0000	0.1457	0.0027	0.0063	0.0001	0.0005	0.0022	0.0054
2000	11	0.5995	0.3868	1.4883	0.0067	0.1392	0.0062	0.0070	0.0005	0.0003	0.0011	0.0076
2000	12	0.4280	0.3592	1.4950	0.0101	0.1315	0.0100	0.0078	0.0001	0.0004	0.0007	0.0111
2001	1	0.3750	0.3258	1.4223	0.0013	0.1229	0.0041	0.0058	0.0000	0.0001	0.0002	0.0044
2001	2	0.7607	0.6732	1.5481	0.0234	0.1172	0.0204	0.0088	0.0005	0.0024	0.0015	0.0243
2001	3	1.5679	0.9600	2.0801	0.0943	0.1303	0.0632	0.0179	0.0100	0.0152	0.0058	0.0842
2001	4	2.5812	2.2242	2.2095	0.2156	0.1808	0.1327	0.0324	0.0280	0.0708	0.0036	0.2071
2001	5	3.0564	3.0570	1.8520	0.2138	0.1832	0.1650	0.0464	0.0209	0.1444	0.0064	0.3158
2001	6	0.8613	1.7524	0.9564	0.0001	0.1709	0.0045	0.0080	0.0040	0.0168	0.0047	0.0260
2001	7	2.8911	2.1995	1.6288	0.0020	0.1612	0.0040	0.0075	0.0008	0.0032	0.0173	0.0246
2001	8	2.5259	2.7870	1.3417	0.0062	0.1515	0.0081	0.0078	0.0003	0.0021	0.0180	0.0282
2001	9	1.3463	1.5734	1.1093	0.0006	0.1429	0.0029	0.0063	0.0001	0.0002	0.0049	0.0081
2001		17.5432	17.2576	1.1093	0.5742	0.1429	0.4238	0.1621	0.0001	0.2564	0.0665	0.7467
Period		57.372	50.518	1.109	2.735	0.143	2.006	0.709	0.000	2.886	0.279	5.171

in table 27 indicate that watershed values for the contents of the base-flow reservoirs are generally 0.1 to 0.2 inch at the end of each water year; this water is potentially available to supply wells. The watershed representation for the contents of the base-flow reservoirs (fig. 43) indicates that at least this amount of water is consistently present, on a watershed scale.

The end-of-year watershed contents of interflow reservoirs is typically very near 0.0000 (table 27). The watershed representation for contents of the interflow

reservoir (fig. 43A) indicates that, unlike the watershed representation of the base-flow reservoirs, the interflow reservoirs fill and deplete rapidly and are most likely to contain water during and shortly after precipitation or spring runoff. Water contained in the interflow reservoirs is, like water contained in the base-flow reservoirs, potentially available to supply wells. However, water in the interflow reservoirs is typically present only for short periods of time related to precipitation or snow-melt events.

**Table 28.** Intrawatershed summary statistics for contemporary simulations (January 1, 1999, through September 30, 2001) for areas of (A) metamorphic, (B) intrusive, and (C) fault-zone rocks and (D) Pikes Peak Granite

[Year, water year (October through September) if month not given; Mo, month; all numbers other than dates in inches; Precip, total precipitation; ET, total evapotranspiration; sm, contents of soil-zone reservoir at end of given period; bfi, total water added to base-flow reservoir; bfr, contents of base flow reservoir at end of accounting period; bf, total base flow discharged to stream; gsnk, total water lost from base-flow reservoir that is not available to support local streamflow; ir, contents of interflow reservoir at end of the accounting period; if, total interflow; ovf, total overland flow; tf, total watershed flow]

Year	Mo	Precip	ET	sm	bfi	bfr	bf	gsnk	ir	if	ovf	tf
A. Metamorphic rocks												
1999	1	0.5239	0.2200	0.3695	0.0000	0.0000	0.0007	0.0003	0.0000	0.0000	0.0008	0.0015
1999	2	0.2708	0.3436	0.3325	0.0000	0.0000	0.0000	0.0000	0.0000	0.0000	0.0008	0.0008
1999	3	0.4485	0.5336	0.2480	0.0000	0.0000	0.0000	0.0000	0.0000	0.0000	0.0009	0.0009
1999	4	6.8452	0.8507	4.1863	0.6242	0.3690	0.1882	0.0670	0.8146	0.1330	0.0197	0.3409
1999	5	3.9007	3.1571	3.5320	0.8114	0.1338	0.7718	0.2748	0.6123	1.2724	0.0433	2.0875
1999	6	1.6838	3.5910	1.6118	0.0084	0.0018	0.1036	0.0369	0.1040	0.5095	0.0145	0.6276
1999	7	2.5087	1.7235	2.3730	0.0086	0.0068	0.0027	0.0010	0.0296	0.0838	0.0164	0.1029
1999	8	4.2358	3.8260	2.3164	0.1546	0.0021	0.1175	0.0418	0.0691	0.2557	0.0396	0.4129
1999	9	1.0845	1.5320	1.8640	0.0001	0.0000	0.0016	0.0006	0.0145	0.0545	0.0065	0.0626
1999		21.5020	15.7774	1.8640	1.6074	0.0000	1.1861	0.4223	0.0145	2.3090	0.1426	3.6377
1999	10	1.0165	1.2032	1.7103	0.0000	0.0000	0.0000	0.0000	0.0029	0.0115	0.0023	0.0138
1999	11	0.6699	0.5979	1.7655	0.0050	0.0022	0.0021	0.0007	0.0030	0.0029	0.0016	0.0065
1999	12	0.9684	0.5683	2.0707	0.0392	0.0102	0.0231	0.0082	0.0065	0.0045	0.0019	0.0294
2000	1	0.4248	0.4568	1.7810	0.0081	0.0007	0.0129	0.0046	0.0013	0.0052	0.0003	0.0184
2000	2	0.6341	0.8126	1.8498	0.0327	0.0054	0.0207	0.0074	0.0077	0.0074	0.0030	0.0310
2000	3	2.4042	1.0872	2.3389	0.0480	0.0114	0.0309	0.0110	0.0073	0.0096	0.0024	0.0429
2000	4	2.2525	2.3801	2.5965	0.0873	0.0040	0.0699	0.0249	0.0196	0.0497	0.0091	0.1287
2000	5	1.4058	2.8852	1.3587	0.0005	0.0000	0.0033	0.0012	0.0040	0.0156	0.0084	0.0273
2000	6	1.6279	1.4275	1.5535	0.0001	0.0001	0.0001	0.0000	0.0009	0.0031	0.0099	0.0131
2000	7	1.3888	1.9810	0.9365	0.0094	0.0008	0.0064	0.0023	0.0063	0.0075	0.0086	0.0225
2000	8	3.3290	2.0390	2.2067	0.0117	0.0030	0.0070	0.0025	0.0024	0.0061	0.0225	0.0356
2000	9	1.5352	1.9562	1.7814	0.0002	0.0001	0.0023	0.0008	0.0005	0.0019	0.0073	0.0115
2000		17.6572	17.3951	1.7814	0.2425	0.0001	0.1788	0.0636	0.0005	0.1249	0.0772	0.3808
2000	10	0.5912	1.0282	1.3208	0.0000	0.0000	0.0001	0.0000	0.0001	0.0004	0.0025	0.0030
2000	11	0.5821	0.4060	1.4924	0.0104	0.0024	0.0059	0.0021	0.0007	0.0005	0.0011	0.0075
2000	12	0.4264	0.3783	1.4914	0.0124	0.0025	0.0091	0.0032	0.0001	0.0006	0.0008	0.0105
2001	1	0.3690	0.3374	1.4142	0.0021	0.0004	0.0030	0.0011	0.0000	0.0001	0.0002	0.0033
2001	2	0.7138	0.6951	1.4763	0.0210	0.0012	0.0149	0.0053	0.0004	0.0005	0.0017	0.0172
2001	3	1.4917	0.9801	1.9445	0.0654	0.0107	0.0412	0.0147	0.0090	0.0084	0.0057	0.0553
2001	4	2.4784	2.2291	2.0871	0.1230	0.0274	0.0783	0.0279	0.0204	0.0263	0.0044	0.1091
2001	5	2.9895	3.0544	1.7850	0.1528	0.0032	0.1305	0.0465	0.0288	0.0794	0.0066	0.2165
2001	6	0.8507	1.6827	0.9513	0.0000	0.0000	0.0024	0.0009	0.0061	0.0227	0.0048	0.0299
2001	7	2.8193	2.0815	1.6851	0.0024	0.0007	0.0013	0.0005	0.0013	0.0049	0.0170	0.0232
2001	8	2.5148	2.9058	1.2797	0.0036	0.0001	0.0030	0.0011	0.0004	0.0013	0.0184	0.0228
2001	9	1.3485	1.5163	1.1095	0.0010	0.0000	0.0008	0.0003	0.0001	0.0003	0.0048	0.0060
2001		17.1752	17.2950	1.1095	0.3941	0.0000	0.2907	0.1035	0.0001	0.1454	0.0681	0.5042
Period		56.334	50.467	1.110	2.244	0.000	1.656	0.589	0.000	2.579	0.288	4.523

In addition to estimates for the contents of the base-flow reservoir at a watershed scale, the simulated results in table 27 indicate about 1.6 inches of recharge to the watershed base-flow reservoir occurred in April and May of 1999, and that much less water (about an order of magnitude less) was recharged to the base-flow reservoir in 2000 and 2001. The watershed representation for contents of

the base-flow reservoirs (fig. 43) generally indicates that contents can undergo relatively rapid changes. Contents typically exhibit a relatively abrupt increase during spring recharge and decrease more slowly. In general, the recession slope for the watershed representation of contents of the base-flow reservoir appears to be about a few hundredths of an inch per year.

**Table 28.** Intrawatershed summary statistics for contemporary simulations (January 1, 1999, through September 30, 2001) for areas of (A) metamorphic, (B) intrusive, and (C) fault-zone rocks and (D) Pikes Peak Granite—Continued

[Year, water year (October through September) if month not given; Mo, month; all numbers other than dates in inches; Precip, total precipitation; ET, total evapotranspiration; sm, contents of soil-zone reservoir at end of given period; bfi, total water added to base-flow reservoir; bfr, contents of base flow reservoir at end of accounting period; bf, total base flow discharged to stream; gsnk, total water lost from base-flow reservoir that is not available to support local streamflow; ir, contents of interflow reservoir at end of the accounting period; if, total interflow; ovf, total overland flow; tf, total watershed flow]

Year	Mo	Precip	ET	sm	bfi	bfr	bf	gsnk	ir	if	ovf	tf
B. Intrusive rocks												
1999	1	0.6078	0.1939	0.4480	0.0000	0.0000	0.0009	0.0001	0.0000	0.0000	0.0011	0.0020
1999	2	0.2877	0.4089	0.4005	0.0000	0.0000	0.0000	0.0000	0.0000	0.0000	0.0006	0.0006
1999	3	0.4547	0.5679	0.2914	0.0000	0.0000	0.0000	0.0000	0.0000	0.0000	0.0006	0.0006
1999	4	6.9142	0.7908	3.7721	0.4484	0.0719	0.3393	0.0373	0.3529	0.1371	0.0092	0.4855
1999	5	4.4471	3.0427	3.6522	1.4646	0.0136	1.3719	0.1509	0.4553	1.6153	0.0464	3.0337
1999	6	1.9327	3.8457	1.7292	0.0118	0.0000	0.0229	0.0025	0.0044	0.4532	0.0169	0.4930
1999	7	2.8099	1.8504	2.6509	0.0189	0.0070	0.0107	0.0012	0.0106	0.0052	0.0184	0.0344
1999	8	3.7093	3.6669	2.2467	0.1798	0.0000	0.1683	0.0185	0.0035	0.2548	0.0330	0.4561
1999	9	1.0055	1.4678	1.7808	0.0000	0.0000	0.0000	0.0000	0.0000	0.0035	0.0052	0.0087
1999		22.1688	15.8349	1.7808	2.1235	0.0000	1.9140	0.2105	0.0000	2.4691	0.1315	4.5146
1999	10	1.0823	1.2170	1.7024	0.0000	0.0000	0.0000	0.0000	0.0000	0.0000	0.0027	0.0028
1999	11	0.6225	0.5631	1.7397	0.0023	0.0002	0.0019	0.0002	0.0000	0.0000	0.0011	0.0030
1999	12	1.0662	0.4174	2.1174	0.0575	0.0017	0.0504	0.0055	0.0082	0.0099	0.0007	0.0610
2000	1	0.5431	0.4225	1.9468	0.0203	0.0000	0.0198	0.0022	0.0001	0.0081	0.0002	0.0281
2000	2	0.5992	0.8725	2.0494	0.0627	0.0000	0.0565	0.0062	0.0018	0.0043	0.0030	0.0637
2000	3	2.5491	1.0514	2.6284	0.1244	0.0015	0.1107	0.0122	0.0030	0.0094	0.0008	0.1209
2000	4	2.2630	2.3382	2.7274	0.2596	0.0001	0.2351	0.0259	0.0083	0.1383	0.0098	0.3832
2000	5	1.6220	3.1557	1.4218	0.0087	0.0000	0.0079	0.0009	0.0001	0.0102	0.0102	0.0283
2000	6	1.4609	1.3827	1.4840	0.0062	0.0001	0.0055	0.0006	0.0022	0.0028	0.0083	0.0166
2000	7	1.6959	2.1505	0.9958	0.0133	0.0000	0.0121	0.0013	0.0018	0.0173	0.0104	0.0399
2000	8	3.6839	2.3020	2.3483	0.0231	0.0005	0.0204	0.0022	0.0011	0.0037	0.0245	0.0485
2000	9	1.2654	1.9340	1.6653	0.0083	0.0002	0.0078	0.0009	0.0009	0.0020	0.0058	0.0156
2000		18.4534	17.8072	1.6653	0.5863	0.0002	0.5280	0.0581	0.0009	0.2060	0.0775	0.8115
2000	10	0.4913	0.8481	1.2820	0.0000	0.0000	0.0002	0.0000	0.0000	0.0009	0.0018	0.0029
2000	11	0.5883	0.3462	1.5091	0.0000	0.0000	0.0000	0.0000	0.0000	0.0000	0.0011	0.0011
2000	12	0.4144	0.3193	1.5269	0.0081	0.0001	0.0072	0.0008	0.0000	0.0000	0.0004	0.0076
2001	1	0.3607	0.3072	1.4550	0.0000	0.0000	0.0001	0.0000	0.0000	0.0000	0.0001	0.0002
2001	2	0.7901	0.6155	1.6764	0.0379	0.0000	0.0341	0.0038	0.0008	0.0079	0.0014	0.0434
2001	3	1.6663	0.9300	2.3024	0.1502	0.0031	0.1326	0.0146	0.0032	0.0159	0.0064	0.1549
2001	4	2.6967	2.2167	2.4386	0.3387	0.0023	0.3058	0.0336	0.0216	0.0833	0.0022	0.3914
2001	5	3.1515	3.0748	2.0327	0.3281	0.0000	0.2977	0.0327	0.0046	0.1823	0.0064	0.4863
2001	6	0.8607	1.8707	1.0258	0.0000	0.0000	0.0000	0.0000	0.0000	0.0045	0.0046	0.0091
2001	7	2.9964	2.3868	1.6383	0.0015	0.0000	0.0014	0.0002	0.0000	0.0000	0.0179	0.0194
2001	8	2.5168	2.6515	1.4764	0.0149	0.0000	0.0135	0.0015	0.0001	0.0049	0.0173	0.0357
2001	9	1.3247	1.6416	1.1615	0.0000	0.0000	0.0000	0.0000	0.0000	0.0001	0.0047	0.0049
2001		17.8578	17.2083	1.1615	0.8795	0.0000	0.7925	0.0872	0.0000	0.2999	0.0644	1.1569
Period		58.480	50.850	1.162	3.589	0.000	3.235	0.356	0.000	2.975	0.273	6.483

The combination of the distributed nature of PRMS and intrawatershed measurements of stream-flow permits simulations for the individual subsurface reservoirs. The results from individual base-flow reservoirs (table 28 and fig. 43) indicate how intrawatershed conditions vary. Figure 43 provides a graphic summary of the contents of the four base-flow

reservoirs and indicates that the Pikes Peak Granite and fault-zone reservoirs have a tendency to receive and retain ground water and slowly release it as base flow that sustains streamflow. The intrusive reservoir, and to a lesser extent the metamorphic reservoir, however, do not retain and slowly release ground water to sustain streamflow. The contents of the

**Table 28.** Intrawatershed summary statistics for contemporary simulations (January 1, 1999, through September 30, 2001) for areas of A) metamorphic, (B) intrusive, and (C) fault-zone rocks and (D) Pikes Peak Granite—Continued

[Year, water year (October through September) if month not given; Mo, month; all numbers other than dates in inches; Precip, total precipitation; ET, total evapotranspiration; sm, contents of soil-zone reservoir at end of given period; bfi, total water added to base-flow reservoir; bfr, contents of base flow reservoir at end of accounting period; bf, total base flow discharged to stream; gsnk, total water lost from base-flow reservoir that is not available to support local streamflow; ir, contents of interflow reservoir at end of the accounting period; if, total interflow; ovf, total overland flow; tf, total watershed flow]

Year	Mo	Precip	ET	sm	bfi	bfr	bf	gsnk	ir	if	ovf	tf
C. Fault-zone rocks												
1999	1	0.8184	0.2540	0.6067	0.0000	0.9566	0.0167	0.0267	0.0000	0.0000	0.0006	0.0172
1999	2	0.3013	0.4887	0.4985	0.0000	0.9191	0.0145	0.0231	0.0000	0.0000	0.0008	0.0153
1999	3	0.4818	0.6642	0.3247	0.0000	0.8792	0.0153	0.0245	0.0000	0.0000	0.0004	0.0158
1999	4	7.6580	0.8183	3.7572	0.1775	1.0190	0.0145	0.0232	0.4685	0.2345	0.0092	0.2582
1999	5	3.7047	3.0481	3.3712	0.8764	1.8288	0.0256	0.0410	0.4313	2.7045	0.0337	2.7639
1999	6	1.8813	3.7291	1.5152	0.0250	1.7762	0.0298	0.0477	0.0035	0.4160	0.0157	0.4615
1999	7	2.7148	1.7022	2.5011	0.0140	1.7132	0.0297	0.0474	0.0031	0.0036	0.0173	0.0506
1999	8	3.6310	3.6739	1.9828	0.1320	1.7660	0.0304	0.0487	0.0048	0.3190	0.0312	0.3806
1999	9	1.0138	1.3538	1.6420	0.0001	1.6920	0.0285	0.0456	0.0000	0.0046	0.0050	0.0382
1999		22.2052	15.7323	1.6420	1.2250	1.6920	0.2051	0.3280	0.0000	3.6822	0.1139	4.0012
1999	10	1.0868	1.2343	1.5358	0.0000	1.6186	0.0282	0.0452	0.0000	0.0000	0.0016	0.0299
1999	11	0.7227	0.6067	1.6120	0.0000	1.5506	0.0262	0.0418	0.0000	0.0000	0.0005	0.0267
1999	12	1.3275	0.4622	2.1922	0.0006	1.4840	0.0259	0.0414	0.0000	0.0000	0.0003	0.0262
2000	1	0.8610	0.5265	2.1044	0.0000	1.4196	0.0248	0.0396	0.0000	0.0000	0.0002	0.0250
2000	2	0.3509	0.9854	2.0658	0.0540	1.4150	0.0225	0.0360	0.0108	0.0280	0.0010	0.0516
2000	3	2.6889	1.0085	2.6827	0.1495	1.5010	0.0244	0.0391	0.0536	0.0927	0.0005	0.1177
2000	4	1.9881	2.3258	2.5268	0.1478	1.5805	0.0263	0.0420	0.0060	0.3713	0.0104	0.4080
2000	5	1.7306	3.1786	1.2714	0.0002	1.5121	0.0264	0.0422	0.0000	0.0058	0.0093	0.0415
2000	6	1.2987	1.2709	1.2864	0.0000	1.4486	0.0244	0.0391	0.0000	0.0000	0.0072	0.0317
2000	7	2.1718	2.3935	1.0129	0.0180	1.4034	0.0243	0.0389	0.0025	0.0204	0.0146	0.0593
2000	8	3.5247	2.2935	2.2283	0.0119	1.3544	0.0234	0.0375	0.0000	0.0024	0.0232	0.0490
2000	9	1.3214	1.9262	1.6176	0.0000	1.2975	0.0219	0.0350	0.0000	0.0000	0.0052	0.0271
2000		19.0731	18.2121	1.6176	0.3821	1.2975	0.2988	0.4778	0.0000	0.5207	0.0740	0.8934
2000	10	0.4140	0.8545	1.1639	0.0000	1.2412	0.0217	0.0346	0.0000	0.0000	0.0013	0.0229
2000	11	0.8188	0.4195	1.5197	0.0000	1.1891	0.0201	0.0321	0.0000	0.0000	0.0008	0.0209
2000	12	0.4402	0.3805	1.5310	0.0000	1.1375	0.0198	0.0317	0.0000	0.0000	0.0004	0.0202
2001	1	0.4462	0.3488	1.4583	0.0000	1.0882	0.0190	0.0304	0.0000	0.0000	0.0000	0.0190
2001	2	0.9874	0.7255	1.8043	0.0000	1.0454	0.0164	0.0263	0.0000	0.0000	0.0007	0.0172
2001	3	1.6593	0.9326	2.4461	0.1030	1.1020	0.0179	0.0286	0.0442	0.0737	0.0053	0.0968
2001	4	2.8787	2.2631	2.5433	0.2195	1.2719	0.0191	0.0305	0.0843	0.3552	0.0035	0.3778
2001	5	3.2023	3.1134	1.9938	0.1972	1.4074	0.0237	0.0379	0.0118	0.5286	0.0067	0.5590
2001	6	0.8924	1.9418	0.9515	0.0004	1.3486	0.0228	0.0364	0.0001	0.0113	0.0049	0.0390
2001	7	3.0796	2.6060	1.4288	0.0000	1.2902	0.0225	0.0360	0.0000	0.0001	0.0190	0.0416
2001	8	2.5668	2.4852	1.5003	0.0000	1.2342	0.0215	0.0344	0.0000	0.0000	0.0171	0.0386
2001	9	1.3499	1.7694	1.0850	0.0000	1.1823	0.0199	0.0319	0.0000	0.0000	0.0068	0.0268
2001		18.7356	17.8404	1.0850	0.5200	1.1823	0.2444	0.3908	0.0000	0.9689	0.0665	1.2799
Period		60.014	51.785	1.085	2.127	1.182	0.748	1.197	0.000	5.172	0.254	6.174

metamorphic and intrusive base-flow reservoirs are, much like interflow, quickly transmitted to streamflow. Contents of the metamorphic and intrusive base-flow reservoirs have large fluctuations, and these portions of the watershed contribute to the rapid changes in the watershed contents of base-flow reservoirs.

Daily values for water-balance terms for watershed and intrawatershed conditions are summarized in table 29. The percentiles in table 29A reiterate that the watershed content of base-flow reservoirs is consistently in the range of 0.1 to 0.2 inch and that the watershed content of interflow reservoirs is very low most of the time (0.0020 for 50 percent of the time, table 29A).

**Table 28.** Intrawatershed summary statistics for contemporary simulations (January 1, 1999, through September 30, 2001) for areas of A) metamorphic, (B) intrusive, and (C) fault-zone rocks and (D) Pikes Peak Granite—Continued

[Year, water year (October through September) if month not given; Mo, month; all numbers other than dates in inches; Precip, total precipitation; ET, total evapotranspiration; sm, contents of soil-zone reservoir at end of given period; bfi, total water added to base-flow reservoir; bfr, contents of base flow reservoir at end of accounting period; bf, total base flow discharged to stream; gsnk, total water lost from base-flow reservoir that is not available to support local streamflow; ir, contents of interflow reservoir at end of the accounting period; if, total interflow; ovf, total overland flow; tf, total watershed flow]

Year	Mo	Precip	ET	sm	bfi	bfr	bf	gsnk	ir	if	ovf	tf
D. Pikes Peak Granite												
1999	1	0.8800	0.2546	0.5785	0.0000	2.2955	0.0409	0.1636	0.0000	0.0000	0.0000	0.0409
1999	2	0.3400	0.5401	0.5454	0.0000	2.1252	0.0341	0.1362	0.0000	0.0000	0.0005	0.0346
1999	3	0.5100	0.7301	0.3342	0.0000	1.9514	0.0348	0.1390	0.0000	0.0000	0.0003	0.0350
1999	4	7.9400	0.7813	2.2006	0.4462	2.2395	0.0316	0.1264	0.0862	0.0218	0.0014	0.0549
1999	5	3.8900	2.8465	1.9117	4.2988	6.1873	0.0702	0.2809	0.6502	1.2291	0.0050	1.3043
1999	6	2.0900	3.3569	0.6584	0.1981	5.8822	0.1007	0.4025	0.0064	0.4458	0.0131	0.5595
1999	7	2.8700	1.4199	2.1004	0.0034	5.4043	0.0963	0.3850	0.0001	0.0043	0.0155	0.1161
1999	8	3.2900	3.1813	1.1349	0.7982	5.7055	0.0994	0.3976	0.0060	0.2615	0.0217	0.3827
1999	9	0.9500	1.1154	0.9506	0.0019	5.2551	0.0905	0.3618	0.0001	0.0041	0.0030	0.0975
1999		22.7600	14.2262	0.9506	5.7467	5.2551	0.5986	2.3930	0.0001	1.9665	0.0605	2.6256
1999	10	1.1900	1.2083	1.0084	0.0000	4.8253	0.0860	0.3438	0.0000	0.0000	0.0009	0.0869
1999	11	0.7300	0.6052	1.0115	0.0000	4.4429	0.0765	0.3059	0.0000	0.0000	0.0000	0.0765
1999	12	1.7000	0.4065	1.4734	0.0000	4.0795	0.0727	0.2907	0.0000	0.0000	0.0000	0.0727
2000	1	0.9500	0.4508	1.6178	0.0000	3.7458	0.0668	0.2669	0.0000	0.0000	0.0000	0.0668
2000	2	0.3300	1.0149	1.7452	0.0000	3.4584	0.0575	0.2299	0.0000	0.0000	0.0006	0.0581
2000	3	2.7900	0.9728	2.2233	0.2377	3.4099	0.0573	0.2289	0.0000	0.0000	0.0001	0.0574
2000	4	1.9700	2.1016	1.6749	1.4663	4.5304	0.0692	0.2766	0.0901	0.3105	0.0068	0.3865
2000	5	1.7600	2.9871	0.5684	0.0522	4.2083	0.0749	0.2994	0.0008	0.0607	0.0061	0.1418
2000	6	1.3500	1.1382	0.7668	0.0003	3.8750	0.0667	0.2668	0.0000	0.0005	0.0064	0.0737
2000	7	2.4100	2.5311	0.5864	0.0517	3.6077	0.0638	0.2552	0.0000	0.0000	0.0144	0.0783
2000	8	3.7800	2.4006	1.9649	0.0000	3.3126	0.0590	0.2360	0.0000	0.0000	0.0220	0.0811
2000	9	1.1300	1.9352	1.1528	0.0000	3.0501	0.0525	0.2100	0.0000	0.0000	0.0027	0.0552
2000		20.0900	17.7524	1.1528	1.8082	3.0501	0.8030	3.2102	0.0000	0.3718	0.0601	1.2348
2000	10	0.4300	0.7863	0.7838	0.0000	2.8006	0.0499	0.1995	0.0000	0.0000	0.0008	0.0507
2000	11	0.8300	0.3286	1.0953	0.0000	2.5786	0.0444	0.1776	0.0000	0.0000	0.0001	0.0445
2000	12	0.4500	0.2960	1.1370	0.0000	2.3677	0.0422	0.1687	0.0000	0.0000	0.0000	0.0422
2001	1	0.4800	0.2597	1.1141	0.0000	2.1741	0.0387	0.1549	0.0000	0.0000	0.0000	0.0387
2001	2	1.0600	0.5881	1.3660	0.0000	2.0128	0.0323	0.1290	0.0000	0.0000	0.0000	0.0323
2001	3	1.8000	0.7792	2.2019	0.2744	2.1174	0.0340	0.1358	0.0036	0.0041	0.0021	0.0401
2001	4	3.0800	2.0591	1.8216	1.7025	3.5914	0.0457	0.1827	0.1484	0.2713	0.0002	0.3173
2001	5	3.2300	2.9627	1.1669	0.7945	4.0449	0.0682	0.2728	0.0107	0.2931	0.0039	0.3653
2001	6	0.9100	1.7022	0.3852	0.0034	3.7275	0.0642	0.2566	0.0001	0.0072	0.0037	0.0751
2001	7	3.1400	2.8061	0.7339	0.0000	3.4227	0.0610	0.2439	0.0000	0.0001	0.0162	0.0773
2001	8	2.6700	2.3218	1.0760	0.0000	3.1428	0.0560	0.2239	0.0000	0.0000	0.0145	0.0705
2001	9	1.3700	1.8542	0.6053	0.0000	2.8937	0.0498	0.1993	0.0000	0.0000	0.0030	0.0528
2001		19.4500	16.7439	0.6053	2.7748	2.8937	0.5865	2.3447	0.0000	0.5758	0.0445	1.2068
Period		62.300	48.722	0.605	10.330	2.894	1.988	7.948	0.000	2.914	0.165	5.067

Simulated intrawatershed results indicate that on a daily basis that there is very little water in the base-flow reservoir for metamorphic rocks and even less water in the intrusive rocks (table 29B and C). The median for daily values is substantially less than the daily mean. In fact, a time series of daily values for the contents of base-flow reservoir in the intrusive rocks is about zero 70 percent of the contemporary simulation

period (70th percentile is 0.0002 inch). Under this condition, only ground water that is not associated with local streamflow is available for withdrawal by wells, and the volume of this water is unknown.

The summaries of GSNK in table 27 and table 28 indicate that, during contemporary simulations, about 0.15 to 0.40 inch of water may be lost from the base-flow reservoir at a watershed scale;

**Table 29.** Summary statistics of daily values for water-balance terms from contemporary simulations in (A) the entire Turkey Creek watershed and for areas of (B) metamorphic, (C) intrusive, and (D) fault-zone rocks and (E) Pikes Peak Granite

[All univariate statistics and percentiles reported in inches; Precip, total precipitation; ET, total evapotranspiration; sm, contents of soil-zone reservoir at end of given period; bfi, total water added to base-flow reservoir; bfr, contents of base-flow reservoir at end of accounting period; bf, total base flow discharged to stream; gsnk, total water lost from base-flow reservoir that is not available to support local streamflow; ir, contents of interflow reservoir at end of the accounting period; if, total interflow; ovf, total overland flow; tf, total watershed flow; Min, minimum; Max, maximum, Stddev, standard deviation; N, number of observations; %, percentage]

A. Entire Turkey Creek watershed

Univariate statistics											
Variable	Mean	Median	Stddev	Min	Max	N					
Precip	0.0571	0.0000	0.1519	0.0000	1.9331	1004					
ET	0.0503	0.0365	0.0442	0.0000	0.1967	1004					
sm	1.6867	1.5812	0.7650	0.1010	4.1275	1004					
bfi	0.0027	0.0000	0.0126	0.0000	0.1582	1004					
bfr	0.1776	0.1733	0.0523	0.1003	0.5031	1004					
bf	0.0020	0.0002	0.0067	0.0001	0.0768	1004					
gsnk	0.0007	0.0003	0.0017	0.0001	0.0195	1004					
ir	0.0337	0.0020	0.1055	0.0000	0.8461	1004					
if	0.0029	0.0001	0.0100	0.0000	0.0929	1004					
ovf	0.0003	0.0000	0.0012	0.0000	0.0251	1004					
tf	0.0052	0.0006	0.0164	0.0001	0.1568	1004					

Percentiles												
Variable	0.1%	1.0%	5.0%	10.0%	20.0%	30.0%	40.0%	50.0%	60.0%	70.0%	80.0%	90.0%
bfr	0.1003	0.1012	0.1085	0.1171	0.1310	0.1471	0.1617	0.1733	0.1821	0.1963	0.2137	0.2402
ir	0.0000	0.0000	0.0000	0.0000	0.0001	0.0006	0.0012	0.0020	0.0037	0.0084	0.0209	0.0668

Correlations											
Variable	Precip	ET	sm	bfi	bfr	bf	gsnk	ir	if	ovf	tf
Precip	1.0000	-0.0534	0.2206	0.3763	0.1295	0.2052	0.1856	0.2190	0.1583	0.8016	0.2396
ET	-0.0534	1.0000	0.5221	0.1058	0.4754	0.2131	0.2217	0.3329	0.3160	0.0685	0.2846
sm	0.2206	0.5221	1.0000	0.4646	0.7085	0.6031	0.6132	0.6303	0.6050	0.2393	0.6326
bfi	0.3763	0.1058	0.4646	1.0000	0.4516	0.8471	0.7982	0.6582	0.6140	0.4375	0.7522
bfr	0.1295	0.4754	0.7085	0.4516	1.0000	0.6170	0.6568	0.7302	0.7001	0.2107	0.6941
bf	0.2052	0.2131	0.6031	0.8471	0.6170	1.0000	0.9907	0.8559	0.8472	0.2353	0.9418
gsnk	0.1856	0.2217	0.6132	0.7982	0.6568	0.9907	1.0000	0.8768	0.8670	0.2038	0.9478
ir	0.2190	0.3329	0.6303	0.6582	0.7302	0.8559	0.8768	1.0000	0.9860	0.3094	0.9732
if	0.1583	0.3160	0.6050	0.6140	0.7001	0.8472	0.8670	0.9860	1.0000	0.2307	0.9724
ovf	0.8016	0.0685	0.2393	0.4375	0.2107	0.2353	0.2038	0.3094	0.2307	1.0000	0.3108
tf	0.2396	0.2846	0.6326	0.7522	0.6941	0.9418	0.9478	0.9732	0.9724	0.3108	1.0000

this water is available for withdrawal by wells but is not available to support local streamflow. On an intra watershed scale, estimates for GSNK indicate that annual total accretions are in the tenths of an inch range for metamorphic-rock (0.21 inch), intrusive-rock (0.13 inch), and fault-zone reservoirs (0.44 inch) and are about 2.9 inches for the Pikes Peak Granite reservoir. The only accounting of GSNK available with PRMS concerns accretions; that is, PRMS provides no information describing how that water behaves, and a ground-water model is required for balance accounting of water that is not associated with streamflow.

**Long-Term Simulations**

The slightly less than 3-year summaries available from the contemporary simulations provide a description of hydrologic conditions during varied climatic conditions; however, the contemporary simulations do not provide a description of how hydrologic conditions are likely to vary over a period of decades. In order to obtain estimates for a longer period of time, long-term simulations were undertaken. Climatologic data from Cheesman Reservoir, with minor adjustments to air-temperature data, were used to obtain the long-term simulations beginning October 1, 1948, and continuing through September 30, 1999, a period of 51 water years.

**Table 29.** Summary statistics of daily values for water-balance terms from contemporary simulations in (A) the entire Turkey Creek watershed and areas of (B) metamorphic, (C) intrusive, and (D) fault-zone rocks and (E) Pikes Peak Granite—Continued

[All univariate statistics and percentiles reported in inches; Precip, total precipitation; *ET*, total evapotranspiration; *sm*, contents of soil-zone reservoir at end of given period; *bfi*, total water added to base-flow reservoir; *bfr*, contents of base-flow reservoir at end of accounting period; *bf*, total base flow discharged to stream; *gsnk*, total water lost from base-flow reservoir that is not available to support local streamflow; *ir*, contents of interflow reservoir at end of the accounting period; *if*, total interflow; *ovf*, total overland flow; *tf*, total watershed flow; Min, minimum; Max, maximum, Stddev, standard deviation; *N*, number of observations; %, percentage]

B. Metamorphic rocks

Univariate statistics

Variable	Mean	Median	Stddev	Min	Max	N
Precip	0.0561	0.0000	0.1525	0.0000	2.0688	1004
<i>ET</i>	0.0503	0.0367	0.0443	0.0000	0.1994	1004
<i>sm</i>	1.6818	1.5825	0.7744	0.1014	4.3055	1004
<i>bfi</i>	0.0022	0.0000	0.0125	0.0000	0.1716	1004
<i>bfr</i>	0.0128	0.0009	0.0461	0.0000	0.5294	1004
<i>bf</i>	0.0016	0.0001	0.0060	0.0000	0.0684	1004
<i>gsnk</i>	0.0006	0.0000	0.0021	0.0000	0.0244	1004
<i>ir</i>	0.0406	0.0029	0.1231	0.0000	0.9904	1004
<i>if</i>	0.0026	0.0001	0.0086	0.0000	0.0763	1004
<i>ovf</i>	0.0003	0.0000	0.0013	0.0000	0.0246	1004
<i>tf</i>	0.0045	0.0005	0.0145	0.0000	0.1473	1004

Percentiles

Variable	0.1%	1.0%	5.0%	10.0%	20.0%	30.0%	40.0%	50.0%	60.0%	70.0%	80.0%	90.0%
<i>bfr</i>	0.0000	0.0000	0.0000	0.0000	0.0000	0.0001	0.0003	0.0009	0.0021	0.0040	0.0077	0.0226
<i>ir</i>	0.0000	0.0000	0.0000	0.0000	0.0002	0.0007	0.0015	0.0029	0.0050	0.0097	0.0256	0.0803

Correlations

Variable	Precip	<i>ET</i>	<i>sm</i>	<i>bfi</i>	<i>bfr</i>	<i>bf</i>	<i>gsnk</i>	<i>ir</i>	<i>if</i>	<i>ovf</i>	<i>tf</i>
Precip	1.0000	-0.0435	0.2267	0.3994	0.1661	0.1661	0.1661	0.1966	0.1372	0.8226	0.2213
<i>ET</i>	-0.0435	1.0000	0.5314	0.0451	0.2056	0.2056	0.2056	0.3417	0.3136	0.0665	0.2765
<i>sm</i>	0.2267	0.5314	1.0000	0.4138	0.6063	0.6063	0.6063	0.6469	0.6172	0.2520	0.6373
<i>bfi</i>	0.3994	0.0451	0.4138	1.0000	0.7132	0.7132	0.7132	0.5819	0.5450	0.4605	0.6563
<i>bfr</i>	0.1661	0.2056	0.6063	0.7132	1.0000	1.0000	1.0000	0.8788	0.8958	0.1902	0.9589
<i>bf</i>	0.1661	0.2056	0.6063	0.7132	1.0000	1.0000	1.0000	0.8788	0.8958	0.1902	0.9589
<i>gsnk</i>	0.1661	0.2056	0.6063	0.7132	1.0000	1.0000	1.0000	0.8788	0.8958	0.1902	0.9589
<i>ir</i>	0.1966	0.3417	0.6469	0.5819	0.8788	0.8788	0.8788	1.0000	0.9902	0.2828	0.9734
<i>if</i>	0.1372	0.3136	0.6172	0.5450	0.8958	0.8958	0.8958	0.9902	1.0000	0.2032	0.9793
<i>ovf</i>	0.8226	0.0665	0.2520	0.4605	0.1902	0.1902	0.1902	0.2828	0.2032	1.0000	0.2858
<i>tf</i>	0.2213	0.2765	0.6373	0.6563	0.9589	0.9589	0.9589	0.9734	0.9793	0.2858	1.0000

The same model characterization of the watershed used for the contemporary simulations, which is based on streamflow data that reflect contemporary water use, was used for the long-term simulations. Water use in the watershed is largely a function of population, and the contemporary amount of ground water withdrawn for use is likely much greater than withdrawals made near the beginning of the long-term simulation period. Consequently, the long-term simulations indicate how the Turkey Creek watershed might respond to the 51 years of precipitation and temperature data used to derive the long-term simulations under current conditions of water use and not under historical conditions of water use.

Results from the long-term simulations are listed in table 30, table 31, and table 32 and are shown in figure 45. The long-term simulations indicate intrawatershed daily central tendencies are slightly higher but similar to contemporary simulation estimates. There is a possibility that the long-term estimates have bias due to the use of precipitation and temperature data from outside the watershed; however, the magnitude of Cheesman annual totals for precipitation is certainly similar to that measured in the Turkey Creek watershed during this study, and the Cheesman data seem to be a reasonable surrogate. Also, the important contribution of long-term

**Table 29.** Summary statistics of daily values for water-balance terms from contemporary simulations in (A) the entire Turkey Creek watershed and areas of (B) metamorphic, (C) intrusive, and (D) fault-zone rocks and (E) Pikes Peak Granite—Continued

[All univariate statistics and percentiles reported in inches; Precip, total precipitation; ET, total evapotranspiration; sm, contents of soil-zone reservoir at end of given period; bfi, total water added to base-flow reservoir; bfr, contents of base-flow reservoir at end of accounting period; bf, total base flow discharged to stream; gsnk, total water lost from base-flow reservoir that is not available to support local streamflow; ir, contents of interflow reservoir at end of the accounting period; if, total interflow; ovf, total overland flow; tf, total watershed flow; Min, minimum; Max, maximum, Stddev, standard deviation; N, number of observations; %, percentage]

C. Intrusive rocks

Univariate statistics

Variable	Mean	Median	Stddev	Min	Max	N
Precip	0.0582	0.0000	0.1534	0.0000	2.0937	1004
ET	0.0506	0.0375	0.0451	0.0000	0.2066	1004
sm	1.7451	1.6427	0.7869	0.0997	4.0257	1004
bfi	0.0036	0.0000	0.0153	0.0000	0.1665	1004
bfr	0.0029	0.0000	0.0105	0.0000	0.1111	1004
bf	0.0032	0.0000	0.0118	0.0000	0.1248	1004
gsnk	0.0004	0.0000	0.0013	0.0000	0.0137	1004
ir	0.0184	0.0002	0.0752	0.0000	0.9416	1004
if	0.0030	0.0000	0.0122	0.0000	0.1505	1004
ovf	0.0003	0.0000	0.0012	0.0000	0.0286	1004
tf	0.0065	0.0002	0.0226	0.0000	0.2140	1004

Percentiles

Variable	0.1%	1.0%	5.0%	10.0%	20.0%	30.0%	40.0%	50.0%	60.0%	70.0%	80.0%	90.0%
bfr	0.0000	0.0000	0.0000	0.0000	0.0000	0.0000	0.0000	0.0000	0.0000	0.0002	0.0012	0.0052
ir	0.0000	0.0000	0.0000	0.0000	0.0000	0.0000	0.0000	0.0002	0.0006	0.0018	0.0057	0.0280

Correlations

Variable	Precip	ET	sm	bfi	bfr	bf	gsnk	ir	if	ovf	tf
Precip	1.0000	-0.0517	0.2109	0.3268	0.2470	0.2470	0.2470	0.2781	0.1827	0.7642	0.2687
ET	-0.0517	1.0000	0.5203	0.1434	0.1921	0.1921	0.1921	0.2587	0.2752	0.0756	0.2520
sm	0.2109	0.5203	1.0000	0.4675	0.5474	0.5474	0.5474	0.5377	0.5351	0.2188	0.5844
bfi	0.3268	0.1434	0.4675	1.0000	0.9426	0.9426	0.9426	0.6787	0.6013	0.3904	0.8349
bfr	0.2470	0.1921	0.5474	0.9426	1.0000	1.0000	1.0000	0.7645	0.7266	0.2746	0.9258
bf	0.2470	0.1921	0.5474	0.9426	1.0000	1.0000	1.0000	0.7645	0.7266	0.2746	0.9258
gsnk	0.2470	0.1921	0.5474	0.9426	1.0000	1.0000	1.0000	0.7645	0.7266	0.2746	0.9258
ir	0.2781	0.2587	0.5377	0.6787	0.7645	0.7645	0.7645	1.0000	0.9788	0.4026	0.9460
if	0.1827	0.2752	0.5351	0.6013	0.7266	0.7266	0.7266	0.9788	1.0000	0.2616	0.9299
ovf	0.7642	0.0756	0.2188	0.3904	0.2746	0.2746	0.2746	0.4026	0.2616	1.0000	0.3385
tf	0.2687	0.2520	0.5844	0.8349	0.9258	0.9258	0.9258	0.9460	0.9299	0.3385	1.0000

simulations is not an exact duplication of watershed climatologic conditions; rather, it is an evaluation of how ground-water conditions are likely to vary during a period of several decades of climatic conditions that are at least similar to climate conditions in the watershed.

The long-term estimates reiterate that the watershed contents of the base-flow reservoirs fluctuate seasonally. The watershed representation of base-flow reservoir contents (fig. 45) indicates that recharge to watershed base-flow reservoir can result in net end-of-year increases of about 0.1 inch (1957, 1969, 1973, and 1995, table 30) and that these increases have a tendency to persist for years. However, during periods with relatively small amounts of precipitation,

simulated results indicate that, on a watershed scale, the contents of the base-flow reservoirs may recede to less than one-tenth of an inch (for example, 1954 and 1956 in table 30). Relatively large annual changes in the contents of the base-flow reservoir are associated with relatively large amounts of ground-water recharge to the watershed. For instance, in water year 1973 the simulated results indicate that the watershed base-flow reservoir received nearly 5 inches of recharge in the spring (bfi of 4.8 inches in 1973, table 30) and that this amount of recharge resulted in a 0.13-inch increase in watershed base-flow reservoir contents at the end of water year 1973 compared to water year 1972 (table 30). In contrast, during water year 1954, the simulated results indicate a low amount



**Table 29.** Summary statistics of daily values for water-balance terms from contemporary simulations in (A) the entire Turkey Creek watershed and areas of (B) metamorphic, (C) intrusive, and (D) fault-zone rocks and (E) Pikes Peak Granite—Continued

[All univariate statistics and percentiles reported in inches; Precip, total precipitation; *ET*, total evapotranspiration; *sm*, contents of soil-zone reservoir at end of given period; *bfi*, total water added to base-flow reservoir; *bfr*, contents of base-flow reservoir at end of accounting period; *bf*, total base flow discharged to stream; *gsnk*, total water lost from base-flow reservoir that is not available to support local streamflow; *ir*, contents of interflow reservoir at end of the accounting period; *if*, total interflow; *ovf*, total overland flow; *tf*, total watershed flow; Min, minimum; Max, maximum, Stddev, standard deviation; N, number of observations; %, percentage]

D. Fault-zone rocks

Univariate statistics

Variable	Mean	Median	Stddev	Min	Max	N
Precip	0.0598	0.0000	0.1636	0.0000	1.9336	1004
<i>ET</i>	0.0516	0.0387	0.0448	0.0000	0.2049	1004
<i>sm</i>	1.6979	1.5644	0.7570	0.1005	3.7985	1004
<i>bfi</i>	0.0021	0.0000	0.0081	0.0000	0.0678	1004
<i>bfr</i>	1.3531	1.3748	0.2569	0.8544	1.8292	1004
<i>bf</i>	0.0007	0.0008	0.0001	0.0005	0.0010	1004
<i>gsnk</i>	0.0012	0.0012	0.0002	0.0008	0.0016	1004
<i>ir</i>	0.0299	0.0000	0.1002	0.0000	1.0888	1004
<i>if</i>	0.0052	0.0000	0.0182	0.0000	0.2111	1004
<i>ovf</i>	0.0003	0.0000	0.0010	0.0000	0.0219	1004
<i>tf</i>	0.0061	0.0009	0.0185	0.0005	0.2120	1004

Percentiles

Variable	0.1%	1.0%	5.0%	10.0%	20.0%	30.0%	40.0%	50.0%	60.0%	70.0%	80.0%	90.0%
<i>bfr</i>	0.8544	0.8606	0.9076	0.9739	1.1070	1.2114	1.2883	1.3748	1.4219	1.4916	1.5879	1.7237
<i>ir</i>	0.0000	0.0000	0.0000	0.0000	0.0000	0.0000	0.0000	0.0000	0.0001	0.0016	0.0121	0.0672

Correlations

Variable	Precip	<i>ET</i>	<i>sm</i>	<i>bfi</i>	<i>bfr</i>	<i>bf</i>	<i>gsnk</i>	<i>ir</i>	<i>if</i>	<i>ovf</i>	<i>tf</i>
Precip	1.0000	-0.0706	0.1847	0.1958	0.0050	0.0049	0.0050	0.1886	0.1327	0.7133	0.1712
<i>ET</i>	-0.0706	1.0000	0.4655	0.2095	0.4194	0.4195	0.4194	0.3039	0.2972	0.0873	0.3011
<i>sm</i>	0.1847	0.4655	1.0000	0.5384	0.3868	0.3868	0.3869	0.6120	0.5868	0.2004	0.5928
<i>bfi</i>	0.1958	0.2095	0.5384	1.0000	0.0383	0.0383	0.0383	0.7720	0.7068	0.2848	0.7132
<i>bfr</i>	0.0050	0.4194	0.3868	0.0383	1.0000	1.0000	1.0000	0.1548	0.1595	0.1327	0.1724
<i>bf</i>	0.0049	0.4195	0.3868	0.0383	1.0000	1.0000	1.0000	0.1547	0.1594	0.1326	0.1723
<i>gsnk</i>	0.0050	0.4194	0.3869	0.0383	1.0000	1.0000	1.0000	0.1549	0.1595	0.1328	0.1724
<i>ir</i>	0.1886	0.3039	0.6120	0.7720	0.1548	0.1547	0.1549	1.0000	0.9830	0.2894	0.9866
<i>if</i>	0.1327	0.2972	0.5868	0.7068	0.1595	0.1594	0.1595	0.9830	1.0000	0.2014	0.9984
<i>ovf</i>	0.7133	0.0873	0.2004	0.2848	0.1327	0.1326	0.1328	0.2894	0.2014	1.0000	0.2562
<i>tf</i>	0.1712	0.3011	0.5928	0.7132	0.1724	0.1723	0.1724	0.9866	0.9984	0.2562	1.0000

of recharge to the watershed base-flow reservoir (0.0326 inch) resulting in an end-of-year reduction of about 0.06 inch compared to 1953. In the 51 years of long-term simulations, several consecutive years with low amounts of precipitation and recharge similar to 1954, a year with relatively small amounts of water in base-flow reservoirs, did not occur. Several consecutive years with low amounts of precipitation and recharge similar to 1954 (or 1964, 1966, 1986, 1989, and so forth), however, would deplete ground-water available to support base flow in the Turkey Creek watershed, and the period of 1966 through 1968 gives some indication of this. The temporal pattern of precipitation described by the 51 years of Cheesman data indicates that several consecutive years of low

precipitation (10 to 14 inches) did not occur in that record. However, global- or regional-scale climate changes or cycles could have a significant effect on the water supply in the Turkey Creek watershed.

Intrawatershed conditions described by the long-term simulations (table 31, table 32, and fig. 45) reiterate many of the observations discussed in the “Contemporary Simulations” section, particularly those concerning differences between the reservoirs and the dynamic nature of the interflow reservoirs. For the entire long-term simulation period, the simulation results indicate that the end-of-year contents of the base-flow reservoir was zero about 60 percent of the period in the intrusive rocks and about 30 percent of the period in the metamorphic rocks. In contrast, in

**Table 29.** Summary statistics of daily values for water-balance terms from contemporary simulations in (A) the entire Turkey Creek watershed and areas of (B) metamorphic, (C) intrusive, and (D) fault-zone rocks and (E) Pikes Peak Granite—Continued

[All univariate statistics and percentiles reported in inches; Precip, total precipitation; ET, total evapotranspiration; sm, contents of soil-zone reservoir at end of given period; bfi, total water added to base-flow reservoir; bfr, contents of base-flow reservoir at end of accounting period; bf, total base flow discharged to stream; gsnk, total water lost from base-flow reservoir that is not available to support local streamflow; ir, contents of interflow reservoir at end of the accounting period; if, total interflow; ovf, total overland flow; tf, total watershed flow; Min, minimum; Max, maximum, Stddev, standard deviation; N, number of observations; %, percentage]

E. Pikes Peak Granite

Univariate statistics

Variable	Mean	Median	Stddev	Min	Max	N
Precip	0.0621	0.0000	0.1739	0.0000	2.0000	1004
ET	0.0485	0.0340	0.0446	0.0000	0.2198	1004
sm	1.1442	1.0945	0.5601	0.0999	2.2431	1004
bfi	0.0103	0.0000	0.0380	0.0000	0.2431	1004
bfr	3.5904	3.5092	1.1735	1.8166	6.2116	1004
bf	0.0020	0.0019	0.0006	0.0010	0.0034	1004
gsnk	0.0079	0.0077	0.0026	0.0040	0.0137	1004
ir	0.0264	0.0000	0.0926	0.0000	1.0021	1004
if	0.0029	0.0000	0.0106	0.0000	0.1175	1004
ovf	0.0002	0.0000	0.0007	0.0000	0.0079	1004
tf	0.0050	0.0021	0.0109	0.0010	0.1208	1004

Percentiles

Variable	0.1%	1.0%	5.0%	10.0%	20.0%	30.0%	40.0%	50.0%	60.0%	70.0%	80.0%	90.0%
bfr	1.8167	1.8625	1.9754	2.1071	2.3857	2.8433	3.2394	3.5092	3.7769	4.1063	4.5168	5.5073
ir	0.0000	0.0000	0.0000	0.0000	0.0000	0.0000	0.0000	0.0000	0.0000	0.0002	0.0066	0.0750

Correlations

Variable	Precip	ET	sm	bfi	bfr	bf	gsnk	ir	if	ovf	tf
Precip	1.0000	-0.0552	0.1860	0.1534	0.0218	0.0218	0.0218	0.1558	0.1133	0.5630	0.1461
ET	-0.0552	1.0000	0.3359	0.2773	0.3894	0.3894	0.3894	0.3461	0.3417	0.1519	0.3649
sm	0.1860	0.3359	1.0000	0.4697	0.0365	0.0365	0.0365	0.4097	0.3877	0.1467	0.3883
bfi	0.1534	0.2773	0.4697	1.0000	0.0932	0.0932	0.0932	0.6770	0.6134	0.1242	0.6099
bfr	0.0218	0.3894	0.0365	0.0932	1.0000	1.0000	1.0000	0.2957	0.3001	0.1607	0.3611
bf	0.0218	0.3894	0.0365	0.0932	1.0000	1.0000	1.0000	0.2957	0.3000	0.1607	0.3611
gsnk	0.0218	0.3894	0.0365	0.0932	1.0000	1.0000	1.0000	0.2957	0.3001	0.1607	0.3611
ir	0.1558	0.3461	0.4097	0.6770	0.2957	0.2957	0.2957	1.0000	0.9887	0.1087	0.9860
if	0.1133	0.3417	0.3877	0.6134	0.3001	0.3000	0.3001	0.9887	1.0000	0.0883	0.9960
ovf	0.5630	0.1519	0.1467	0.1242	0.1607	0.1607	0.1607	0.1087	0.0883	1.0000	0.1569
tf	0.1461	0.3649	0.3883	0.6099	0.3611	0.3611	0.3611	0.9860	0.9960	0.1569	1.0000

areas of fault-zone rocks and Pikes Peak Granite, base-flow reservoirs contained water through the entire long-term simulation. During water year 1954, simulation results indicate that for 75 percent of the time, the contents of the intrusive-rock base-flow reservoir were insufficient to support base flow.

**Simulation Results and Their Implications to Water Supply**

In order to give simulated results context with respect to water-supply issues, some discussion of water use in the watershed is required. It is important to note that, in this report, the term “water use”

indicates the amount of water withdrawn from wells; it does not describe consumption or the amount of withdrawn water that is returned to the hydrologic system, but simply describes the amount of water required to satisfy estimated withdrawals from wells. It also is important to note that the PRMS watershed characterization is for the current conditions of water use—that is, the effects of current estimated withdrawals, whether they be depleted streamflow in some areas or a steady but small contribution of return flow to streamflow in other areas, are characterized by the calibrated model.

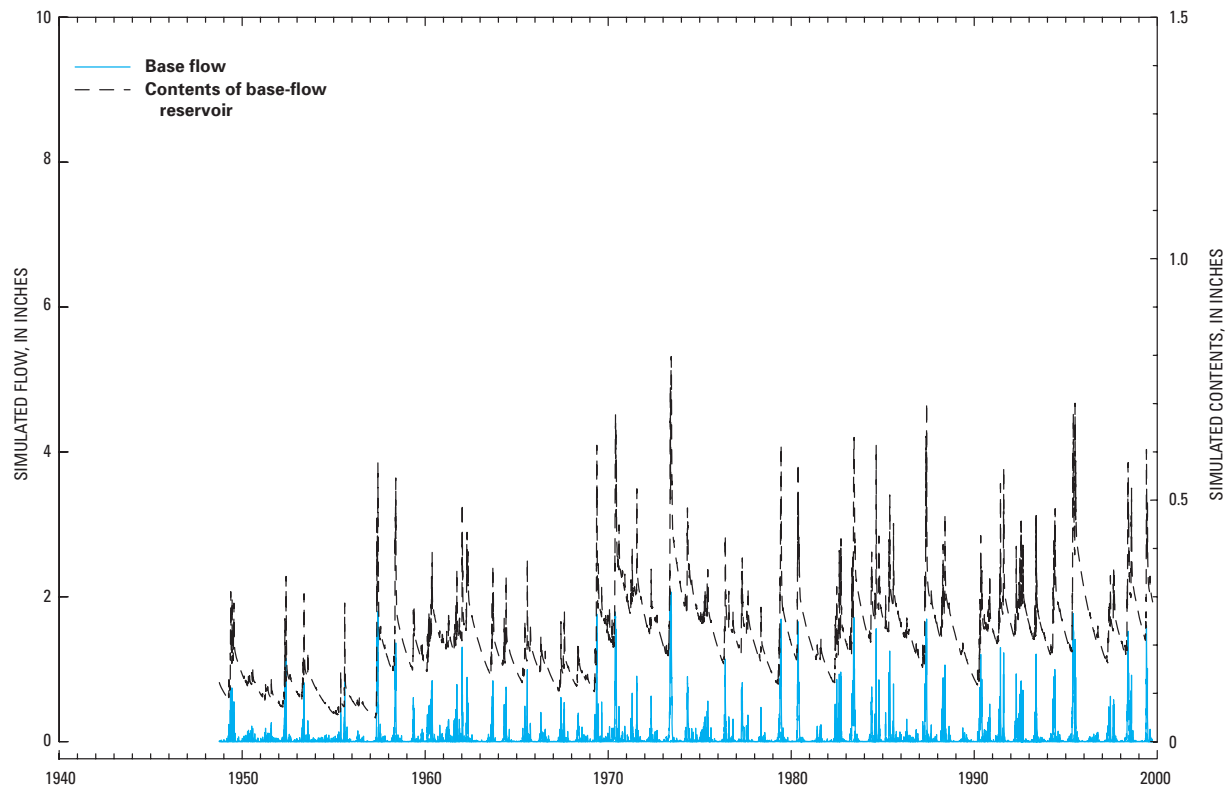
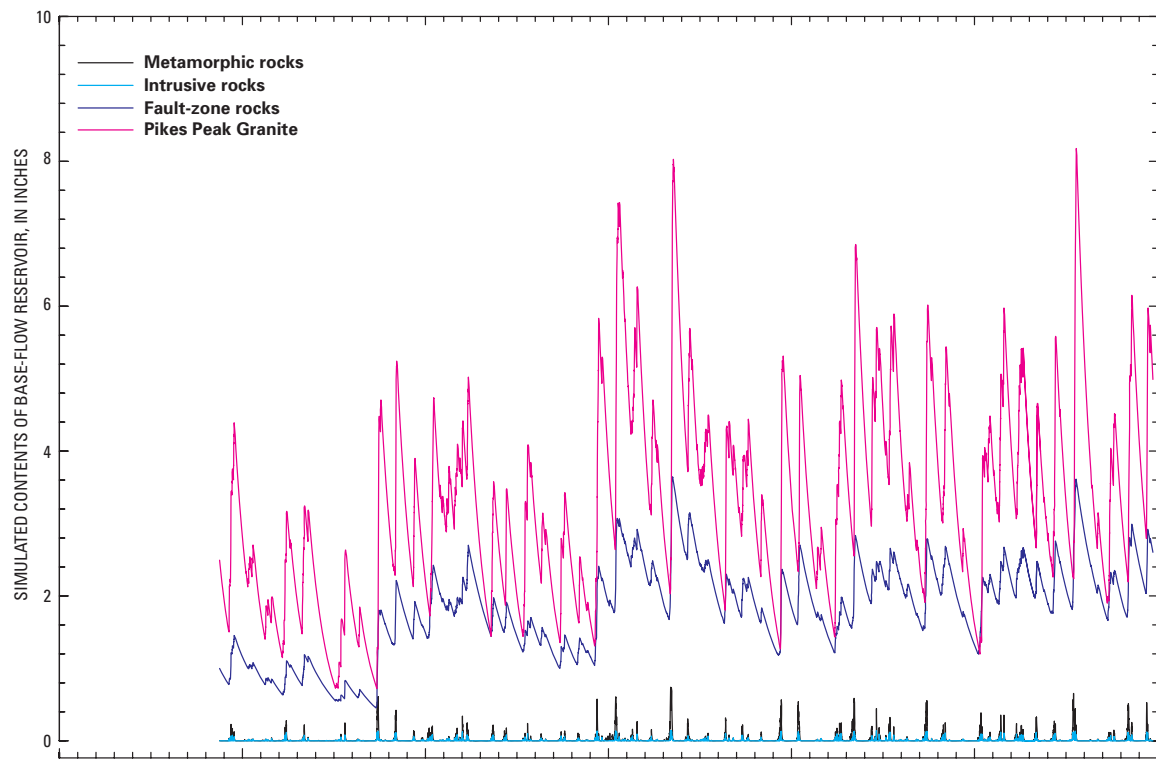


**Figure 45.** Watershed hydrographs of long-term simulated results.













**Table 32.** Summary statistics of daily values for water-balance terms from long-term simulations for (A) the entire Turkey Creek watershed and for areas of (B) metamorphic, (C) intrusive, and (D) fault-zone rocks and (E) Pikes Peak Granite

[All univariate statistics and percentiles reported in inches; Precip, total precipitation; ET, total evapotranspiration; sm, contents of soil-zone reservoir at end of given period; bfi, total water added to base-flow reservoir; bfr, contents of base-flow reservoir at end of accounting period; bf, total base flow discharged to stream; gsnk, total water lost from base-flow reservoir that is not available to support local streamflow; ir, contents of interflow reservoir at end of the accounting period; if, total interflow; ovf, total overland flow; tf, total watershed flow; Min, minimum; Max, maximum; Stddev, standard deviation; N, number of observations; %, percentage]

A. Entire Turkey Creek Watershed

Univariate statistics											
Variable	Mean	Median	Stddev	Min	Max	N					
Precip	0.0469	0.0000	0.1461	0.0000	2.6500	18627					
ET	0.0406	0.0258	0.0415	0.0000	0.2249	18627					
sm	2.3514	2.2973	0.8457	0.1374	4.1913	18627					
bfi	0.0038	0.0000	0.0165	0.0000	0.1812	18627					
bfr	0.1983	0.1944	0.0844	0.0423	0.7757	18627					
bf	0.0029	0.0002	0.0091	0.0000	0.1029	18627					
gsnk	0.0010	0.0003	0.0023	0.0001	0.0266	18627					
ir	0.0255	0.0015	0.0736	0.0000	0.9793	18627					
if	0.0021	0.0001	0.0068	0.0000	0.1067	18627					
ovf	0.0003	0.0000	0.0011	0.0000	0.0268	18627					
tf	0.0053	0.0005	0.0154	0.0000	0.1899	18627					

Percentiles												
Variable	0.1%	1.0%	5.0%	10.0%	20.0%	30.0%	40.0%	50.0%	60.0%	70.0%	80.0%	90.0%
bfr	0.0439	0.0519	0.0742	0.0957	0.1261	0.1549	0.1743	0.1944	0.2122	0.2315	0.2562	0.2929
ir	0.0000	0.0000	0.0000	0.0000	0.0000	0.0002	0.0005	0.0015	0.0037	0.0084	0.0225	0.0644

Correlations											
Variable	Precip	ET	sm	bfi	bfr	bf	gsnk	ir	if	ovf	tf
Precip	1.0000	0.0189	0.1313	0.2827	0.0705	0.1427	0.1152	0.1311	0.0918	0.7796	0.1788
ET	0.0189	1.0000	0.2145	0.1381	0.2996	0.2429	0.2618	0.3618	0.3444	0.1081	0.3037
sm	0.1313	0.2145	1.0000	0.3805	0.4162	0.4814	0.4922	0.4388	0.4234	0.1550	0.4827
bfi	0.2827	0.1381	0.3805	1.0000	0.4478	0.8532	0.8051	0.6232	0.5765	0.3590	0.7841
bfr	0.0705	0.2996	0.4162	0.4478	1.0000	0.5968	0.6359	0.6051	0.5873	0.1021	0.6199
bf	0.1427	0.2429	0.4814	0.8532	0.5968	1.0000	0.9920	0.8257	0.8140	0.1845	0.9641
gsnk	0.1152	0.2618	0.4922	0.8051	0.6359	0.9920	1.0000	0.8498	0.8394	0.1440	0.9679
ir	0.1311	0.3618	0.4388	0.6232	0.6051	0.8257	0.8498	1.0000	0.9877	0.1875	0.9387
if	0.0918	0.3444	0.4234	0.5765	0.5873	0.8140	0.8394	0.9877	1.0000	0.1379	0.9339
ovf	0.7796	0.1081	0.1550	0.3590	0.1021	0.1845	0.1440	0.1875	0.1379	1.0000	0.2392
tf	0.1788	0.3037	0.4827	0.7841	0.6199	0.9641	0.9679	0.9387	0.9339	0.2392	1.0000

The contemporary (2001) estimate for the number of occupied households in the watershed is about 4,900, and the SEO estimates, for permitting purposes, that household use is 300 gallons per day, or about 1,650 acre-feet for the entire watershed on an annual basis. Records from local residential supply systems (Diana Hunter, Indian Hills Water District, written commun., 2001; Norman Lewis, Homestead Water District, written commun., 2001; and Roger Migchelbrink, Will-O-Wisp Water District, oral commun., 2001), which represent the use for about 600 households, indicate that water use, at least for

these 600 or so households, is about 200 gallons per day or about 67 percent of the commonly cited 300 gallons per day amount. On the basis of this information this report will bracket estimates of daily water withdrawals as about 200 to 300 gallons per day per household. This amount of water, referred to as “estimated withdrawals” in this report, corresponds to a watershed depth of 0.43 to 0.65 inch per year, or 0.0012 to 0.0018 inch per day. These values are small; however, the values of many terms in the water balance summaries in tables 28–32, such as input to and contents of the base-flow reservoirs, also are small.

**Table 32.** Summary statistics of daily values for water-balance terms from long-term simulations for (A) the entire Turkey Creek watershed and areas of (B) metamorphic, (C) intrusive, and (D) fault-zone rocks and (E) Pikes Peak Granite—Continued

[All univariate statistics and percentiles reported in inches; Precip, total precipitation; ET, total evapotranspiration; sm, contents of soil-zone reservoir at end of given period; bfi, total water added to base-flow reservoir; bfr, contents of base-flow reservoir at end of accounting period; bf, total base flow discharged to stream; gsnk, total water lost from base-flow reservoir that is not available to support local streamflow; ir, contents of interflow reservoir at end of the accounting period; if, total interflow; ovf, total overland flow; tf, total watershed flow; Min, minimum; Max, maximum, Stddev, standard deviation; N, number of observations; %, percentage]

B. Metamorphic Rocks

Univariate statistics											
Variable	Mean	Median	Stddev	Min	Max	N					
Precip	0.0469	0.0000	0.1461	0.0000	2.6500	18627					
ET	0.0414	0.0266	0.0419	0.0000	0.2283	18627					
sm	2.3960	2.3270	0.8708	0.1380	4.3536	18627					
bfi	0.0035	0.0000	0.0165	0.0000	0.1905	18627					
bfr	0.0201	0.0007	0.0639	0.0000	0.7313	18627					
bff	0.0026	0.0001	0.0083	0.0000	0.0945	18627					
gsnk	0.0009	0.0000	0.0029	0.0000	0.0337	18627					
ir	0.0297	0.0021	0.0838	0.0000	1.1221	18627					
if	0.0018	0.0001	0.0056	0.0000	0.0907	18627					
ovf	0.0003	0.0000	0.0011	0.0000	0.0271	18627					
tf	0.0062	0.0012	0.0160	0.0002	0.2242	18627					

Percentiles												
Variable	0.1%	1.0%	5.0%	10.0%	20.0%	30.0%	40.0%	50.0%	60.0%	70.0%	80.0%	90.0%
bfr	0.0000	0.0000	0.0000	0.0000	0.0000	0.0000	0.0002	0.0007	0.0019	0.0047	0.0131	0.0474
ir	0.0000	0.0000	0.0000	0.0000	0.0000	0.0002	0.0008	0.0021	0.0049	0.0108	0.0271	0.0780

Correlations											
Variable	Precip	ET	sm	bfi	bfr	bf	gsnk	ir	if	ovf	tf
Precip	1.0000	0.0223	0.1343	0.2713	0.0923	0.0923	0.0923	0.1066	0.0659	0.7867	0.1477
ET	0.0223	1.0000	0.2243	0.1107	0.2639	0.2639	0.2639	0.3646	0.3371	0.1101	0.3108
sm	0.1343	0.2243	1.0000	0.3676	0.4968	0.4968	0.4968	0.4321	0.3970	0.1594	0.4827
bfi	0.2713	0.1107	0.3676	1.0000	0.7385	0.7385	0.7385	0.5711	0.5222	0.3384	0.6976
bfr	0.0923	0.2639	0.4968	0.7385	1.0000	1.0000	1.0000	0.8476	0.8367	0.1174	0.9706
bff	0.0923	0.2639	0.4968	0.7385	1.0000	1.0000	1.0000	0.8476	0.8367	0.1174	0.9706
gsnk	0.0923	0.2639	0.4968	0.7385	1.0000	1.0000	1.0000	0.8476	0.8367	0.1174	0.9706
ir	0.1066	0.3646	0.4321	0.5711	0.8476	0.8476	0.8476	1.0000	0.9881	0.1542	0.9427
if	0.0659	0.3371	0.3970	0.5222	0.8367	0.8367	0.8367	0.9881	1.0000	0.0983	0.9363
ovf	0.7867	0.1101	0.1594	0.3384	0.1174	0.1174	0.1174	0.1542	0.0983	1.0000	0.1939
tf	0.1477	0.3108	0.4827	0.6976	0.9706	0.9706	0.9706	0.9427	0.9363	0.1939	1.0000

Various water-balance terms can be compared to estimated withdrawals to evaluate their relative magnitudes and also the effects of the withdrawals on the watershed system. Comparisons to recharge are considered unrealistic principally because much recharge leaves the watershed as streamflow. If interflow is discounted, due to its intermittent nature as described in the “Runoff Modeling” section, then water associated with base flow becomes the next term of interest. The

PRMS watershed characterization provides quantitative estimates of all terms related to base flow as described in equation 3 from the “Watershed Characterization Using the Precipitation-Runoff Modeling System” section; equation 3 is essentially a water balance for the base-flow reservoir. A term that is not described by equation 3 is the total amount of ground water in the system (the product of aquifer volume and porosity). Although estimates of porosity are presented in this report, the total

**Table 32.** Summary statistics of daily values for water-balance terms from long-term simulations for (A) the entire Turkey Creek watershed and areas of (B) metamorphic, (C) intrusive, and (D) fault-zone rocks and (E) Pikes Peak Granite—Continued

[All univariate statistics and percentiles reported in inches; Precip, total precipitation; ET, total evapotranspiration; sm, contents of soil-zone reservoir at end of given period; bfi, total water added to base-flow reservoir; bfr, contents of base-flow reservoir at end of accounting period; bf, total base flow discharged to stream; gsnk, total water lost from base-flow reservoir that is not available to support local streamflow; ir, contents of interflow reservoir at end of the accounting period; if, total interflow; ovf, total overland flow; tf, total watershed flow; Min, minimum; Max, maximum, Stddev, standard deviation; N, number of observations; %, percentage]

C. Intrusive rocks

Univariate statistics						
Variable	Mean	Median	Stddev	Min	Max	N
Precip	0.0469	0.0000	0.1461	0.0000	2.6500	18627
ET	0.0398	0.0247	0.0415	0.0000	0.2197	18627
sm	2.3793	2.3411	0.8418	0.1346	4.0987	18627
bfi	0.0047	0.0000	0.0198	0.0000	0.1904	18627
bfr	0.0037	0.0000	0.0137	0.0000	0.1424	18627
bf	0.0042	0.0000	0.0154	0.0000	0.1600	18627
gsnk	0.0005	0.0000	0.0017	0.0000	0.0176	18627
ir	0.0140	0.0000	0.0517	0.0000	1.0063	18627
if	0.0022	0.0000	0.0082	0.0000	0.1603	18627
ovf	0.0002	0.0000	0.0011	0.0000	0.0269	18627
tf	0.0067	0.0001	0.0222	0.0000	0.2435	18627

Percentiles												
Variable	0.1%	1.0%	5.0%	10.0%	20.0%	30.0%	40.0%	50.0%	60.0%	70.0%	80.0%	90.0%
bfr	0.0000	0.0000	0.0000	0.0000	0.0000	0.0000	0.0000	0.0000	0.0000	0.0001	0.0011	0.0070
ir	0.0000	0.0000	0.0000	0.0000	0.0000	0.0000	0.0000	0.0000	0.0002	0.0011	0.0055	0.0277

Correlations											
Variable	Precip	ET	sm	bfi	bfr	bf	gsnk	ir	if	ovf	tf
Precip	1.0000	0.0190	0.1220	0.2737	0.1994	0.1994	0.1994	0.1770	0.1095	0.7623	0.2152
ET	0.0190	1.0000	0.1993	0.1543	0.1940	0.1940	0.1940	0.2929	0.3035	0.1100	0.2522
sm	0.1220	0.1993	1.0000	0.3737	0.4313	0.4313	0.4313	0.4045	0.4017	0.1448	0.4550
bfi	0.2737	0.1543	0.3737	1.0000	0.9458	0.9458	0.9458	0.6354	0.5634	0.3561	0.8822
bfr	0.1994	0.1940	0.4313	0.9458	1.0000	1.0000	1.0000	0.7340	0.6926	0.2569	0.9630
bf	0.1994	0.1940	0.4313	0.9458	1.0000	1.0000	1.0000	0.7340	0.6926	0.2569	0.9630
gsnk	0.1994	0.1940	0.4313	0.9458	1.0000	1.0000	1.0000	0.7340	0.6926	0.2569	0.9630
ir	0.1770	0.2929	0.4045	0.6354	0.7340	0.7340	0.7340	1.0000	0.9832	0.2532	0.8855
if	0.1095	0.3035	0.4017	0.5634	0.6926	0.6926	0.6926	0.9832	1.0000	0.1617	0.8586
ovf	0.7623	0.1100	0.1448	0.3561	0.2569	0.2569	0.2569	0.2532	0.1617	1.0000	0.2857
tf	0.2152	0.2522	0.4550	0.8822	0.9630	0.9630	0.9630	0.8855	0.8586	0.2857	1.0000

amount of ground water in the system remains unknown because the dimensions of the system, or aquifer volume, are unknown. The map surface dimensions, or x and y, are presumed to be the watershed; however, the depth dimension, or z, is not known.

An evaluation of equation 3 using results listed in table 27, table 28, table 30, or table 31 indicates that the  $\Delta BFR$  is often negative, which indicates that the contents of the base-flow reservoir are being depleted. Should the contents of the base-flow reservoir be

completely depleted, not only will there be no base flow, but GSNK, which comes from the base-flow reservoirs, also will be zero. If the contents of base-flow reservoirs are zero, ground water can still leave the watershed by evapotranspiration, in areas where the water table is shallow, by underflow, by withdrawals made for domestic use, or in various combinations of all three. Under these conditions, streamflow will not resume until the contents of base-flow reservoirs becomes greater than zero.

**Table 32.** Summary statistics of daily values for water-balance terms from long-term simulations for (A) the entire Turkey Creek watershed and areas of (B) metamorphic, (C) intrusive, and (D) fault-zone rocks and (E) Pikes Peak Granite—Continued

[All univariate statistics and percentiles reported in inches; Precip, total precipitation; ET, total evapotranspiration; sm, contents of soil-zone reservoir at end of given period; bfi, total water added to base-flow reservoir; bfr, contents of base-flow reservoir at end of accounting period; bf, total base flow discharged to stream; gsnk, total water lost from base-flow reservoir that is not available to support local streamflow; ir, contents of interflow reservoir at end of the accounting period; if, total interflow; ovf, total overland flow; tf, total watershed flow; Min, minimum; Max, maximum, Stddev, standard deviation; N, number of observations; %, percentage]

D. Fault-zone rocks

Univariate statistics

Variable	Mean	Median	Stddev	Min	Max	N
Precip	0.0469	0.0000	0.1461	0.0000	2.6500	18627
ET	0.0392	0.0246	0.0409	0.0000	0.2207	18627
sm	2.1868	2.1627	0.7770	0.1428	3.9116	18627
bfi	0.0025	0.0000	0.0088	0.0000	0.0728	18627
bfr	1.6690	1.7157	0.5955	0.3865	3.4256	18627
bf	0.0009	0.0009	0.0003	0.0002	0.0019	18627
gsnk	0.0015	0.0015	0.0005	0.0003	0.0030	18627
ir	0.0297	0.0000	0.0889	0.0000	1.1633	18627
if	0.0050	0.0000	0.0158	0.0000	0.2230	18627
ovf	0.0002	0.0000	0.0010	0.0000	0.0263	18627
tf	0.0062	0.0012	0.0160	0.0002	0.2242	18627

Percentiles

Variable	0.1%	1.0%	5.0%	10.0%	20.0%	30.0%	40.0%	50.0%	60.0%	70.0%	80.0%	90.0%
bfr	0.3945	0.4774	0.6101	0.7990	1.1068	1.3728	1.5653	1.7157	1.8648	2.0097	2.1765	2.4059
ir	0.0000	0.0000	0.0000	0.0000	0.0000	0.0000	0.0000	0.0000	0.0006	0.0040	0.0191	0.0818

Correlations

Variable	Precip	ET	sm	bfi	bfr	bf	gsnk	ir	if	ovf	tf
Precip	1.0000	0.0196	0.1343	0.2725	0.0163	0.0163	0.0163	0.1737	0.1109	0.7735	0.1583
ET	0.0196	1.0000	0.2048	0.1965	0.1702	0.1702	0.1702	0.3498	0.3457	0.1116	0.3508
sm	0.1343	0.2048	1.0000	0.4270	0.2038	0.2038	0.2038	0.4789	0.4576	0.1539	0.4643
bfi	0.2725	0.1965	0.4270	1.0000	0.1046	0.1046	0.1046	0.7435	0.6784	0.3613	0.6927
bfr	0.0163	0.1702	0.2038	0.1046	1.0000	1.0000	1.0000	0.1724	0.1744	0.0277	0.1939
bf	0.0163	0.1702	0.2038	0.1046	1.0000	1.0000	1.0000	0.1724	0.1744	0.0277	0.1939
gsnk	0.0163	0.1702	0.2038	0.1046	1.0000	1.0000	1.0000	0.1724	0.1744	0.0277	0.1939
ir	0.1737	0.3498	0.4789	0.7435	0.1724	0.1724	0.1724	1.0000	0.9863	0.2421	0.9896
if	0.1109	0.3457	0.4576	0.6784	0.1744	0.1744	0.1744	0.9863	1.0000	0.1574	0.9979
ovf	0.7735	0.1116	0.1539	0.3613	0.0277	0.0277	0.0277	0.2421	0.1574	1.0000	0.2186
tf	0.1583	0.3508	0.4643	0.6927	0.1939	0.1939	0.1939	0.9896	0.9979	0.2186	1.0000

Comparison of estimates for ground-water withdrawals made for domestic wells to simulated results for the entire watershed contents of the base-flow reservoirs indicates that, on a watershed basis, there is typically more than enough water in storage to meet estimates of contemporary (2001) demands for withdrawals. In fact, the daily time series of watershed contents in the base-flow reservoirs indicates that requirements for daily estimated withdrawals (0.0012 to 0.0018 inch) are exceeded greater than 99.9 percent of the long-term simulation period (table 32A). Intrawatershed estimates indicate that the minimum contents for base-flow

reservoirs for the fault-zone rocks and Pikes Peak Granite always exceed estimated withdrawals. The contents for base-flow reservoirs in the metamorphic and intrusive rocks, however, are frequently between 50 and 60 percent for metamorphic rocks and about 80 percent for granitic rocks (table 32), less than estimates for daily withdrawals. Although water associated with base flow appears to be adequate to maintain current estimated withdrawals in the Pikes Peak Granite and fault-zone areas, the simulated results indicate that this is not the case in the metamorphic and intrusive rock areas of the watershed.

**Table 32.** Summary statistics of daily values for water-balance terms from long-term simulations for (A) the entire Turkey Creek watershed and areas of (B) metamorphic, (C) intrusive, and (D) fault-zone rocks and (E) Pikes Peak Granite—Continued

[All univariate statistics and percentiles reported in inches; Precip, total precipitation; ET, total evapotranspiration; sm, contents of soil-zone reservoir at end of given period; bfi, total water added to base-flow reservoir; bfr, contents of base-flow reservoir at end of accounting period; bf, total base flow discharged to stream; gsnk, total water lost from base-flow reservoir that is not available to support local streamflow; ir, contents of interflow reservoir at end of the accounting period; if, total interflow; ovf, total overland flow; tf, total watershed flow; Min, minimum; Max, maximum, Stddev, standard deviation; N, number of observations; %, percentage]

E. Pikes Peak Granite

Univariate statistics

Variable	Mean	Median	Stddev	Min	Max	N
Precip	0.0469	0.0000	0.1461	0.0000	2.6500	18627
ET	0.0353	0.0202	0.0402	0.0000	0.2217	18627
sm	1.3478	1.3099	0.5676	0.1316	2.2431	18627
bfi	0.0088	0.0000	0.0328	0.0000	0.2587	18627
bfr	3.1366	3.0133	1.2973	0.6440	7.9146	18627
bf	0.0017	0.0017	0.0007	0.0004	0.0044	18627
gsnk	0.0069	0.0066	0.0029	0.0014	0.0174	18627
ir	0.0244	0.0000	0.0858	0.0000	1.2981	18627
if	0.0027	0.0000	0.0096	0.0000	0.1574	18627
ovf	0.0002	0.0000	0.0008	0.0000	0.0214	18627
tf	0.0046	0.0019	0.0099	0.0004	0.1598	18627

Percentiles

Variable	0.1%	1.0%	5.0%	10.0%	20.0%	30.0%	40.0%	50.0%	60.0%	70.0%	80.0%	90.0%
bfr	0.6562	0.7912	1.3022	1.5466	1.9813	2.3316	2.6641	3.0133	3.3711	3.7289	4.1855	4.8865
ir	0.0000	0.0000	0.0000	0.0000	0.0000	0.0000	0.0000	0.0000	0.0000	0.0004	0.0070	0.0585

Correlations

Variable	Precip	ET	sm	bfi	bfr	bf	gsnk	ir	if	ovf	tf
Precip	1.0000	0.0219	0.1290	0.3039	0.0292	0.0292	0.0292	0.2090	0.1331	0.7127	0.1853
ET	0.0219	1.0000	0.1807	0.2865	0.2435	0.2435	0.2435	0.3788	0.3811	0.1192	0.3937
sm	0.1290	0.1807	1.0000	0.3516	0.0843	0.0843	0.0843	0.3067	0.2964	0.1467	0.3028
bfi	0.3039	0.2865	0.3516	1.0000	0.1230	0.1230	0.1230	0.6313	0.5526	0.3956	0.5714
bfr	0.0292	0.2435	0.0843	0.1230	1.0000	1.0000	1.0000	0.2327	0.2373	0.0639	0.3054
bf	0.0292	0.2435	0.0843	0.1230	1.0000	1.0000	1.0000	0.2327	0.2373	0.0639	0.3054
gsnk	0.0292	0.2435	0.0843	0.1230	1.0000	1.0000	1.0000	0.2327	0.2373	0.0639	0.3054
ir	0.2090	0.3788	0.3067	0.6313	0.2327	0.2327	0.2327	1.0000	0.9801	0.2930	0.9830
if	0.1331	0.3811	0.2964	0.5526	0.2373	0.2373	0.2373	0.9801	1.0000	0.1904	0.9946
ovf	0.7127	0.1192	0.1467	0.3956	0.0639	0.0639	0.0639	0.2930	0.1904	1.0000	0.2652
tf	0.1853	0.3937	0.3028	0.5714	0.3054	0.3054	0.3054	0.9830	0.9946	0.2652	1.0000

**SUMMARY**

The Turkey Creek watershed has a drainage area of 47.2 square miles and lies southwest of Denver in the foothills of the Rocky Mountains at elevations between about 6,000 and 10,500 feet. The watershed has about 11,000 residents that occupy about 4,900 households—a density of about one household per 6 acres. Domestic water is derived from local ground water, and the majority of residents obtain water from household wells completed in fractured crystalline rock. Most withdrawn water is returned to the ground-water system through ISDS's.

Geology in the watershed consists of many types of Precambrian fractured metamorphic and intrusive crystalline rocks that have been deformed by folds and faults to produce many brittle features in the watershed; water contained in these rocks occurs dominantly in fractures. The many different types of rocks can be combined into three groups (metamorphic, intrusive, and their faulted equivalents) and a fourth subgroup (Pikes Peak Granite) that have unique fracture characteristics.

Direct measurements of evapotranspiration made at two sites in the watershed representing forest and meadow environments indicate that a large amount of

precipitation in the Turkey Creek watershed is returned to the atmosphere. At the forest site, where evapotranspiration was sometimes limited by water availability, the mean evapotranspiration for 3 calendar years of measurements beginning in 1999 was 82.9 percent of measured precipitation; during a relatively dry calendar year (2000) evapotranspiration was as much as 95.4 percent of measured precipitation. At the meadow site, where evapotranspiration was not often limited by water availability, calendar year 2001 evapotranspiration was about 1.2 times as much as at the forest site and, due to augmentation by shallow ground water, exceeded measured precipitation. The results of daily evaluations of evapotranspiration and related processes indicate that water can percolate to below the soil zone most effectively in the spring when evapotranspiration rates are low.

Surface-water records for Turkey Creek near the mouth of the canyon, through 2001, indicate that streamflow in the watershed is seasonal due to precipitation and snowmelt in spring. Although streamflow generally recedes to less than about 1 cubic foot per second later in the year, Turkey Creek is rarely dry. Short-term streamflow records collected at four subbasins that represent intrusive and fault-zone rocks and Pikes Peak Granite during the spring of 2001 indicate that (1) intrusive-rock areas of the watershed generally have poorly sustained streams that frequently go dry during rainless periods and (2) areas of Pikes Peak Granite and fault-zone rocks have well-sustained streamflow. Synoptic measurements of streamflow made at many sites in the watershed during the summer and fall 2001 corroborate these findings and are the basis for characterizing metamorphic areas as having poorly sustained streamflow.

Ground-water-level measurements collected historically (from about 1973 through 1983), monthly beginning in 1998, continuously beginning in May 2001, and synoptically in September 2001, indicate a ground-water system that responds directly to precipitation. Historical measurements in USGS monitoring wells indicate a seasonal pattern, similar to surface water, in which ground-water levels rise in the spring and then steadily recede to about consistent levels annually. Contemporary measurements from the same USGS monitoring wells do not indicate a long-term downward trend in water levels; rather, annual low water levels are determined by the length of rainless periods. Additional contemporary water-level measurements indicate that water levels in some wells can

fluctuate many tens of feet on an annual basis. Results from synoptic water-level measurements made in September 2001 indicate a water-table surface that is similar to the watershed topography. The synoptic data indicate a mean depth to water of about 105 feet; however, in the parts of the watershed where topographic relief is large, depths to water may exceed 300 ft.

Water quality was evaluated principally on the basis of samples from about 110 wells and 22 streams collected on a nearly quarterly basis during water year 1999; samples were analyzed for major ions, nutrients, and minor elements. These data indicate that ground water and surface water in the Turkey Creek watershed are calcium-bicarbonate to calcium-chloride types of water that rarely fail to meet applicable Federal or State recommended drinking-water standards. However, concentrations for some water-quality properties and constituents in ground water, such as specific conductance, calcium, magnesium, sodium, chloride, and nitrate plus nitrite, appear to have increased significantly since the last similar sampling effort of ground-water quality in the 1970's. In addition, concentrations for chloride in ground water and surface water, together with regional measurements of chloride in precipitation and a few samples that describe bromide concentrations in ground and surface water, indicate that water in the Turkey Creek watershed is being affected by residential development in the watershed. The likely source of these effects is from salt-containing traction materials used on roads, or effluent from ISDS's, or both.

Water-quality sampling and analyses conducted in an effort to determine the extent, if any, of ISDS influence on water quality did not produce definitive results. Correlations among potential ISDS-related water-quality properties and constituents such as specific conductance, chloride, nitrate plus nitrite, and boron are not consistently strong and do not identify a single, simple process involved in the genesis of Turkey Creek watershed water quality. Reconnaissance-level samples of ground and surface water in 2001 that were analyzed for wastewater compounds indicate that some wastewater compounds are present in ground and surface water, perhaps with a higher incidence in surface water. On the basis of this study, it is not possible to determine if ISDS effluent is, or is not, a strong contributor to either ground-water or surface-water quality. Additional questions regarding preferential flow paths for ISDS effluent remain unanswered.

An additional reconnaissance-level sampling effort, conducted by the Jefferson County Health Department, obtained analyses of tritium content from 24 ground-water samples. The results of these samples indicate that some ground water in the Turkey Creek watershed was recharged before the nuclear testing era of the 1950's and 1960's; however, most water appears to be of recent age.

Spatial distributions of water-quality properties and constituents such as specific conductance, chloride, nitrate plus nitrite and boron, have few definitive patterns. However, the southwestern part of the Turkey Creek watershed, which is topographically similar to other parts of the watershed, has the lowest concentrations of these water-quality properties and constituents. Supporting this finding are differences in medians at greater than 90-percent significance ( $p < 0.10$ ) between water-quality properties and constituents, including specific conductance, all major cations, chloride, sulfate, and nitrate plus nitrite, determined for water from the Pikes Peak Granite in the southwest part of the watershed compared to the rest of the watershed. The relatively low concentrations in the Pikes Peak Granite are most likely a function of dilution, related to the relatively large amounts of ground water estimated to be present in the southwestern part of the watershed.

A methodology involving fracture-network analysis, watershed runoff modeling, and knowledge of hydrologic conditions was undertaken to assess the quantity of ground water in the watershed. Estimates of potential porosity were made for the four rock groups defined on the basis of geologic mapping and detailed analysis of outcrop-scale measurements of fracture characteristics. The estimates of potential porosity are very small, indicating that the fractured bedrock aquifer has a small amount of space in which water can exist. The magnitude of the porosity estimates is in the hundredths to tenths of a percent range for metamorphic and intrusive rocks and in range of 1 to 9 percent for the fault-zone rocks.

Knowledge of hydrologic conditions in the watershed was used with additional intrawatershed measurements of precipitation and temperature to calibrate a physically based, distributed-parameter runoff model (PRMS). The runoff model characterization of the rock groups as interflow and base-flow reservoirs facilitates watershed and intrawatershed estimates of ground water associated with streamflow. The runoff model characterization also uses a term (GSNK) to track losses from base-flow reservoirs—water that is lost from the base-flow reservoirs is ground water that is not associated

with local streamflow. The initial runoff model calibration was adjusted on the basis of detailed evapotranspiration measurements available from two sites within the watershed, and the final calibration produces a good match between simulated and measured streamflow and a close match between simulated and measured runoff and evapotranspiration.

Contemporary watershed model simulations for the period January 1, 1999, through September 30, 2001, indicate that, on the entire watershed scale, there is typically more than enough ground water in base-flow reservoirs to meet estimates of daily ground-water withdrawals made for domestic supply. Intrawatershed conditions, however, vary. Watershed model estimates indicate that the Pikes Peak Granite and fault-zone areas receive recharge and transmit it to streamflow in a relatively consistent fashion; as a result, there is nearly always (greater than 99.9 percent of time, table 29) enough recoverable ground water in base-flow reservoirs to support estimates of daily ground-water withdrawals made for domestic supply. This is not the case, however, in the metamorphic and intrusive rock areas where field measurements indicate streams are poorly sustained and simulated results from the watershed model indicate that there is frequently (between 60 and 70 percent of the time for metamorphic and between 80 and 90 percent of the time for intrusive) not enough water in base-flow reservoirs to support estimates of daily ground-water withdrawals made for domestic supply. In these poorly sustained areas most recharge to the ground-water system is transmitted to streams quickly as base flow. When a base-flow reservoir becomes depleted there will be no base flow in the associated area, and ground water that is not associated with local streamflow becomes the only source of water available to wells. Once withdrawals from this source are replaced, or recharged, base flow in the watershed can resume.

Long-term simulations from October 1, 1948, through September 30, 1999, were made using precipitation and temperature data from a climatologic station at Cheesman Reservoir in the vicinity of the Turkey Creek watershed. Long-term simulations were done to evaluate watershed conditions over a period of several decades by using climatic conditions that are similar to those in the Turkey Creek watershed. The results of the long-term simulations confirm that, on a watershed scale, the contents of base-flow reservoirs are consistently capable of meeting contemporary (2001) estimates of ground-water withdrawals made

for domestic supply in the Turkey Creek watershed. The long-term results also indicate that the end-of-the-water-year contents of watershed base-flow reservoirs may be less than one-tenth of an inch under conditions of low annual precipitation (10 to 14 inches per year). In addition, the long-term simulations indicate that the watershed-scale recession for the watershed contents of the base-flow reservoirs can be as much as about 0.06 inch per year during years with low precipitation. Together, these simulated results indicate that multiple years of low precipitation combined with relatively small amounts of water in base-flow reservoirs, a condition that is not present in the 51-year record of precipitation used for the long-term simulations, could deplete base-flow resources that support streamflow, at a watershed scale, in the Turkey Creek watershed. In this case the only source for domestic ground water in the watershed would be ground water that is not associated with local streamflow. The long-term simulations underpin the findings of the contemporary simulations that indicate ground water that supports base flow in the metamorphic and intrusive rock areas of the watershed is frequently depleted: between 50 and 60 percent for metamorphic rocks and about 80 percent for intrusive rocks. Although the long-term simulations indicate slightly higher estimates of annual accretions to ground-water storage not associated with streamflow, the magnitude of the long-term estimates are on the order of tenths of an inch. These observations reiterate the importance of ground water that is not associated with local streamflow to domestic water supply in the Turkey Creek watershed.

## SELECTED REFERENCES

- Allmendinger, R.W., 1995, Stereonet—Orientation data analysis computer code: Absoft Corporation.
- American Society for Testing Materials, 1999, Standard specification for reagent water, D 1193–99: West Conshohocken, Pa., American Society for Testing Materials Subcommittee D19.02, 2 p.
- Anderson, D.E., Verma, S.B., and Rosenberg, N.J., 1984, Eddy correlation measurements of CO<sub>2</sub>, latent heat, and sensible heat fluxes over a crop surface: *Boundary Layer Meteorol.*, v. 29, p. 263–272.
- Baldocchi, D.D., 1994, A comparative study of mass and energy exchange over a closed C3 (wheat) and an open C4 (corn) canopy—I. The partitioning of available energy into latent and sensible heat exchange: *Agricultural and Forest Meteorology*, v. 67, p. 191–220.
- Bartholoma, S.D., 1997, comp., User's manual for National Water Information System of the U.S. Geological Survey, Chapter 3, Automated Data Processing System: U.S. Geological Survey Open-File Report 97–635, 219 p.
- Berndt, H.W., 1960, Precipitation and streamflow of a Colorado front range watershed: Station Paper no. 47: Rocky Mountain Forest and Range Experiment Station, U.S. Forest Service.
- Bevan, Keith, 1997, *Topmodel—A critique: Hydrological Process*, v. 11, John Wiley and Sons, p 1069–1085.
- Bidlake, W.R., Woodham, W.M., and Lopez, M.A., 1993, Evapotranspiration from areas of native vegetation in west-central Florida: U.S. Geological Survey Open-File Report 93–415, 35 p.
- Black, T.A., 1979, Evapotranspiration from Douglas fir stands exposed to soil water deficits: *Water Resources Research*, v. 15, no. 1, p. 164–170.
- Bowen, I.S., 1926, The ratio of heat losses by conduction and by evaporation from any water surface: *Physics Review*, v. 27, p. 779–787.
- Bruce, B.W., and McMahon, P.B., 1997, Shallow ground-water quality of selected land-use/aquifer settings in the South Platte River Basin, Colorado and Nebraska, 1993–95: U.S. Geological Survey Water-Resources Investigations Report 97–4229, 48 p.
- 1998, Shallow ground-water quality of selected land-use/aquifer settings in the South Platte River Basin, Colorado and Nebraska, 1993–95: U.S. Geological Survey Water-Resources Investigations Report 97–4229, 48 p.
- Brutsaert, Wilfried, 1982, *Evaporation into the atmosphere*: Boston, D. Reidel Publishing Co., 299 p.
- Bryant, Bruce, 1974, Reconnaissance geologic map of the Conifer quadrangle, Jefferson County, Colorado: U.S. Geological Survey Geologic Quadrangle Maps of the United States, Map MF–597, scale 1:24,000.
- Bryant, Bruce, Miller, R.D., and Scott, G.R., 1973, Geologic map of the Indian Hills quadrangle, Jefferson County, Colorado: U.S. Geological Survey Geologic Quadrangle Maps of the United States, Map GQ–1073, scale 1:24,000.
- Bryant, Bruce, Offield, T.W., and Schmidt, W., 1975, Relations between thermal, photographic, and topographic linears and mapped and measured structures in a Precambrian terrain in Colorado: U.S. Geological Survey, *Journal of Research*, v. 3, no. 3, p. 295–303.
- Caine, J.S., 2001, Fracture network, fault zone, and geologic data collected from the Turkey Creek watershed, Colorado Rocky Mountain Front Range: U.S. Geological Survey Open-File Report 01–416, 46 p.
- Caine, J.S., Evans, J.P., and Forster, C.B., 1996, Fault zone architecture and permeability structure: *Geology*, v. 24, p. 1025–1028.



- Caine, J.S., and Forster, C.B., 1999, Fault zone architecture and fluid flow—Insights from field data and numerical modeling, *in* Haneberg, W.C., Mozley, P.S., Moore, J.C., and Goodwin, L.B., eds., *Faults and subsurface fluid flow in the shallow crust: American Geophysical Union Geophysical Monograph 113*, p. 101–127.
- Calder, I.R., 1977, A model of transpiration and interception loss from a spruce forest in Plynlimon, central Wales: *Journal of Hydrology*, v. 33, p. 247–265.
- Campbell, G.S., Mugaas, J.N., and King, J.R., 1978, Measurement of long-wave radiant flux in organismal energy budgets—A comparison of three methods: *Ecology*, v. 59, no. 6, p. 1277–1281.
- Char, S.J., 2000, Bedrock geology of the Turkey Creek drainage basin, Jefferson County, Colorado: U.S. Geological Survey Open-File Report 00–265.
- Chow, Ven Te, ed., 1964, *Handbook of applied hydrology*: New York, McGraw-Hill.
- Claassen, H.C., and Halm, D.R., 1996, Estimates of evapotranspiration or effective moisture in Rocky Mountain watersheds from chloride ion concentrations in stream baseflow: *Water Resources Research*, v. 32, no. 2, p. 363–372.
- Colorado Climate Center, 1984, Analysis of Colorado average annual precipitation for the 1951–1980 period: Fort Collins, Colorado State University, Climatology Report 84–4.
- 2002, Colorado Climate Center, Data access, daily data: accessed October 1, 2002, at URL <http://climate.atmos.colostate.edu/>
- Colorado Department of Public Health and Environment, 1998, Regulation no. 32, Classification and numeric standards for Arkansas River basin: Colorado Department of Public Health and Environment, Water Quality Control Commission, variously paginated.
- 2000, Regulation no. 31, The basic standards and methodologies for surface water (5 CCR 1002–31): Colorado Department of Public Health and Environment, Water Quality Control Commission, variously paginated.
- Cressie, Noel, 1991, *Statistics for spatial data*: New York, Wiley, 900 p.
- Croft, A.R., and Monninger, L.V., 1953, Evapotranspiration and other water losses on some aspen forest types in relation to water available for stream flow: *Transactions, American Geophysical Union*, v. 34, no. 4, p. 563–574.
- Davis, S.N., Cecil, L.D., Zreda, Mark, and Moysey, Stephen, 2001, Chlorine-36, bromide, and the origin of spring water: *Chemical Geology*, v. 179, p. 3–16.
- Davis, S.N., Whittemore, D.O., and Fabryka-Martin, J., 1998, Uses of Cl<sup>-</sup>/bromide ratios in studies of potable water: *Ground Water*, v. 36, p. 338–350.
- Dershowitz, William, Lee, G., Geier, J., Foxford, T., LaPointe, P., and Thomas, A., 1996, *FractMan™—Interactive discrete feature data analysis, geometric modeling, and exploration simulation—User documentation, version 2.5*: Redman Wash., Golder Associates, Inc.
- Drever, J.I., 1988, *The geochemistry of natural waters* (2d ed.): Englewood Cliffs, N.J., Prentice-Hall, 437 p.
- Drew, L.J., Karlinger, M.R., Armstrong, T.R., and Moore, R.B., 1999, Relations between igneous and metamorphic rock fracture patterns and groundwater yield from the variography of water-well yields—Pinardville quadrangle, New Hampshire: *Natural Resources Research*, v. 8, no. 2, p. 137–152.
- Fenneman, N.M., 1931, *Physiography of the western United States*: New York, McGraw-Hill, 531 p.
- Fetter, C.W., Jr., 1980, *Applied hydrogeology*: Columbus Ohio, Charles E. Merrill Publishing Company, 488 p.
- Fitzjarrald, D.R., Stormwind, B.L., Fisch, G., and Cabral, O.M.R., 1988, Turbulent transport observed just above the Amazon forest: *Journal of Geophysical Research*, v. 93, p. 1551–1563.
- Flynn, J.L., and Barber, L.B., 2000, Quality of ground water and surface water in an area of individual sewage disposal system use near Barker Reservoir, Nederland, Colorado, August–September 1998: U.S. Geological Survey Open-File Report 00–214, 8 p.
- Folger, P.F., 1995, A multidisciplinary study of the variability of dissolved 222Rn in ground water in a fractured crystalline rock aquifer and its impact on indoor air: Golden, Colorado School of Mines, Ph.D. dissertation, 181 p.
- Freeze, R.A., and Cherry, J.A., 1979, *Groundwater*: New York, Prentice-Hall Inc., 604 p.
- Fuchs, Marcel, and Tanner, C.B., 1968, Calibration and field test of soil heat flux plates: *Soil Science Society of America Proceedings*, v. 32, p. 326–328.
- Garcia, K.T., Maddy, D.W., Lopp, L.E., Jackson, D.L., Coupe, R.H., and Schertz, T.L., 1997, User's manual for the National Water Information System of the U.S. Geological Survey, Chapter 2, Water-Quality System: U.S. Geological Survey Open-File Report 97–634, 253 p.
- German, E.R., 2000, Regional evaluation of evapotranspiration in the Everglades: U.S. Geological Survey Water-Resources Investigations Report 00–4217, 48 p.
- Goulden, M.L., Munger, J.W., Fan, S.M., Daube, B.C., and Wofsy, S.C., 1996, Measurements of carbon sequestration by long-term eddy covariance—Methods and a critical evaluation of accuracy: *Global Change Biology*, v. 2, p. 169–182.
- Granato, G.E., and Smith, K.P., 2000, Automated ground water monitoring system and method: U.S. Patent Document 6,021,664, date February 8, 2000, 20 p.

- Granier, Andre, 1985, Une nouvelle methode pour la mesure du flux de seve brute dans le tronc des arbres: *Annales des Sciences Forestieres*, v. 42, p. 193–200.
- Gray, D.M., and Male, D.H., eds., 1981, *Handbook of snow*: Toronto, Pergamon Press, 776 p.
- Hall, D.C., Hillier, D.E., Nickum, E., and Dorrance, W.G., 1981, Effects of residential wastewater-treatment systems on ground-water quality in west-central Jefferson County, Colorado: U.S. Geological Survey Water-Resources Investigations Open-File Report 81–73, 65 p.
- Hall, D.C., and Johnson, C.J., 1979, Drinking-water quality and variations in water levels in the fractured crystalline-rock aquifer, west-central Jefferson County, Colorado: U.S. Geological Survey Water-Resources Investigations Report 79–94, 89 p.
- Harrison, J.E., and Moench, R.H., 1961, Joints in Precambrian rocks, Central City-Idaho Springs area, Colorado: U.S. Geological Survey Professional Paper 374–B, 14 p.
- Hay, L.E., Wilby, R.L., and Leavesley, G.H., 2000, A comparison of delta change and downscaled GCM scenarios for three mountainous basins in the United States: *Journal of American Water Resources Association*, v. 36, no. 2, p. 387–397.
- Helsel, D.R., and Hirsch, R.M., 1992, *Statistical methods in water resources—Studies in environmental science 49*: New York, Elsevier, 529 p.
- Hem, J.D., 1985, *Study and interpretation of the chemical characteristics of natural water (3d ed.)*: U.S. Geological Survey Water-Supply Paper 2254, 263 p.
- Hewlett, J.D., 1961, Soil moisture as a source of baseflow from a steep mountain watershed: U.S. Forest Service, Southeast Forest Experimental Station 132, 11 p.
- Hofstra, W.E., and Hall, D.E., 1975a, Geologic control of supply and quality of water in the mountainous part of Jefferson County, Colorado: *Colorado Geological Survey Bulletin* 36, 51 p.
- 1975b, Hydrologic and water-quality data in western Jefferson County, Colorado: Colorado Department of Natural Resources, Colorado Water Resources Basic Data Release 36, 51 p.
- Horowitz, A.J., Demas, C.R., and Fitzgerald, K.K., 1994, U.S. Geological Survey protocol for the collection and processing of surface-water samples for the subsequent determination of inorganic constituents in filtered water: U.S. Geological Survey Open-File Report 94–539, 57 p.
- Isaaks, E.H., and Srivastava, R.M., 1989, *An introduction to applied geostatistics*: New York, Oxford University Press, 561 p.
- Jensen, S.K., and Domingue, J.O., 1988, Extracting topographic structure from digital elevation data for geographic system analysis: *Photogrammetric Engineering and Remote Sensing*, v. 54, p. 1593.
- Kaimal, J.C., and Finnigan, J.J., 1994, *Atmospheric boundary layer flows, their structure and measurement*: New York, Oxford University Press, 289 p.
- Kamb, W.B., 1959, Petrofabric observations from Blue Glacier, Washington, in relation to theory and experiment: *Journal of Geophysical Research*, v. 64, no. 11, p. 1891–1909.
- Kaufmann, M.R., 1984, A canopy model (RM-CWU) for determining transpiration of subalpine forests—II. Consumptive water use in two watersheds: *Canadian Journal of Forest Research*, v. 14, p. 227–232.
- Kaufmann, M.R., 1985, Species differences in stomatal behavior, transpiration, and water use efficiency in subalpine forests, in Tigerstedt, P.M.A., Puttonen, P., and Koski, V., eds., *Crop physiology of forest trees*: Helsinki, Finland, University of Helsinki, 350 p.
- Knuth, Martin, Jackson, J.L., and Whittemore, D.O., 1990, An integrated approach to identifying the salinity source contaminating a ground-water supply: *Ground Water*, v. 28, no. 2, p. 207–214.
- Leavesley, G.H., Lichty, R.W., Troutman, B.M., and Saindon, L.G., 1983, *Precipitation runoff modeling system—User’s manual*: U.S. Geological Survey Water-Resources Investigations Report 83–4238, 207 p.
- Leavesley, G.H., Restrepo, P.J., Markstrom, S.L., Dixon, M., and Stannard, L.G., 1996, *The modular modeling system (MMS)—User’s manual*: U.S. Geological Survey Open-File Report 96–151, 175 p.
- Lickus, R.J., and LeRoy, L.W., 1968, Precambrian structure and stratigraphy along the mountain front west of Golden, Jefferson County, Colorado—A reconnaissance study, in Hollister, J.C., and Weimer, R.J., eds., *Geophysical and geological studies of the relationships between the Denver earthquakes and the Rocky Mountain Arsenal well—Part A: Golden, Colo., Quarterly of the Colorado School of Mines*, v. 63, no. 1, p. 129–165.
- Lundberg, Angela, 1993, Evaporation of intercepted snow—Review of existing and new measurement methods: *Journal of Hydrology*, v. 151, p. 267–290.
- Mays, L.W., 1996, ed., *Water resources handbook*: New York, McGraw-Hill, variously paginated.
- Michel, R.L., 1989, Tritium deposition in the continental United States, 1953–83: U.S. Geological Survey Water-Resources Investigations Report 89–4072, 46 p.
- Moore, C.J., 1976, Eddy flux measurements above a pine forest: *Quarterly Journal Royal Meteorological Society*, v. 102, p. 913–918.

- Morgan, Karen, 2000, Spatial analysis and modeling of geochemical distribution to assess fracture flow in Turkey Creek Basin, Jefferson County, Colorado: Golden, Colorado School of Mines, unpublished Master's thesis, 194 p.
- Nie, Dalin, and Kanemasu, E.T., 1989, A comparison of net radiation on slopes: Proceedings, 19th Conference on Agricultural and Forest Meteorology, March 7–10, Charleston, S.C., American Meteorology Society, p. 142–143.
- Nnyamah, J.U., and Black, T.A., 1977, Rates and patterns of water uptake in a Douglas-fir stand: *Soil Science Society of America Journal*, v. 41, p. 972–979.
- Ohmura, Atsumu, 1982, Objective criteria for rejecting data for Bowen ratio flux calculations: *Journal of Applied Meteorology*, v. 21, p. 595–598.
- Priestley, C.H.B., and Taylor, R.J., 1972, On the assessment of surface heat flux and evaporation using large-scale parameters: *Monthly Weather Review*, v. 100, p. 81–92.
- REBS, Inc., 1995. REBS Q\*7.1 Net Radiometer Manual, Rev. 3: Radiation and Energy Balance Systems, Inc., Seattle, Wash.
- Rantz, S.E., 1978, Measurement and computation of streamflow—v. 1, Measurement of stage and discharge, and v. 2, Computation of discharge: U.S. Geological Survey Water-Supply Paper 2175, 630 p.
- Risch, M.R., and Robinson, B.A., 2000, Use of borehole and surface geophysics to investigate ground-water quality near a road-deicing salt-storage facility, Valparaiso, Indiana: U.S. Geological Survey Water-Resources Investigations Report 00–4070, 47 p.
- Rutter, A.J., Morton, A.J., and Robins, P.C., 1975, A predictive model of rainfall interception in forests—II. Generalization of the model and comparison with observations in some coniferous and hardwood stands: *Journal of Applied Ecology*, v. 12, p. 367–380.
- Scott, G.R., 1972, Geologic map of the Morrison quadrangle, Jefferson County, Colorado: U.S. Geological Survey Geologic Quadrangle Map I–790–A, scale 1:24,000.
- Sheridan, D.M., Reed, J.C., Jr., and Bryant, Bruce, 1972, Geologic map of the Evergreen quadrangle, Jefferson County, Colorado: U.S. Geological Survey Geologic Quadrangle Map I–786–A, scale 1:24,000.
- Shuttleworth, W.J., Gash, J.H.C., Lloyd, C.R., McNeil, D.D., Moore, C.J., and Wallace, J.S., 1988, An integrated micrometeorological system for evaporation measurement: *Agriculture and Forest Meteorology*, v. 43, p. 295–317.
- Snow, D.T., 1968, Hydraulic characteristics of fractured metamorphic rocks of the Front Range and implications to the Rocky Mountain Arsenal well: *Golden, Colorado School of Mines Quarterly*, v. 63, no. 1, 32 p.
- 1972, Mountain ground water supplies: *The Mountain Geologist*, v. 10, no. 1, p. 19–24.
- Sonnenberg, S.A., and Bolyard, D.W., 1997, Tectonic history of the Front Range in Colorado, *in* Bolyard, D.W., and Sonnenberg, S.A., eds., *Geologic history of the Colorado Front Range: Rocky Mountain Association of Geologists, 1997 RMS–AAPG Field Trip Number 7 Guide*, p. 1–7.
- Spittlehouse, D.L., and Black, T.A., 1979, Determination of forest evapotranspiration using Bowen ratio and eddy correlation measurements: *Journal of Applied Meteorology*, v. 18, p. 647–653.
- Stannard, D.I., 1993, Comparison of Penman-Monteith, Shuttleworth-Wallace, and modified Priestley-Taylor evapotranspiration models for wildland vegetation in semiarid rangeland: *Water Resources Research*, v. 29, no. 5, p. 1379–1392.
- Stannard, D.I., Blanford, J.H., Kustas, W.P., Nichols, W.D., Amer, S.A., Schmugge, T.J., and Weltz, M.A., 1994, Interpretation of surface flux measurements in heterogeneous terrain during the Monsoon '90 experiment: *Water Resources Research*, v. 30, no. 5, p. 1227–1239.
- Stevens, M.R., Johncox, D.A., and Cox, J.R., 1997, Hydrologic and water quality data, Guanella Pass area, Colorado, water year 1995: U.S. Geological Survey Open-File Report 97–2004, 87 p.
- Sumner, D.M., 1996, Evapotranspiration from successional vegetation in a deforested area of the Lake Wales Ridge, Florida: U.S. Geological Survey Water-Resources Investigations Report 96–4244, 38 p.
- Sutphin, D.M., Drew, L.J., Schenemeyer, J.H., and Burton, W.C., 2000, Characteristics of water-well yields in part of the Blue Ridge geologic province in Loudoun County, Virginia: *Natural Resources Research*, v. 10, no. 1, p. 19.
- Swinbank, W.C., 1951, The measurement of vertical transfer of heat and water vapor by eddies in the lower atmosphere: *Journal of Meteorology*, v. 8, no. 3, p. 135–145.
- Tanner, C.B., 1960, Energy-balance approach to evapotranspiration from crops: *Soil Science Society of America Proceedings*, v. 24, p. 1–9.
- Tanner, B.D., and Greene, J.P., 1989, Measurement of sensible heat and water-vapor fluxes using eddy-correlation methods: Final report prepared for U.S. Army Dugway Proving Grounds, U.S. Army, Dugway, Utah, 17 p.
- Thompson, J.R., 1974, Energy budget measurements over three cover types in eastern Arizona: *Water Resources Research*, v. 10, no. 5, p. 1045–1048.
- Tomusiak, S.R.A., Caine, J.S., and Ge, S., 2000, Linking field-based discrete fracture models to hydrogeology—Characterization of the fractured crystalline aquifer, Turkey Creek watershed, near Denver, Colorado: Geological Society of America, 2000 Annual Meeting, Reno, Nev., Abstracts with Programs, v. 37, p. A63.

- Troutman, B.M., 1985, Errors and parameter estimation in precipitation-runoff modeling, parts 1 and 2: *Water Resources Research*, v. 21, no. 8, p. 1195–1222.
- Tweto, Ogden, and Sims, P.K., 1963, Precambrian ancestry of the Colorado Mineral Belt: *Geological Society of America Bulletin*, v. 74, p. 991–1014.
- U.S. Army Corps of Engineers, 1956, Summary report of the snow investigations—Snow hydrology: Portland, Oreg., U.S. Army Corps of Engineers, North Pacific Division, 437 p.
- U.S. Department of Agriculture, 1980, Soil survey of the Golden area, Colorado: U.S. Department of Agriculture, 405 p.
- 1995, Soil survey geographic (SSURGO) database—Data use information: Miscellaneous publication number 1527, variously paginated.
- 1999, Soil Survey geographic database for Golden area, Colorado, parts of Denver, Douglas, Jefferson, and Park Counties: Ft. Worth, Texas, U.S. Department of Agriculture-Natural Resources Conservation Service, Soil Survey Division, National SSURGO Data base, Ref. No. CO641.
- U.S. Environmental Protection Agency, 1991, National Secondary Drinking Water Standards: U.S. Environmental Protection Agency Publication #570/9-91-019 FS, Office of Water.
- 1996, Drinking-water regulations and health advisories: Washington D.C., Office of Water, Report EPA 822-R-96-001 [unpaginated].
- 1999, National Primary Drinking Water Standards: U.S. Environmental Protection Agency Pub. #816/F-99-018, Office of Water.
- U.S. Geological Survey, 1942–1953, Surface-water supply of the Missouri River basin. Annual Reports as follows: 1942, Water-Supply Paper 956; 1943, Water-Supply Paper 976; 1944, Water-Supply Paper 1006; 1945, Water-Supply Paper 36; 1946, Water-Supply Paper 1056; 1947, Water-Supply Paper 1086; 1948, Water-Supply Paper 1116; 1949, Water-Supply Paper 1146; 1950, Water-Supply Paper 1176; 1951, Water-Supply Paper 1210; 1952, Water-Supply Paper 1240; 1953, Water-Supply Paper 1280.
- 1997 to present, National field manual for the collection of water-quality data: U.S. Geological Survey Techniques of Water-Resources Investigations, book 9, chaps. A1–A9, 2 v., variously paginated.
- 2001, National Atmospheric Deposition Program, accessed November 21, 2001, at URL <http://nadp.sws.uiuc.edu>
- Vengosh, Avner, and Pankratov, Irena, 1998, Chloride/bromide and chloride/fluoride ratios of domestic sewage effluents and associated contaminated ground water: *Ground Water*, v. 36, no. 5, p. 815–824.
- Verma, S.B., Baldocchi, D.D., Anderson, D.E., Matt, D.R., and Clement, R.J., 1986, Eddy fluxes of CO<sub>2</sub>, water vapor, and sensible heat over a deciduous forest: *Boundary-Layer Meteorology*, v. 36, p. 71–91.
- Viger, 1998, An interface for the treatment of spatial information in modeling: accessed November 11, 2000, at URL [http://wwwbr.cr.usgs.gov/projects/SW\\_precip\\_runoff/weasel/index.html](http://wwwbr.cr.usgs.gov/projects/SW_precip_runoff/weasel/index.html)
- Viger, R.L., Markstrom, S.L., and Leavesley, G.H., 1998, An interface for the treatment of spatial information used in watershed modeling and water resource management: Proceedings of the First Federal Interagency Hydrologic Modeling Conference, April 19–23, 1998, Las Vegas, Nevada, v. 2, p. 73–80.
- Voss, C.I., 2000, Is simple analysis the best for complex environments?—Subsurface waste isolation in crystalline rock: 2000 Annual Meeting, Reno, Nevada, Geological Society of America Abstracts with Programs, v. 32, p. A–63.
- Waltz, J.P., 1972, Methods of geologic evaluation of pollution potential at mountain homesites: *Ground Water*, v. 10, no. 1, p. 42–49.
- Webb, E.K., Pearman, G.I., and Leuning, R., 1980, Correction of flux measurements for density effects due to heat and water vapour transfer: *Quarterly Journal of Royal Meteorology Society*, v. 106, p. 85–100.
- Weeks, E.P., Weaver, H.L., Campbell, G.S., and Tanner, B.D., 1987, Water use by saltcedar and by replacement vegetation in the Pecos River flood plain between Acme and Artesia, New Mexico: U.S. Geological Survey Professional Paper 491–G, 33 p.
- Wolock, D.M., 1997, STATSGO soil characteristics for the conterminous United States: accessed November 11, 2000, at URL <http://water.usgs.gov/GIS/metadata/usgswrd/muid.html>

---

---

# APPENDIX

---

---



## Brittle Structures of the Turkey Creek Watershed

Figure 3 shows fracture network orientation data from nine localities collected along natural outcrops in the Turkey Creek watershed. The figure includes equal-area plots to indicate the strike, dip, and number of fractures mapped in a particular area. In the equal-area plots, orientation, or strike and dip, of a fracture is represented by a point; in figure 3 the points on the diagram have been contoured so that the darker the area the more points are represented. Points located near the edge of the diagram represent vertical-dipping fractures and points near the center represent horizontal-dipping fractures. To determine the strike, or azimuth direction of a fracture, locate a point or center of a closed contour, locate a position 90 degrees clockwise, then go straight to the edge of the diagram and that azimuth positions the strike of the fracture; for reference, north is at the top of the diagram and east is at 90 degrees clockwise. Points or areas plotted between the outside and center of the diagram represent dip angles between 0 degrees, or horizontal (center), and 90 degrees, or vertical (edge).

Over 1,300 measurements of individual fractures were recorded, 1,066 were used in the fracture analysis (Caine, 2001). Of the measurements used, approximately 99 percent are joints, as indicated by the lack of striations, mullions, displaced compositional layers, and so forth. Most of the observed fractures are planar to slightly curvilinear in the intrusive rocks and slightly curvilinear to curvilinear in the metamorphic rocks. Many fractures, particularly in the intrusive rocks, have curving tips. The curvature may be critical in hydraulically linking otherwise planar and parallel fractures. In general, most fractures are short, a few meters in trace length. Aperture, the distance between the walls of a crack measured perpendicular to the walls, generally ranges from indistinguishable to several millimeters wide. There are rare apertures that are easily visible, weathered cracks, several centimeters wide. In general, most apertures were less than 1 millimeter wide. Most fractures in the intrusive rocks, and in many metamorphic rocks, are stained by iron oxides (field identified as hematite) that become diffuse a few millimeters to a few centimeters into the rock. Other mineral fillings are rare, so most of the observed joints are open fractures. Fracture intensities are on the order of 10 fractures per meter in the fault zones and pegmatite dikes to more typical values of 3 to 4 fractures per meter in

the other rock groups. The term fracture intensity is used here as an indicator of how many fractures were observed in any given outcrop. Fracture spacing is relatively uniform in the intrusive rocks and pegmatites. In the metamorphic rocks and fault zones, local heterogeneities in composition, layer thickness, and proximity to preexisting structures have a large influence on fracture spacing, intensity, and orientation.

Fracture-set mean orientations and dispersions in the intrusive rocks are generally strongly clustered and thus have low dispersions (fig. 3). At two sites in the large central pluton in the watershed, Nobel and Harrington, generally similar fracture-set mean orientations are shown (fig. 3). In each case there is a subordinate fracture set steeply dipping northeast-southwest, and a dominant northwest-southeast steeply dipping set (fig. 3). The Nobel site also has a northwest-southeast steeply dipping set of fractures. This site is very close to the pluton margin where the north-south set is roughly parallel to the contact with the metamorphic rocks (fig. 3). Other than the north-south set, the similarity in mean orientation and dispersion, as well as other field indicators such as morphology, indicate that within individual plutons brittle fracturing of the intrusive rocks occurred rather uniformly. Computed fracture intensities in the intrusive rocks are quite uniform and range from 2.0 to 2.5  $m^2/m^3$  (see "Fracture Intensity and Calibration of Fracture Network Models to Field Data" section for discussion of how fracture intensity was derived).

Additional features observed in the intrusive rocks were small-scale (less than 1 m wide) fracture zones. These structures form localized and bounded zones of high-intensity fracturing relative to the surrounding rock. Fracture intensity in these zones is on the order of tens of fractures per meter in contrast to three to four fractures per meter in the surrounding rocks. The occurrence of fracture zones is on the order of one zone per approximately 7 to 12 meters. Because of the high fracture intensity of these zones relative to the surrounding rock, the zones may act as important localized areas of infiltration and aquifer recharge. In contrast, infiltration in the surrounding rock through very small-aperture, low-intensity fractures may be low. An additional heterogeneity found in the intrusive rocks is a myriad of dikes, wall and roof pendants, and other assorted apophyses that appear to vary randomly in scale and morphology. These features represent local (a few meters to hundreds of meters long) heterogeneities that have variably responded to

brittle deformation due to emplacement-related juxtaposition of metamorphic and intrusive rocks with a variety of rheological properties.

In contrast to the intrusive rocks, fracture sets in the metamorphic rocks exhibit a heterogeneity in orientation from one location to another (fig. 3). The fracture sets have moderate dispersion, and preexisting fabrics clearly have a large influence on orientation, intensity, and morphology. Computed fracture intensities also are heterogeneous and range from  $1.6 \text{ m}^2/\text{m}^3$  to  $5.0 \text{ m}^2/\text{m}^3$  for the four localities studied. The metamorphic rocks exhibit a qualitative structural hierarchy of brittle fracturing that probably is controlled by primary and secondary features. Compositional layering and foliation also may influence fracture intensity and morphology. Variations in fracture intensity and morphology are highly scale-dependent. Picking a representative block of fractured rock of a particular type at a particular scale is difficult for this rock group.

Finally, there are many distinct styles of fault zones within the Turkey Creek watershed. Localized deformation zones composed of brecciated and mineralized host rock occur in one-kilometer-long, relatively narrow, curvilinear fault zones (fig. 3) where displacement of lithologic units can be documented. Although some of these features show very low intensities of fault-related subsidiary fracturing, most likely the initial brittle fractures were mineral filled in the early stages of faulting and subsequently assimilated into the fault zone, and they are locally jointed due to postfaulting deformation and (or) exhumation. These features likely act as partial localized barriers to ground-water flow in some subsurface locations but may also be short-circuited by discrete jointing (Caine and Forster, 1999).

In contrast to the localized deformation zones are the unusually wide zones (tens of meters to more than several kilometers wide) of intense brittle fracturing and associated alteration (figs. 2 and 3). Fracture-network data were collected from two such fault zones where there was sufficient exposure along road cuts—the only data-collection localities that were not natural outcrops. The US40 fault-zone locality is outside of the watershed but is representative of wide fault zones within the watershed, such as the C73 locality. The US40 locality is found in the Junction Ranch-Paradise Hills fault zone, and the C73 locality is found in the Conifer-Aspen Park fault zone (fig. 3). General observations also were made along several other road cuts in the watershed. Figure 3 shows that

fracture orientations are diffuse and heterogeneous between the fault zones studied. Although there is fracture-network orientation heterogeneity within each fault zone, the overall style of fault-related fracturing is consistent within each of these fault zones. There are typically several sets of steeply dipping fractures and highly diffuse sets of subhorizontal fractures (fig. 3). Fracture trace lengths are generally short with mean values just over 0.5 m, and individual fractures most commonly truncate against other fractures to form a highly interconnected network. The fractures are commonly slightly curvilinear and have apertures typically less than 1 mm wide. Most of the fractures in the fault zones are stained by iron oxides (field identification indicates limonite) that have extensively migrated into the interfracture rock mass as either Liesegang bands (nested and fracture-symmetric bands or rings of higher and lower iron indicative of diffusion processes) or more massively diffused oxide staining. Computed fracture intensities also are consistent at the two fault zones studied and are on the order of  $27 \text{ m}^2/\text{m}^3$ . These intensities are very high relative to other brittle structures.

Although no fracture-network data were collected in the pegmatite dikes, these features, which are meters up to about a kilometer long, are yet another heterogeneity that is superimposed on both the intrusive and metamorphic rocks in the watershed. One important and possibly significant observation is that the fracture intensity of these morphologically irregular features is about 10 times higher than the host rock into which they intrude, regardless of host rock type. It is not clear if the brittle fracturing is related to primary emplacement-related strain that was released during exhumation in the near subsurface, or to tectonic strains, or to some combination of both.

## Fracture Data Analysis, Model Construction, and Matching Models to Data

The flowchart in figure A1 summarizes the steps required for the comprehensive analysis and modeling of natural fracture data to generate input parameters for simulation of fracture porosity. A spreadsheet program, Stereonet (Allmendinger, 1995), and FracMan (Dershowitz and others, 1996) by Golder Associates, Inc., were the primary computer codes used for derivation of model parameters from the field data.



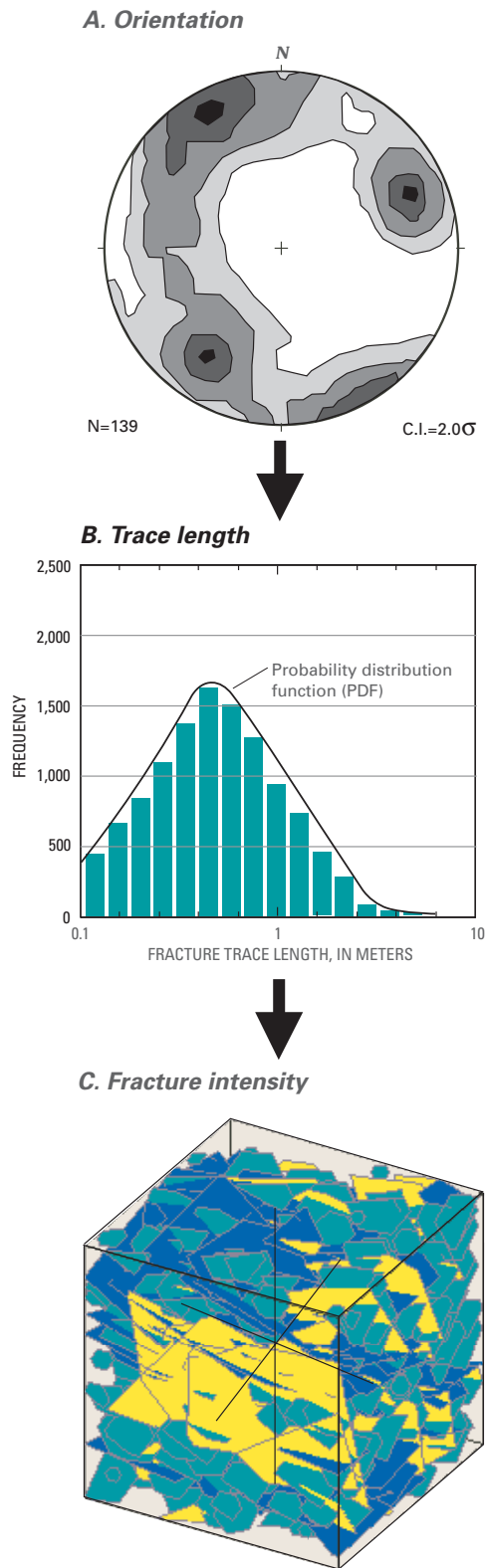


**Figure A1.** Flow chart showing how discrete fracture-network model parameters are modeled to lead to the construction of a single best-fit model.

The analyses used in this study assume that fracture sets with a mean orientation and dispersion can be distinguished from one another and that their individual physical properties control the hydraulic behavior of the fracture networks as a whole at a variety of scales. All other fracture-set parameters, such as trace length, are then calculated on a set-by-set basis. Although natural fracture sets can be distinguished by a number of parameters, the sets assigned in this study are based exclusively on orientation. This is primarily due to the lack of unique mineralization signatures, age markers, and general uniformity of length and morphology in any given set.

FracMan is a discrete fracture-network data-analysis and synthetic fracture-network generator computer code. FracMan creates rectangular regions that are filled with synthetic fractures whose properties statistically relate to the field data. When constructing a fracture network, FracMan initially selects a fracture center point from a random number for the first fracture in the first fracture set. It then randomly selects an orientation and length from the statistical distribution for that set, assigns these values to a fracture, and randomly places the synthetic fracture in the specified model domain. The next fracture is created with a new center point, in a position defined by a fracture spacing model for that set. The above process is repeated until the first set has been completely created in accordance with the specified fracture intensity for that set. Each successive set is created until the fracture network is complete. Additionally, as each fracture in each set is created in the network, random fracture truncations and free tips are created in accordance with the field data for that set. Following is a description of how each fracture network parameter is developed for input into FracMan.

### Fracture Set Designation

Raw orientation data are plotted on a lower hemisphere equal-area plot and then contoured using the Kamb method (Kamb, 1959, figure 13). Clusters of the raw and contoured data are segregated and the mean orientation and Fisher dispersion for each cluster (set) are calculated. The choice of any individual set is based on the tightness of the cluster and observations made in the field. Each fracture in each set and its corresponding data (for example, position, trace length, and terminations) are segregated to form a new set-specific, comprehensive database.

## Fracture Length Simulation

The trace-length means, standard deviations, and probability distribution functions (PDF, the type of curve that best fits a parameter frequency distribution plot) are determined for each set from the raw data. A PDF is plotted for the raw trace-length data by using FracMan. Fracture termination style (for example, free tips and truncations by neighboring fractures or fractures that freely intersect other fractures) also is incorporated into the fracture-length distributions. In order to create a synthetic trace-length distribution and derive its mean and PDF that best matches the field data, simulated trace planes and scanlines are set up that have the same orientations and sizes as those in the field from which the data were collected (Dershowitz and others, 1996). Multiple simulations of fracture traces are generated with the code FracSize (a module of FracMan). The initial simulation is started with a mean fracture radius, standard deviation, and distribution based on the field data. Simulations are repeated until a satisfactory match between the simulated and measured fractures are obtained. The criteria for a good fit are arbitrarily based on the results of Kolmogorov-Smirnov (K-S) and Chi-squared (Chi2) tests (Dershowitz and others, 1996). For most simulations, 90 percent or better significance was sought for both K-S and Chi2. Unfortunately, many of the data were difficult to fit at such high degrees of significance. The mean percent significance for all simulated fracture sets using K-S was 93.5 percent and using Chi2 was 69.0 percent.

## Fracture Spacing

Fracture spacing was assumed to be best represented by a uniform distribution. The Enhanced Baecher spacing model (Dershowitz and others, 1996) in FracMan was found to yield fracture-network models that best match the field observations. The Enhanced Baecher model locates fracture centers in a model domain using a Poisson distribution and allows for fracture terminations at intersections with preexisting fractures (Dershowitz and others, 1996). The Enhanced Baecher model produces fracture sets with relatively uniform spatial distributions and minimal clustering, as was generally observed in the field. All fractures in this study are simulated as smooth, parallel-walled, hexagonal plates.

## Fracture Intensity and Calibration of Fracture Network Models to Field Data

Fracture intensity can be expressed as fracture area per unit volume (that is,  $m^2/m^3 = 1/m$ , or  $P_{32}$  in FracMan). The term fracture density is sometimes interchanged with fracture intensity, which is more formally defined here as the number of fractures per unit line length (that is,  $1/m$ , or  $P_{10}$  in FracMan). Because fracture-dominated fluid flow and fracture intensity occur in a three-dimensional volume, three-dimensional modeling is appropriate in this case. Because fracture intensity in a volume cannot be directly measured, it can only be simulated from scanline fracture intensity or  $P_{10}$  data. Because the dimensions of fracture area per unit volume ( $P_{32}$ ) and number of fractures per unit line length ( $P_{10}$ ) are the same (that is,  $1/\text{length}$ ),  $P_{32}$  can be derived from  $P_{10}$ . Fracture intensity is estimated by matching, or calibrating, simulated fracture lengths and intensities to the field data.

First, a three-dimensional, cubic simulation region or model domain is defined using FracMan for each locality that is slightly larger than the longest scanline measured in the field at that locality. There were at least three and up to nine scanlines measured at each locality. Within the model domain, the three most orthogonal scanlines are simulated. These are simulated with the same orientation and length as those measured in the field, and the positions of the simulated and measured scanlines in the domain are assumed to be random as are the actual scanlines in the field. Model  $P_{10}$ 's are then calculated for each fracture set on each scanline by running Monte Carlo simulations using an initial supplied value for  $P_{32}$  (usually starting with the observed  $P_{10}$  value). This is repeated using a Monte Carlo-style simulation process until the input  $P_{32}$  value results in a close match to the observed  $P_{10}$ . A close match is determined by calculating the relative error for each simulation. Thus, for each of 100 realizations of a fracture network constructed with the same statistical parameters but a different initial seed, the resulting number of simulated fracture intersections ( $M_i$ ) with each model scanline is compared with the observed number of intersections ( $O_i$ ) from the real scanlines. The relative percent error ( $(M_i - O_i) / O_i \times 100$ ) is then calculated for each run, and the input  $P_{32}$  is adjusted until the error is arbitrarily less than 10 percent.

The next step in the process is to further adjust  $P_{32}$  using all of the fracture sets in the full model domains and the three most orthogonal scanlines for the location being simulated. All nonfault-zone model domains are 15-m cubes. The fault-zone model domains are 2-m cubes. Once reasonable estimates of fracture density ( $P_{32}$ ) are derived from the scanline fracture-intensity data ( $P_{10}$ ) matching process described above, a similar process of populating the full model domains with all fracture sets can be started. A first estimate for the  $P_{32}$  for each fracture set is again run 100 times using a Monte Carlo-style simulation. The number of intersections for each simulated fracture set on each scanline is compared with the observed data, and the mean relative error is again calculated for all of the 100 realizations. The  $P_{32}$ 's are then systematically adjusted, within reasonable values compared to the field data, until the mean relative error for each scanline is arbitrarily within about 20 percent of the observations.

For most of the simulations the full-model, single scan-line calibrations are well within 20 percent mean relative error. However, there are several fracture-set  $P_{32}$  outliers that would not calibrate to within 20 percent. Because this study is designed to generate fracture-network models that generically represent the field data, the results are acceptable. Moreover, the final step in this process is to choose the best single fracture-network model generated by one random seed, which has the lowest relative percent error. For each of the models, the error for simulated fracture sets along each model scanline is within 20 percent, and generally less than 10 percent, and the mean total error for all of the models is 3.7 percent. The best model for each location was saved and used for calculating fracture porosity scenarios as described in the "Estimates of Potential Fracture Network Porosity" section.

## Spatial Analysis of Well-Construction Data and Ground-Water Levels

A brief analysis of spatial characteristics for reported well yield was done to determine if the available data were sufficient to define any spatial patterns in aquifer characteristics. The analysis included geostatistical techniques that can be referred to as "variogram analysis." Variogram analysis is a

precursor to techniques that use existing measurements to estimate conditions at unmeasured locations. Detailed descriptions of variogram mechanics are available in texts (Isaaks and Srivastava, 1989; Cressie, 1991), and only the general nature of such analysis is discussed here.

An essential goal of variogram analysis is to evaluate the spatial association for, in this study, reported well yields. The analysis helps answer the question, "In general, are the reported yields for wells that are closely located to each other more similar than the reported yields for wells that are not closely located?" A convenient way to evaluate spatial association is to compute differences in reported yields for all possible pairings of wells, and then to express variability of the computed differences, often in a graph called a variogram, as a function of the distance between wells. For example, wells that are close to each other may have relatively small differences in reported yields, and the variability of differences in reported yields is relatively low. As the distance between wells increases, differences in reported yields may increase, which will reflect an increased variability.

In the example above, the initial values on a variogram (those for wells with very small separation distances) would indicate a minimum value. As the separation distance increases, the variogram value rises to the maximum value for variability and may remain at a relatively constant value. The minimum variogram value, commonly called a nugget, represents the expected amount of variability in reported yields for closely spaced wells. The maximum value, commonly called the sill, represents the expected amount of variability for relatively large well spacings. The value for well spacing associated with the sill, commonly called the range, is an approximation of the largest well spacing for which the members of a pair of wells have some amount of spatial association. If the observed variability for pairs is influenced by direction, it is useful to develop graphical representation for a series of variograms that describe spatial association and the way it varies with direction. This graphical representation is called a variogram surface map. The variogram surface map can be thought of as a representation of a series of variograms made through a full circle of directions.

## Evapotranspiration Measurement Methods

The eddy-correlation method, used at the forest site, does not rely on the surface energy balance but uses direct measurements of the turbulent eddy motions and the water or heat content of the eddies above a plant canopy to compute  $E$  and  $H$  (Swinbank, 1951). Although movement of air (wind) is primarily horizontal, vertical motions of parcels, or eddies, of air are superimposed on the overall horizontal movement. Transport of any constituent (water, heat, carbon dioxide, pollutants) between the surface and the atmosphere occurs through these vertical motions. For example, if evaporation is occurring, then on average, upward-moving eddies are more humid than downward-moving eddies. Sensible heat flux is the heat that moves between the surface and the atmosphere due to a temperature difference. And if sensible heat is moving upward, then on average, upward-moving eddies are warmer than downward-moving eddies. By making very rapid measurements of vertical windspeed and concentration (vapor density, temperature, and so forth) at a point, many eddies are sampled and the data reflect the mean fluxes from the underlying surface. Mathematically, these ideas can be written as:

$$E = \overline{w'\rho_v'} \quad (\text{A1a})$$

and

$$H = \rho C_p \overline{w'T'} \quad (\text{A1b})$$

where

- $E$  is the mass flux of water vapor (grams per square meter per second),
  - $H$  is sensible heat flux (watts per square meter),
  - $w$  is the vertical component of windspeed (meters per second),
  - $\rho_v$  is vapor density (grams per cubic meter),
  - $\rho$  is air density (grams per cubic meter),
  - $C_p$  is the specific heat capacity of air (joules per gram per degree Celsius),
  - $T$  is air temperature (degrees Celsius), and
- primes (') denote deviations from means over some time period.

In this formulation, overbars ( $\overline{\quad}$ ) denote means over the same time period,  $\overline{w'\rho_v'}$  is the covariance of  $w$  and  $\rho_v$ , and  $\overline{w'T'}$  is the covariance of  $w$  and  $T$ . At the forest site,  $w'$ ,  $\rho_v'$ , and  $T'$  were sampled eight times per second and the covariances were calculated every 30 minutes on a digital data logger. A sonic anemometer was used to measure  $w'$  and  $T'$ , and a krypton hygrometer was used to measure  $\rho_v'$ . Eddy correlation sensors were placed at 57 ft above land surface on a 60-ft-tall tower; mean tree height was 39 ft. Placement of the sensors well above the canopy (about 1.5 times canopy height) ensures that small-scale variability in the turbulent flow field, caused by spacing between individual trees, is removed. Corrections were made to the raw measurements to account for density effects (Webb and others, 1980) and for the sensitivity of the krypton hygrometer to oxygen (Tanner and Greene, 1989). Also, coordinate rotation was applied to account for the slight slope ( $3.75^\circ$ ) at the site (Kaimal and Finnigan, 1994). At an ideal site, accuracy of eddy-correlation measurements is considered to be about 5 to 10 percent on a daily time step and about 2 to 3 percent on a monthly time step (Shuttleworth and others, 1988). Values of  $E$  in grams per square meter per second can be converted to  $ET$  rates in inches per day by multiplying by 3.402.

Eddy-correlation sensors do not operate when their sensing surfaces become wet during or after precipitation. When these surfaces dry out, the measurements resume. During the 3 years of study, the eddy-correlation sensors were inoperative (down) 16.2 percent of the time (which was about evenly divided between day time and night time). If sensors were down for more than two consecutive 30-minute periods,  $ET$  was estimated using a modified Priestley-Taylor equation for potential  $ET$  (Priestley and Taylor, 1972). Potential  $ET$  occurs from a wet or "well-watered" surface. It was reasoned that if sensors were wet for an extended period, the forest canopy was in all likelihood also wet and potential  $ET$  was occurring. The Priestley-Taylor equation is driven by net radiation, soil heat flux, and air temperature. If sensors were down for one or two 30-minute periods,  $H$  and  $LE$  were simply set to their respective values from the last 30-minute period before they went down. These short downtimes are often associated with very brief showers, where canopy surfaces may remain mostly dry but a single raindrop or snowflake can render the

sensor(s) inoperative. A potential *ET* estimate is inappropriate during these times, whereas an estimate from about an hour earlier is justified.

Net radiation,  $R_n$ , soil heat flux,  $G$ , and change in heat stored in the canopy,  $\Delta S$ , also were measured at the forest site to provide a check on the eddy-correlation measurements. If all measurements are accurate, then the left side of equation 1 (in text) will equal the right side. If the two sides are unequal, the difference is the energy-balance closure.  $R_n$  was measured using a Radiation Energy Balance Systems (REBS), Inc., model Q\*7.1 net radiometer, placed at 53.4 ft above land surface (14 ft above the treetops). The sensor was located south of the tower about 5.8 ft from the nearest tower leg and was maintained level. Corrections were made to the raw measurements to account for the sloping surface at the site (Nie and Kanemasu, 1989) and for the effects of windspeed (REBS, 1995).  $G$  was measured using the combination method (Fuchs and Tanner, 1968). Three soil-heat flux plates were buried at a depth of 3.1 inches to measure the flux of heat at this depth,  $G_d$ . Three sets of four thermocouples were buried at depths of 0.4, 1.2, 2.0, and 2.8 inches to measure the mean temperature of the soil from the surface to the 3.1-inch depth. These temperatures were used with estimates of the specific heat capacity of the soil ( $C_s$ ) to calculate  $\Delta ST$ , the change in heat stored in the 3.1-inch layer. The soil heat flux at the surface,  $G$ , was calculated as the sum of  $G_d$  and  $\Delta ST$ .  $C_s$  was computed from measurements of bulk density and water content of the soil. A few volumetric soil samples were obtained to measure bulk density, and water content (soil moisture) was measured onsite every 30 minutes.  $G$  is a small but significant term in the energy balance of the forest on a 30-minute basis, but  $G$  is very near zero on a daily basis because heat that penetrates the soil during the day typically is liberated back to the atmosphere at night. Although measurements to calculate  $\Delta S$  were made at this site, the calculation requires information about forest biomass and distribution that has not yet been determined. Because  $\Delta S$  typically is smaller than  $G$  on a daily basis, it was not calculated in this report and was assumed to be zero.

Accuracy of eddy-correlation measurements often is difficult to assess because independent measurements of the turbulent fluxes ( $H$  and  $LE$ )

usually are not made concurrently. In wildland settings, usually the only guideline available to estimate the accuracy of eddy-correlation measurements is the energy-balance closure. However, this is not always conclusive because errors may exist in any of the terms in equation 1. Over periods of a day or more, errors in  $G$  or  $\Delta S$  are likely to be very small because the terms themselves are small.  $R_n$  is the largest single term in equation 1, however, and could potentially contain significant errors. Comparisons were made between daily values of  $(R_n - G)$  and  $(H + LE)$  measured at the forest site, using only days when all sensors were operational (594 days).  $\Delta S$  was not included because it is very small on a daily basis and is virtually zero averaged over the whole study period. On average, the turbulent flux ( $H + LE$ ) was 80.05 percent of the available energy ( $R_n - G$ ). Daily values of  $(H + LE)$  are well correlated with ( $r^2 = 0.913$ ) but significantly less than daily values of  $(R_n - G)$ . This amount of disparity between available energy and turbulent flux is not uncommon (Moore, 1976; Weeks and others, 1987; Fitzjarrald and others, 1988; Bidlake and others, 1993; Goulden and others, 1996; Sumner, 1996; German, 2000). Very good energy-balance closures have also been obtained at some sites, however (Anderson and others, 1984; Verma and others, 1986; Shuttleworth and others, 1988; Stannard, 1993; Stannard and others, 1994; Baldocchi, 1994). There is ongoing debate regarding the reasons for lack of energy-balance closure. There are good reasons to believe that the model of net radiometer used in this study overmeasures net radiation (Campbell and others, 1978; G.S. Campbell, Washington State University, written commun., 1980), and there is little reason to suspect problems with the eddy-correlation method. Therefore, *ET* results for this forest site will be based on the raw eddy-correlation measurements, uncorrected for energy-balance closure. Until the energy-balance question is resolved, however, the possibility exists that these *ET* values significantly underestimate the true *ET*.

The Bowen-ratio method, used at the meadow site, relies on the assumption of zero energy-balance closure (eq. 1) to compute latent-heat flux,  $LE$ . The Bowen ratio,  $B$ , is the ratio of sensible to latent-heat flux,  $H/LE$ . If  $B$  can be measured along with  $R_n$ ,  $G$ , and  $\Delta S$ , equation 1 can be used to compute both  $H$  and  $LE$ . If the eddy diffusivities for heat and water vapor

are equal, then the ratio of the fluxes is equal to the ratio of the vertical gradients (or differences) in concentration (Bowen, 1926). Mathematically, this can be stated as:

$$B = \gamma \frac{\Delta T}{\Delta e} \quad (\text{A2})$$

where

$B$  is the Bowen ratio (unitless),

$\gamma$  is the psychrometric constant (kilopascals per degree Celsius),

$\Delta T$  is the vertical temperature difference over some interval above the plant canopy (degrees Celsius), and

$\Delta e$  is the vertical vapor pressure difference over that same interval (kilopascals).

Using the definition of  $B$  from above, equation 1 (in text) can be rewritten as:

$$LE = \frac{R_n - G - \Delta S}{1 + B} \quad (\text{A3})$$

and  $LE$  can be divided by  $L$  to obtain  $E$ .

$R_n$  and  $G$  were measured at the meadow site using methods and sensor models identical to those used at the forest site. No attempt was made to measure  $\Delta S$  at the meadow site because the biomass of the grass canopy is small enough that  $\Delta S$  is insignificant. Measurement of  $\Delta T$  and  $\Delta e$  typically requires specialized methods to remove bias between upper and lower sensors because the differences often are of similar magnitude to sensor bias. For this study, sensor bias was removed by interchanging positions of the two sensors on regular intervals (Tanner, 1960) and averaging the readings. At the meadow site, two ventilated solid-state temperature-humidity probes were deployed at heights of 6.8 ft and 3.5 ft above land surface. Data were collected for 15 minutes, the probes were interchanged, and data were collected for another 15 minutes. Assuming the bias between sensors remains constant over one-half hour, averaging the two 15-minute periods together to compute half-hour differences eliminates sensor bias. These differences were used to compute half-hour values of  $B$  by using equation A2 and half-hour values of  $LE$  by using equation A3. Bowen-ratio data were filtered following the method described in Ohmura (1982) to eliminate

problems caused by small measurement errors near sunrise and sunset. If  $-0.7 > B > -1.3$ , or computed  $H$  and  $LE$  were of opposite sign to  $\Delta T$  and  $\Delta e$ , respectively (that is, counter-gradient flux was indicated), then  $LE$  was set to zero. The raw measured values of daily  $ET$  at the meadow site were reduced by 20.0 percent because net radiation,  $R_n$ , is used to calculate  $ET$  using the Bowen-ratio method (eq. A3 in Appendix) and was believed to be overmeasured using this model of net radiometer. This adjustment is intended to remove  $ET$  measurement bias between the two sites caused by methodological differences. As with the eddy-correlation results, until the energy-balance question is resolved, the possibility exists that the Bowen-ratio  $ET$  values significantly underestimate the true  $ET$  at the meadow site.

## Quality Assurance and Quality Control

The integrity of analytical and sampling procedures can be evaluated using milliequivalent balances, quality-control samples, and duplicate samples; about 37 percent of all samples analyzed as part of this study were quality-control samples. Milliequivalent balances commonly are used to evaluate analytical integrity, whereas various quality-control samples are used to evaluate both analytical and sampling integrity.

### Milliequivalent Balances

Concentrations in milligrams per liter may be converted to milliequivalents by adjusting those concentrations for their formula weights and chemical charges. The resulting milliequivalent concentrations are used to compute milliequivalent balances by summing cation and anion milliequivalents and comparing those two sums. Assuming that cations and anions are the major contributors to the ionic content of sampled water, the two sums should be equal. The milliequivalent balance typically is computed with this equation:

$$\left| \frac{\Sigma c - \Sigma a}{\Sigma c + \Sigma a} \right| \times 100 \quad (\text{A4})$$

where  $\Sigma c$  is the sum of the cation milliequivalent concentrations and  $\Sigma a$  is the sum of the anion milliequivalent concentrations.

A frequency table showing the distribution of milliequivalent balances for samples collected as part of this study (table A1) indicates that about 88 percent of all samples for which milliequivalent balances are available are within plus or minus 7.5 percent. These analyses represent the typical performance of the laboratories involved, when making analytical determinations for this study. Of the remaining 27 samples, 21 are dilute water (relatively low ionic content) that have no results for potassium. Because the samples are dilute, the absence of results for potassium may account for the apparent lack of balance. The remaining six samples represent results that are not well balanced, indicating that some of the major-ion results have higher than typical error bars.

### Quality-Control Samples

The validity of quality-control samples was ensured by using inorganic-free water provided by the USGS Ocala, Fla., laboratory (American Society for Testing Materials D1193, 1999). Detection of measurable concentrations for any water-quality constituent in quality-control samples indicates a possibility that

**Table A1.** Frequency distribution for milliequivalent balances

[Note: Interval, interval of milliequivalent balance values;  
Absolute frequency number of milliequivalent balances in interval]

Interval	Absolute frequency	Absolute frequency (percent)	Cumulative frequency (percent)
-22.5 -	-20	2	0.905
-20 -	-17.5	0	0.000
-17.5 -	-15	3	1.357
-15 -	-12.5	2	0.905
-12.5 -	-10	8	3.620
-10 -	-7.5	6	2.715
-7.5 -	-5	13	5.882
-5 -	-2.5	32	14.480
-2.5 -	0	41	18.552
0 -	2.5	77	34.842
2.5 -	5	29	13.122
5 -	7.5	2	0.905
7.5 -	10	1	0.452
10 -	12.5	0	0.000
12.5 -	15	1	0.452
15 -	17.5	0	0.000
17.5 -	20	0	0.000
20 -	22.5	1	0.452
22.5 -	25	0	0.000
25 -	27.5	0	0.000
27.5 -	30	0	0.000
30 -	32.5	0	0.000
32.5 -	35	0	0.000
35 -	37.5	1	0.452
37.5 -	40	1	0.452
40 -	42.5	0	0.000
42.5 -	45	1	0.452
Total	221	100.000	

analytical or sampling procedures have introduced some error into reported concentrations. Table A2 lists results for quality-control samples in which measurable concentrations for water-quality constituents were detected. Results for all bacteriological samples collected in June 1999 were rejected due to the presence of total coliform bacteria in bacteriological blanks. No other data were rejected; however, some discussion of the detections in quality-control samples is warranted.

The most commonly detected constituents in the quality-control samples are minor elements, and the most prominent of those detections are three reported detections of antimony at concentrations of about 50 µg/L using inductively coupled plasma (ICP) methods. In this study, the ICP method was used principally to detect cations; however, the method also provides results for minor elements. In this study, the atomic adsorption graphite furnace (AAGF) method was used to detect minor elements because it is generally known to be more sensitive to minor elements than ICP methods. For the three ICP detections of antimony at concentrations of about 50 µg/L, the AAGF results indicate no detectable antimony. The same is true for all other reported detections for minor elements in table A2 with ICP methodology. AAGF methodology did detect minor elements at low concentrations in 17 (or about 6 percent of AAGF quality-control analyses) quality-control samples analyzed mostly in the fall 1998. No AAGF results were rejected as part of this study; however, the results for detections of minor elements at low concentrations with AAGF methodology indicates some uncertainty for AAGF concentrations.

Additional detections in quality-control samples involved nutrients. There were two detections of total phosphorus at 0.02 mg/L, a level that is the detection limit for methods used in this study. The low level and frequency for total phosphorus in quality-control samples were noted but were not identified as cause to reject total phosphorus results. A detection of nitrate plus nitrite as nitrogen at a concentration of 3.82 mg/L in a preservative blank was attributed to field error.

Water for field blanks associated with the wastewater-compound analyses was obtained at the USGS NWQL. Sample bottles of blank water were kept open to the air during sample collection and processing to expose the field blank to the same potential sources of contamination as the environmental

**Table A2.** List of detections in quality-control samples

[Note: Control number refers to unique number assigned to each sample by USEPA; Sample identifier defines type of quality control sample with characters 1-3 (QCA and QCD - equipment blanks, QCB - field blank, QCC and QCE - preservative blanks, QCX - bacteriological blank); Collection date is mmddyy (month, day, year); collection time is hhmm (hours, minutes); Analytical method, AAGF GROUP - atomic adsorption graphite furnace, ICP - inductively coupled plasma; Phase, D - dissolved; --, not available or applicable; µg/L, microgram per liter]

Control number	Sample identifier	Collection		Water-quality constituent	Analytical method	Phase	Result	Units
		date	time					
-----								
Equipment blanks (total collected = 112)								
8-183303	QCA-T1-1	091498	1216	TITANIUM	ICP GROUP	D	2.00	µg/L
8-183348	QCA-T2-2	091598	1441	TITANIUM	ICP GROUP	D	2.00	µg/L
8-183438	QCA-T3-2	091698	1025	LEAD	AAGF GROUP	D	1.00	µg/L
8-183326	QCD-T1-5	091898	1040	AMMONIA (as N)	--	--	0.05	mg/L
8-183446	QCD-T3-3	091898	1323	AMMONIA (as N)	--	--	0.08	mg/L
8-183416	QCD-T2-5	092198	1144	AMMONIA (as N)	--	--	0.05	mg/L
8-183418	QCA-T2-6	092298	1530	TITANIUM	ICP GROUP	D	1.00	µg/L
8-183338	QCA-T1-8	092398	1043	COPPER	AAGF GROUP	D	1.00	µg/L
8-183453	QCA-T3-5	092398	1101	ANTIMONY	ICP GROUP	D	53.0	µg/L
8-183601	QCA-SW-01	092498	1115	ARSENIC	AAGF GROUP	D	1.60	µg/L
8-172347	QCD-SW-2	031799	1045	TOTAL PHOSPHORUS	--	--	0.02	mg/L
8-182072	QCA-T3-5	062299	1345	SILVER	AAGF GROUP	D	0.20	µg/L
-----								
Field blanks (total collected = 38)								
8-183344	QCB-T2-1	091498	1255	TITANIUM	ICP GROUP	D	3.00	µg/L
8-183349	QCB-T2-2	091598	1441	TITANIUM	ICP GROUP	D	2.00	µg/L
8-183409	QCB-T2-4	091898	1035	ARSENIC	AAGF GROUP	D	1.00	µg/L
8-183334	QCB-T1-7	092298	1350	TITANIUM	ICP GROUP	D	1.00	µg/L
8-183419	QCB-T2-6	092298	1530	LEAD	AAGF GROUP	D	0.60	µg/L
8-183454	QCB-T3-5	092398	1101	ANTIMONY	ICP GROUP	D	50.0	µg/L
8-183454	QCB-T3-5	092398	1101	ARSENIC	AAGF GROUP	D	1.10	µg/L
8-183424	QCB-T2-7	092398	1345	TITANIUM	ICP GROUP	D	1.00	µg/L
8-183602	QCB-SW-01	092498	1115	LEAD	AAGF GROUP	D	0.70	µg/L
8-183616	QCB-SW-03	092998	1255	COPPER	AAGF GROUP	D	0.60	µg/L
8-182018	QCB-T1-2	061699	1215	COPPER	AAGF GROUP	D	0.70	µg/L
8-182028	QCB-T3-2	061699	1315	COPPER	AAGF GROUP	D	0.60	µg/L
-----								
Preservative blanks (total collected = 113)								
8-183442	QCE-T3-2	091698	1025	TOTAL PHOSPHORUS	--	--	0.02	mg/L
8-183310	QCC-T1-2	091598	1030	TITANIUM	ICP GROUP	D	3.00	µg/L
8-183437	QCE-T3-1	091598	1115	NITRATE/NITRITE (N)	--	--	3.82	mg/L
8-183350	QCC-T2-2	091598	1441	TITANIUM	ICP GROUP	D	3.00	µg/L
8-183450	QCC-T3-4	092198	1405	ANTIMONY	AAGF GROUP	D	0.60	µg/L
8-183450	QCC-T3-4	092198	1405	THALLIUM	AAGF GROUP	D	0.90	µg/L
8-183450	QCC-T3-4	092198	1405	ZINC	ICP GROUP	D	4.00	µg/L
8-183617	QCC-SW-03	092998	1255	ANTIMONY	ICP GROUP	D	48.0	µg/L
8-182079	QCC-T1-6	061499	1625	COPPER	AAGF GROUP	D	1.30	µg/L
8-182089	QCC-T3-6	061499	1615	COPPER	AAGF GROUP	D	1.20	µg/L
8-182009	QCC-T2-1	061599	1215	COPPER	AAGF GROUP	D	0.90	µg/L
8-182696	QCC-T1-7	062399	1045	CHROMIUM	AAGF GROUP	--	1.30	µg/L
-----								
Bacteriological blanks (total collected = 26)								
8-170641	QCX-T1-7	062399	1045	Total Coliform	--	--	1	--
8-182532	QCX-T2-7	062399	1140	Total Coliform	--	--	1	--
8-182533	QCX-T3-7	062399	1210	Total Coliform	--	--	1	--



samples. No detections were reported from the three field-blank samples. One of the two laboratory blanks from the April 2001 sampling showed four estimated concentrations, but the values were below the method reporting level (MRL). The other laboratory blank showed two estimated concentrations, both below the MRL. The laboratory blank from the September 2001 sampling showed no concentrations above the MRL. Laboratory procedures adjust the MRL upward for the environmental samples to account for potential contamination documented in the blank samples. In general, the compounds detected in blanks do not show values above censoring limits in the environmental sample results of the same lot.

### Duplicate Samples

Duplicate samples are collected to test repeatability, and they were prepared by collecting two aliquots of water for each analysis. In theory the results from each aliquot should be the same; deviations describe laboratory precision or problems with field techniques. The results of duplicate samples from this study were evaluated by computing relative percent differences (rpd's) for different categories that

were defined on the basis of analytical methodology (table A3). The rpd was computed with the following equation:

$$rpd = \left[ \frac{C1 - C2}{(C1 + C2)/2} \right] \times 100 \quad (A5)$$

where

- C1 is the concentration for aliquot 1, and
- C2 is the concentration for aliquot 2.

Table A3 indicates that the highest rpd, from -123 to 178, occurred in ICP analyses. An arbitrarily defined rpd bracket from -20 to 20 contains 83.5 percent of ICP analyses. The other analysis categories, especially cations and anions, contain a larger percentage of samples in the -20 to 20 rpd bracket. These results indicate that confidence in reported results is highest for cations and anions and somewhat lower for other analyses.

Tritium results showed good reproducibility in laboratory replicates, with mean percent difference at about 10 percent. Laboratory standard deviations of counting error were generally smaller than plus or minus 2 tritium units. Field duplicates had a mean rpd of about 5 percent.

**Table A3.** Statistics for relative percent differences in duplicate samples

[Note: Q25, 25th percentile; Q75, 75th percentile; Bracket, percentage of samples greater than -20 and less than 20 relative percent difference; N, number of samples]

Analysis category	Mean	Median	Q25	Q75	Minimum	Maximum	Bracket	N
Total organic carbon	2.24	0	-5.71	8.33	-53.97	62.07	88.57	35
Nutrients	5.26	0	-0.37	5.36	-128.87	111.11	88.50	87
AAGF metals	3.56	0	-1.45	10.85	-104.00	85.71	84.78	92
ICP metals	1.23	0	-1.50	1.95	-123.57	178.29	83.50	358
Cations	-0.95	0	-0.64	0.82	-84.71	28.18	98.50	133
Anions	-0.07	0	-0.25	1.26	-181.68	47.51	96.03	151

**Table A4. Selected site characteristics for water levels measured in fall 2001**

[USGS id, 15-digit NWIS identifier; Local, local id; Cell, refers to project grid identifier; Permit, well permit number from State Engineers Office; Latitude and Longitude, degrees minutes and seconds determined with commercial Global Positioning units and referenced to North American Datum of 1927; Elev, altitude above mean sea level determined from 1:24,000 topographic maps and referenced to National Geodetic Vertical Datum of 1929; MP, height of measuring point above land surface; Date, month day and year of measurement; Time, hours and minutes of measurement; DTW, measured depth from measuring point to water in well; na, not applicable, unk, unknown]

USGS id	Local	Cell	Permit	Latitude	Longitude	Elev	Measuring point description	MP	Date	Time	DTW	Status
393035105204500	na	4	166346	393034.5	1052045.4	9255	top of casing	0.40	09/27/01	1410	116.48	recently pumped
393039105200700	na	5	198794	393038.8	1052006.5	9030	top of casing	1.00	10/02/01	1445	449.00	recently pumped
393116105210900	na	21	148360	393115.5	1052109.0	9530	top of casing	0.00	09/27/01	1819	148.60	affected by nearby pumping
393101105205100	na	22	169640	393100.5	1052050.5	9460	top of casing	0.50	10/02/01	1600	150.00	recently pumped
393059105195900	na	24	unk	393058.7	1051959.0	8635	land surface	0.00	10/02/01	1345	0.00	recently pumped
393106105193100	na	25	107927	393106.3	1051931.2	8600	plug in top of casing	0.00	10/02/01	1400	19.44	recently pumped
393107105184300	na	26	75757	393106.7	1051843.0	8480	top of casing	1.00	09/24/01	1107	201.11	pumping
393119105183200	na	26	144671	393119.0	1051832.0	8285	top of casing	0.40	09/26/01	1500	69.65	recently pumped
393139105220000	na	39	105205	393139.2	1052200.0	9330	top of casing	0.00	09/27/01	1409	23.28	recently pumped
393129105213600	na	40	159879	393128.8	1052136.1	9605	top of casing	0.79	09/27/01	1703	56.05	affected by nearby pumping
393116105202400	na	42	78268	393116.1	1052024.4	8810	top of casing	0.20	09/27/01	1245	98.21	recently pumped
393139105141200	GW009	53	unk	393138.7	1051410.6	8365	top of casing	1.00	09/28/01	1830	287.00	recently pumped
393144105135600	GW011	54	unk	393143.5	1051357.8	8445	top of casing	1.00	09/28/01	1800	312.00	recently pumped
393203105220400	na	58	176711	393202.5	1052204.1	8960	top of casing	0.89	09/27/01	1628	11.84	affected by nearby pumping
393159105213500	na	59	184392	393159.2	1052135.4	9095	top of casing	1.60	09/27/01	1451	167.30	recently pumped
393153105211400	na	60	114268	393153.1	1052114.4	8950	top of casing	0.92	09/27/01	1536	109.16	recently pumped
393150105194600	na	62	162862	393149.6	1051946.1	8245	top of casing	0.38	09/26/01	1340	215.40	recently pumped
393157105193400	na	63	161441	393156.5	1051933.8	8245	top of casing	0.75	09/26/01	1300	72.75	recently pumped
393206105204800	GWK08	64	unk	393206.4	1052046.0	8445	top of casing	1.00	09/26/01	1210	4.50	recently pumped
393153105180700	na	65	13467	393152.7	1051806.8	8235	top of casing	1.50	09/26/01	1520	48.40	recently pumped
393202105183200	na	65	unk	393202.1	1051832.2	8060	top of casing	1.10	09/25/01	1216	12.00	recently pumped
393204105180200	GW004	66	unk	393205.0	1051759.5	8275	top of casing	0.75	09/26/01	1550	30.17	recently pumped
393206105141800	GW007	72	unk	393204.3	1051415.9	7915	top of casing	1.10	09/26/01	1120	128.83	recently pumped
393202105135200	na	73	126079	393201.6	1051351.5	7985	top of casing	0.30	09/26/01	1030	47.56	recently pumped
393240105205600	na	79	unk	393240.2	1052056.1	8660	top of casing	0.82	09/26/01	1416	60.25	affected by nearby pumping
393240105205600	na	79	193063	393239.8	1052056.1	8655	top of casing	0.50	09/26/01	1402	54.70	affected by nearby pumping
393234105201800	GWJ03	80	unk	393233.8	1052016.4	8620	top of casing	1.20	09/26/01	1547	137.50	affected by nearby pumping
393230105201000	GWJ02	81	unk	393229.7	1052008.8	8505	top of casing	0.67	09/26/01	1523	86.82	recently pumped
393216105184100	na	83	173558	393216.1	1051841.1	8230	top of casing	1.30	09/26/01	1140	185.00	recently pumped
393233105181300	na	84	unk	393232.7	1051813.0	8245	top of casing	1.20	10/03/01	1315	100.71	recently pumped
393249105163800	na	86	140549	393248.5	1051638.0	7915	top of casing	1.50	09/27/01	1045	32.03	recently pumped
393237105162900	GW099	87	unk	393236.8	1051626.2	8150	plug in top of casing	1.80	10/02/01	1840	16.92	pumping
393221105152700	na	89	unk	393221.2	1051527.1	7910	top of casing	0.30	10/02/01	1115	26.70	recently pumped
393238105152000	GW004	89	unk	393240.0	1051516.9	7790	top of casing	0.90	09/26/01	1405	51.86	recently pumped
393413105135800	GW004	89	unk	393413.0	1051355.8	7400	top of casing	1.00	09/26/01	1400	24.37	recently pumped
393231105144000	GW006	91	unk	393230.5	1051438.6	7770	top of casing	1.80	09/26/01	1500	127.55	recently pumped
393226105133100	na	92	unk	393226.0	1051331.0	7805	top of casing	-0.20	09/28/01	1430	195.00	recently pumped
393228105133800	na	92	182209	393228.0	1051338.0	8015	top of casing	1.10	09/28/01	1500	332.00	recently pumped
393237105222900	GWK05	96	unk	393136.7	1052227.4	9910	top of casing	0.95	09/27/01	1158	183.50	affected by nearby pumping
393241105214500	na	97	unk	393241.0	1052145.0	8795	top of casing	1.75	09/26/01	1836	64.27	recently pumped
393241105214500	na	97	163824	393241.3	1052145.0	8790	top of casing	1.50	09/26/01	1815	67.29	recently pumped
393243105220000	na	97	131563	393243.4	1052200.1	8870	top of casing	1.00	09/26/01	1924	159.04	recently pumped
393245105210100	na	98	63571	393244.9	1052101.4	8665	top of casing	0.67	09/26/01	1738	73.74	recently pumped
393242105202000	GW101	99	unk	393241.2	1052018.8	8560	top of casing	0.69	09/26/01	1715	101.66	affected by nearby pumping

**Table A4. Selected site characteristics for water levels measured in fall 2001—Continued**

[USGS id, 15-digit NWIS identifier; Local, local id; Cell, refers to project grid identifier; Permit, well permit number from State Engineers Office; Latitude and Longitude, degrees minutes and seconds determined with commercial Global Positioning units and referenced to North American Datum of 1927; Elev, altitude above mean sea level determined from 1:24,000 topographic maps and referenced to National Geodetic Vertical Datum of 1929; MP, height of measuring point above land surface; Date, month day and year of measurement; Time, hours and minutes of measurement; DTW, measured depth from measuring point to water in well; na, not applicable; unk, unknown]

USGS id	Local	Cell	Permit	Latitude	Longitude	Elev	Measuring point description	MP	Date	Time	DTW	Status
393417105192800	na	99	unk	393416.8	1051928.0	8035	top of casing	1.50	09/25/01	1710	55.24	recently pumped
393300105194400	GW104	100	unk	393300.1	1051941.2	8075	top of casing	1.25	09/25/01	1840	40.35	recently pumped
393303105191700	na	101	160087	393302.8	1051916.8	8230	top of casing	0.00	09/26/01	1748	324.00	recently pumped
393259105185700	GW707	102	unk	393301.6	1051855.0	7910	top of casing	0.65	09/25/01	1040	14.40	recently pumped
393244105172600	GW005	105	unk	393243.3	1051723.5	8175	plug in top of casing	-6.00	09/26/01	1040	78.15	recently pumped
393245105170000	na	106	156090	393244.9	1051700.4	8030	top of casing	0.70	09/25/01	1335	14.96	recently pumped
393250105155100	na	107	71984	393250.1	1051550.6	7850	top of casing	1.00	09/25/01	1230	62.28	recently pumped
393301105153100	MH8	108	unk	393301.2	1051529.9	8095	top of casing	1.00	09/26/01	1230	14.64	static
393245105145000	GW005	109	unk	393245.6	1051447.8	7900	top of casing	2.20	09/26/01	1300	55.45	recently pumped
393316105192400	na	120	137486	393315.9	1051923.8	8105	top of casing	0.00	09/25/01	1710	161.80	recently pumped
393308105184900	GW709	121	unk	393308.5	1051846.5	7970	top of casing	0.75	09/25/01	1400	85.65	recently pumped
393316105182400	na	122	unk	393316.1	1051823.8	8045	top of casing	0.50	10/02/01	1245	26.96	recently pumped
393320105184000	na	122	unk	393319.7	1051840.0	8030	top of casing	0.10	09/25/01	1700	109.65	recently pumped
393318105170400	na	124	130385	393318.2	1051703.8	8290	top of casing	0.70	09/25/01	1407	82.17	recently pumped
393322105165000	na	125	96541	393322.0	1051649.9	8250	top of casing	0.80	10/02/01	1155	42.38	recently pumped
393306105161300	na	126	163851	393306.4	1051613.1	8330	top of casing	1.10	09/25/01	1525	188.39	recently pumped
393324105152300	na	127	152613	393323.7	1051523.2	8210	top of casing	0.70	09/26/01	1030	56.46	recently pumped
393308105145500	GW001	128	unk	393307.7	1051453.4	7910	top of casing	0.90	09/26/01	1345	137.23	pumping
393308105132100	na	131	unk	393307.6	1051321.4	7335	top of casing	0.60	10/02/01	940	26.44	recently pumped
393334105192500	GW103	139	unk	393333.9	1051923.2	7915	top of casing	1.10	09/25/01	1817	35.90	pumping
393350105184300	MH5	140	unk	393351.3	1051851.8	7815	plug in top of casing	1.00	09/25/01	1135	33.00	static
393347105180300	na	141	99212	393346.5	1051803.1	8350	top of casing	0.30	09/25/01	1625	109.90	recently pumped
393344105171400	MH6.2	143	unk	393344.3	1051714.2	8352	top of casing	1.00	10/03/01	955	11.07	static
393344105155100	na	145	75392	393344.0	1051550.5	8645	top of casing	0.80	09/28/01	1200	201.50	recently pumped
393334105153600	na	146	155910	393333.8	1051536.1	8445	top of casing	1.50	09/26/01	1125	189.75	recently pumped
393332105150800	MH7	147	unk	393331.6	1051505.1	8310	top of casing	1.10	09/27/01	1540	61.12	static
393411105193400	na	158	83100	393411.0	1051934.4	8045	top of casing	0.65	09/25/01	1624	69.55	recently pumped
393417105183800	na	159	unk	393417.0	1051838.0	7755	top of casing	1.50	09/27/01	1430	7.23	recently pumped
393404105182200	GW002	160	unk	393403.6	1051819.5	7930	top of casing	1.50	09/25/01	1224	168.40	recently pumped
393401105152000	na	165	192690	393400.7	1051519.5	8230	top of casing	-0.40	09/28/01	1000	84.80	recently pumped
393405105151400	na	166	185829	393404.8	1051513.8	7985	top of casing	0.75	09/28/01	920	141.70	recently pumped
393413105132200	GW003	169	unk	393413.6	1051319.8	7185	top of casing	0.80	09/25/01	1340	11.70	recently pumped
393401105124600	GW007	170	unk	393419.0	1051250.8	7265	top of casing	0.90	09/25/01	1000	128.60	pumping
393442105193900	na	177	67402	393442.4	1051938.8	8130	top of casing	0.69	09/25/01	1500	156.95	recently pumped
393432105180300	na	180	92639	393431.6	1051802.8	8055	top of casing	1.00	09/25/01	1520	190.50	recently pumped
393448105170100	GWH01	181	unk	393446.8	1051657.4	7685	top of casing	0.30	09/25/01	1025	103.35	recently pumped
393444105165500	GWH03	182	unk	393443.8	1051653.2	7670	top of casing	0.70	09/24/01	1425	45.22	recently pumped
393437105160700	GW13	183	unk	393437.4	1051605.5	7890	top of casing	0.25	09/28/01	1105	76.80	recently pumped
393429105154700	na	184	155281	393429.1	1051546.8	7885	top of casing	0.50	09/28/01	1205	12.72	recently pumped
393424105134800	GW005	187	unk	393424.0	1051346.0	7405	top of casing	1.90	09/28/01	1100	83.40	recently pumped
393437105183900	na	188	100105	393436.5	1051838.6	7720	top of casing	0.90	09/25/01	1315	10.15	recently pumped
393447105132700	na	188	187827	393446.5	1051327.1	7350	top of casing	0.60	09/25/01	1125	101.30	recently pumped
393426105130000	GW009	189	unk	393424.8	1051258.5	7045	top of casing	1.00	09/25/01	1235	5.30	recently pumped
393504105183200	na	198	19859	393503.7	1051832.7	7775	plug in top of casing	-0.10	09/25/01	1810	33.15	recently pumped
393503105174400	na	199	88930	393503.1	1051744.1	7855	top of casing	0.90	09/25/01	1110	76.05	recently pumped

**Table A4. Selected site characteristics for water levels measured in fall 2001—Continued**

[USGS id, 15-digit NWIS identifier; Local, local id; Cell, refers to project grid identifier; Permit, well permit number from State Engineers Office; Latitude and Longitude, degrees minutes and seconds determined with commercial Global Positioning units and referenced to North American Datum of 1927; Elev, altitude above mean sea level determined from 1:24,000 topographic maps and referenced to National Geodetic Vertical Datum of 1929; MP, height of measuring point above land surface; Date, month day and year of measurement; Time, hours and minutes of measurement; DTW, measured depth from measuring point to water in well; na, not applicable, unk, unknown]

USGS id	Local	Cell	Permit	Latitude	Longitude	Elev	Measuring point description	MP	Date	Time	DTW	Status
393459105165701	MH4	200	unk	393459.6	1051655.5	7685	top of casing	0.10	09/24/01	1527	100.56	static
393452105151900	na	203	141447	393451.8	1051518.6	7470	top of casing	1.67	09/27/01	1150	91.82	recently pumped
393531105172700	na	219	51645	393530.5	1051727.2	8150	top of casing	1.00	09/27/01	1030	148.88	recently pumped
393532105150500	GWF02	223	unk	393531.6	1051503.2	7435	top of casing	1.00	09/28/01	1250	30.50	recently pumped
393536105140800	na	224	53567	393536.0	1051408.0	7250	top of casing	0.40	09/27/01	1130	22.34	recently pumped
393522105133800	na	225	53567	393522.0	1051338.0	7330	top of casing	0.30	09/27/01	1800	174.25	recently pumped
393552105172900	na	237	78185	393552.0	1051728.6	7990	top of casing	0.50	09/27/01	1300	162.25	recently pumped
393557105170200	na	238	117459	393557.1	1051701.8	7975	top of casing	0.25	09/27/01	1330	290.30	recently pumped
393547105165100	na	239	79269	393546.9	1051650.8	7725	top of casing	0.58	09/27/01	1430	76.98	recently pumped
393547105151500	na	241	73879	393546.5	1051515.2	7500	top of plate	0.50	09/28/01	1350	66.53	recently pumped
393547105144900	na	242	83170	393546.5	1051449.2	7400	top of casing	1.50	10/01/01	1125	75.52	recently pumped
393552105143600	GWF09	243	unk	393551.5	1051434.1	7420	top of casing	0.30	10/01/01	1045	49.42	recently pumped
393551105140100	na	244	104479	393551.0	1051401.0	7370	top of casing	0.40	09/27/01	1330	350.00	recently pumped
393604105132200	GWF02	245	unk	393604.3	1051320.6	6840	top of casing	0.25	09/24/01	1105	34.98	recently pumped
393543105123700	na	246	152277	393543.0	1051237.2	7285	top of casing	0.75	09/24/01	1140	54.19	recently pumped
393616105165000	na	258	131231	393615.6	1051650.4	7810	top of casing	1.00	09/27/01	1650	94.55	recently pumped
393625105161400	na	259	159923	393625.0	1051614.0	7965	top of casing	1.00	09/27/01	1100	228.00	recently pumped
393609105152300	na	260	131580	393608.5	1051523.1	7635	top of casing	0.50	09/28/01	1430	na .00	recently pumped
393641105152000	na	261	37790	393613.5	1051520.0	7670	top of casing	1.30	09/27/01	1030	100.90	recently pumped
393643105165600	na	276	175105	393642.8	1051656.2	7895	top of casing	0.60	10/01/01	1400	101.49	recently pumped
393640105164400	GWF15	277	unk	393643.1	1051640.5	7895	top of casing	1.50	09/25/01	1745	24.93	pumping
393643105163600	na	277	unk	393643.4	1051635.8	7895	top of casing	0.70	09/25/01	1824	50.63	recently pumped
393634105154500	na	278	197500	393634.0	1051545.0	7865	top of casing	0.30	09/27/01	1700	204.00	recently pumped
393637105134300	na	282	198923	393637.3	1051342.5	6900	top of casing	0.95	09/27/01	1042	401.80	recently pumped
393710105164900	na	296	89582	393709.7	1051649.4	8170	top of casing	0.20	09/25/01	1900	168.55	recently pumped
393710105165000	na	296	unk	393709.5	1051650.2	8175	top of casing	0.80	09/25/01	1920	158.81	recently pumped
393713105155300	na	298	197797	393713.2	1051553.0	7525	top of casing	0.70	09/24/01	1720	105.09	recently pumped
393721105153100	na	298	189222	393720.8	1051530.6	7475	top of casing	0.00	10/02/01	1030	287.00	recently pumped
393711105145200	na	299	226879	393710.5	1051452.4	7095	top of casing	0.70	09/28/01	1000	66.68	affected by nearby pumping
393723105135800	na	301	118865	393723.1	1051358.2	7300	top of casing	0.00	09/28/01	1132	375.00	pumping
393721105131100	na	302	unk	393711.9	1051310.6	6605	top of casing	0.88	09/24/01	1314	58.80	recently pumped
393738105171000	na	314	54005	393738.4	1051709.8	8410	top of casing	0.20	10/02/01	1300	368.00	recently pumped
393727105164900	na	315	100062	393726.9	1051648.5	8205	top of casing	0.40	10/01/01	1500	125.84	recently pumped
393745105160100	na	316	111412	393745.3	1051601.1	7435	top of casing	-0.40	09/24/01	1420	91.58	recently pumped
393728105151700	na	317	5681433	393728.0	1051517.0	7135	ticg	0.70	09/27/01	1900	7.00	recently pumped
393734105151300	na	318	190413	393733.6	1051512.5	7090	top of casing	0.60	09/24/01	1800	20.49	recently pumped
393753105155300	na	335	97142	393753.2	1051553.0	7325	top of casing	0.20	09/24/01	1500	53.04	affected by nearby pumping
393756105154400	na	336	unk	393756.4	1051544.4	7275	top of casing	1.50	09/24/01	1655	40.43	recently pumped
393125105220900	na	na	217016	393124.7	1052208.5	9790	top of casing	0.95	09/27/01	1323	113.80	affected by nearby pumping
393228105205900	na	na	202663	393228.4	1052058.9	8955	top of casing	0.64	09/26/01	1236	329.40	affected by nearby pumping
393359105141100	na	na	unk	393358.5	1051411.4	7490	top of casing	0.40	10/04/01	1245	17.79	recently pumped
393403105142300	na	na	unk	393402.5	1051423.2	7445	top of casing	0.40	10/04/01	1245	15.06	recently pumped